frontiers | Research Topics

Combined abiotic interactions in woody plants

Edited by
Hülya Torun, Srdjan Stojnic and Claudia Cocozza

Coordinated by
Peter Petrík

Published in
Frontiers in Plant Science

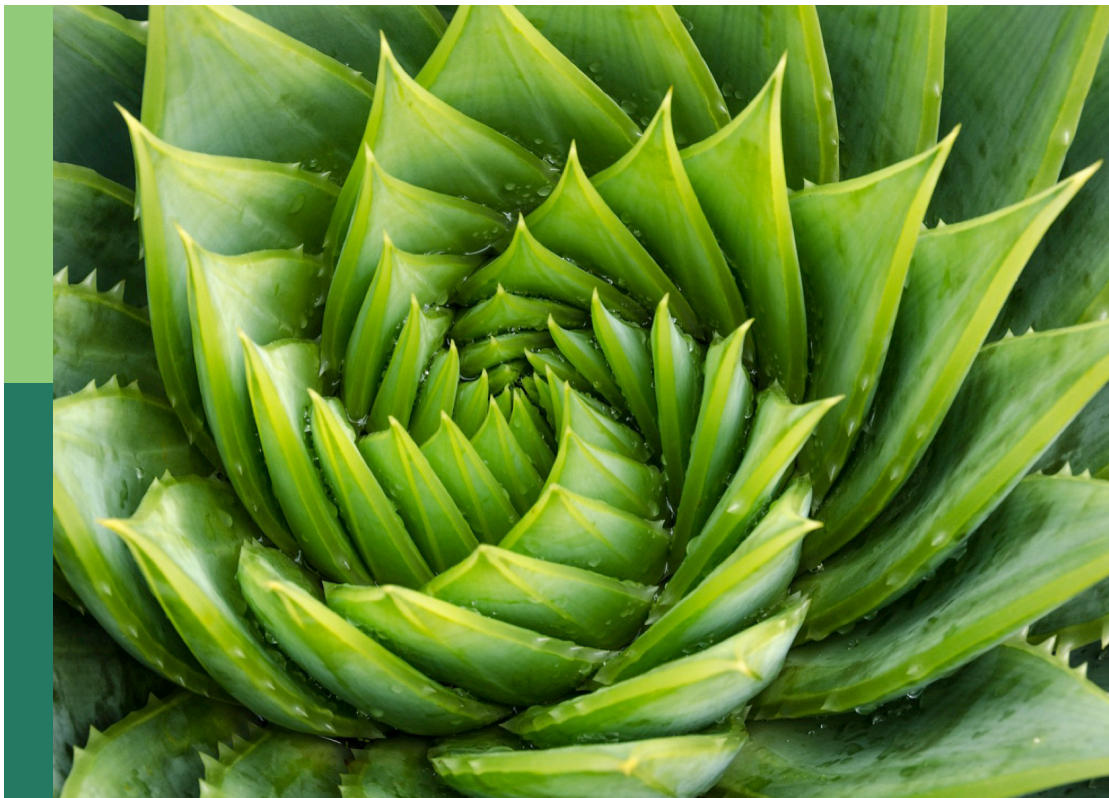

ISSN 1664-8714
ISBN 978-2-8325-5229-2
DOI 10.3389/978-2-8325-5229-2

About Frontiers

Frontiers is more than just an open access publisher of scholarly articles: it is a pioneering approach to the world of academia, radically improving the way scholarly research is managed. The grand vision of Frontiers is a world where all people have an equal opportunity to seek, share and generate knowledge. Frontiers provides immediate and permanent online open access to all its publications, but this alone is not enough to realize our grand goals.

Frontiers journal series

The Frontiers journal series is a multi-tier and interdisciplinary set of open-access, online journals, promising a paradigm shift from the current review, selection and dissemination processes in academic publishing. All Frontiers journals are driven by researchers for researchers; therefore, they constitute a service to the scholarly community. At the same time, the *Frontiers journal series* operates on a revolutionary invention, the tiered publishing system, initially addressing specific communities of scholars, and gradually climbing up to broader public understanding, thus serving the interests of the lay society, too.

Dedication to quality

Each Frontiers article is a landmark of the highest quality, thanks to genuinely collaborative interactions between authors and review editors, who include some of the world's best academicians. Research must be certified by peers before entering a stream of knowledge that may eventually reach the public - and shape society; therefore, Frontiers only applies the most rigorous and unbiased reviews. Frontiers revolutionizes research publishing by freely delivering the most outstanding research, evaluated with no bias from both the academic and social point of view. By applying the most advanced information technologies, Frontiers is catapulting scholarly publishing into a new generation.

What are Frontiers Research Topics?

Frontiers Research Topics are very popular trademarks of the *Frontiers journals series*: they are collections of at least ten articles, all centered on a particular subject. With their unique mix of varied contributions from Original Research to Review Articles, Frontiers Research Topics unify the most influential researchers, the latest key findings and historical advances in a hot research area.

Find out more on how to host your own Frontiers Research Topic or contribute to one as an author by contacting the Frontiers editorial office: frontiersin.org/about/contact

Combined abiotic interactions in woody plants

Topic editors
Hülya Torun — Düzce University, Türkiye
Srdjan Stojnic — University of Novi Sad, Serbia
Claudia Cocozza — University of Florence, Italy

Topic coordinator
Peter Petrík — Karlsruhe Institute of Technology (KIT), Germany

Citation
Torun, H., Stojnic, S., Cocozza, C., Petrík, P., eds. (2024). *Combined abiotic interactions in woody plants*. Lausanne: Frontiers Media SA.
doi: 10.3389/978-2-8325-5229-2

Table of contents

frontiers | Frontiers in Plant Science

TYPE Editorial
PUBLISHED 17 July 2024
DOI 10.3389/fpls.2024.1455459

OPEN ACCESS

EDITED AND REVIEWED BY
Dominik K. Großkinsky,
Austrian Institute of Technology (AIT), Austria

*CORRESPONDENCE
Peter Petrík
peter.petrik@kit.edu

RECEIVED 26 June 2024
ACCEPTED 10 July 2024
PUBLISHED 17 July 2024

CITATION
Torun H, Cocozza C, Petrík P and Stojnic S (2024) Editorial: Combined abiotic interactions in woody plants.
Front. Plant Sci. 15:1455459.
doi: 10.3389/fpls.2024.1455459

Editorial: Combined abiotic interactions in woody plants

Hülya Torun[1], Claudia Cocozza[2], Peter Petrík[3,4]* and Srdjan Stojnic[5]

[1]Department of Biosystem Engineering, Faculty of Agriculture, Düzce University, Düzce, Türkiye, [2]Department of Agriculture, Food, Environment and Forestry (DAGRI), University of Florence, Florence, Italy, [3]Karlsruhe Institute of Technology (KIT), Institute of Meteorology and Climate Research-Atmospheric Environmental Research, Institut für Meteorologie und Klimaforschung Atmosphärische Umweltforschung (IMK-IFU), Garmisch-Partenkirchen, Germany, [4]Chair of Forest Botany, Institute of Forest Botany and Forest Zoology, Technical University of Dresden (TUD), Tharandt, Germany, [5]Institute of Lowland Forestry and Environment, University of Novi Sad, Novi Sad, Serbia

KEYWORDS

drought, heat stress, heavy metals, light, ROS, temperature, trees

Editorial on the Research Topic
Combined abiotic interactions in woody plants

1 Introduction

Combined abiotic stress interactions, such as the simultaneous occurrence of drought and high temperatures, significantly impact plants' physiology, growth, and survival. The occurrence of multiple stressors often exacerbates the effects of each other, leading to compounded challenges for plants (Zandalinas and Mittler, 2022). Additionally, the energy expenditure required to combat multiple stresses can deplete the plant's reserves, hindering its growth and reproductive capabilities (Maurya et al.). Over time, such compounded stresses can lead to reduced ecosystem productivity, altered species composition, and potentially increased plant mortality rates. Understanding stress interaction effects is essential due to the complexity of climate change, which is increasing both the frequency and severity of droughts and heatwaves across the globe (Tripathy et al., 2023). The impact of these two stressors can have devastating effects on sites already affected by other abiotic stressors such as higher soil salinity, heavy metals or other ecotoxic chemicals. Moreover, the land use legacy can also amplify negative impact on trees, especially in urban ecosystems (Cui et al.). The articles in this Research Topics explored the effects of drought and heat stress, light availability and heavy metal stress on the growth and physiology of trees.

2 Drought and heat stress

The co-occurrence of drought and heat stress is one of the most common stress interactions in nature. Drought conditions can limit water availability, reducing the tree's ability to cool itself through transpiration, while high temperatures can increase water loss and further strain the tree's water balance. The heat stress can also damage photosynthetic apparatus thus further negatively affecting the carbon balance and growth (Yuan et al.). The

heat-drought stress combination can therefore lower water uptake, impair photosynthesis, reduce water-use efficiency, increase reactive oxygen species (ROS) generation, reduce growth and heighten mortality risk. The abiotic stressors can also weaken the tree's overall health, making it more susceptible to diseases and pests (Teshome et al., 2020). There are multiple options with which we can try to reduce the negative impact of drought and heat stress in forest ecosystems. The application of N can improve the water-use efficiency and growth of drought prone forests in desert regions (Bai et al.). Besides, the exogenous application of plant phytohormones such as auxins, cytokinins, gibberellins, abscisic acid, salicylic acid, jasmonic acid etc. whether prior to or concurrent with the onset of drought and heat stress, has been demonstrated to enhance thermotolerance in plants and to facilitate the maintenance of internal water balance (Paul et al., 2018; Li et al., 2021; Seleiman et al., 2021; Huang et al., 2023). Another important co-factor that can positively improve drought tolerance of forest ecosystems is the selection of drought resistant clones or cultivars (Vuksanović et al.).

3 Light, water and temperature

An important factor of the drought-heat interaction in forest ecosystems is the light availability. The incoming light intensity is affected by overall stand structure, tree density and canopy arrangement. The open canopy forests show greater photosynthetic efficiency and growth (Čater et al.), but at the same time provide less shade and therefore less optimal microclimate under drought and heat stress in regard to water balance (Zavadilová et al., 2023). The incoming light quantity also affects the nutrient availability and accumulation in leaves. The trees in forest understory have a higher leaf N/P ratio than ones in forest edges or gaps (Zhang et al.). The higher N/P ratio can positively affect photosynthesis and synthesis of secondary metabolites, but can negatively impact ATP production and overall metabolic activity. The interaction between light availability and abiotic stressors is still under-explored for tree species. New research in this direction is especially needed as thinning, the most common practice in forest management to alter the canopy structure and light regime in forest ecosystems.

4 Drought and heavy metal stress

Drought and heavy metal stress interact synergistically in plants, creating a compounded adverse effect on their physiology and growth. Drought conditions limit water availability, causing stomatal closure to reduce transpiration, which in turn restricts CO_2 intake and diminishes photosynthetic efficiency. Concurrently, heavy metal stress, caused by elements like cadmium, lead, and arsenic, disrupts root function and nutrient uptake, further impairing water absorption and leading to additional dehydration (Sitko et al., 2021). This combination exacerbates nutrient imbalances as heavy metals compete with essential nutrients, such as calcium and zinc, for uptake. Both stresses independently generate ROS, but together they significantly elevate ROS levels, overwhelming the plant's antioxidant defenses and causing extensive cellular damage (Kostić et al.). Exogenous application of phytohormones or other biotechnological compounds, such as salicylic acid, can alleviate or reduce the negative impact of the combined drought and heavy metal stress (Torun et al.). The understanding of the interaction of heavy metal stress with other abiotic stressors, as well as, the effectivity of biotechnological applications is critical for phytoremediation and land remediation practices.

5 Concluding remarks and future perspectives

In conclusion, the interplay between multiple abiotic stressors, such as drought and high temperatures, exerts a profound impact on the physiology, growth, and survival of plants. The simultaneous occurrence of these stressors amplifies their individual effects, presenting compounded challenges that strain the energy reserves of plants and hinder their growth and reproductive success. Understanding these interactions is crucial, especially in the context of climate change, which is intensifying the frequency and severity of droughts and heatwaves globally. The detrimental effects of combined stresses are even more pronounced in environments already compromised by other abiotic factors like soil salinity, heavy metals, or ecotoxic chemicals. Future research should include multi-stress studies with more than two stressors. Moreover, there is a gap in knowledge regarding the impact of seasonal timing (spring vs. summer), severity and stress duration in trees. The research focused on biotechnological applications or breeding with regard to multiple-stressors is also needed to reach effective adaptation strategies for climate change.

Author contributions

HT: Supervision, Writing – original draft. CC: Supervision, Writing – original draft. PP: Writing – original draft. SS: Supervision, Writing – original draft.

Conflict of interest

The authors declare that the research was conducted in the absence of any commercial or financial relationships that could be construed as a potential conflict of interest.

Publisher's note

References

Huang, J., Hartmann, H., Ogaya, R., Schöning, I., Reichelt, M., Gershenzon, J., et al. (2023). Hormone and carbohydrate regulation of defense secondary metabolites in a Mediterranean forest during drought. *Environ. Exp. Bot.* 209, 105298. doi: 10.1016/j.envexpbot.2023.105298

Li, N., Euring, D., Cha, J. Y., Lin, Z., Lu, M., Huang, L.-J., et al. (2021). Plant hormone-mediated regulation of heat tolerance in response to Global climate change. *Front. Plant Sci.* 11, 2020. doi: 10.3389/fpls.2020.627969

Paul, S., Wildhagen, H., Janz, D., and Polle, A. (2018). Drought effects on the tissue- and cell-specific cytokinin activity in poplar. *AoB Plants* 10, 1–8. doi: 10.1093/aobpla/plx067

Seleiman, M. F., Al-Suhaibani, N., Ali, N., Akmal, M., Alotaibi, M., Refay, Y., et al. (2021). Drought Stress Impacts on Plants and Different Approaches to Alleviate Its Adverse Effects. *J. Plant*. 10 (2), 259. doi: 10.3390/plants10020259

Sitko, K., Opała-Owczarek, M., Jemioła, G., Gieroń, Ż., Szopiński, M., Owczarek, P., et al. (2021). Effect of drought and heavy metal contamination on growth and photosynthesis of silver birch trees growing on post-industrial heaps. *Cells* 11, 53. doi: 10.3390/cells11010053

Teshome, D. T., Zharare, G. E., and Naidoo, S. (2020). The threat of the combined effect of biotic and abiotic stress factors in forestry under a changing climate. *Front. Plant Sci.* 11. doi: 10.3389/fpls.2020.601009

Tripathy, K. P., Mukherjee, S., Mishra, A. K., Mann, M. E., and Williams, A. P. (2023). Climate change will accelerate the high-end risk of compound drought and heatwave events. *Proc. Natl. Acad. Sci. U.S.A.* 120, e2219825120. doi: 10.1073/pnas.2219825120

Zandalinas, S. I., and Mittler, R. (2022). Plant responses to multifactorial stress combination. *New Phytol.* 234, 1161–1167. doi: 10.1111/nph.18087

Zavadilová, I., Szatniewska, J., Stojanović, M., Fleischer, P., Vágner, L., Pavelka, M., et al. (2023). The effect of thinning intensity on sap flow and growth of Norway spruce. *J. For. Sci.* 69, 205–216. doi: 10.17221/17/2023-JFS

frontiers | Frontiers in Plant Science

TYPE Original Research
PUBLISHED 14 October 2022
DOI 10.3389/fpls.2022.946141

OPEN ACCESS

EDITED BY
Virginia Hernandez-Santana,
Institute of Natural Resources and Agrobiology of Seville (CSIC), Spain

REVIEWED BY
Maria A. Pérez-Fernádez,
Universidad Pablo de Olavide, Spain
Doudou Li,
Chinese Academy of Medical Sciences and Peking Union Medical College, China

*CORRESPONDENCE
Qiaoling Yan
qlyan@iae.ac.cn

SPECIALTY SECTION
This article was submitted to Plant Abiotic Stress, a section of the journal Frontiers in Plant Science

RECEIVED 17 May 2022
ACCEPTED 09 September 2022
PUBLISHED 14 October 2022

CITATION
Yuan J, Yan Q, Wang J, Xie J and Li R (2022) Different responses of growth and physiology to warming and reduced precipitation of two co-existing seedlings in a temperate secondary forest.
Front. Plant Sci. 13:946141.
doi: 10.3389/fpls.2022.946141

Different responses of growth and physiology to warming and reduced precipitation of two co-existing seedlings in a temperate secondary forest

Junfeng Yuan[1,2,3], Qiaoling Yan[1,2]*, Jing Wang[4], Jin Xie[5] and Rong Li[1,2,3]

[1]Qingyuan Forest Chinese Ecosystem Research Network (CERN), National Observation and Research Station, Shenyang, China, [2]Chinese Academy of the Sciences (CAS) Key Laboratory of Forest Ecology and Management, Institute of Applied Ecology, Shenyang, China, [3]University of Chinese Academy of Sciences, Beijing, China, [4]School of Life Sciences, Zhengzhou University, Zhengzhou, China, [5]Key Laboratory of Agricultural Water Resources, Hebei Key Laboratory of Soil Ecology, Center for Agricultural Resources Research, Institute of Genetic and Developmental Biology, Chinese Academy of Sciences, Shijiazhuang, China

Warming and precipitation reduction have been concurrent throughout this century in most temperate regions (e.g., Northeast China) and have increased drought risk to the growth, migration, or mortality of tree seedlings. Coexisting tree species with different functional traits in temperate forests may have inconsistent responses to both warming and decreased precipitation, which could result in a species distribution shift and change in community dynamics. Unfortunately, little is known about the growth and physiological responses of coexisting species to the changes in these two meteorological elements. We selected two coexisting species in a temperate secondary forest of Northeast China: *Quercus mongolica* Fischer ex Ledebour (drought-tolerant species) and *Fraxinus mandschurica* Rupr. (drought-intolerant species), and performed an experiment under strictly controlled conditions simulating the predicted warming (+2°C, +4°C) and precipitation reduction (-30%) compared with current conditions and analyzed the growth and physiology of seedlings. The results showed that compared with the control, warming (including +2°C and +4°C) increased the specific area weight and total biomass of *F. mandschurica* seedlings. These were caused by the increases in foliar N content, the activity of the PSII reaction center, and chlorophyll content. A 2°C increase in temperature and reduced precipitation enhanced root biomass of *Q. mongolica*, resulting from root length increase. To absorb water in drier soil, seedlings of both species had more negative water potential under the interaction between +4°C and precipitation reduction. Our results

demonstrate that drought-tolerant species such as *Q. mongolica* will adapt to the future drier conditions with the co-occurrence of warming and precipitation reduction, while drought-intolerant species will accommodate warmer environments.

KEYWORDS

warming, drought-intolerance species, foliar N content, root biomass, specific area weight

Introduction

The natural and anthropogenic activities have largely changed global climatic conditions, which pose a threat to life on earth (Hodson, 2017). Moreover, the global surface temperature has increased during the past decades and it is expected to continue rising by 0.3-4.8°C at the end of this century (IPCC, 2013). Warming and a shift in precipitation patterns have caused and exacerbated regional drought conditions, especially in mid/high-latitude temperate regions (IPCC, 2013; Li et al., 2017). Northeast China is located in the middle and high latitudes of the northern hemisphere and has experienced a much more rapid warming trend than the national and global scales for the last decades (Piao et al., 2010). Furthermore, the precipitation amounts of Northeast China have approximately decreased by 30% and suffered from increased drought risk in recent studies (Gao et al., 2020). Taken together, Northeast China is typical among the areas where warming and drought will be concurrent throughout this century. These climatic alterations may potentially alter the interaction between plants and their environment, and thus alter forest structure and function because of certain species migration or mortality. Accordingly, to improve the ability to forecast forest dynamics, there is a compelling need to assess the responses of plants to these combined changes in temperature and precipitation (Hu et al., 2013).

Most previous studies analyzed the effects of climate change on adult trees (Morin et al., 2010) without considering seedlings. However, seedlings are more sensitive to climate variability than adult counterparts due to their limited root system and leaf areas, leading to less carbohydrate accumulation and resource acquisition in seedlings that cannot cope well with abrupt environmental changes (Lloret et al., 2009). Thus, seedling recruitment is considered a critical stage for the successful establishment of tree species. The previous study has indicated that the seedling mortality of dominant tree species in temperate forests increased, and seedling growth was limited under future climates (Yang et al., 2012). The shrink of distribution and even a decrease in community species richness may happen in temperate regions in the future.

A temperature increase and a precipitation decrease are expected to affect individual growth, carbon or biomass accumulation and allocation pattern, and physiological processes, and thus change species survival, establishment, and the composition of ecosystems (Hu et al., 2013; Reich et al., 2018). In general, warming will promote individual growth and photosynthesis as long as the temperature does not exceed the optimum range in alpine ecosystems and polar regions, but it is still uncertain for temperate regions (Milbau et al., 2017; Han et al., 2019). Yun et al. (2016) found warming enhanced the growth of root collar diameter and increased chlorophyll contents of *Pinus densiflora* Sieb. et Zucc. seedlings. A meta-analysis of data from 24 studies showed that the above-ground biomass, growth, and photosynthesis increased with elevated temperatures (Wu et al., 2011). However, decreased precipitation usually suppresses total leaf area to decrease water loss, increases root length and root biomass to enhance water uptake capacity responding to reduced soil moisture, and finally limits the growth of plants (Rodgers et al., 2018). Hence, when considering the combined effects of temperature and water on seedling growth in the future, individual performance might determine the balance of response to warming and precipitation reduction. However, there is little information about the interactive effects of warming and decreased rainfall on seedlings' growth and physiology.

The impacts of warming and reduced precipitation on the growth and physiology of seedlings differed across changing intensity (Taeger et al., 2015) and among species (Matías et al., 2016). Although the 2 °C temperature increase is used for most works (Xiao et al., 2019; Lyons et al., 2020), it is not representative of many sites, where projected temperature alterations by the end of the current century have been well above 2 °C, e.g., the Tibetan Plateau (Zhao et al., 2022) and northern latitude mountains (Nogués-Bravo et al., 2007). As a consequence, a larger temperature magnitude is needed for the

Abbreviations: SLW, specific leaf weight; $RCD_{inc,}$ mean periodic increment of root collar diameter; R_{inc}, mean periodic increment of maximum root length; H_{inc}, mean periodic increment of height; Ψ, water potential; CP, current precipitation; FP, future precipitation.

study. The responses of different species to climate change depend on exogenous and endogenous factors, such as habitats and species traits. The habitat can shape the endogenous climate stress tolerance of species, where species from xeric habitats are more adapted to warming and lower water availability than those from humid habitats. For example, *Pinus halepensis* Mill. and *Pinus pinaster* Ait. from drier habitats (lowland) showed a higher survival and better performance in warming and direr habitats than in humid habitats (high-elevation) (Matías et al., 2016). Different functional traits of species (e.g., shade tolerance and drought tolerance) also facilitate trees to accommodate environmental alternations (Richter et al., 2012). This induced the majority of research to focus on the comparison among various provenances and families of species (Kueppers et al., 2017; Zhu et al., 2020). But the consequences of warming and decreased precipitation could be of paramount importance for coexisting species with contrasting traits since inconsistent responses of these coexisting species to climate change could result in a species distribution shift and change in community dynamics (Chmura et al., 2017; Reich et al., 2018). Unfortunately, little is known about the growth and physiological responses of coexisting species to both warming and decreased precipitation.

Secondary forest is the main forest type across the world and Northeast China, accounting for 60% and 72% of forest area, respectively (Zhu et al., 2018). However, compared with the primary stands, there have been many problems in secondary forests, e.g., productivity losses and stability and resilience declines. These problems are radically caused by the poor regeneration capacity of dominant species (Yu et al., 2017). As a consequence, improving their natural regeneration would determine the future destiny of secondary forests. Evaluating seedling performance to climate alterations is vital to enhance regeneration and consequently restore secondary forests. Specifically, projected warming and drought both will induce lower soil moisture. Thus, the traits related to water balance might play a key role in the future performance of seedlings. As precious commercial timber species, *Quercus mongolica* Fischer ex Ledebour and *Fraxinus mandschurica* Rupr are dominant and co-existing in secondary forests of Northeast China. In addition, *Q. mongolica* is mainly distributed in uphill xeric environments with sunny slopes and belongs to a drought-tolerant species (Dai et al., 2020). While *F. mandshurica* belongs to a drought-intolerant species and tends to grow in comparatively humid sites such as river banks and shady slopes (Liu et al., 2015). The response of these coexisting species with contrasting traits to both warming and decreased precipitation is an essential means of predicting the community dynamics of secondary forests.

Here, we selected two-year-old seedlings of *Q. mongolica* and *F. mandschurica*, and conducted a controlled experiment to compare their physiology and growth under simulated current climatic patterns and projected future climatic scenarios. The patterns of warming included three temperature scenarios (i.e., control, +2°C, and +4°C) and two precipitation scenarios (i.e., control and -30%). We hypothesized that (i) warming would alleviate the effects of precipitation reduction on the seedling physiology and growth, and (ii) seedlings of the drought-tolerant species, *Q. mongolica*, are better adapted to future climate change (warming, precipitation reduction, and their co-occurrence) than seedlings of the drought-intolerant species, *F. mandshurica*. We expect that the different responses of coexisting species to warming and reduced precipitation can provide us with information on future community dynamics and restoration by promoting natural regeneration under climate changes in temperate secondary forests.

Materials and methods

Experimental setup

Two-year-old seedlings of the two tree species with the same height (12.7 cm and 9.6 cm for *Q. mongolica* and *F. mandshurica*, respectively) and root collar diameter (1.75 cm and 1.62 cm for *Q. mongolica* and *F. mandshurica*, respectively) were collected from Qingyuan Forest CERN, Northeast China (41°51'N, 124°54'E). There are typical temperate broadleaved secondary forests in Qingyuan Forest CERN. The average annual rainfall in the study area ranges from 700 and 850 mm, 80% of which falls from June to August. The mean annual temperature is +4.7°C. The coldest month is January with a mean air temperature of -12.1°C, and the hottest month is July with a mean air temperature of +21.0°C.

Seedlings were collected on 1st June 2020 and then were immediately transferred to tubular PVC pots (7.5 cm in diameter and 40 cm high) filled with soil. The soil in pots was derived from topsoil from secondary forests in Qingyuan Forest CERN to a depth of 0-10 cm, passed through a 1 cm sieve to remove smaller stones and other impurities, and then autoclaved at 121 °C for 2 h.

After planting, all seedlings were thoroughly irrigated and placed into three incubators (MGC-450BP-2L, inner space with 0.7 m length × 0.55 m width × 1.14 m height) that simulated three temperature scenarios (control, +2°C, and +4°C treatments, respectively) with the temperature treatment as a whole plot factor (Table 1): (i) 'control temperature', representing the mean monthly day and night temperature of the Qingyuan Forest CERN during the growing season from 2005 to 2019; (ii) '+2°C treatment', simulating an increase of 2°C in day and night mean temperature respecting to the temperature at the Qingyuan Forest CERN by 2055; (iii) '+4°C treatment', simulating 4°C increase than control temperature records by the end of the 21st century (Nogués-Bravo et al., 2007). The weekly temperatures (day/night, in °C) of the study area (Qingyuan Forest CERN) during the 16-week experiment were developed for the three temperature scenarios (control, +2°C, and +4°C treatments, respectively) (Table 1).

TABLE 1 Weekly temperatures (day/night, in °C) and light time of day or night (day/night, in hours) during the experiment development in different conditions: control, +2 °C, and +4 °C.

Week	Equivalent	Control	+2 °C	+4 °C	Light time
1-4	June	21.9/15.3	23.9/17.3	25.9/19.3	14.5/9.5
5-8	July	24/18.5	26/20.5	28/22.5	14.5/9.5
9-12	August	23.1/18.3	25.1/20.3	27.1/22.3	13/11
13-16	September	18/11.5	20/13.5	22/15.5	12/12

These values were obtained as monthly mean from the meteorological stations of Qingyuan Forest CERN during the 2005-2019 series.

Two precipitation treatments representing current and future precipitation (CP and FP hereafter) respectively were set up in each incubator, and were applied as a subplot factor: (i) 'current precipitation', derived from the mean precipitation of Qingyuan County (~20 km away from Qingyuan Forest CERN) during the growing season (June-September) for 1963-2013 series (138.1 mm); (ii) 'future precipitation', simulated precipitation reduction by 30% based on the previous level, as projected of Qingyuan County, Northeast China (96.7 mm). Total precipitation amounts were split into 32 irrigation events (twice per week) from the 1st experimental week to the 16th week. Thus, our experiment was designed with three factors (temperature, precipitation, and species), in which temperature included three levels and both other factors included two levels, fully crossed with 15 replicated seedlings per factor combination ($2 \times 3 \times 15 = 90$ seedlings).

For the whole experiment, light intensity in each incubator was constantly fixed at a photosynthetic photon flux density of 105 μmol m^2 s^{-1} for daytime, which represented the light availability for the understory with moderate openness. The light time was in line with the monthly day length which was based on the time of sunrise and sunset per month in Qingyuan Forest CERN (see Table 1), rising gradually at dawn and decreasing at dusk for around one extra hour. To avoid any possible chamber effects, all seedlings were rotated through three different incubators every ten days by randomizing each seedling position within each incubator.

Soil moisture (volumetric water content) was recorded twice a week (two days after each watering event) by using the time-domain reflectometer (TDR) (SM200; Delta-T Devices, Cambridge, UK) during the whole experiment. The TDR with three steel rods was vertically inserted at 5 cm of the soil surface in each pot. The soil moisture was measured on the half of seedlings (i.e., N = 8 per species and treatment combination). Temperatures within the incubators were periodically checked with independent temperature devices (iButton, DS1922L) continuously logged to ensure the temperature accuracy of different treatments. To measure temperature, the temperature device was installed in the center of the incubator and logged at 1-hour intervals. The study was performed for 16 weeks from 26 June 2020 to 16 October 2020 at incubators.

Seedling measurement

Before we transplanted seedlings, an initial measure of growth variables (i.e., root collar diameter (RCD), height, and maximum root length) was conducted for all seedlings. The RCD was recorded at a constant height (1 cm above the soil surface) using a digital caliper, and seedling height was measured as the distance from the root collar to the tip of the top bud. The seedlings were laid on a flat surface and the roots were straightened to measure the maximum root length. The maximum root length was measured from the base of the stem to the tip of the root system. At the end of the experiment, we again measured the final three growth variables of all seedlings.

The leaf areas of nine fresh plants for each treatment were measured by the high-resolution scanner (Founder Z1600, China). The acquired pictures were analyzed by computer image analysis software (Díaz-Barradas et al., 2010). In addition, the maximum photochemical efficiency of photosystem II (Fv/Fm) and the plant water potential (Ψ) of three replicates per treatment were measured before the final harvest of seedlings (Tuna et al., 2008; Zheng et al., 2019). Fv/Fm was recorded with a portable fluorometer (FMS2, Hansatech Instruments, UK) at predawn. A fiber-optic encased in a light-tight chamber was inserted onto the leaf clip, and the healthy and fully expanded leaves were exposed to measured light (0.05 μmol m^{-2} s^{-1}). After getting the minimum fluorescence yield (F_0), the leaves were given a saturating pulse of actinic light (300 mmol m^{-2} s^{-1}) for 0.7 s to read a maximum fluorescence yield (Fm). The maximum quantum yield of photosystem II (Fv/Fm) was calculated as $Fv/Fm = (Fm - F_0)/Fm$. A fully expanded mature leaf in the upper canopy was randomly selected to measure the water potential (Ψ) by using a pressure bomb (range: 0-15 MPa; PMS, Manofrígido, Lisbon, Portugal). Ψ was recorded on the same day at predawn (03:00-05:00). Then nine intact plants were divided into three parts (i.e., leaves, shoots, and roots), and the harvested roots were carefully washed to remove the remnants of soil. The three parts of the seedlings were oven-dried at 60°C for 72 h to a constant weight, and the dry biomass of each part was recorded.

Carbon and nitrogen analyses

We randomly collected nine plants and divided them into three groups per treatment combination to analyze carbon and nitrogen concentrations. Dried leaves were ground to powder, passed through a 0.25 mm (60 mesh) sieve, and analyzed for total carbon and nitrogen concentrations. Foliar carbon (C) and nitrogen (N) concentrations were measured by an elemental analyzer (vario MICRO cube; Elementar Analyser Systeme GmbH, Hessen Hanau, Germany). Finally, we calculated the C:N by dividing foliar carbon concentrations by nitrogen concentrations.

Determination of chlorophyll pigments

Before final harvest, fresh leaves (500 mg) from two seedlings per treatment were cut up into three groups and homogenized with 10 mL acetone (80%), and then chlorophyll was extracted from the homogenized plant materials to avoid light for 1-2 days. The absorbance of the supernatant was read at 645 nm and 663 nm using a spectrophotometer (UA1880, Jinghua Instruments, China). The relative amount of chlorophyll a, chlorophyll b, and the total content of chlorophyll were calculated according to the following equations:

$$Chlorophyll\ a\ (mg/g) = (12.7 \times A663 - 2.69 \times A645)V/W \quad (1)$$

$$Chlorophyll\ b\ (mg/g) = (12.9 \times A645 - 4.68 \times A663)V/W \quad (2)$$

$$Total\ Chlorophyll\ (mg/g) = (20.2 \times A645 + 8.02 \times A663)V/W \quad (3)$$

where A663 and A645 are the absorbances at 645 nm and 663 nm. V is the final volume of chlorophyll extract in 80% acetone. W is the fresh weight of tissue extracted (500 mg) (Arnon, 1949).

The ratio of chlorophyll a and chlorophyll b (chlorophyll a: b) was calculated by chlorophyll a content divided by chlorophyll b content.

Data analysis

To evaluate the mean periodic increment of RCD (RCD_{inc}), height (H_{inc}), and maximum root length (R_{inc}), we calculated the difference between the final measured value (V_{T1}) and initial value (V_{T0}) for these three growth variables as follows:

$$RCD_{inc}/\ H_{inc}/\ R_{inc} = V_{T1} - V_{T0}$$

The specific leaf weight was determined by the leaf area divided by the leaf dry weight. The root-shoot ratio was calculated by root dry weight divided by the total dry weight of the leaf and stem.

The variation in soil moisture among the different treatments was tested by repeated-measures analysis of variances (ANOVA). The differences in increment of height, RCD and root length, total biomass, root-shoot ratio, Ψ, Fv/Fm, total chlorophyll content, chlorophyll a: b, foliar nitrogen content, and C:N were tested by using three-way ANOVAs across the different factors and interactions. Tukey's *post hoc* tests were used to further examine the variances across treatment levels. The effect of the experimental incubators could not be assumed as a factor in the ANOVAs since plants were rotated within and between incubators during the whole experiment which minimized the compound effect. The assumption of normality of data was evaluated with a normal probability plot and Shapiro-Wilk tests. The homogeneity of variances was assessed using Levene's test (Kardol et al., 2006; Buters et al., 2019). Non-normal variables were transformed (log, square root, etc.) to meet the statistical requirements when necessary. A *p*-value less than 0.05 was regarded as statistically significant. All the analyzes were performed with R version 4.0.4 (R Core Team, 2021). A car package (Fox and Weisberg, 2011) was used for normality tests and ANOVAs. A Lsmeans package (Lenth, 2016) was used for Tukey's *post hoc* tests. The results were shown as mean ± S.E. throughout the paper.

Results

Soil moisture

Soil moisture was affected by three factors (temperature, precipitation, and species) and their interactions during the experiment. Soil moisture in CP conditions was significantly higher than in FP conditions for both species for all three temperature scenarios (40.8 ± 0.1 vs 34.0 ± 0.1%; F = 1331.8, $P< 0.0001$). Under the two precipitation treatments, the lowest soil moisture was in the +4°C treatment (35.7%) for both species (see Supplementary Figure 1).

Seedling growth and biomass allocation pattern

The mean periodic increment in root collar diameter (RCD_{inc}) was significantly affected by temperature, species, and their interactions. For *F. mandschurica*, RCD_{inc} under control temperature (0.76 mm) was greatly less than that under +2°C (1.42 mm) and +4°C (1.55 mm) treatments, while no difference was

detected between these two increased temperature scenarios (Figure 1A). The mean periodic increment in total height (H_{inc}) was little affected by species. There was a significant effect of temperature and species on specific leaf weight (SLW). SLW in the control temperature was lower than in the +2°C and +4°C treatments (Figure 1B). Total biomass was determined by temperature and species, but unaffected by precipitation levels and any interactions among the three factors. Seedlings at +2°C treatment had maximum final biomass (1.5 g) (Figure 1C).

Furthermore, there were significant interactions of species × temperature and species × precipitation on the mean periodic increment in root length (R_{inc}). For *Q. mongolica*, seedlings in FP showed an obvious increase in root length than those in CP (Figure 2). In addition, *F. mandschurica* seedlings in +2°C and +4°C treatments had a longer root length than those in the control (Table 2).

However, a significant interaction among three factors was detected in the root-shoot ratio. For *Q. mongolica* under +2°C,

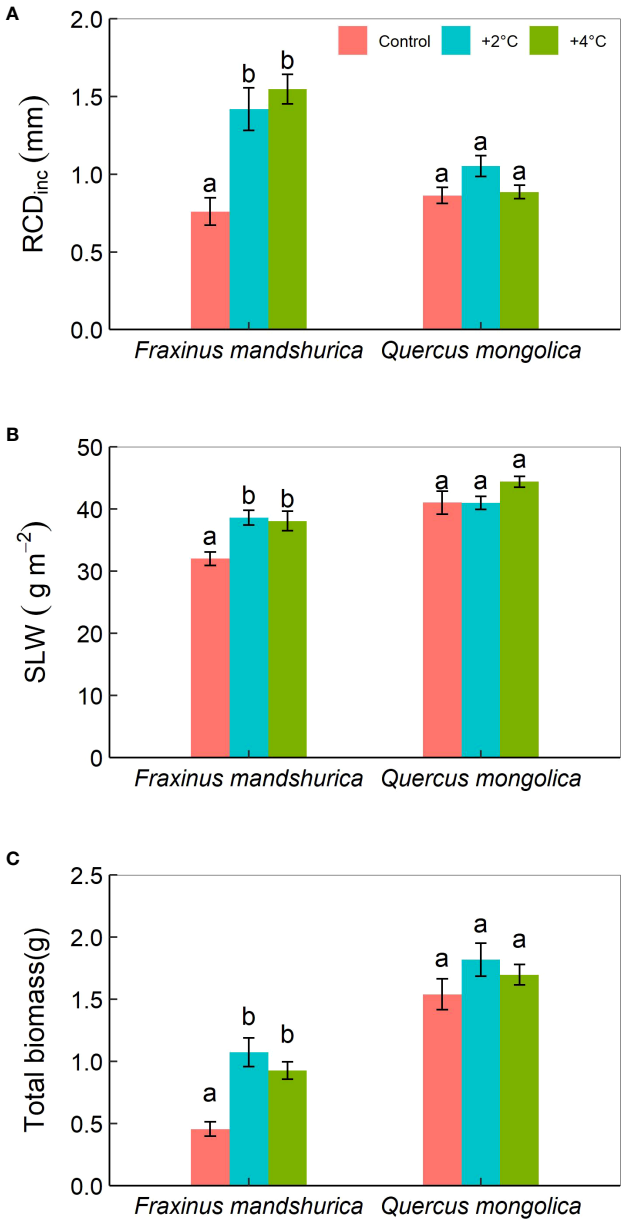

FIGURE 1
The mean periodic increment in root collar diameter (RCD_{inc}) **(A)** and specific leaf weight (SLW) **(B)**, and total biomass **(C)** for different species growing under the three temperatures (control; +2°C; +4°C). The data were presented as the mean ± S.E. Different lowercase letters indicated significant differences ($P<0.05$) between temperature treatments for the same species.

10.3389/fpls.2022.946141

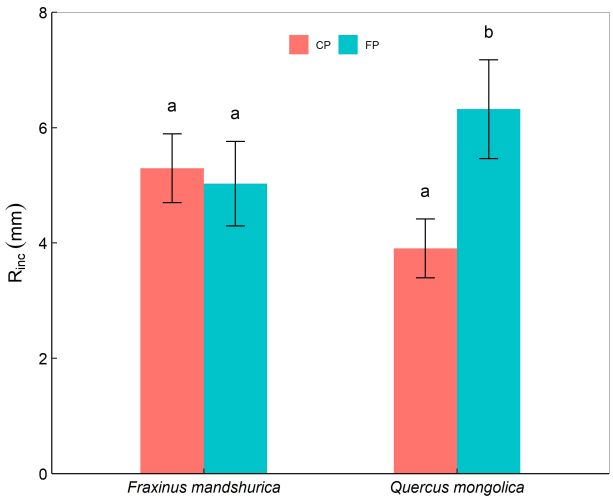

FIGURE 2
The mean periodic increment in maximum root length (R_{inc}) of *Quercus mongolica* and *Fraxinus mandschurica* seedlings across the species and irrigating (current precipitation, CP; future precipitation, FP) treatments. The data were presented as the mean ± S.E. Different lowercase letters indicated significant differences (P<0.05) between precipitation treatments in the same species.

seedlings from FP exhibited a higher root-shoot ratio than from CP, but no significant variance in the root-shoot ratio was observed for *F. mandschurica* (Figure 3).

Physiological variables of seedlings

Fv/Fm was significantly affected by temperature treatment and species. Overall, plants from the control temperature performed a lower Fv/Fm than the rest two temperature treatments (Figure 4A). In addition, there was a significant interaction between temperature and precipitation treatment on the water potential of seedlings. Under +4°C, both species from FP showed a lower water potential than seedlings from CP (Figure 4B).

Total chlorophyll content was affected by temperature levels, species, and their interaction. For *Q. mongolica*, seedlings at +4°C treatment had a higher chlorophyll content than those at +2°C and

TABLE 2 Summary of statistics (F and P values).

	F	*P*	F	*P*	F	*P*	F	*P*	F	*P*	F	*P*
	RCD_{inc}		**H_{inc}**		**R_{inc}**		**Final biomass**		**Root- shoot ratio**		**SLW**	
Temperature	13.67	**0.00**	0.29	0.75	2.24	0.11	7.31	**0.00**	27.70	**0.00**	4.66	**0.01**
Precipitation	0.01	0.94	0.00	0.95	2.30	0.13	1.31	0.26	0.09	0.77	1.08	0.30
Species	21.52	**0.00**	3.82	**0.05**	0.26	0.61	101.55	**<0.0001**	293.84	**<0.0001**	27.93	**0.00**
T×P	0.54	0.59	1.31	0.27	0.34	0.71	0.12	0.89	1.79	0.17	0.23	0.79
T×S	12.39	**0.00**	0.30	0.74	5.01	**0.01**	1.52	0.22	2.94	0.06	2.37	0.10
P×S	0.35	0.56	0.75	0.39	4.87	**0.03**	0.10	0.75	0.16	0.69	2.33	0.13
S×T×P	0.66	0.52	0.90	0.41	1.59	0.21	0.30	0.74	3.40	**0.04**	0.13	0.88
	Ψ		Fv/Fm		Total chlorophyll		Chlorophyll a:b		N concentration		C:N ratio	
Temperature	0.82	0.44	28.05	**0.00**	78.02	**<0.0001**	93.83	**<0.0001**	5.81	**0.01**	4.03	**0.03**
Precipitation	2.54	0.11	0.84	0.36	1.19	0.28	0.94	0.34	0.96	0.34	1.60	0.22
Species	47.85	**0.00**	42.47	**0.00**	9.59	**0.00**	1.40	0.24	3.42	0.08	12.13	**0.00**
T×P	4.32	**0.02**	0.16	0.85	1.14	0.33	1.32	0.27	1.05	0.37	1.23	0.31
T×S	1.82	0.17	0.39	0.68	12.29	**0.00**	7.54	**0.00**	3.62	**0.04**	2.69	0.09
P×S	0.23	0.63	0.78	0.38	0.92	0.34	0.39	0.53	3.10	0.09	3.74	0.07
S×T×P	0.04	0.96	0.14	0.87	0.72	0.49	0.84	0.44	1.53	0.24	2.36	0.12

Differences in all variables were tested by using factorial ANOVA (F values) across the different experimental factors (temperature, T; species, S; precipitation, P). Significant results were in bold. RCD_{inc}, mean periodic increment of root collar diameter (RCD); H_{inc}, mean periodic increment of height; R_{inc}, mean periodic increment of maximum root length; SLW, specific leaf weight.

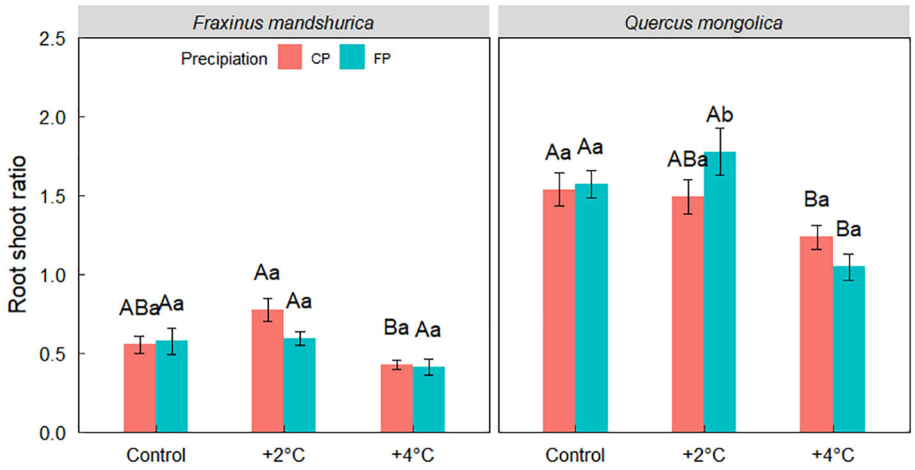

FIGURE 3
The root-shoot ratio of *Quercus mongolica* and *Fraxinus mandschurica* seedlings across the temperature (control; +2°C; +4°C) and irrigating (current precipitation, CP; future precipitation, FP) treatments. The data were presented as the mean ± S.E. Different capital letters indicated significant differences ($P<0.05$) among temperature treatments. Different lowercase letters indicated significant differences ($P<0.05$) between precipitation treatments in the same temperature condition and species.

control temperatures (Table 2). For *F. mandschurica*, significant differences in any temperature treatment on chlorophyll contents were observed, following the order: +4°C>+2°C>control temperature (Figure 5A). The ratio of chlorophyll a and chlorophyll b was affected by temperature levels and the interactions between temperature and species, showing that seedlings in +4°C had a lower ratio of chlorophyll a and chlorophyll b than those in +2°C and control treatments for two species (Figure 5B).

Foliar nitrogen concentration differed between temperatures and temperature × species interaction. For *F. mandschurica*, nitrogen concentration under +4°C treatment was greatly more than that under +2°C and control treatments (Figure 5C). C:N differed among temperature treatments and species (Figure 5D). Compared to the control treatment, C:N ratio of seedlings at the +4°C treatment significantly decreased by ~7.8% (Table 2).

Discussion

In this research, we evaluated the effects of warming and decreased precipitation on the seedling performance of *Q. mongolica* and *F. mandschurica*. Temperature manipulations increased root collar diameter, specific leaf weight, total biomass, chlorophyll contents, nitrogen concentration, and Fv/Fm, but reduced the ratio of chlorophyll a/b and the C:N ratio. In addition, temperature and precipitation had no pronounced effects on seedlings' height. Decreased precipitation only induced longer roots. When +2°C and precipitation acted concomitantly, an increased root-shoot ratio was observed. A temperature of +4°C and reduced precipitation induced more negative water potential. The two species did not respond to climatic manipulations in the same manner, with *F. mandschurica* responding more to warming and *Q. mongolica* responding to warming plus precipitation reduction. The different responses of the two species to climate change could provide us with more information about community dynamics in the future.

The effect of climatic change on seedling growth

The root collar diameter and height are the most common indicators in regeneration research (Nissinen et al., 2020). It is widely reported that moderate warming can stimulate plant growth (Noh et al., 2021). In our study, warming (both +2°C and +4°C) increased the root collar diameter of the seedlings (Figure 1A). Similar results were obtained by (Fisichelli et al., 2014; Han et al., 2015), who found a 3 °C increase in temperature promoted an increase in root collar diameter in *Pinus koraiensis* Siebold et Zuccarini and *Abies holophylla* Maxim, by 10% and 7%, respectively. The growth of root collar diameter is derived from the activity of cambium, which begins with the increase of seedling height in spring and continues to grow even after the seedling stops growing (Yun et al., 2016). The height growth is related to a stem originating from the previous bud, which starts with bud sprouting in spring and stops with budburst in early spring

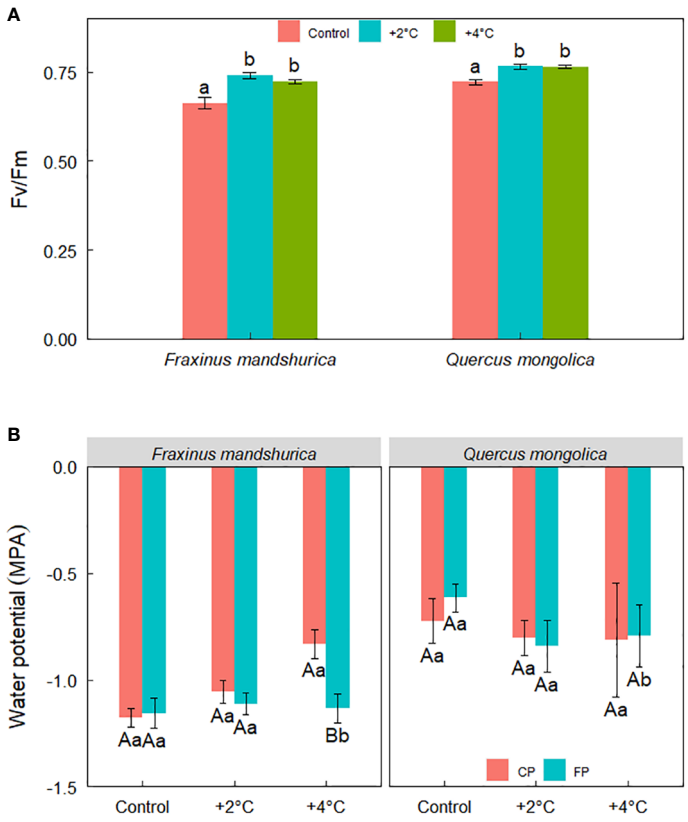

FIGURE 4
Fv/Fm for different species growing under the three temperatures (control; +2°C; +4°C) **(A)** and water potential across temperatures, precipitation treatments, and species **(B)**. The data were presented as the mean ± S.E. Different lowercase letters indicated significant differences (P<0.05) between temperature treatments in the same species for Fv/Fm. Different lowercase letters indicated significant differences (P<0.05) between precipitation treatments at the same species and temperature level while different capital letters indicated significant differences (P<0.05) between temperature treatments in the same species and precipitation level for water potential.

(Kramer and Kozlowski, 1979). According to our results, warming had a positive effect on the root collar diameter of the seedlings while there was no obvious difference detected in seedling height among temperature treatments. The difference in the origination of root collar diameter and height might result in their inconsistent response to warming. We cultivated seedlings from June when the stem had stopped growing. Therefore, a response in seedling height would be expected to early spring and long-term warming. For example, the total heights of Silver birch (*Betula pendula* Roth.) and Scots pine (*Pinus sylvestris* L.), seedlings under the warming treatment were greater than under ambient environments after two growing seasons, while there were no differences observed during the first growing season (Nissinen et al., 2020). These outcomes speculate that seedling height does not immediately respond to climate alterations, at least in the short term. Height and root collar diameter do not represent the seedling growth performance due to lateral extension growth (Lu et al., 2018). Since the carbon storage of plants could be characterized by biomass, which is a better indicator of growth variations to environmental change. *F. mandschurica* had higher biomass under the +2°C and +4°C treatments than the control. The results were supported by (Prieto et al., 2009), who showed that warming increased the growth and total biomass of *Pinus halepensis* L. Increased biomass with warming might be owing to photosynthesis enhancement in the study areas (Slot et al., 2018). Our results imply that biomass was sensitive to climate variations (e.g., temperature). We hypothesized that drought-tolerant species like *Q. mongolica* could be more adapted to future climate changes than *F. mandschurica* (hypothesis 2). Our findings demonstrate the increase in root collar and biomass was consistent with the opinion that warming could promote growth but disagree with hypothesis 2, that there would be a greater growth increase in *F. mandschurica* compared to *Q. mongolica*.

Trees could enhance resource efficiency by adjusting portioning to different organs of biomass to adapt to conditions (Chmura et al., 2017). However, the response of specific species to

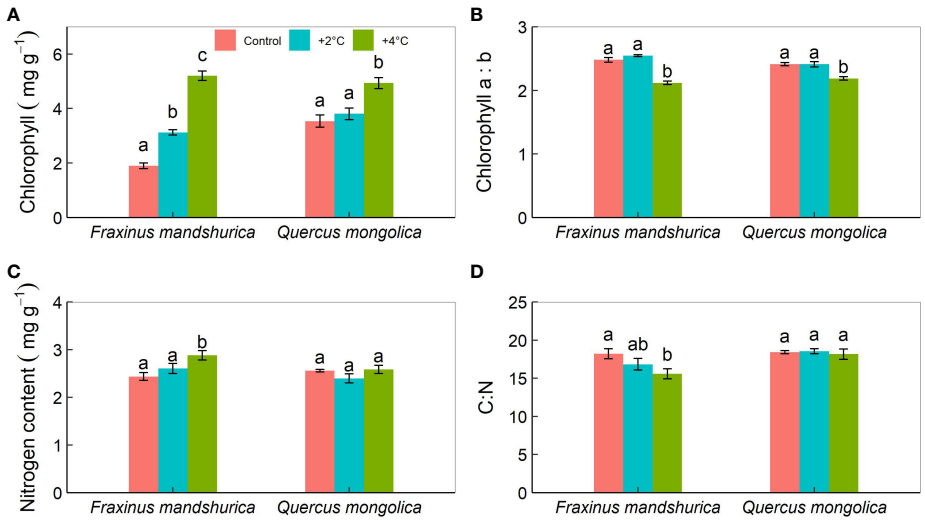

FIGURE 5
Total chlorophyll content **(A)**, the ratio of chlorophyll a:b **(B)**, nitrogen content **(C)**, and the ratio of C:N **(D)** in leaves for different species growing under the three temperatures (control; +2°C; +4°C). The data were presented as the mean ± S.E. Different lowercase letters indicated significant differences (P<0.05) between temperature treatments for the same species.

changed environmental conditions is still unclear. Warming and precipitation reduction might have a contrasting effect on the biomass allocation pattern, depending on the trade-off mechanism for the adaption to temperature and the acquisition of water. In our case, *Q. mongolica* under the +4 °C condition had a lower root-shoot ratio than under +2°C and control conditions, and the same trend was found in *F. mandschurica*, which indicates that +4°C improves above-ground carbon storage for the two species. Moreover, combined with seedlings' growth, warming might promote seedlings' growth by increasing the allocation of carbon aboveground (Noh et al., 2020). Under +2°C, *Q. mongolica* from FP had a higher root-shoot ratio than seedlings from CP. This increase in the proportion of biomass allocated to the root could enhance the resistance of *Q. mongolica* to drought and induce more imbalance in water ecology (Grossnickle, 2012). Furthermore, this demonstrates that *Q. mongolica* is more sensitive to decreased soil moisture than *F. mandschurica*. In addition, root length is a paramount trait that is required to obtain water and nutrient resources in deeper soil layers (Kuster et al., 2012). The longer root of *Q. mongolica* with future precipitation alterations indicates that the root performance of *Q. mongolica* is consistent with the distribution of soil moisture. However, warming only affected the root length of *F. mandschurica*. Therefore, our results do not support that warming alleviates the effects of precipitation reduction (hypothesis 1). Numerous studies confirmed that oaks are drought-tolerant species with expanding their distribution in drier environments (Hu et al., 2013), and our results support that drought-tolerant species like *Q. mongolica* would expand their competitive advantage in future arid environments rather than warming environments (hypothesis 2).

Leaf traits and particularly specific leaf weight (SLW) are considered highly informative (Scheepens et al., 2010), as SLW reflects the capacity of plants' carbon assimilation. In general, SLW increases with greater photosynthesis and carbon accumulation (Grassi et al., 2001). For *F. mandschurica*, the seedlings exhibited a greater SLW in the +4°C environment than in the +2°C and control environments. Previous studies showed that warmer environments enhance photosynthesis and net primary productivity (Rustad et al., 2001; Wu et al., 2011), and our results supported the above view through the SLW change. Through the seedlings' growth performance, we overturn hypothesis 2 because *F. mandschurica* grew better than *Q. mongolica* in warming treatments.

Climatic change effect on seedling physiology

The Fv/Fm ratio is considered to show damage to the PSII reaction center and is a good indicator of the conversion efficiency of intrinsic energy in the PSII reaction center (Ismail et al., 2014). Fv/Fm showed a trend where seedlings from the two species in the +4°C and +2°C environments had higher values than the seedlings in the control environment. This indicates that warming might promote the activity of the PSII reaction center. In addition, the two warming treatments enhanced total chlorophyll content for both species, but only +4°C had an

obvious increase compared to the control for *Q. mongolica*. The elevated temperature often promotes the concentration of pigments, such as chlorophyll and other chemical tissues (An et al., 2017), thus we speculate that an increase of 4°C and 2°C might provide a near-optimal temperature range for chlorophyll synthesis and enhance the efficiency usage of radiation energy. *Q. mongolica* grows in warmer environments, such as ridges and sunny slopes, than *F. mandschurica*, thus *Q. mongolica* needs a higher temperature to synthesize chlorophyll than *F. mandschurica*. The increase in activity of the PSII reaction center and pigments might be two important reasons for the upregulation of photosynthesis under elevated temperatures during the growing season (Song et al., 2019). In our study, the chlorophyll a/b ratio decreased with temperature, indicating that chlorophyll b is more sensitive to warming than chlorophyll a. The chlorophyll a/b ratio reflects plants acclimatized to low-light environments (Wang et al., 2021). Therefore, in our study, the chlorophyll a/b ratio diminished with temperature suggesting that seedlings might not adapt to low light conditions in the warmer future. FP resulted in more negative water potential than CP for seedlings under the +4°C condition. This result indicates that the interaction of +4°C and precipitation reduction induces harsh conditions. Reduced precipitation provoked a decrease in water potential and an increase in root length but had no impact on seedling growth, which suggests that reduced precipitation does not limit the growth of seedlings for the two species. This phenomenon might result from the fact that the study site is in a humid region and decreased precipitation does not provoke a large reduction in soil moisture to limit growth.

The experimental warming reduced the foliar C/N ratio, and seedlings under the +4°C condition had a lower C/N ratio than under the control condition, which was mainly induced by a foliar nitrogen concentration increase, especially in *F. mandschurica*. Warming promotes soil nitrogen mineralization, thus increasing foliar nitrogen content (Xu et al., 2012). In Harvard forests, a 5 °C increase in soil temperature provided more available nitrogen for plants (Melillo et al., 2002). In addition, the biogeochemical hypothesis indicates that the increase of foliar N concentrate under elevated temperature is correlated to strengthened plant photosynthesis and increased plant nitrogen absorption capacity of (Zhang and Wang, 2021). The above two pathways could explain higher foliar nitrogen in a warming scenario. Further, 75% of foliar N concentrate is used for synthetic chlorophyll, which is supported by our results with higher chlorophyll contents under warming scenarios. Furthermore, a foliar N increase also confirmed an increase in the seedlings' growth and was associated with increases in foliar photosynthesis activity. The seedling's physiological performance in foliar N, Fv/Fm, and pigments are consistent with the fact that that warming promotes seedling growth. Furthermore, the physiological performances of *F. mandschurica* are better than *Q. mongolica* under the warming context, which suggests that *F. mandschurica* is more adapted to warming environments. Therefore, our results disagreed with hypothesis 2.

Conclusions

Evaluating the responses of coexisting species with contrasting functional traits to projected climate changes is paramount in predicting the regeneration patterns of tree species and community dynamics. Our results indicated that interspecific differences largely decided the seedlings' performance in future climatic conditions. *F. mandschurica* (a drought-intolerant species) seemed to be less sensitive to precipitation reduction, but have higher plasticity (e.g., SLW and foliar nitrogen content) in adapting to warming. A drought-tolerant species such as *Q. mongolica* actively accommodated precipitation reduction by increasing root length and inducing more negative water potential. In addition, warming promoted the seedling growth of the two species while reduced precipitation and warming with precipitation reduction merely induced traits related to the water balance in *Q. mongolica.* In the future, drought-tolerant species (e.g., *Q. mongolica*) might expand their range to drier (warming and precipitation co-occurrence) regions whereas *F. mandschurica* is better adaptative to warming environments. However, enclosed environments might underestimate the impacts of reduced precipitation and warming, and similar studies should be conducted in the field.

Data availability statement

The raw data supporting the conclusions of this article will be made available by the authors, without undue reservation.

Author contributions

QY conceived the ideas and designed the study. JY, JW, JX, and RL collected field data. JY analyzed the data and led the writing of first draft of manuscript. QY and JY substantially contributed to revising the manuscript. All authors contributed critically to the draft and gave final approval for publication.

Funding

This research was funded by the National Natural Science Foundation of China (U1808201), and the National Key R & D Program of China (2020YFA0608100).

Acknowledgments

We thank Prof. Jiaojun Zhu for his suggestions on the design of the study. We thank Miss Ting Zhang and Xinlei Yu for their help during the sample measurements. We thank Dr. Deliang Lu and Lining Song for their suggestions on the statistical analysis.

Conflict of interest

The authors declare that the research was conducted in the absence of any commercial or financial relationships that could be construed as a potential conflict of interest.

Publisher's note

All claims expressed in this article are solely those of the authors and do not necessarily represent those of their affiliated organizations, or those of the publisher, the editors and the reviewers. Any product that may be evaluated in this article, or claim that may be made by its manufacturer, is not guaranteed or endorsed by the publisher.

Supplementary material

The Supplementary Material for this article can be found online at: https://www.frontiersin.org/articles/10.3389/fpls.2022.946141/full#supplementary-material

References

An, J., Han, S., Chang, H., Park, M. J., Kim, S., Hwang, J., et al. (2017). Physiological and growth responses to experimental warming in first-year seedlings of deciduous tree species. *Turk. J. Agric. For.* 41, 175–182. doi: 10.3906/tar-1611-106

Arnon, D. I. (1949). Copper enzymes in isolated chloroplasts. polyphenoloxidase in *Beta vulgaris*. *Plant Physiol. (Rockv).* 24, 1–15. doi: 10.1104/pp.24.1.1

Buters, T., Belton, D., and Cross, A. T. (2019). Seed and seedling detection using unmanned aerial vehicles and automated image classification in the monitoring of ecological recovery. *Drones* 3, 53. doi: 10.3390/drones3030053

Chmura, D. J., Modrzynski, J., Chmielarz, P., and Tjoelker, M. G. (2017). Plasticity in seedling morphology, biomass allocation and physiology among ten temperate tree species in response to shade is related to shade tolerance and not leaf habit. *Plant Biol. (Stuttg).* 19, 172–182. doi: 10.1111/plb.12531

Dai, J., Liu, H., Wang, Y., Guo, Q., Hu, T., Quine, T., et al. (2020). Drought-modulated allometric patterns of trees in semi-arid forests. *Commun. Biol.* 3, 405. doi: 10.1038/s42003-020-01144-4

Díaz-Barradas, M. C., Zunzunegui, M., Ain-Lhout, F., Jáuregui, J., Boutaleb, S., Álvarez-Cansino, L., et al. (2010). Seasonal physiological responses of argania spinosa tree from Mediterranean to semi-arid climate. *Plant Soil.* 337, 217–231. doi: 10.1007/s11104-010-0518-8

Fisichelli, N., Wright, A., Rice, K., Mau, A., Buschena, C., and Reich, P. B. (2014). First-year seedlings and climate change: Species-specific responses of 15 north American tree species. *Oikos.* 123, 1331–1340. doi: 10.1111/oik.01349

Gao, S., Wang, Y., Yu, S., Huang, Y., Liu, H., Chen, W., et al. (2020). Effects of drought stress on growth, physiology and secondary metabolites of two Adonis species in northeast China. *Sci. Hortic-Amsterdam.* 259, 108795. doi: 10.1016/j.scienta.2019.108795

Grassi, G., Colom, M. R., and Minotta, G. (2001). Effects of nutrient supply on photosynthetic acclimation and photoinhibition of one-year-old foliage of. *Picea abies.* 111, 245–254. doi: 10.1034/j.1399-3054.2001.1110217.x

Grossnickle, S. C. (2012). Why seedlings survive: Influence of plant attributes. *New For.* 43, 711–738. doi: 10.1007/s11056-012-9336-6

Han, S. H., Kim, S., Chang, H., and Li, G. (2019). Increased soil temperature stimulates changes in carbon, nitrogen, and mass loss in the fine roots of *Pinus koraiensis* under experimental warming and drought. *Turk. J. Agric. For.* 43, 80–87. doi: 10.3906/tar-1807-162

Han, S., Lee, S. J., Yoon, T. K., Han, S. H., Lee, J., Kim, S., et al. (2015). Species-specific growth and photosynthetic responses of first-year seedlingsof four coniferous species to open-field experimental warming. *Turk. J. Agric. For.* 39, 342–349. doi: 10.3906/tar-1408-117

Hodson, R. (2017). Climate change. *Nature.* 550, S53. doi: 10 1038/550S53a

Hu, B., Simon, J., and Rennenberg, H. (2013). Drought and air warming affect the species-specific levels of stress-related foliar metabolites of three oak species on acidic and calcareous soil. *Tree Physiol.* 33, 489–504. doi: 10.1093/treephys/tpt025

IPCC (2013). *Climate change 2013: The physical science basis: Working group I contribution to the fifth assessment report of the intergovernmental panel on climate change* (Cambridge, UK: Cambridge University Press).

Ismail, I. M., Basahi, J. M., and Hassan, I. A. (2014). Gas exchange and chlorophyll fluorescence of pea (*Pisum sativum* l.) plants in response to ambient ozone at a rural site in Egypt. *Sci. Total Environ.* 497-498, 585–593. doi: 10.1016/j.scitotenv.2014.06.047

Kardol, P., Bezemer, T. M., and van der Putten, W. H. (2006). Temporal variation in plant-soil feedback controls succession. *Ecol. Lett.* 9, 1080–1088. doi: 10.1111/j.1461-0248.2006.00953.x

Kramer, P. J., and Kozlowski, T. T. (1979). Physiology of Woody Plants. New York: Academic Press. 811 p.

Kueppers, L. M., Conlisk, E., Castanha, C., Moyes, A. B., Germino, M. J., de Valpine, P., et al. (2017). Warming and provenance limit tree recruitment across and beyond the elevation range of subalpine forest. *Glob Chang Biol.* 23, 2383–2395. doi: 10.1111/gcb.13561

Kuster, T. M., Arend, M., Günthardt-Goerg, M. S., and Schulin, R. (2012). Root growth of different oak provenances in two soils under drought stress and air warming conditions. *Plant Soil.* 369, 61–71. doi: 10.1007/s11104-012-1541-8

Lenth, R. V. (2016). Least-squares means: the R Package lsmeans. *J.Stat. Softw.* 69, 1–33. doi: 10.18637/jss.v069

Liu, Y. Y., Song, J., Wang, M., Li, N., Niu, C. Y., and Hao, G. Y. (2015). Coordination of xylem hydraulics and stomatal regulation in keeping the integrity of xylem water transport in shoots of two compound-leaved tree species. *Tree Physiol.* 35, 1333–1342. doi: 10.1093/treephys/tpv061

Li, Y., Zhou, G., and Liu, J. (2017). Different growth and physiological responses of six subtropical tree species to warming. *Front. Plant Sci.* 8, 1511 doi: 10.3389/fpls.2017.01511

Lloret, F., Peñuelas, J., Prieto, P., Llorens, L., and Estiarte, M. (2009). Plant community changes induced by experimental climate change: Seedling and adult species composition. *Perspect. Plant Ecol.* 11, 53–63. doi: 10.1016/j.ppees.2008.09.001

Lu, D., Wang, G. G., Yan, Q. L., Gao, T., and Zhu, J. J. (2018). Effects of gap size and within-gap position on seedling growth and biomass allocation: Is the gap partitioning hypothesis applicable to the temperate secondary forest ecosystems in northeast China? *For Ecol. Manage.* 429, 351–362. doi: 10.1016/j.foreco.2018.07.031

Lyons, C. L., Branfireun, B. A., McLaughlin, J., and Lindo, Z. (2020). Simulated climate warming increases plant community heterogeneity in two types of boreal peatlands in north–central Canada. *J. Veg Sci.* 31, 908–919. doi: 10.1111/jvs.12912

Matías, L., Castro, J., Villar-Salvador, P., Quero, J. L., and Jump, A. S. (2016). Differential impact of hotter drought on seedling performance of five ecologically distinct pine species. *Plant Ecol.* 218, 201–212. doi: 10.1007/s11258-016-0677-7

Melillo, J. M., Steudler, P. A., Aber, J. D., Newkirk, K., Lux, H., Bowles, F. P., et al. (2002). Soil warming and carbon-cycle feedbacks to the climate system. *Science.* 298, 2173–2176. doi: 10.1126/science.1074153

Milbau, A., Vandeplas, N., Kockelbergh, F., and Nijs, I. (2017). Both seed germination and seedling mortality increase with experimental warming and fertilization in a subarctic tundra. *AoB Plants.* 9, plx040. doi: 10.1093/aobpla/plx040

Morin, X., Roy, J., Sonie, L., and Chuine, I. (2010). Changes in leaf phenology of three European oak species in response to experimental climate change. *New Phytol.* 186, 900–910. doi: 10.1111/j.1469-8137.2010.03252.x

Nissinen, K., Virjamo, V., Kilpeläinen, A., Ikonen, V. P., Pikkarainen, L., Ärväs, I. L., et al. (2020). Growth responses of boreal scots pine, Norway spruce and silver birch seedlings to simulated climate warming over three growing seasons in a controlled field experiment. *Forests.* 11, 943. doi: 10.3390/f11090943

Nogués-Bravo, D., Araújo, M. B., Errea, M. P., and Martínez-Rica, J. P. (2007). Exposure of global mountain systems to climate warming during the 21st century. *Global Environ. Change* 17, 420–428. doi: 10.1016/j.gloenvcha.2006.11.007

Noh, N. J., Crous, K. Y., Li, J., Choury, Z., Barton, C. V. M., Arndt, S. K., et al. (2020). Does root respiration in Australian rainforest tree seedlings acclimate to experimental warming? *Tree Physiol.* 40, 1192–1204. doi: 10.1093/treephys/tpaa056

Noh, N. J., Kim, G. J., Son, Y., and Cho, M. S. (2021). Early growth responses of *Larix kaempferi* (Lamb.) carr. seedling to short-term extreme climate events in summer. *Forests.* 12, 1595. doi: 10.3390/f12111595

Piao, S., Ciais, P., Huang, Y., Shen, Z., Peng, S., Li, J., et al. (2010). The impacts of climate change on water resources and agriculture in China. *Nature.* 467, 43–51. doi: 10.1038/nature09364

Prieto, P., Peñuelas, J., Llusià, J., Asensio, D., and Estiarte, M. (2009). Effects of experimental warming and drought on biomass accumulation in a Mediterranean shrubland. *Plant Ecol.* 205, 179–191. doi: 10.1007/s11258-009-9608-1

Reich, P. B., Sendall, K. M., Stefanski, A., Rich, R. L., Hobbie, S. E., and Montgomery, R. A. (2018). Effects of climate warming on photosynthesis in boreal tree species depend on soil moisture. *Nature.* 562, 263–267. doi: 10.1038/s41586-018-0582-4

Richter, S., Kipfer, T., Wohlgemuth, T., Calderon, Guerrero., C., Ghazoul, J., and Moser, B. (2012). Phenotypic plasticity facilitates resistance to climate change in a highly variable environment. *Oecologia.* 169, 269–279. doi: 10.1007/s00442-011-2191-x

Rodgers, V. L., Smith, N. G., Hoeppner, S. S., and Dukes, J. S. (2018). Warming increases the sensitivity of seedling growth capacity to rainfall in six temperate deciduous tree species. *AoB Plants.* 10, ply003. doi: 10.1093/aobpla/ply003

Rustad, L., Campbell, J., Marion, G., Norby, R., Mitchell, M., Hartley, A., et al. (2001). A meta-analysis of the response of soil respiration, net nitrogen mineralization, and aboveground plant growth to experimental ecosystem warming. *Oecologia.* 126, 543–562. doi: 10.1007/s004420000544

Scheepens, J. F., Frei, E. S., and Stocklin, J. (2010). Genotypic and environmental variation in specific leaf area in a widespread alpine plant after transplantation to different altitudes. *Oecologia.* 164, 141–150. doi: 10.1007/s00442-010-1650-0

Slot, M., Winter, K., and Timothy, Paine, C. E. (2018). High tolerance of tropical sapling growth and gas exchange to moderate warming. *Funct. Ecol.* 32, 599–611. doi: 10.1111/1365-2435.13001

Song, X., Zhou, G., Ma, B. L., Wu, W., Ahmad, I., Zhu, G., et al. (2019). Nitrogen application improved photosynthetic productivity, chlorophyll fluorescence, yield and yield components of two oat genotypes under saline conditions. *Agronomy.* 9, 115. doi: 10.3390/agronomy9030115

Taeger, S., Sparks, T. H., and Menzel, A. (2015). Effects of temperature and drought manipulations on seedlings of scots pine provenances. *Plant Biol. (Stuttg).* 17, 361–372. doi: 10.1111/plb.12245

Tuna, A. L., Kaya, C., Dikilitas, M., and Higgs, D. (2008). The combined effects of gibberellic acid and salinity on some antioxidant enzyme activities, plant growth parameters and nutritional status in maize plants. *Environ. Exp. Bot.* 62, 1–9. doi: 10.1016/j.envexpbot.2007.06.007

Wang, Y. B., Huang, R. D., and Zhou, Y. F. (2021). Effects of shading stress during the reproductive stages on photosynthetic physiology and yield characteristics of peanut (*Arachis hypogaea* linn.). *J. Integr. Agr.* 20, 1250–1265. doi: 10.1016/s2095-3119(20)63442-6

Wu, Z., Dijkstra, P., Koch, G. W., PeÑUelas, J., and Hungate, B. A. (2011). Responses of terrestrial ecosystems to temperature and precipitation change: A meta-analysis of experimental manipulation. *Glob Chang Biol.* 17, 927–942. doi: 10.1111/j.1365-2486.2010.02302.x

Xiao, D. R., Yan, P. F., Zhan, P. F., Zhang, Y., Liu, Z. Y., Tian, K., et al. (2019). Temperature variations in simulated warming alter photosynthesis of two emergent plants in plateau wetlands, China. *Ecosphere.* 10, e02792. doi: 10.1002/ecs2.2729

Xu, Z., Yin, H., Xiong, P., Wan, C., and Liu, Q. (2012). Short-term responses of *Picea asperata* seedlings of different ages grown in two contrasting forest ecosystems to experimental warming. *Environ. Exp. Bot.* 77, 1–11. doi: 10.1016/j.envexpbot.2011.10.011

Yang, Y., Wang, G., Yang, L., and Guo, J. (2012). Effects of drought and warming on biomass, nutrient allocation, and oxidative stress in*Abies fabri* in eastern Tibetan plateau. *J. Plant Growth Regul.* 32, 298–306. doi: 10.1007/s00344-012-9298-0

Yu, L. Z., Liu, L. F., Wang, X. G., Sun, Y. R., Kong, X. W., Gao, T., et al. (2017). Discussion on the protection and restoration technology of secondary forest ecosystems in northeast China. *Chin. J. Ecology.* 36, 3243–3248. doi: 10.13292/j.1000-4890.201711.024

Yun, S. J., Han, S., Han, S. H., Kim, S., Li, G., Park, M., et al. (2016). Short-term effects of warming treatment and precipitation manipulation on the ecophysiological responses of *Pinus densiflora* seedlings. *Turk. J. Agric. For.* 40, 621–630. doi: 10.3906/tar-1511-68

Zhang, X., and Wang, S. (2021). Joint control of plant ecological strategy by climate, regeneration mode, and ontogeny in northeastern Chinese forests. *Ecol. Evol.* 11, 6703–6715. doi: 10.1002/ece3.7522

Zhao, D., Zhu, Y., Wu, S., and Lu, Q. (2022). Simulated response of soil organic carbon density to climate change in the northern Tibet permafrost region. *Geoderma.* 405, 115455. doi: 10.1016/j.geoderma.2021.115455

Zheng, Y., Li, F., Hao, L., Yu, J., Guo, L., Zhou, H., et al. (2019). Elevated CO_2 concentration induces photosynthetic down-regulation with changes in leaf structure, non-structural carbohydrates and nitrogen content of soybean. *BMC Plant Biol.* 19, 255. doi: 10.1186/s12870-019-1788-T

Zhu, Y., Chen, C., Guo, Y., Fu, S., and Chen, H. Y. H. (2020). Linking leaf-level morphological and physiological plasticity to seedling survival and growth of introduced Canadian sugar maple to elevated precipitation under warming. *For Ecol. Manage.* 457, 117758. doi: 10.1016/j.foreco.2019.117758

Zhu, J. J., Yan, Q., Yu, L. Z., Zhang, J. X., Yang, K., and Gao, T. (2018). Support ecological restoration and sustainable management of forests in northeast China based on research of forest ecology and demonstrations. *Bull. Chin. Acad. Sci.* 33, 107–118. doi: 10.16418/j.issn.1000-3045.2018.01.012

frontiers | Frontiers in Plant Science

TYPE Original Research
PUBLISHED 01 December 2022
DOI 10.3389/fpls.2022.1003266

OPEN ACCESS

EDITED BY
Iftikhar Ali,
State Key Laboratory of Molecular Developmental Biology (CAS), China

REVIEWED BY
Atsushi Kume,
Kyushu University, Japan
Feng Xu,
Yangtze University, China

*CORRESPONDENCE
Xiaoke Wang
wangxk@rcees.ac.cn

SPECIALTY SECTION
This article was submitted to Plant Abiotic Stress, a section of the journal Frontiers in Plant Science

RECEIVED 26 July 2022
ACCEPTED 28 October 2022
PUBLISHED 01 December 2022

CITATION
Cui B, Wang X, Su Y, Gong C, Zhang D, Ouyang Z and Wang X (2022) Responses of tree growth, leaf area and physiology to pavement in *Ginkgo biloba* and *Platanus orientalis*. *Front. Plant Sci.* 13:1003266. doi: 10.3389/fpls.2022.1003266

Responses of tree growth, leaf area and physiology to pavement in *Ginkgo biloba* and *Platanus orientalis*

Bowen Cui[1,2], Xuming Wang[3], Yuebo Su[4], Cheng Gong[1], Danhong Zhang[1,2], Zhiyun Ouyang[1,2] and Xiaoke Wang[1,2,5]*

[1]State Key Laboratory of Urban and Regional Ecology, Research Center for Eco-Environmental Sciences, Chinese Academy of Sciences, Beijing, China, [2]College of Resources and Environment, University of Chinese Academy of Sciences, Beijing, China, [3]Key Laboratory for Subtropical Mountain Ecology (Ministry of Science and Technology and Fujian Province Funded), College of Geographical Sciences, Fujian Normal University, Fuzhou, China, [4]Shenzhen Academy of Environmental Sciences, Shenzhen, China, [5]Beijing Urban Ecosystem Research Station, Chinese Academy of Sciences, Beijing, China

Trees growing on paved lands endure many environmental stresses in the urban environment. However, the morphological and physiological mechanisms underlying tree adaptation to pavement in the field are less known. In this study, we investigated 40 sites where *Ginkgo biloba* and *Platanus orientalis* grow on adjacent pairs of paved and vegetated plots in parks and roadsides in Beijing, China. Relative to the vegetated land, the mean increments in the diameter at breast height and height in the paved land were significantly decreased by 44.5% and 31.9% for *G. biloba* and 31.7% and 60.1% for *P. orientalis*, respectively. These decreases are related to both the decrease in assimilation products due to the reductions in leaf area, leaf total nitrogen content, and chlorophyll content and the increase in energy cost due to the synthesis of more soluble sugar and proline for mitigating stress. The increase in leaf soluble sugar content, proline content, and $\delta^{13}C$ indicated that trees could adapt to the paved land through the regulation of osmotic balance and the enhancement of water-use efficiency. Piecewise structural equation models showed that trees growing on the paved land are stressed by compounding impacts of the leaf morphological and physiological changes. Therefore, it is critical to explore the complex response of plant morphological and physiological traits to the pavement-induced stress for improving tree health in urban greening.

KEYWORDS

urban trees, pavement, tree growth, leaf morphology and physiology, carbon isotopes

Introduction

Urban trees could provide multiple ecosystem services that are significantly beneficial to residents, such as improving air quality (Nowak et al., 2018), reducing noise pollution (Margaritis and Kang, 2017), increasing carbon sequestration (Nowak and Crane, 2002), and cooling air and surfaces (Armson et al., 2012) through shading effects and evaporative processes (Upreti et al., 2017; Wang et al., 2019). In recent years, urban tree planting programs have been carried on in many cities (Koesera et al., 2014), such as New York's Million Trees initiative (City of New York, 2011) and Beijing's Million Mu (Chinese unit of land area = 1/15 ha) Tree Planting initiative, to maximize and sustain ecological services (Pincetl et al., 2013). Because of the shortage of land available for tree planting in the urban context, paved lands such as roadside and public square have been deployed widely for planting more trees. However, the paved land does not favor plant growth because it alters soil microenvironments through increased soil surface and rhizospheric temperature (Arnfield, 2003; Tang et al., 2011), decreased rainwater infiltration (Lee and Heaney, 2003), aggravated soil compaction (Philip and Azlin, 2005), inhibited soil–air gas exchange (Feng et al., 2002; Balakina et al., 2005), reduced nutrient availability (Zhao et al., 2012), and changed energy and water balances (Morgenroth and Buchan, 2009). In general, the urban paved land is compacted with road rollers for smoothing. The compacted substrate could restrict plant growth by narrowing the soil pore spaces through which root tips extend and young roots expand radially (Grabosky et al., 2009). When compacted soils were encountered as they grow beyond the planting pits, the tree root growth was hindered due to the reduced soil porosity and water infiltration (Gregory et al., 2006; Pitt et al., 2008). Trees growing on the paved land have to endure a number of stresses [e.g., drought, heat, soil compaction, and pollution (Chen et al., 2017)] and disturbances [e.g., infrastructure installations and maintenance work, vandalism, and car accidents (Mullaney et al., 2015b)]. So, trees growing on the paved land often have high mortality rates, short average life spans, and low growth (Day and Amateis, 2011; Sand et al., 2018). Mueller and Day (2005) reported that *Nerium oleander* saplings planted in open lawn sites have better growth than those in sites surrounded by an impervious pavement. Chen et al. (2017) discovered that the pavement-induced rise in surface temperature decreased the survival and growth of the *Acer truncatum* sapling. Moser et al. (2017) found significant stem growth reductions in a highly paved public square compared with a contrasting more open and greener square. In contrast, some results showed that trees grow similarly or even greater under the paved soil than the non-paved one (Morgenroth, 2011; Morgenroth and Visser, 2011; Fini et al., 2017; Fini et al., 2022). Therefore, more investigations should be conducted to understand why trees respond inconsistently to the pavement.

The leaf, as the most important component that can transfer solar energy into chemical energy to support all life processes, is very plastic in response to environmental changes. The leaf can readily respond to stresses by alteration of its morphological and physiological traits. Mullaney et al. (2015b) explored the effects of different pavement types on the leaf total nitrogen (TN), stomatal conductance, and $\delta^{13}C$ of *Melaleuca quinquenervia* at different growth stages, which were all correlated with photosynthetic capacity. The pavement induced a reduction in chlorophyll content and an increment in malondialdehyde (MDA) in *A. truncatum* leaves (Chen et al., 2016). However, little is known about how the leaf morphological characteristics adapt to the pavement, including leaf area and specific leaf area (SLA), both of which can be strongly affected by environmental stress (Parkhurst and Loucks, 1972; Poorter et al., 2009).

In this study, two species of common urban trees, one gymnosperm, *Ginkgo biloba*, and one angiosperm, *Platanus orientalis*, are studied because they are the most widely planted urban trees (Dmuchowski et al., 2019; Vrinceanu et al., 2021) and highly resistant to drought (Roloff et al., 2009) at sites that each has adjacent pairs of paved and vegetated lands. The environmental factors, tree growth, and leaf morphological and physiological traits are investigated *in situ*. The following three questions will be answered: 1) Are there differences in soil temperature, moisture, and nutrient between paved and vegetated lands? 2) What changes in leaf morphological and physiological traits occur to adapt to the paved land? 3) Do *G. biloba* and *P. orientalis* respond differently to the paved land?

Materials and methods

Study sites

This study was conducted in the urban area of Beijing (39° 56′N, 116°20′E). It is the capital of China with more than 20 million residents and is characterized by a typical continental monsoon climate with distinct seasons. The mean annual precipitation and temperature are around 500 mm and 11°C–12°C, respectively. The soils are mixtures of original fluvo-aquic soil, fine sand, and clay and vary with site history and construction. The average saturated soil water content and hydraulic conductivity were 40.6% and 2.4×10^{-4} ($cm \cdot s^{-1}$), respectively (Xie et al., 1998).

In parks and roadsides within the 5th Ring Road of Beijing, spatially balanced study sites were selected (Figure 1A). A total of 40 sites were finally selected, of which 25 sites were for *G. biloba* that were located in 19 parks and six roadsides, and 15 sites were for *P. orientalis* that were located in 12 parks and three roadsides. At each site, one of two species of *G. biloba* and *P. orientalis* grows at adjacently paired plots: paved and vegetated lands (Figures 1B, C). Paved lands are mostly covered by marble or impervious brick and a small amount by pervious brick on

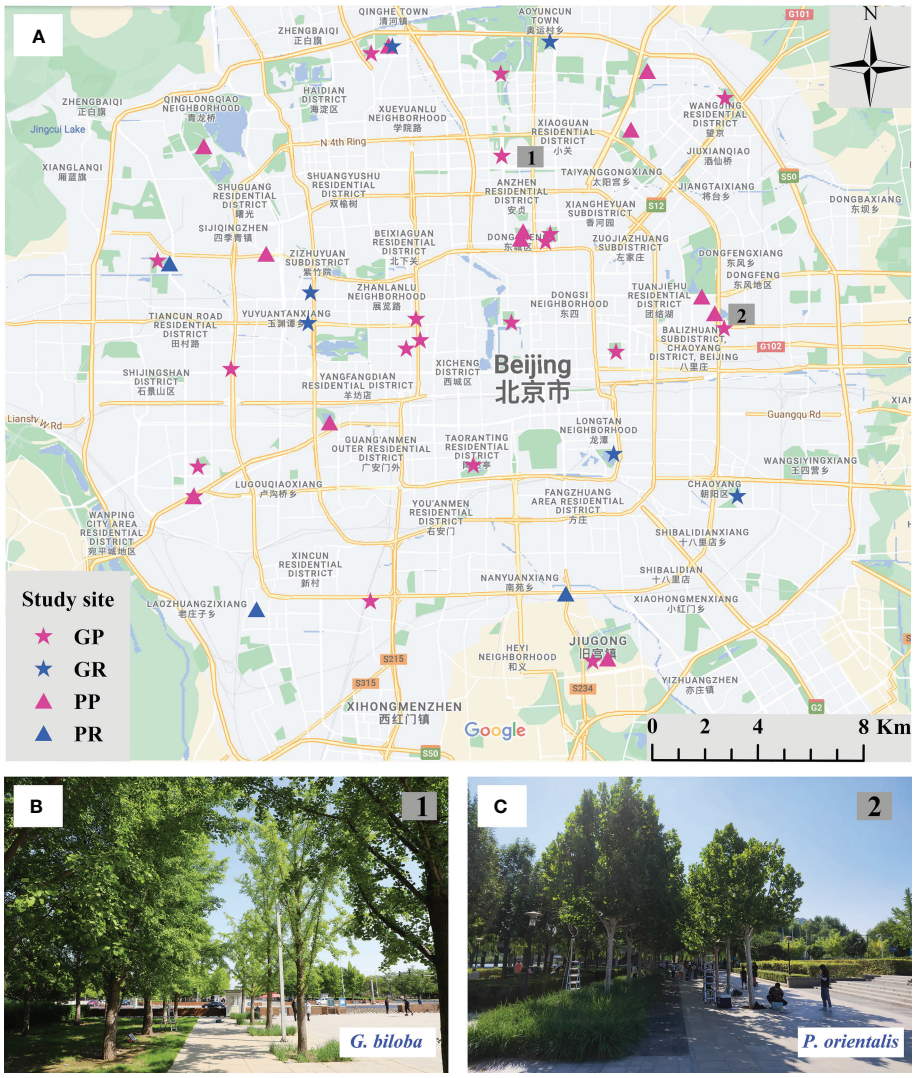

FIGURE 1
Location of the 40 study sites **(A)** for *Ginkgo biloba* at parks (GP) and at roadsides (GR) and for *Platanus orientalis* at parks (PP) and at roadsides (PR). Study sites of *G biloba* in Minzuyuan park **(B)** and *P. orientalis* in Honglingjin park **(C)**. At each study site, trees grow at adjacently paired plots: vegetated land and paved land.

which trees grow in pits usually in the size of 2 m × 2 m and 1 m × 1 m for park and roadside, respectively. Soils under the paved land were usually compacted for supporting the expected pavement loading. Vegetated lands are occupied by turf, shrub, or ruderal plants. Meanwhile, the trees at each site have the same age and are managed equally, and at each plot, there are more than three individuals of target trees. The tree ages varied from 20 to 40 years in different study sites for both *G. biloba* and *P. orientalis*, which were inferred from the size of the trees, including the diameter at breast height (DBH) and height, which are shown in Figure 2. Study sites where trees were pruned during the experiment were not counted in this study.

Field measurements

On each pair of paved and vegetated plots, we measured DBH, height, crown radius, and leaf area density (LAD; total one-sided leaf area per unit volume) of 560 individuals of *G. biloba* and *P. orientalis* in both years of 2018 and 2021 at the interval of 3 years. DBH was measured with a steel dendrometer band at 1.3 m aboveground, except in the case of buttressed stems, which were measured above the buttress to avoid overestimation (Condit, 1998). Height was determined as the height from the root collar to the top of the highest living bud using a Nikon Forestry Pro (Nikon Vision, Tokyo, Japan) laser

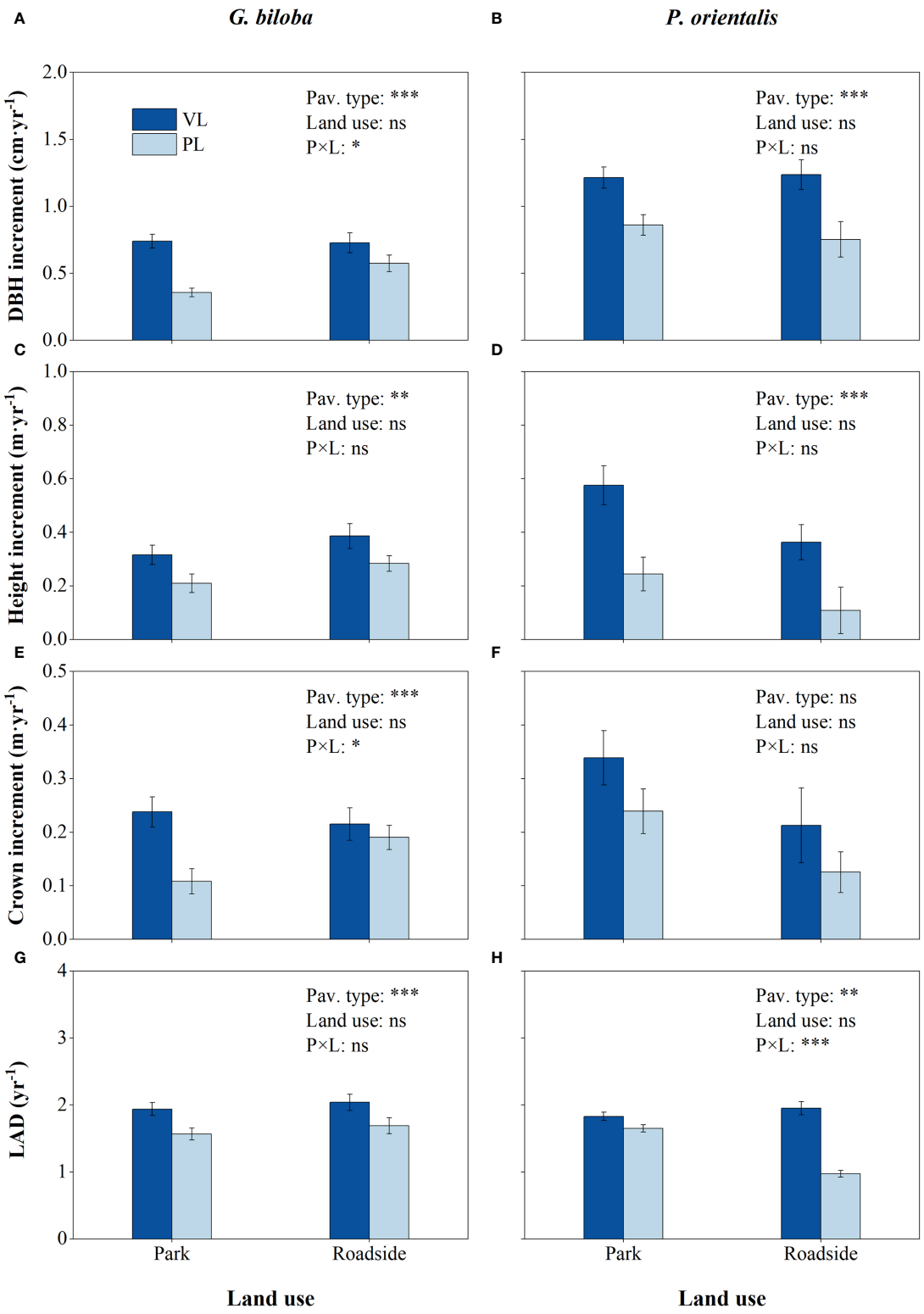

FIGURE 2
Results from the linear mixed-effects model (LMM) testing for the differences in the DBH increment **(A, B)**, height increment **(C, D)**, crown increment **(E, F)**, and leaf area density (LAD) **(G, H)** vs. the pavement type (VL, vegetated land; PL, paved land), land use (park and roadside), and their interactions. *, $P < 0.05$; **, $P < 0.01$; ***, $P < 0.001$; ns, not significant. Data represent mean ± SE.

rangefinder to the accuracy of 0.1 m. Crown radius was the average distance from the center of the trunk to the farthest point below branch tips in four directions, north, south, east, and west, which was measured using a linear tape. LAD was measured by the LAI-2000 Plant Canopy Analyzer (Li-Cor, Inc., Lincoln, NE, USA).

At each pit where trees were measured, the surface temperature, soil temperature, and soil moisture were remeasured during each investigation. The surface temperature and soil temperature were measured using an infrared thermometer (Optris MS, Optris GmbH, Berlin, Germany) and soil thermometer (SYS-TP101, SYS, Liaoning, China). The soil moisture was measured using TDR300 (Spectrum Technologies Inc., Plainfield, IL, USA).

Soil sampling and analysis

Soils were sampled at paired plots of 15 study sites (eight sites for *G. biloba* and seven sites for *P. orientalis*) in October 2021. In each plot, soil (0–20 cm) was collected at three randomly selected tree pits using a soil drill (4-cm diameter) and mixed as a composite soil sample. A total of 90 soil samples were collected. Soil samples were kept in a ziplock plastic bag. After transferring to the laboratory, soil samples were stored at -20°C for further analysis.

After removing litters, stones, and debris, the soil samples were homogenized by passing through a 10-mesh (2-mm) sieve and then air-dried at 22°C for 15 days. All samples were ground using a grinding machine and passed through a 200-mesh (0.075-mm) sieve. Grinding blade and sieves were carefully sterilized by using 75% alcohol and cleaned with water to avoid cross-contamination between samples. Samples of approximately 20 mg were used to analyze the elemental concentration. The TN and total carbon (TC) contents of the leaves were measured by an elemental analyzer (Vario EL III, Elementar, Hanau, Germany).

Leaf sampling and measurement

Leaves were sampled from 35 study sites in August 2021, including 21 sites for *G. biloba* and 14 sites for *P. orientalis*. Three healthy individual trees (i.e., three replicates) were selected at each plot. Branches were randomly removed using scissors from four directions (i.e., east, south, west, and north) in the central canopy of the selected tree. Sufficient fresh leaves were collected from the removed 3-year-old branches. There were three replicates of leaf samples for each plot. Leaf samples were kept in ziplock plastic bags and stored with ice bags in a portable cooler box, then transferred to the laboratory. Ten leaves were chosen randomly from each bag to measure the leaf area, leaf relative water content (RWC), and SLA. For the rest of these leaf samples, five leaves were selected randomly and cleaned to remove dust and debris using deionized water. The leaf edges for both species and leaf veins for *P. orientalis* were removed, then cut into strips about 1–2 mm wide using scissors. The leaf strips were kept frozen at -40°C until further processing.

In the laboratory, fresh leaves were first weighed, then the leaf area was measured using a leaf area meter (LI-3000C, Li-Cor, USA), and then leaves were taken to full water saturation for 24 h and weighed again. Finally, the leaves were dried for 72 h at 75°C and weighed again. SLA was calculated as the ratio of the leaf area to the dry leaf weight. RWC was calculated using the following equation:

$$\mathrm{RWC} = \frac{(Fresh\ \ leaf\ \ mass - Dry\ \ leaf\ \ mass)}{(Fully\ \ water - saturated\ \ leaf\ \ mass - Dry\ \ leaf\ \ mass)} \quad (1)$$

The chlorophyll and carotenoid contents were analyzed using the methods of Li et al. (2018). Fresh leaves (0.1 g) were treated with 10 ml of 95% ethanol solution in the dark for about 48 h at 4°C until completely fading. During the extraction of chlorophyll, the leaves were shaken 6–8 times a day to ensure complete extraction. The chlorophyll (a + b) (Chl a+b) content and carotenoid content were measured by using the specific absorption coefficients (664, 649, and 470 nm) following Lichtenthaler (1987).

The MDA content was analyzed according to the method of Heath and Packer (1968) based on the thiobarbituric acid (TBA) reaction. Fresh leaves (0.1 g) were mixed with 1 ml of 10% trichloroacetic acid (TCA) and ground to homogenate and then centrifuged at 8,000g for 10 min. The supernatant at 100 µl was mixed with 100 µl of 0.6% TBA. The mixture was incubated at 100°C for 60 min and quickly cooled on ice. Then, the solution was centrifuged at 10,000g for 10 min, and the MDA content was measured by using specific absorption coefficients (600, 532, and 450 nm). The MDA values were expressed as the percentage of fresh matter.

The soluble sugar content was determined using the anthrone method proposed by Yemm and Willis (1954). Approximately 0.1 g of fresh leaves were placed into a mortar and then ground to homogenate with 1 ml of distilled water. The solution was bathed for 10 min at 100°C and centrifuged for 10 min at 8,000g. The supernatant at 0.5 ml was diluted with distilled water to a final volume of 10 ml. Then, 40 µl of the solution was mixed with 40 µl distilled water, 20 µl anthrone reagent, and 200 µl of 98% H_2SO_4, and the solution was heated at 95°C for 10 min. The solution was cooled to room temperature, and the absorbance was determined spectrophotometrically at 620 nm. The soluble sugar content in the samples was calculated from a standard curve and on a fresh weight basis.

The free proline content was measured according to the method of Bates et al. (1973). Fresh leaves (0.1 g) were extracted in 1 ml of 3% sulfo-salicylic acid. Then, 0.25 ml of the filtrate was

mixed with 0.25 ml of acid ninhydrin followed by 0.25 ml of glacial acetic acid. All samples were incubated at 100°C for 60 min and cooled in an ice bath, and 0.5 ml of toluene was added to the solution and mixed vigorously. The chromophore-containing toluene was aspirated, and the absorbance was read at 520 nm on a microplate spectrophotometer (Spectramax 190, Molecular Devices, San Jose, CA, USA). The proline concentration in the samples was determined from a standard curve and calculated on a fresh weight basis.

The element content and carbon stable isotope were analyzed in leaves collected from 15 study sites, the same study sites as the soil samples. The leaf samples were dried at 75°C, ground, and stored in a desiccator until further analysis. The TN and TC contents were determined using the same method as for soil samples, with approximately 7 mg of leaf sample used in the analysis. Relative C stable isotope abundances were determined by combustion in an elemental analyzer (FLASH 2000, Thermo Fisher Scientific, Waltham, MA, USA) operated in continuous-flow mode and connected to an isotope ratio mass spectrometer (Delta V Advantage, Thermo Fisher Scientific, Waltham, MA, USA), with samples of ca. 1.3 mg used in the analysis. The carbon isotope composition ($\delta^{13}C$) was used to report the carbon isotope ratio of the sample relative to the standard and was determined by the following equation (2):

$$\delta^{13}C = \left(R_{sample}/R_{standard} - 1\right) \times 1000(‰) \quad (2)$$

where R is the ratio of the heavy to the light isotopes in the sample or the respective standard. The CO_2 standard gas calibration, control of reproducibility, and accuracy of the isotope abundance measurements in the leaf samples followed the protocol described by Gebauer and Schulze (1991).

The carbon isotope discrimination, $\Delta^{13}C$, was calculated following Farquhar et al. (1982):

$$\Delta^{13}C = \frac{(\delta_{air} - \delta_{leaf})}{(1 - \delta_{leaf}/1000)} \quad (3)$$

where δ_{leaf} is the $\delta^{13}C$ of the leaves and δ_{air} is the $\delta^{13}C$ of the atmospheric CO_2 and takes the value of -10‰ ± 0.9‰ according to the results of a site at 10-m altitude in Beijing during the vegetated season (Pang et al., 2016). Given that the leaf conductance to water vapor (k) is 1.6 times the conductance to CO_2, $\Delta^{13}C$ can be converted to intrinsic water-use efficiency (iWUE) as follows (Ma et al., 2021):

$$\text{iWUE} = \frac{c_a}{k} \cdot \frac{b - \Delta - f' \frac{\Gamma^*}{c_a}}{b - a_s + \frac{g_{sc}}{g_m} \cdot (b - a_m)} \quad (4)$$

where c_a is the CO_2 mole fraction in the atmosphere; b (29‰) and f (11‰) represent the fractionations due to Rubisco carboxylation and photorespiration, respectively; $a_b = 1 + b$, $a_f = 1 + f$, and $f' = fa_b/a_f$. Γ^* (35) is the CO_2 compensation point in the absence of mitochondrial respiration; a_s (4.4‰) is the fractionation during CO_2 diffusion through the stomata; g_{sc}/g_m (0.8) was the ratio between the stomatal conductance to CO_2 (g_{sc}) and the mesophyll conductance (g_m). a_m (1.8‰) is the fractionation associated with CO_2 dissolution and diffusions in mesophyll.

Statistical analyses

The effects of the pavement and land use types on the environmental factors, tree growth, and morphological and physiological traits were tested by a linear mixed-effects model (LMM) using the "lmer" function in LMER4 package (Bates et al., 2015). The pavement type and land use type were modeled as fixed factors and the site as a random effect to account for the nested sampling design. Tukey's honest significant difference (HSD) test was performed using the R package "emmeans" to test differences between the paved land and the unpaved land. Pearson's correlation coefficients were calculated between the tree growth and foliar traits to investigate the effect of the leaf physiological and morphological traits, $\delta^{13}C$, and leaf and soil nutrient content on the tree growth.

To determine whether the leaf morphological or physiological traits had a stronger link to the tree growth in *G. biloba* and *P. orientalis*, we performed structural equation models (SEMs) using the R packages "piecewiseSEM" (Lefcheck, 2016). Without an established framework for the leaf trait–growth relationships, we initially excluded these from the model framework. Fisher's C statistic was used as the goodness-of-fit, and the final model was considered to have an adequate overall fit to the observed data when the model had a nonsignificant C value ($P > 0.05$) (Shipley, 2009).

The data analysis was conducted using the R language (R, version 4.0, http://www.R-project.org).

Results

Environmental factors

There were significant differences in the surface temperature, soil temperature, and moisture between the paved land and the vegetated land in both parks and roadsides for both species except for the soil moisture of *G. biloba* in roadsides (Figure 3). Compared with the vegetated land, the surface temperatures in the paved land were 4.02°C and 3.15°C higher in parks and roadsides for *G. biloba*, respectively ($P< 0.001$), and 3.47°C and 5.60°C higher in parks and roadsides for *P. orientalis*, respectively ($P< 0.001$); the soil temperatures in the paved land were 2.00°C and 1.80°C higher at parks and roadsides for *G. biloba*, respectively ($P< 0.001$), and 0.92°C and 1.94°C higher at parks and roadsides for *P. orientalis*, respectively ($P< 0.001$); and the soil moistures in the paved land were 2.24% lower ($P< 0.001$)

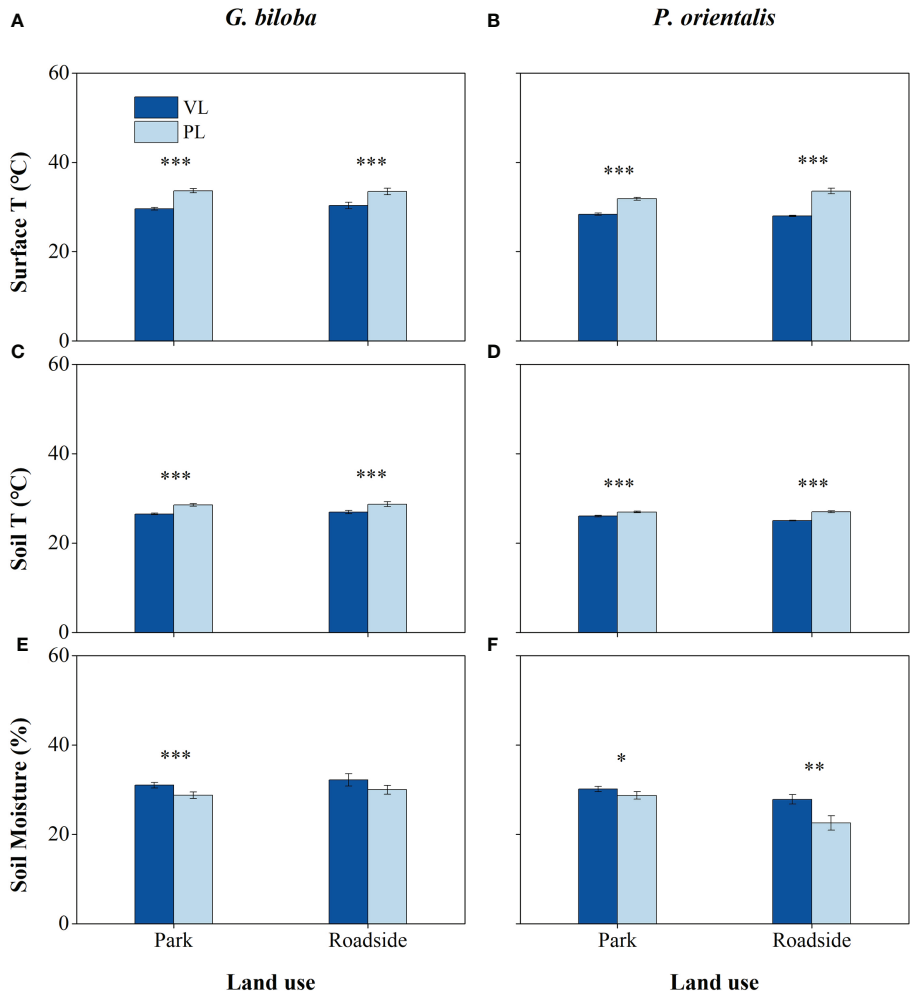

FIGURE 3
The surface temperature **(A, B)**, soil temperature **(C, D)**, and soil moisture **(E, F)** of the vegetated land (VL) and the paved land (PL) at the park and roadside for *Ginkgo biloba* and *Platanus orientalis*. Error bars indicate the standard error of the mean. *, **, *** indicate statistically significant differences between VL and PL at $P< 0.05$, $P< 0.01$, and $P< 0.001$, respectively.

in parks for *G. biloba* and 1.45% and 5.27% lower in parks and roadsides for *P. orientalis*, respectively ($P< 0.05$). No significant differences in the soil TN, TC, and C/N ratios were found between the paved land and the vegetated land in parks for both species (Figures 4A–C).

Tree growth

Relative to the vegetated land (Figure 2), the mean DBH increment, height increment, and LAD in the paved land were significantly decreased by 44.5%, 31.9%, and 18.9% for *G. biloba* and by 31.7%, 60.1%, and 18.7% for *P. orientalis*, respectively; the crown increment of *G. biloba* in the paved land significantly decreased by 44.9% ($P< 0.05$).

The effects of the pavement type on the tree growth varied with the land use type (Figure 2). Relative to the vegetated land, the reductions in the DBH increment in the paved land were significantly ($P< 0.05$) higher at the park than at the roadside for *G. biloba*, while the reduction in the LAD was significantly ($P< 0.001$) lower at the park than at the roadside for *P. orientalis*.

Leaf morphology and physiology

Compared with the vegetated land (Figure 5), the mean leaf area in the paved land significantly ($P< 0.001$) decreased by 20.0% and 21.6% for *G. biloba* and *P. orientalis*, respectively; the mean SLA in the paved land significantly ($P< 0.01$) decreased by 12.6% for *P. orientalis*.

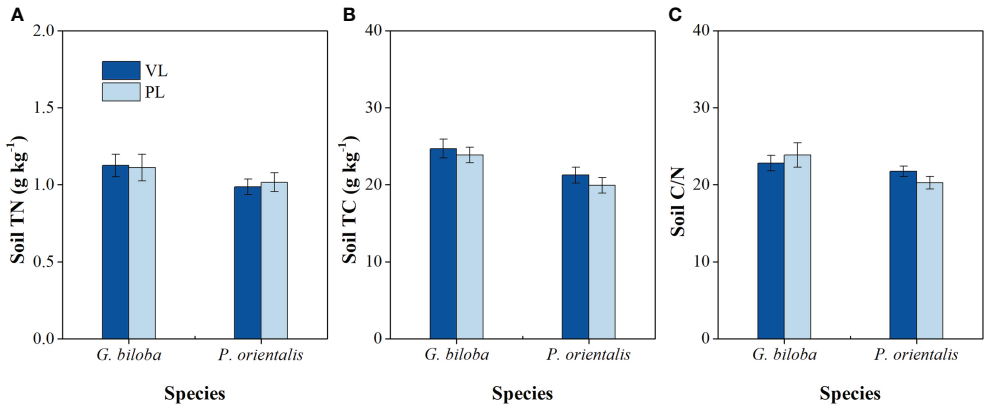

FIGURE 4
The differences in the soil total nitrogen (TN) **(A)**, soil total carbon (TC) **(B)**, and soil C/N ratio **(C)** between the vegetated land (VL) and the paved land (PL) at the park for *Ginkgo biloba* and *Platanus orientalis*. Error bars indicate the standard error of the mean.

Relative to the vegetated land (Figure 6), the mean Chl a+b content in the paved land significantly decreased by 22.2% and 19.6% for *G. biloba* and *P. orientalis*, respectively ($P< 0.001$), and the mean Chl/Car by 17.8% for *G. biloba*; the mean Chl a/b in the paved land significantly increased by 6.3% and 8.9% for *G. biloba* and *P. orientalis*, respectively.

Relative to the vegetated land (Figure 7), the mean soluble sugar content in the paved land significantly ($P< 0.01$) increased by 25.2% and 20.5% and proline content by 29.7% and 25.1% for *G. biloba* and *P. orientalis*, respectively; the mean MDA content in the paved land significantly increased by 14.4% for *G. biloba*.

Leaf total nitrogen and total carbon content and carbon isotope composition ($\delta^{13}C$)

Compared with the vegetated land, the leaf TN and C/N ratio in the paved land significantly decreased by 16.8% and 24.1% for *G. biloba*, respectively (Figures 8A, C); the $\delta^{13}C$ values in the paved land were 0.96‰ and 1.01‰ higher for *G. biloba* and *P. orientalis*, respectively; the iWUE values in the paved land were 10.9% and 11.3% higher for *G. biloba* and *P. orientalis*, respectively; and the $\Delta^{13}C$ values in the paved land were 1.01‰ and 1.06‰ lower for *G. biloba* and *P. orientalis*, respectively (Figures 8D–F).

Correlation between the tree growth and the foliar traits

At the parks, the tree growth was significantly related to the leaf area but not the leaf water content and SLA for *G. biloba* and *P. orientalis* ($P< 0.05$; Figures 9A, B). As for the leaf physiology, the tree growth was significantly positively associated with the chlorophyll but negatively with the soluble sugar, MDA, and proline for both species. The tree growth and $\delta^{13}C$ also showed a significantly positive correlation for both species ($P< 0.05$; Figures 9C, D). In addition, the leaf TN was significantly positively correlated with the tree growth for *G. biloba*.

Tree growth response to the pavement in relation to the leaf area and proline

Piecewise SEMs provide evidence that the response of the tree growth to the pavement can be negatively related to the leaf area indirectly through the proline content for *G. biloba*. Although there were no significantly direct relations of the pavement to the proline content in *G. biloba* (Figure 10), the proline content can be indirectly related to the pavement through the leaf area ($P< 0.05$; Figures 10A, C). The proline content was related to the DBH and height of *G. biloba* (Figures 9A, B). Therefore, the DBH of *G. biloba* can be inhibited by the leaf area directly and also indirectly through the proline content. The height of *G. biloba* was only indirectly affected by the leaf area through the proline content.

Discussion

Stresses of the paved land on the tree growth

Trees growing on the paved land were strongly inhibited. This study showed that the DBH increment and the height

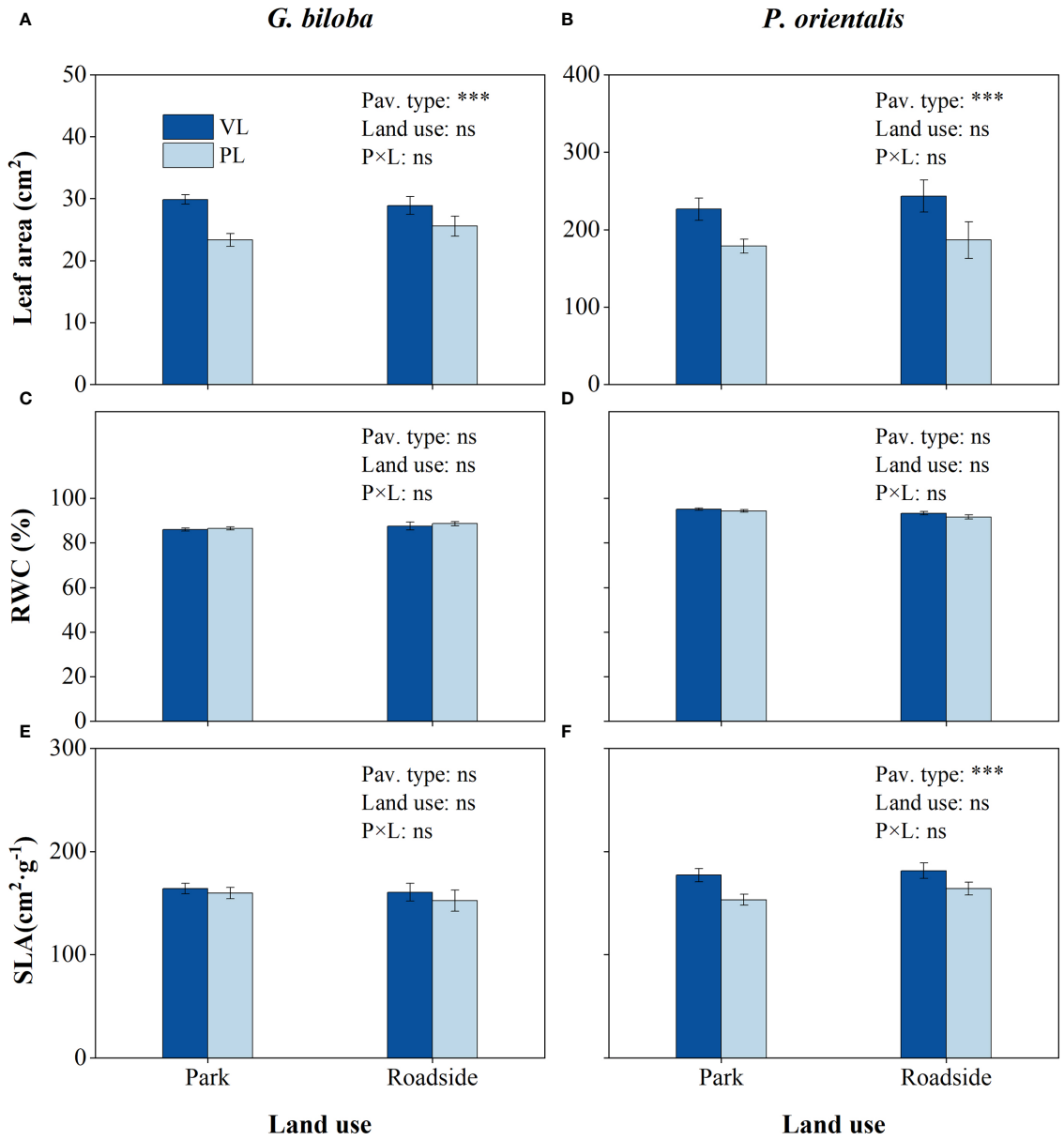

FIGURE 5
Results from the linear mixed-effects model (LMM) testing for the differences in leaf area **(A, B)**, relative water content (RWC) **(C,D)**, and specific leaf area (SLA) **(E, F)** vs. the pavement type (VL, vegetated land; PL, paved land), land use (park and roadside), and their interactions. ***, $P<$ 0.001; ns, not significant. Data represent mean ± SE.

increment significantly declined in the paved land, as widely observed in previous studies with different pavements (Sanders and Grabosky, 2014; Sand et al., 2018).

A higher LAD would block more amount of solar radiation and has a higher cooling effect on the surface temperature (Gillner et al., 2015). In addition, all materials of the paved surface in urban settings usually have a low albedo and thermal capacity, absorbing a large amount of solar radiation, and no evaporation can occur (Krayenhoff and Voogt, 2010; Fini et al., 2017), then the paved land heats up considerably. In conclusion, the paved land has a higher surface and soil temperature as shown in this study (Figure 3). The soil water balance mainly depends on the water input, soil evaporation, and plant transpiration (Daly and Porporato, 2005). The paved surface has low permeability (Chen et al., 2011; Pataki et al., 2011; Savi et al., 2015), preventing or delaying rainwater infiltration into

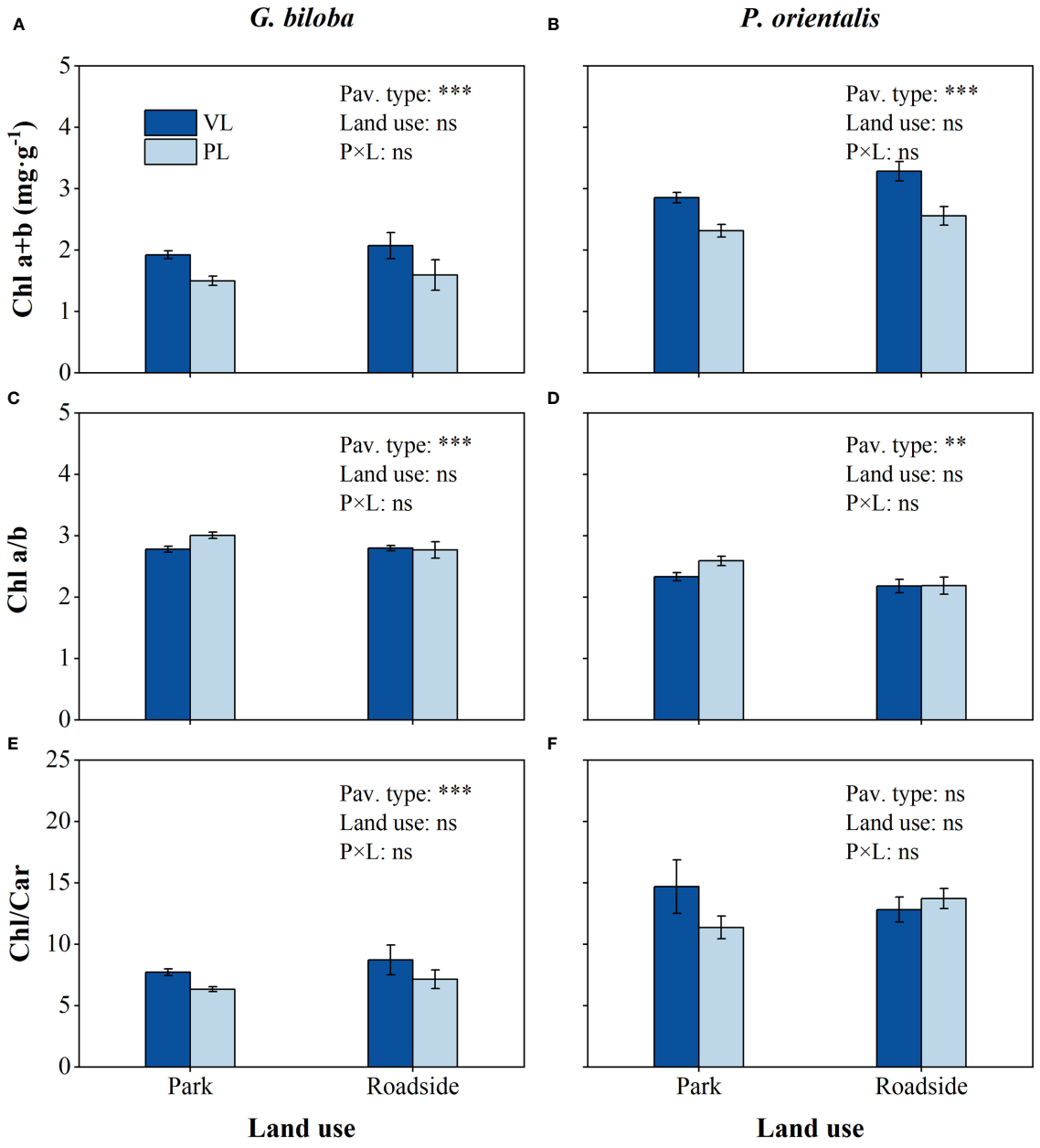

FIGURE 6
Results from the linear mixed-effects model (LMM) testing for the differences in the content of Chl a+b **(A, B)**, Chl a/b **(C, D)**, and Chl/Car **(E, F)** vs. the pavement type (VL, vegetated land; PL, paved land), land use (park and roadside), and their interactions. **, $P < 0.01$; ***, $P < 0.001$; ns, not significant. Data represent mean ± SE.

the soil. Therefore, the soil moisture under the paved land was lower than that under the vegetated land.

For most temperate tree species, the optimal temperature range for the root is 10°C–25°C (Pregitzer et al., 2000). The root growth and leaf conductance would be decreased when the soil temperature is greater than 30°C (Graves, 1994). A high soil temperature can reduce the soil and plant hydraulic conductance and water uptake (Kramer and Boyer, 1995) by increasing the water viscosity and membrane permeability and also by reducing the new fine root production (Rahman et al., 2014). Therefore, the pavement-induced high temperature might contribute to the reductions in tree DBH and height increment for *G. biloba* and *P. orientalis* on the paved land. In the continental climate with unevenly seasonal distribution in rainfall, such as Beijing, the soil

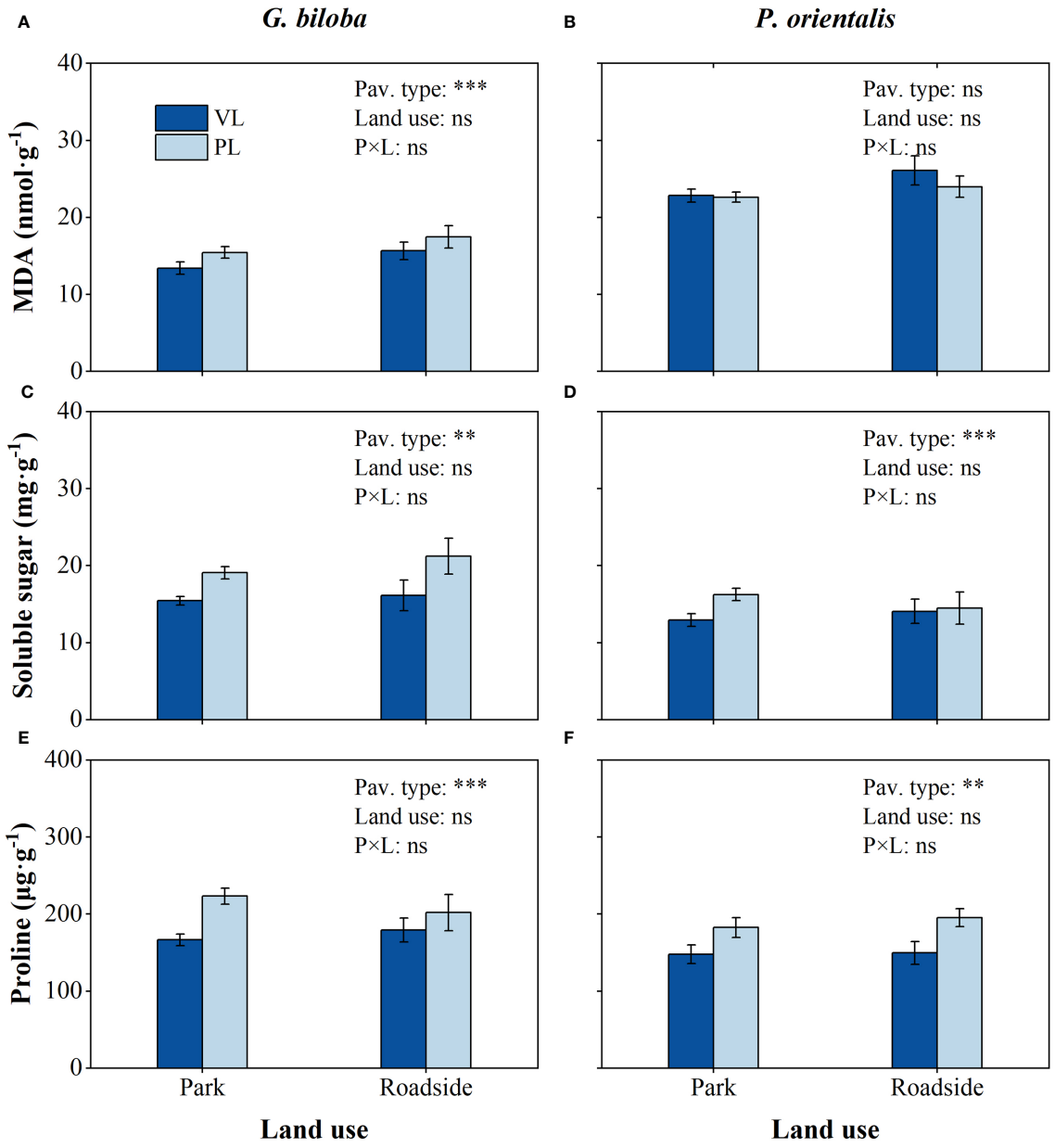

FIGURE 7
Results from the linear mixed-effects model (LMM) testing for the differences in the content of Malondialdehyde (MDA) **(A, B)**, soluble sugar **(C, D)**, and proline **(E, F)** vs. the pavement type (VL, vegetated land; PL, paved land), land use (park and roadside), and their interactions. **, $P< 0.01$; ***, $P< 0.001$; ns, not significant. Data represent mean ± SE.

moisture is one of the important factors limiting the tree growth. Under the paved land, rainfall is intercepted, and the soil moisture might even worsen, as shown in this study (Figure 3). The pavement-induced low soil moisture might be another cause of reduction in the tree growth.

In addition, urban areas are characterized by huge microclimatic heterogeneity depending on the structure of the sites (Moser et al., 2017). Compared with the vegetated land, the paved land has been shown to have high levels of solar radiation (Kjelgren and Clark, 1992), air temperature, and vapor pressure deficit (Kirschbaum, 2004) and further enhance the evaporative demand, then exacerbate drought stress to trees in the paved land (Moser et al., 2016). So, in a future study, it would better to monitor more factors for each tree.

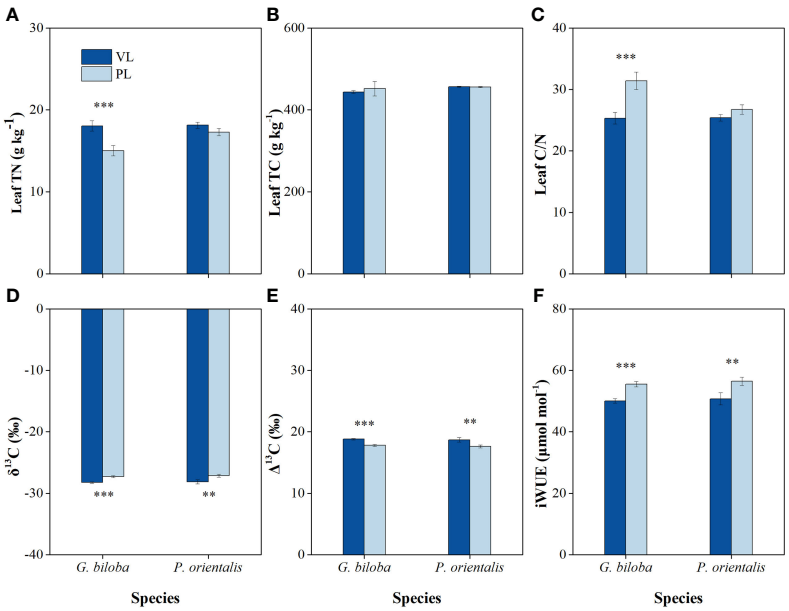

FIGURE 8
The differences in the leaf total nitrogen (TN) **(A)**, leaf total carbon (TC) **(B)**, leaf C/N ratio **(C)**, carbon isotope composition ($\delta^{13}C$) value **(D)**, carbon isotope discrimination ($\Delta^{13}C$) value **(E)**, and intrinsic water-use efficiency (iWUE) **(F)** between the vegetated land (VL) and the paved land (PL) at the park for *G biloba* and *P. orientalis*. Error bars indicate the standard error of the mean. ** and *** indicate statistically significant differences between VL and PL at $P< 0.01$ and $P< 0.001$, respectively.

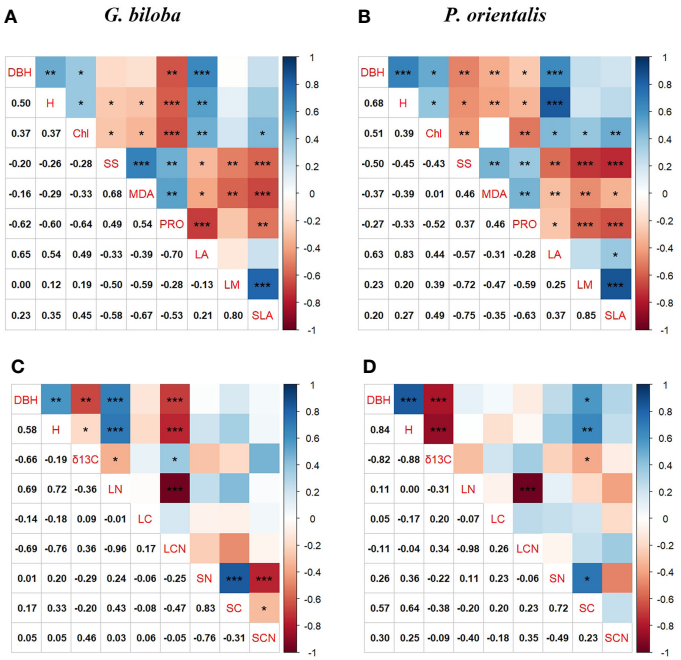

FIGURE 9
Pearson's correlations among the tree growth, leaf physiology, and leaf morphology for *G biloba* **(A)** and *P. orientalis* **(B)**, respectively, and among the tree growth, carbon isotope composition ($\delta^{13}C$), and leaf and soil nutrient content for *G biloba* **(C)** and *P. orientalis* **(D)**, respectively. Asterisks represent statistical significance (*, $P< 0.05$; **, $P< 0.01$; ***, $P< 0.001$).

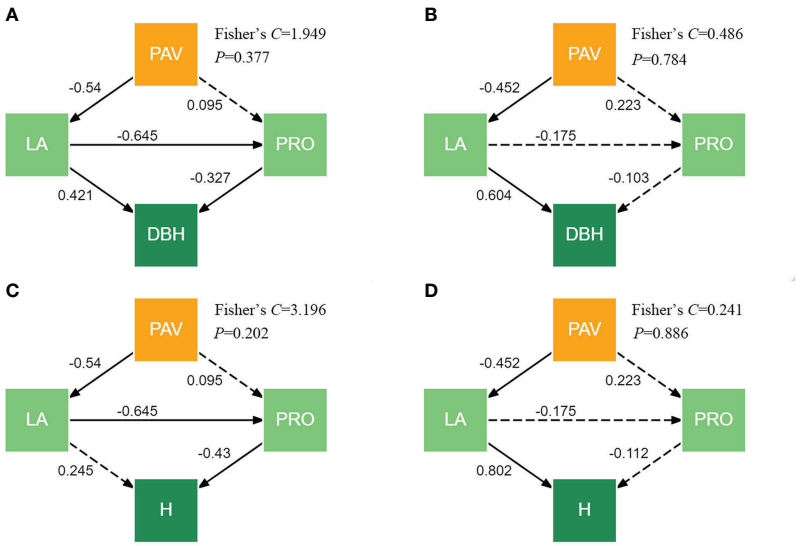

FIGURE 10
Piecewise SEMs showing the direct and indirect effects of the pavement (PAV), leaf area (LA), and proline (PRO) content on the DBH and height (H) for *G. biloba* **(A, C)** and *P. orientalis* **(B, D)**. Solid arrows represent significant effects ($P < 0.05$), and the dashed arrows indicate nonsignificant effects ($P > 0.05$).

Air pollution could have a stronger influence than the climate on the tree growth (Locosselli et al., 2019). Matsumoto et al. (2022) found that *Rhododendron pulchrum*, *Rhaphiolepis*, and *Prunus yedoensis* all had a higher restriction of maximum photosynthesis. Therefore, the combined effects of the pavement and air pollution require further study in the future.

Alterations of the leaf morphology and physiology under the paved land

The leaf is the critical component for the tree to utilize light energy and evaporate water that are essential to drive biological processes. However, the leaf is easily altered by changes in the environment. The stresses of the paved land would alter the leaf morphology and physiology. This study showed significant reductions in the leaf area, chlorophyll, and N contents and increases in the MDA and $\delta^{13}C$ for *G. biloba* and/or *P. orientalis*.

Under drought stress brought by the paved land, the leaf area of both species and SLA of *P. orientalis* become smaller in this study. It is generally thought that smaller leaves can shed heat more quickly to reduce the evaporative cooling in drier climates (McDonald et al., 2003). Plants with lower SLA tend to devote most of their energy and nutrients to building defensive structures or increasing leaf tissue density to prevent excessive dehydration (Garnier et al., 2001). In contrast, Zhang et al. (2022) reported a lower SLA but not leaf size in *Cinnamomum camphora* under an impervious pavement. Therefore, the responses of the leaf morphology to the pavement can be species specific.

As a component of the photosynthetic machinery, chlorophyll absorbs light energy and is involved in energy transfer in the course of photosynthesis (Von Wettstein et al., 1995; Blankenship, 2002). In this study, the leaves in the paved land have a significantly declined chlorophyll content. This can be caused by the reduced biochemical activities of the chlorophyll biosynthetic enzymes under drought stress (Dalal and Tripathy, 2012). Meanwhile, plants would increase the mass fraction of the non-photosynthetic (vascular and sclerenchyma) tissues under drought stress, which allows optimization of water use (Ivanova et al., 2018). The reduced chlorophyll content on the paved land will limit photosynthesis and the tree growth.

A significant decline in the leaf TN content under the paved land occurred for *G. biloba* in this study (Figure 4). However, there is no significant difference in the soil TN content. Therefore, the declined leaf TN content can be caused by the declined uptake of plant nutrients due to the reduced transpiration under drought stress. As one of the main macroelements needed for plant growth, nitrogen in plants is an elementary component of the chlorophyll nucleic acids, multiple coenzymes, vitamins, and plant hormones (Hammad and Ali, 2014). Therefore, a low leaf TN could reduce photosynthesis (Evans, 1989b) and then the growth of *G. biloba*.

As the final product of plasma membrane peroxidation, the molality concentration of MDA can reflect the degree of plant damage (Mittler, 2002; Zandalinas et al., 2016). In this study,

only *G. biloba* showed a significant increase in MDA under the paved land, indicating a higher degree of damage to cell membranes for *G. biloba*.

Adaptation of the trees to the paved land

Plants could adapt to an unfavorable environment by several biochemical or biophysical processes, such as the regulation of osmotic balance and the ratio of photosynthetic pigments, and enhancement of the water-use efficiency.

Under drought stress, plants will regulate the osmotic balance to decrease the osmotic potential and maintain the turgor of the mesophyll (Sevanto et al., 2014) by accumulating osmotic adjustment substances such as soluble sugar and proline (Ashraf and Foolad, 2007; Szabados and Savoure, 2010; Lamke and Baurle, 2017; Bechtold and Field, 2018). In this study, the leaf proline and soluble sugar were significantly increased under the paved land in *G. biloba* and *P. orientalis* leaves, which is consistent with the reports on *Camellia oleifera* under drought stress (He et al., 2020), indicating that there is an adaptive mechanism for trees to regulate osmotic substances under the paved land. According to the optimal nitrogen partitioning among the photosynthetic components (Evans, 1989a; Hikosaka and Terashima, 1995), the Chl a/b ratio increases in response to N limitation (Kitajima and Hogan, 2003). Controlling the Chl a/b ratio was also one way to adapt the photosynthetic function to high-light and arid environments (Björkman, 1981). Therefore, the increased Chl a/b ratio could be an adaptation to lower soil moisture under the paved land for both species and also an adaptation to lower TN for *G. biloba*. The de-epoxidized carotenoid zeaxanthin plays additional important roles as a thylakoid stabilizer and as an antioxidant upon desiccation (Havaux, 1998; Fernandez-Marin et al., 2013). Therefore, the lower Chl/Car is also a measure of chloroplast protection (Fernandez-Marin et al., 2020).

Under the paved land, leaf $\delta^{13}C$ abundance increased (Figure 8). Plants discriminate against ^{13}C during photosynthetic CO_2 fixation (Duranceau et al., 1999). Enzymes in the photosynthetic pathway would discriminate against the heavier molecule, $^{13}CO_2$, and preferentially use the lighter molecule, $^{12}CO_2$ (Mullaney et al., 2015a). While under drought stress, a greater proportion of $^{13}CO_2$ is fixed in leaves owing to the reduced internal $^{12}CO_2$ concentrations in leaves caused by stomatal closure (Farquhar et al., 1989; Handley et al., 1997). The $\delta^{13}C$ enrichment under the paved land could reduce photosynthesis due to the reducing gas exchange and then inhibited the growth. Meanwhile, as one strategy to adapt to drought stress, the plant must save water use for production, i.e., enhance water-use efficiency. In this study, the time-integrated measurements of iWUE are inferred from the ^{13}C stable isotopic composition ($\delta^{13}C$) of plant material (Farquhar et al., 1989). Under the paved land, the iWUE increased significantly for both *G. biloba* and *P. orientalis*, implying that trees have adapted to the paved land by the tradeoff between carbon use and water loss for trees in the pavement. Kagotani et al. (2013) also found that the long-term leaf WUE of *Prunus yedoensis* is higher at the sites with a high air temperature and low soil water content due to a smaller leaf $\Delta^{13}C$ in Kyoto city.

Compounding effects of the leaf morphological and physiological traits

In this study, there were significant correlations between the leaf morphological and physiological traits (Figure 9), indicating that trees growing on the paved land have altered simultaneously in leaf morphological and physiological properties.

Leaf photosynthesis is subjected to both stomatal limitations and non-stomatal limitations (NSLs) (Buckley and Diaz-Espejo, 2015). Generally, stomatal limitations and NSLs to photosynthesis operate concurrently and are coordinated with each other (Flexas et al., 2008; Gago et al., 2016). Under the paved land, a small leaf area incurs less stomata for taking up CO_2 into carbohydrates. The simultaneous changes in the leaf morphology and physiology will reduce the photosynthetic rate per area. In addition, the LAD under the paved land was significantly lower than under the vegetated land. Then, the photosynthetic production as well as the growth of an individual tree was reduced. The close relationships between leaf traits and tree growth (Figure 9) showed that each trait of either leaf morphology or physiology influences the tree growth independently. However, these leaf traits might influence the tree growth dependently. As shown in Figures 10A, C, the leaf area reduction under the paved land influences the DBH of *G. biloba* both directly and indirectly through the proline content and the height of *G. biloba* not directly but through the proline content. This implies the importance of the confounding effects of the leaf morphology and physiology in understanding the mechanism underlying the tree response to environmental stress.

Species difference in the tolerance to the paved land

This study confirmed that both tree species investigated are significantly impacted by the paved land in growth and leaf morphology and physiology; however, there was still a difference between *G. biloba* and *P. orientalis* in the tolerance to the paved land. The leaf MDA content increased under the paved land significantly for *G. biloba* but not for *P. orientalis*, indicating that the ability to preserve the membrane stability is weaker for *G. biloba* than for *P. orientalis*. The leaf TN content was reduced by the paved land significantly for *G. biloba* but not for *P. orientalis*. All of these suggest that *G. biloba* might be more vulnerable to the stress under the paved land than *P. orientalis*. While only *P. orientalis* had a significant decrease in

the SLA under the paved land. All of these may be caused by the differences in the anatomy of the leaf venation structure and the stem xylem structure. As a palmately veined species, *P. orientalis* has main veins but not *G. biloba*, with parallel veins in dichotomy, and a higher vein length per unit area (VLA) than *G. biloba* (Sack and Scoffoni, 2013). Under drought stress, the main vein density and thick-walled conduits of *P. orientalis* are both increased, implying increased construction costs per unit surface area and then lower SLA. *P. orientalis* is a diffuse-porous species while *G. biloba* is a non-porous species. Diffuse-porous species usually had a higher water transport efficiency than non-porous species under drought stress (Dai et al., 2020). Therefore, there were different adaptation mechanisms to the pavement in the SLA, leaf TN content, and MDA for *G. biloba* and *P. orientalis*.

Because of its importance to cultural and esthetic values in China, *G. biloba* has become one of the most popular tree species in urban greening in China ranging from subtropical to temperate climatic zones. Considering the low tolerance to the paved land, *G. biloba* is not recommended for planting on the paved land except when a good irrigation system is guaranteed.

Conclusions

Trees have been planted widely on the paved land for offsetting the limitation of land and providing more ecosystem services in the urban context. The high soil temperature and low soil moisture have exerted significant stress on the tree growth, which was manifested in the field by decreased DBH and height increments, leaf area, and leaf chlorophyll content but increased MDA, as compared with the vegetated land. However, trees could adapt to the paved land stress by regulating the osmotic balance through increasing the leaf proline and soluble sugar contents and increasing water-use efficiency through decreasing the leaf area and stomatal conductance. The reduction in tree growth on the paved land is related to the changes in the leaf morphology and physiology. Compared with *G. biloba*, *P. orientalis* showed different adaptations to the pavement-induced stresses in the SLA, leaf TN content, and MDA, which imply that they responded by different pathways. To mitigate high-temperature and low-moisture stresses on trees growing on paved lands, silvicultural measures such as irrigation should be conducted in time.

Data availability statement

The raw data supporting the conclusions of this article will be made available by the authors, without undue reservation.

Ethics statement

Written informed consent was obtained from the individual(s) for the publication of any potentially identifiable images or data included in this article.

Author contributions

BC and XKW designed the study. BC, YS and DZ conducted the field survey and laboratory analyses. BC, XMW and CG analyzed the data. BC and XMW wrote the manuscript. XKW and ZO reviewed and edited the manuscript. All authors contributed to the article and approved the submitted version.

Acknowledgment

We especially thank Chao Wang, Yang Yao, Zhen Li and Shuai Zhang for the field work. Special appreciations are given to the reviewers for their constructive suggestions on revision. This work was supported by grants from the National Natural Science Foundation of China (No. 41571053 and No. 71533005).

Conflict of interest

The authors declare that the research was conducted in the absence of any commercial or financial relationships that could be construed as a potential conflict of interest.

The handling editor declared a shared affiliation with the authors BC, CG, DZ, ZO and XW at the time of the review.

Publisher's note

Supplementary material

The Supplementary Material for this article can be found online at: https://www.frontiersin.org/articles/10.3389/fpls.2022.1003266/full#supplementary-material

References

Armson, D., Stringer, P., and Ennos, A. R. (2012). The effect of tree shade and grass on surface and globe temperatures in an urban area. *Urban For. Urban Gree* 11, 245–255. doi: 10.1016/j.ufug.2012.05.002

Arnfield, A. J. (2003). Two decades of urban climate research: A review of turbulence, exchanges of energy and water, and the urban heat island. *Int. J. Climatol* 23, 1–26. doi: 10.1002/joc.859

Ashraf, M., and Foolad, M. R. (2007). Roles of glycine betaine and proline in improving plant abiotic stress resistance. *Environ. Exp. Bot.* 59, 206–216. doi: 10.1016/j.envexpbot.2005.12.006

Balakina, J. N., Makarova, O. V., Bondarenko, V. V., Koudstaal, L. J., Ros, E. J., Koolen, A. J., et al. (2005). Simulation of oxygen regime of tree substrates. *Urban For. Urban Gree* 4, 23–35. doi: 10.1016/j.ufug.2005.06.001

Bates, D., Machler, M., Bolker, B. M., and Walker, S. C. (2015). Fitting linear mixed-effects models using lme4. *J. Stat. Softw.* 67, 1–48. doi: 10.18637/jss.v067.i01

Bates, L. S., Waldren, R. P., and Teare, I. D. (1973). Rapid determination of free proline for water-stress studies. *Plant Soil* 39, 205–207. doi: 10.1007/BF00018060

Bechtold, U., and Field, B. (2018). Molecular mechanisms controlling plant growth during abiotic stress. *J. Exp. Bot.* 69, 2753–2758. doi: 10.1093/jxb/ery157

Björkman, O. (1981). *Responses to different quantum flux densities* (Heidelberg: Springer Berlin), 57–107.

Blankenship, R. E. (2002). Molecular mechanism of photosynthesis. *Blackwell Sci.* doi: 10.1002/9780470758472

Buckley, T. N., and Diaz-Espejo, A. (2015). Partitioning changes in photosynthetic rate into contributions from different variables. *Plant Cell Environ.* 38, 1200–1211. doi: 10.1111/pce.12459

Chen, Y., Jiang, B., Wang, X., and Li, L. (2016). Responses of growth and photosynthetic characteristics of *Acer truncatum* seedlings to hardening pavements. *Chin. J. Ecol.* 35, 3258–3265. [in Chinese].

Chen, Y. Y., Wang, X. K., Jiang, B., Wen, Z., Yang, N., and Li, L. (2017). Tree survival and growth are impacted by increased surface temperature on paved land. *Landscape Urban Plann.* 162, 68–79. doi: 10.1016/j.landurbplan.2017.02.001

Chen, L. X., Zhang, Z. Q., Li, Z. D., Tang, J. W., Caldwell, P., and Zhang, W. J. (2011). Biophysical control of whole tree transpiration under an urban environment in northern China. *J. Hydrol.* 402, 388–400. doi: 10.1016/j.jhydrol.2011.03.034

City of New York (2011). *MillionTreesNYC (retrived 01.06.11)*. Available at: http://www.milliontreesnyc.org/html/home/home.shtml.

Condit, R. (1998). *Tropical forest census plots* (Georgetown, Texas: Springer-Verlag, Berlin and R. G. Lands Company).

Dai, Y. X., Wang, L., and Wan, X. C. (2020). Frost fatigue and its spring recovery of xylem conduits in ring-porous, diffuse-porous, and coniferous species in situ. *Plant Physiol. Biochem.* 146, 177–186. doi: 10.1016/j.plaphy.2019.11.014

Dalal, V. K., and Tripathy, B. C. (2012). Modulation of chlorophyll biosynthesis by water stress in rice seedlings during chloroplast biogenesis. *Plant Cell Environ.* 35, 1685–1703. doi: 10.1111/j.1365-3040.2012.02520.x

Daly, E., and Porporato, A. (2005). A review of soil moisture dynamics: From rainfall infiltration to ecosystem response. *Environ. Eng. Sci.* 22, 9–24. doi: 10.1089/ees.2005.22.9

Day, S. D., and Amateis, R. L. (2011). Predicting canopy and trunk cross-sectional area of silver linden (*Tilia tomentosa*) in confined planting cutouts. *Urban For. Urban Gree* 10, 317–322. doi: 10.1016/j.ufug.2011.08.001

Dmuchowski, W., Bragoszewska, P., Gozdowski, D., Baczewska-Dabrowska, A. B., Chojnacki, T., Jozwiak, A., et al. (2019). Strategy of ginkgo biloba l. in the mitigation of salt stress in the urban environment. *Urban For. Urban Gree* 38, 223–231. doi: 10.1016/j.ufug.2019.01.003

Duranceau, M., Ghashghaie, J., Badeck, F., Deleens, E., and Cornic, G. (1999). $\delta^{13}C$ of CO_2 respired in the dark in relation to $\delta^{13}C$ of leaf carbohydrates in *Phaseolus vulgaris* l. under progressive drought. *Plant Cell Environ.* 22, 515–523. doi: 10.1046/j.1365-3040.1999.00420.x

Evans, J. R. (1989a). Partitioning of nitrogen between and within leaves grown under different irradiances. *Aust. J. Plant Physiol.* 16, 533–548. doi: 10.1071/PP9890533

Evans, J. R. (1989b). Photosynthesis and nitrogen relationships in leaves of C_3 plants. *Oecologia* 78, 9–19. doi: 10.1007/BF00377192

Farquhar, G. D., Ehleringer, J. R., and Hubick, K. T. (1989). Carbon isotope discrimination and photosynthesis. *Annu. Rev. Plant Physiol. Plant Mol. Biol.* 40, 503–537. doi: 10.1146/annurev.pp.40.060189.002443

Farquhar, G. D., Oleary, M. H., and Berry, J. A. (1982). On the relationship between carbon isotope discrimination and the inter-cellular carbon-dioxide concentrations in leaves. *Aust. J. Plant Physiol.* 9, 121–137. doi: 10.1071/PP9820121

Feng, G., Wu, L., and Letey, J. (2002). Evaluating aeration criteria by simultaneous measurement of oxygen diffusion rate and soil-water regime. *Soil Sci.* 167, 495–503. doi: 10.1097/00010694-200208000-00001

Fernandez-Marin, B., Kranner, I., Sebastian, M. S., Artetxe, U., Laza, J. M., Vilas, J. L., et al. (2013). Evidence for the absence of enzymatic reactions in the glassy state. a case study of xanthophyll cycle pigments in the desiccation-tolerant moss syntrichia ruralis. *J. Exp. Bot.* 64, 3033–3043. doi: 10.1093/jxb/ert145

Fernandez-Marin, B., Nadal, M., Gago, J., Fernie, A. R., Lopez-Pozo, M., Artetxe, U., et al. (2020). Born to revive: molecular and physiological mechanisms of double tolerance in a paleotropical and resurrection plant. *New Phytol.* 226, 741–759. doi: 10.1111/nph.16464

Fini, A., Frangi, P., Comin, S., Vigevani, I., Rettori, A. A., Brunetti, C., et al. (2022). Effects of pavements on established urban trees: Growth, physiology, ecosystem services and disservices. *Landscape Urban Plann.* 226, 104501. doi: 10.1016/j.landurbplan.2022.104501

Fini, A., Frangi, P., Mori, J., Donzelli, D., and Ferrini, F. (2017). Nature based solutions to mitigate soil sealing in urban areas: Results from a 4-year study comparing permeable, porous, and impermeable pavements. *Environ. Res.* 156, 443–454. doi: 10.1016/j.envres.2017.03.032

Flexas, J., Ribas-Carbo, M., Diaz-Espejo, A., Galmes, J., and Medrano, H. (2008). Mesophyll conductance to CO_2: current knowledge and future prospects. *Plant Cell Environ.* 31, 602–621. doi: 10.1111/j.1365-3040.2007.01757.x

Gago, J., Daloso, D. D., Figueroa, C. M., Flexas, J., Fernie, A. R., and Nikoloski, Z. (2016). Relationships of leaf net photosynthesis, stomatal conductance, and mesophyll conductance to primary metabolism: A multispecies meta-analysis approach. *Plant Physiol.* 171, 265–279. doi: 10.1104/pp.15.01660

Garnier, E., Shipley, B., Roumet, C., and Laurent, G. (2001). A standardized protocol for the determination of specific leaf area and leaf dry matter content. *Funct. Ecol.* 15, 688–695. doi: 10.1046/j.0269-8463.2001.00563.x

Gebauer, G., and Schulze, E. D. (1991). Carbon and nitrogen isotope ratios in different compartments of a healthy and a declining *Picea abies* forest in the fichtelgebirge, Ne Bavaria. *Oecologia* 87, 198–207. doi: 10.1007/BF00325257

Gillner, S., Vogt, J., Tharang, A., Dettmann, S., and Roloff, A. (2015). Role of street trees in mitigating effects of heat and drought at highly sealed urban sites. *Landscape Urban Plann.* 143, 33–42. doi: 10.1016/j.landurbplan.2015.06.005

Grabosky, J., Haffner, E., and Bassuk, N. (2009). Plant available moisture in stone soil media for use under pavement while allowing urban tree root growth. *Arboricult. Urban For.* 35, 271–278. doi: 10.48044/jauf.2009.041

Graves, W. R. (1994). Urban soil temperatures and their potential impact on tree growth. *J. Arboricult.* 20, 24–27. doi: 10.48044/jauf.1994.005

Gregory, J. H., Dukes, M. D., Jones, P. H., and Miller, G. L. (2006). Effect of urban soil compaction on infiltration rate. *J. Soil Water Conserv.* 61, 117–124.

Hammad, S. A. R., and Ali, O. A. M. (2014). Physiological and biochemical studies on drought tolerance of wheat plants by application of amino acids and yeast extract. *Ann. Agric. Sci.* 59, 133–145. doi: 10.1016/j.aoas.2014.06.018

Handley, L. L., Robinson, D., Scrimgeour, C. M., Gordon, D., Forster, B. P., Ellis, R. P., et al. (1997). Correlating molecular markers with physiological expression in hordeum, developing approach using stable isotopes. *New Phytol.* 137, 159–163. doi: 10.1046/j.1469-8137.1997.00820.x

Havaux, M. (1998). Carotenoids as membrane stabilizers in chloroplasts. *Trends Plant Sci.* 3, 147–151. doi: 10.1016/S1360-1385(98)01200-X

Heath, R. L., and Packer, L. (1968). Photoperoxidation in isolated chloroplasts. i. kineticsand stoichiometry of fatty acid peroxidation. *Arch. Biochem. Biophys.* 125, 189–198. doi: 10.1016/0003-9861(68)90654-1

He, X. S., Xu, L. C., Pan, C., Gong, C., Wang, Y. J., Liu, X. L., et al. (2020). Drought resistance of *Camellia oleifera* under drought stress: Changes in physiology and growth characteristics. *PloS One* 15, 7. doi: 10.1371/journal.pone.0235795

Hikosaka, K., and Terashima, I. (1995). A model of the acclimation of photosynthesis in the leaves of C_3 plants to sun and shade with respect to nitrogen use. *Plant Cell Environ.* 18, 605–618. doi: 10.1111/j.1365-3040.1995.tb00562.x

Ivanova, L. A., Yudina, P. K., Ronzhina, D. A., Ivanov, L. A., and Holzel, N. (2018). Quantitative mesophyll parameters rather than whole-leaf traits predict response of C_3 steppe plants to aridity. *New Phytol.* 217, 558–570. doi: 10.1111/nph.14840

Kagotani, Y., Fujino, K., Kazama, T., and Hanba, Y. T. (2013). Leaf carbon isotope ratio and water use efficiency of urban roadside trees in summer in Kyoto city. *Ecol. Res.* 28, 725–734. doi: 10.1007/s11284-013-1056-7

Kirschbaum, M. U. F. (2004). Direct and indirect climate change effects on photosynthesis and transpiration. *Plant Biol.* 6, 242–253. doi: 10.1055/s-2004-820883

Kitajima, K., and Hogan, K. P. (2003). Increases of chlorophyll a/b ratios during acclimation of tropical woody seedlings to nitrogen limitation and high light. *Plant Cell Environ.* 26, 857–865. doi: 10.1046/j.1365-3040.2003.01017.x

Kjelgren, R. K., and Clark, J. R. (1992). Microclimates and tree growth in three urban spaces. *Hortic. Res. Inst.* 10, 139–145. doi: 10.24266/0738-2898-10.3.139

Koesera, A. K., Gilman, E. F., Paz, M., and Harchick, C. (2014). Factors influencing urban tree planting program growth and survival in Florida, united states. *Urban For. Urban Gree* 13, 655–661. doi: 10.1016/j.ufug.2014.06.005

Kramer, P. J., and Boyer, J. S. (1995). *Water relations of plants and soil* (San Diego: Academic Press), ISBN: .

Krayenhoff, E. S., and Voogt, J. A. (2010). Impacts of urban albedo increase on local air temperature at daily-annual time scales: model results and synthesis of previous work. *J. Appl. Meteorol. Climatol* 49, 1634–1648. doi: 10.1175/2010JAMC2356.1

Lamke, J., and Baurle, I. (2017). Epigenetic and chromatin-based mechanisms in environmental stress adaptation and stress memory in plants. *Genome Biol.* 18, 124. doi: 10.1186/s13059-017-1263-6

Lee, J. G., and Heaney, J. P. (2003). Estimation of urban imperviousness and its impacts on storm water systems. *J. Water Resour. Plann. Manage-Asce* 129, 419–426. doi: 10.1061/(ASCE)0733-9496(2003)129:5(419)

Lefcheck, J. S. (2016). PIECEWISESEM: Piecewise structural equation modelling in r for ecology, evolution, and systematics. *Methods Ecol. Evol.* 7, 573–579. doi: 10.1111/2041-210X.12512

Lichtenthaler, H. K. (1987). Chlorophylls and carotenoids: Pigments of photosynthetic biomembranes. *Methods Enzymol.* 148, 350–382. doi: 10.1016/0076-6879(87)48036-1

Li, Y., He, N. P., Hou, J. H., Xu, L., Liu, C. C., Zhang, J. H., et al. (2018). Factors influencing leaf chlorophyll content in natural forests at the biome scale. *Front. Ecol. Evol.* 6. doi: 10.3389/fevo.2018.00064

Locosselli, G. M., de Camargo, E. P., Moreira, T. C. L., Todesco, E., Andrade, M. D., de Andre, C. D. S., et al. (2019). The role of air pollution and climate on the growth of urban trees. *Sci. Total Environ.* 666, 652–661. doi: 10.1016/j.scitotenv.2019.02.291

Margaritis, E., and Kang, J. (2017). Relationship between green space-related morphology and noise pollution. *Ecol. Indic.* 72, 921–933. doi: 10.1016/j.ecolind.2016.09.032

Ma, W. T., Tcherkez, G., Wang, X. M., Schaufele, R., Schnyder, H., Yang, Y. S., et al. (2021). Accounting for mesophyll conductance substantially improves ^{13}C-based estimates of intrinsic water-use efficiency. *New Phytol.* 229, 1326–1338. doi: 10.1111/nph.16958

Matsumoto, M., Kiyomizu, T., Yamagishi, S., Kinoshita, T., Kumpitsch, L., Kume, A., et al. (2022). Responses of photosynthesis and long-term water use efficiency to ambient air pollution in urban roadside trees. *Urban Ecosyst.* 25, 1029–1042. doi: 10.1007/s11252-022-01212-z

McDonald, P. G., Fonseca, C. R., Overton, J. M., and Westoby, M. (2003). Leaf-size divergence along rainfall and soil-nutrient gradients: is the method of size reduction common among clades? *Funct. Ecol.* 17, 50–57. doi: 10.1046/j.1365-2435.2003.00698.x

Mittler, R. (2002). Oxidative stress, antioxidants and stress tolerance. *Trends Plant Sci.* 7, 405–410. doi: 10.1016/S1360-1385(02)02312-9

Morgenroth, J. (2011). Root growth response of *platanus orientalis* to porous pavements. *Arboricult. Urban For.* 37, 45–50. doi: 10.48044/jauf.2011.007

Morgenroth, J., and Buchan, G. D. (2009). Soil moisture and aeration beneath pervious and impervious pavements. *Arboricult. Urban For.* 35, 135–141. doi: 10.48044/jauf.2009.024

Morgenroth, J., and Visser, R. (2011). Aboveground growth response of *Platanus orientalis* to porous pavements. *Arboricult. Urban For.* 37, 1–5. doi: 10.48044/jauf.2011.001

Moser, A., Rahman, M. A., Pretzsch, H., Pauleit, S., and Rötzer, T. (2017). Inter- and intraannual growth patterns of urban small-leaved lime (*Tilia cordata* mill.) at two public squares with contrasting microclimatic conditions. *Int. J. Biometeorol.* 61, 1095–1107. doi: 10.1007/s00484-016-1290-0

Moser, A., Rotzer, T., Pauleit, S., and Pretzsch, H. (2016). The urban environment can modify drought stress of small-leaved lime (*Tilia cordata* mill.) and black locust (*Robinia pseudoacacia* l.). *Forests* 7, 77. doi: 10.3390/f7030071.

Mueller, E. C., and Day, T. A. (2005). The effect of urban ground cover on microclimate, growth and leaf gas exchange of oleander in phoenix, Arizona. *Int. J. Biometeorol.* 49, 244–255. doi: 10.1007/s00484-004-0235-1

Mullaney, J., Lucke, T., and Trueman, S. J. (2015a). The effect of permeable pavements with an underlying base layer on the growth and nutrient status of urban trees. *Urban For. Urban Gree* 14, 19–29. doi: 10.1016/j.ufug.2014.11.007

Mullaney, J., Trueman, S. J., Lucke, T., and Bai, S. H. (2015b). The effect of permeable pavements with an underlying base layer on the ecophysiological status of urban trees. *Urban For. Urban Gree* 14, 686–693. doi: 10.1016/j.ufug.2015.06.008

Nowak, D. J., and Crane, D. E. (2002). Carbon storage and sequestration by urban trees in the USA. *Environ. pollut.* 116, 381–389. doi: 10.1016/S0269-7491(01)00214-7

Nowak, D. J., Hirabayashi, S., Doyle, M., McGovern, M., and Pasher, J. (2018). Air pollution removal by urban forests in Canada and its effect on air quality and human health. *Urban For. Urban Gree* 29, 40–48. doi: 10.1016/j.ufug.2017.10.019

Pang, J. P., Wen, X. F., and Sun, X. M. (2016). Mixing ratio and carbon isotopic composition investigation of atmospheric CO_2 in Beijing, China. *Sci. Total Environ.* 539, 322–330. doi: 10.1016/j.scitotenv.2015.08.130

Parkhurst, D. F., and Loucks, O. L. (1972). Optimal leaf size in relation to environment. *J. Ecol.* 60, 505–537. doi: 10.2307/2258359

Pataki, D. E., McCarthy, H. R., Litvak, E., and Pincetl, S. (2011). Transpiration of urban forests in the Los Angeles metropolitan area. *Ecol. Appl.* 21, 661–677. doi: 10.1890/09-1717.1

Philip, E., and Azlin, Y. N. (2005). Measurement of soil compaction tolerance of *Lagestromia speciosa* (L.) pers. using chlorophyll fluorescence. *Urban For. Urban Gree* 3, 203–208. doi: 10.1016/j.ufug.2005.04.003

Pincetl, S., Gillespie, T., Pataki, D. E., Saatchi, S., and Saphores, J. D. (2013). Urban tree planting programs, function or fashion? Los Angeles and urban tree planting campaigns. *GeoJournal* 78, 475–493. doi: 10.1007/s10708-012-9446-x

Pitt, R., Chen, S. E., Clark, S. E., Swenson, J., and Ong, C. K. (2008). Compaction's impacts on urban storm-water infiltration. *J. Irrig. Drain. Eng.* 134, 652–658. doi: 10.1061/(ASCE)0733-9437(2008)134:5(652)

Poorter, H., Niinemets, U., Poorter, L., Wright, I. J., and Villar, R. (2009). Causes and consequences of variation in leaf mass per area (LMA): a meta-analysis. *New Phytol.* 182, 565–588. doi: 10.1111/j.1469-8137.2009.02830.x

Pregitzer, K. S., King, J. A., Burton, A. J., and Brown, S. E. (2000). Responses of tree fine roots to temperature. *New Phytol.* 147, 105–115. doi: 10.1046/j.1469-8137.2000.00689.x

Rahman, M. A., Armson, D., and Ennos, A. R. (2014). Effect of urbanization and climate change in the rooting zone on the growth and physiology of *Pyrus calleryana*. *Urban For. Urban Gree* 13, 325–335. doi: 10.1016/j.ufug.2013.10.004

Roloff, A., Korn, S., and Gillner, S. (2009). The climate-Species-Matrix to select tree species for urban habitats considering climate change. *Urban For. Urban Gree* 8, 295–308. doi: 10.1016/j.ufug.2009.08.002

Sack, L., and Scoffoni, C. (2013). Leaf venation: structure, function, development, evolution, ecology and applications in the past, present and future. *New Phytol.* 198, 983–1000. doi: 10.1111/nph.12253

Sanders, J. R., and Grabosky, J. C. (2014). 20 years later: Does reduced soil area change overall tree growth? *Urban For. Urban Gree* 13, 295–303. doi: 10.1016/j.ufug.2013.12.006

Sand, E., Konarska, J., Howe, A. W., Andersson-Skold, Y., Moldan, F., Pleijel, H., et al. (2018). Effects of ground surface permeability on the growth of urban linden trees. *Urban Ecosyst.* 21, 691–696. doi: 10.1007/s11252-018-0750-1

Savi, T., Bertuzzi, S., Branca, S., Tretiach, M., and Nardini, A. (2015). Drought-induced xylem cavitation and hydraulic deterioration: risk factors for urban trees under climate change? *New Phytol.* 205, 1106–1116. doi: 10.1111/nph.13112

Sevanto, S., McDowell, N. G., Dickman, L. T., Pangle, R., and Pockman, W. T. (2014). How do trees die? a test of the hydraulic failure and carbon starvation hypotheses. *Plant Cell Environ.* 37, 153–161. doi: 10.1111/pce.12141

Shipley, B. (2009). Confirmatory path analysis in a generalized multilevel context. *Ecology* 90, 363–368. doi: 10.1890/08-1034.1

Szabados, L., and Savoure, A. (2010). Proline: a multifunctional amino acid. *Trends Plant Sci.* 15, 89–97. doi: 10.1016/j.tplants.2009.11.009

Tang, C. S., Shi, B., Gao, L., Daniels, J. L., Jiang, H. T., and Liu, C. (2011). Urbanization effect on soil temperature in nanjing, China. *Energy Build.* 43, 3090–3098. doi: 10.1016/j.enbuild.2011.08.003

Upreti, R., Wang, Z. H., and Yang, J. C. (2017). Radiative shading effect of urban trees on cooling the regional built environment. *Urban For. Urban Gree* 26, 18–24. doi: 10.1016/j.ufug.2017.05.008

Von Wettstein, D., Gough, S., and Kannangara, C. G. (1995). Chlorophyll biosynthesis. *Plant Cell* 7, 1039–1057. doi: 10.2307/3870056

Vrinceanu, D., Berghi, O. N., Cergan, R., Dumitru, M., Ciuluvica, R. C., Giurcaneanu, C., et al. (2021). Urban allergy review: Allergic rhinitis and asthma with plane tree sensitization (Review). *Exp. Ther. Med.* 21, 275. doi: 10.3892/etm.2021.9706

Wang, C. H., Wang, Z. H., Wang, C. Y., and Myint, S. W. (2019). Environmental cooling provided by urban trees under extreme heat and cold waves in US cities. *Remote Sens. Environ.* 227, 28–43. doi: 10.1016/j.rse.2019.03.024

Xie, Y. H., Huang, G. H., and Zhao, L. X. (1998). Spatial variability of field soil properties. *J. China Agric. Univ.* 3, 41–45. [in Chinese]

Yemm, E. W., and Willis, A. J. (1954). The estimation of carbohydrates in plant extracts by anthrone. *Biochem. J.* 57, 508–514. doi: 10.1042/bj0570508

Zandalinas, S. I., Rivero, R. M., Martinez, V., Gomez-Cadenas, A., and Arbona, V. (2016). Tolerance of citrus plants to the combination of high temperatures and drought is associated to the increase in transpiration modulated by a reduction in abscisic acid levels. *BMC Plant Biol.* 16, 105. doi: 10.1186/s12870-016-0791-7

Zhang, C., Liu, H. H., Huang, N., Zhang, F. Y., Meng, Y. Q., Wang, J. A., et al. (2022). Coordination of leaf hydraulic and economic traits in *Cinnamomum camphora* under impervious pavement. *BMC Plant Biol.* 22, 347. doi: 10.1186/s12870-022-03740-4

Zhao, D., Li, F., Wang, R. S., Yang, Q. R., and Ni, H. S. (2012). Effect of soil sealing on the microbial biomass, n transformation and related enzyme activities at various depths of soils in urban area of Beijing, China. *J. Soils Sediments* 12, 519–530. doi: 10.1007/s11368-012-0472-6

frontiers | Frontiers in Plant Science

TYPE Original Research
PUBLISHED 16 December 2022
DOI 10.3389/fpls.2022.1052565

OPEN ACCESS

EDITED BY
Akash Tariq,
Xinjiang Institute of Ecology and Geography (CAS), China

REVIEWED BY
Maierdang Keyimu,
Xinjiang Institute of Ecology and Geography (CAS), China
Zeeshan Ahmed,
Xinjiang Institute of Ecology and Geography(CAS), China

*CORRESPONDENCE
Zhipeng Sha
zp_sha@163.com
Ruiheng Lyu
lvrh514723@126.com

†These authors have contributed equally to this work and share first authorship

SPECIALTY SECTION
This article was submitted to Plant Abiotic Stress, a section of the journal Frontiers in Plant Science

RECEIVED 24 September 2022
ACCEPTED 25 November 2022
PUBLISHED 16 December 2022

CITATION
Zhang Y, Cheng X, Sha Z, Lekammudiyanse MU, Ma W, Dayananda B, Li S and Lyu R (2022) Environmental drivers of the leaf nitrogen and phosphorus stoichiometry characteristics of critically endangered *Acer catalpifolium*. *Front. Plant Sci.* 13:1052565. doi: 10.3389/fpls.2022.1052565

Environmental drivers of the leaf nitrogen and phosphorus stoichiometry characteristics of critically endangered *Acer catalpifolium*

Yuyang Zhang[1†], Xiaoyu Cheng[1†], Zhipeng Sha[2*], Manuja U. Lekammudiyanse[3], Wenbao Ma[4], Buddhi Dayananda[5], Shuang Li[6] and Ruiheng Lyu[1*]

[1]The National-Local Joint Engineering Laboratory of High Efficiency and Superior-Quality Cultivation and Fruit Deep Processing Technology on Characteristic Fruit Trees, College of Horticulture and Forestry Sciences, Tarim University, Alar, China, [2]Faculty of Morden Agricultural Engineering, Kunming University of Science and Technology, Kunming, China, [3]Coastal Marine Ecosystems Research Centre, Central Queensland University, Gladstone, QLD, Australia, [4]Ecological Restoration and Conservation of Forests and Wetlands Key Laboratory of Sichuan Province, Sichuan Academy of Forestry, Chengdu, China, [5]School of Agriculture and Food Sciences, The University of Queensland, Brisbane QLD, Australia, [6]State Key Laboratory of Environmental Criteria and Risk Assessment, Chinese Research Academy of Environmental Sciences, Beijing, China

Acer catalpifolium is a perennial deciduous broad-leaved woody plant, listed in the second-class protection program in China mainly distributed on the northwest edge of Chengdu plain. However, extensive anthropogenic disturbances and pollutants emissions (such as SO_2, NH_3 and NO_X) in this area have created a heterogeneous habitat for this species and its impacts have not been systematically studied. In this study, we investigated the leaf nitrogen (N) and phosphorus (P) content of *A. catalpifolium* in the natural distribution areas, and a series of simulation experiments (e.g., various water and light supply regimes, different acid and N deposition levels, reintroduction management) were conducted to analyze responses of N and P stoichiometric characteristics to environmental changes. The results showed that leaf nitrogen content (LNC) was 14.49 ~ 25.44 mg g^{-1}, leaf phosphorus content (LPC) was 1.29~3.81 mg g^{-1} and the N/P ratio of the leaf (L-N/P) was 4.87~13.93. As per the simulation experiments, LNC of *A. catalpifolium* is found to be relatively high at strong light conditions (80% of full light), high N deposition (100 and 150 kg N ha^{-1}), low acidity rainwater, reintroduction to understory area or N fertilizer applications. A high level of LPC was found when applied with 80% of full light and moderate N deposition (100 kg N ha^{-1}). L-N/P was high under severe shade (8% of full light), severe N deposition (200 kg N ha^{-1}), and reintroduction to gap and undergrowth habitat; however, low L-N/P was observed at low acidity rainwater or P fertilizer application. The nutrient supply facilitates corresponding elements uptake, shade tends to induce P limitation and soil acidification shows N limitation.

Our results provide theoretical guidance for field management and nutrient supply regimes for future protection, population rejuvenation of this species and provide guidelines for conservation and nutrient management strategies for the endangered species.

KEYWORDS

environmental factors, N/P ratio(L-N/P), leaf nitrogen content (LNC), leaf phosphorus content (LPC), Acer catalpifolium

Introduction

Ecological stoichiometry explains the relationship between the structure, function, and elements of the ecosystem in which plants themselves live (Elser and Hamilton, 2007; Sardans et al., 2012b). In plant leaf stoichiometry, N and P play an important role in the study of vegetation composition, ecosystem function, and nutrient constraints (Allen and Gillooly, 2009). The variation patterns of N and P concentrations and N/P ratio in leaves (L-N/P) and their influencing factors (biological and abiotic) have been widely reported (Reich and Oleksyn, 2004; Han et al., 2005; Ågren, 2008). Based on the previous findings, a series of hypotheses were constructed to explain the causes of leaf stoichiometry changes such as the biogeochemical cycle hypothesis, temperature-physiology hypothesis, plant growth rate hypothesis, and soil substrate age hypothesis (Chadwick et al., 1999; McGroddy et al., 2004; Ågren, 2008).

The biogeochemical hypothesis proposed that the storage capacity of the plant's available nutrients in the soil is an important driving factor in the current status of leaf nutrients (McGroddy et al., 2004). The N from the environment (96.3 Tg N yr^{-1} of atmospheric N was deposited into the terrestrial ecosystems in 2016 (Ackerman et al., 2018)) into the system effectively improves the utilization and absorption of N by plants. A comprehensive analysis of 201 research reports found that simulated N deposition could increase the leaf nitrogen content (LNC) in terrestrial ecosystems, but leaf phosphorus concentration (LPC) was weak in response to N deposition (Sardans et al., 2017). Furthermore, previous studies suggested that N addition can significantly reduce the P concentration of plants aboveground due to massive imbalance of availability N and P which stimulates plant to take up more N but limit P uptake (Li et al., 2016b; Deng et al., 2017). In contrast, some studies have shown that N deposition increases the absorption of N and P by plants (Braun et al., 2009; Huang et al., 2012).

The temperature-physiology hypothesis suggests that plant metabolism is highly sensitive to temperature (Reich and Oleksyn, 2004). With the decrease in temperature, plant physiological domestication and adaptation increased LNC and LPC, while L-N/P increased accordingly (Reich and Oleksyn, 2004). Studies that used global databases have shown that LNC and LPC were higher in high latitudes than in low latitudes (Tian et al., 2017), and the change from relative P limitation to N limitation increased with the increase in latitude (Du et al., 2020). The soil substrate age hypothesis also predicts that the restriction of phosphorus from the Arctic (relatively young geologically) to tropical regions increases gradually, and is mainly limited by less weathered phosphate rock (Chadwick et al., 1999a).

The plant growth rate hypothesis has suggested that the relative growth rate of plants depends on the rate of protein synthesis (subject to phosphorus-rich ribosomal RNA) indicated plants relative growth rate mainly determined by the P concentration or P:N ratio of plants (Ågren, 2008; Peng et al., 2011). Under drought conditions, plants allocate more resources to growth and energy metabolism including the allocation of N, P and other elements to roots to facilitate water absorption (Gargallo-Garriga et al., 2014; Gargallo-Garriga et al., 2015). According to the results of literature integration analysis, drought can improve LNC on the whole but has no significant impact on LPC (Sardans et al., 2017). However, an arid environment can reduce the ability of plants to absorb and utilize nutrients and restrict plant growth (He and Dijkstra, 2014), which conforms to the plant growth rate hypothesis as a whole.

Experiments on field fertilization of plants show that the N:P of plants also have high internal stability (Demars and Edwards, 2007; Yu et al., 2010; Yu et al., 2011). However, N:P of a plant itself is not completely consistent with N:P in its habitat (water, air, and soil), which might be the reason for the plant's ability in absorbing and storing nutrients to adapt to the habitat (Chapin et al., 1990; Chapin et al., 1993). This phenomenon is known as "resource supply-demand", which is an asymmetric matching phenomenon of plants' adaptation to their local environment (Güsewell, 2004). The stoichiometric characteristics of plants are usually defined by their limiting elements, which can be explained by "Liebig's law of the minimum" (von Liebig, 1855). The demand for chemical elements in plants is limited by the element with the smallest supply (known as the limiting

element), which has an important influence on the growth rate, population structure, and structural stability of plants (Vitousek et al., 2010). Hence, the study of plant restrictive elements is the premise to restore the population and judge the law of population development (Elser and Hamilton, 2007; Vitousek et al., 2010), N:P is an important indicator of plant nutrient restriction. Previous studies have suggested that low L-N/P (< 14) and high N:P (> 16) were driven by the N limitation and phosphorus limitation respectively, and the moderate L-N/P (14 < N:P < 16) can be the reason of both N and P limitation (Güsewell, 2004; Wassen et al., 2005).

Plant stoichiometry characteristics can be further affected by climate change scenarios (Vitousek et al., 2010). Due to anthropogenic activities (such as the burning of fossil fuels, transportation, and intensive agriculture), global reactive N emissions rise sharply, which can differ the N and P inputs in the terrestrial ecosystem (Vitousek et al., 2010). Moreover, an integrated analysis has shown that the significant changes in leaf stoichiometry are related to the increased CO_2 concentration, drought conditions, and P enrichment (Sardans et al., 2017).

Acer catalpifolium Rehd. belongs to the family Sapindaceae and is a large broad-leaved deciduous tree with a tall and straight trunk, which has been listed in the "wild plants with extremely small populations" (WPESP) rescue and protection plan due to the critically endangered status in China (Zhang et al., 2020). Previous field investigation stated the narrow distribution of this species (mainly in the rain zone of west China) and serious obstacle to the regeneration of natural population (Zhang et al., 2018). This distribution area is affected by anthropogenic emissions with large N deposition and frequent acid rains which have profoundly affected the *A. catalpifolium* habitat (Du et al., 2020; Zhang et al., 2021a; Zhang et al., 2021b), however, it is still unclear how these emissions change the N and P content in the soil and at what level these changes can affect the growth of *A. catalpifolium*. We conducted field investigations combined with a series of simulation experiments to analyze the driving factors of L-N/P as well as the response to different environmental change scenarios.

Materials and methods

Field investigation

In November 2017, mature and healthy *A. catalpifolium* leaves were collected from the natural populations from Leibo, Yibin, Dujiangyan, Ya'an, Emei mountain, and Pingwu regions in Sichuan province. A total of 22 sampling sites were selected from the above locations, and nine samples were taken from artificial planting *A. catalpifolium* forest (10 years old) in Emei mountain. Three healthy plants were selected from each sampling site, and 10 healthy and intact leaves were collected from each plant. In addition, soil samples were collected (n=6) at each corresponding sampling site. Part of the collected soil samples were stored in a -20 °C refrigerator before measuring the available N content, and the rest was air-dried to measure other properties (including soil pH, organic matter, total N, available P and K). The longitude and latitude, altitude, tree height, and diameter at breast height (DBH) of the sampling sites were recorded (detailed procedure refer to Zhang et al. (2018)).

Simulation experiment

The simulation experiments were carried out in Beijing (different water and light simulation experiments) and Tangchang Town of Sichuan Province (simulated acid and N deposition experiments). The seedlings of *A. catalpifolium* used in simulation experiments were grown in a seedbed that contained Burozem and bark sawdust humus. After one month of cultivation, the seedlings with similar growth characteristics were transplanted into pots (one plant per pot) and prepared for experimental treatments. The size of the pot was 35cm × 45cm, the soil used for potting was same as that in the seedbed, both Burozem and bark sawdust humus, soil organic matter 2.52%; total N 0.14%; total P 0.24%; total K 0.47%; available P 27.21 mg kg^{-1}; available K 134.68 mg kg^{-1}.

Simulated different water and light conditions experiment

After transplantation, seedlings were placed in three light conditions (L1, L2, and L3 represented 80%, 50% (using single layer black nylon mesh net), and 8% (using double layer black nylon mesh net) of total light, respectively) which were manipulated by the different layers of black mesh nylon nets, and four water treatments (W1, W2, W3, and W4 represented 35%, 55%, 75% and 95% water holding capacity, respectively). Each treatment was replicated six times (Zhang et al., 2019).

Simulated acid deposition experiment

The acid deposition experiment was conducted from 1st May 2017 to 31st October 2018 and was set up as two acid deposition patterns (leaf and soil application) × two acid rain types (sulfuric acid dominant acid rain, and nitric acid balanced acid rain) × three acidity gradients (pH 2.5, 3.5 and 4.5). The control (CK) also included and only received filtered water. The sulfuric acid dominant acid rain applied to leaf and soil was expressed as SL (SL2.5, SL3.5, and SL4.5) and SS (SS2.5, SS3.5 and SS4.5) respectively, nitric acid balanced acid rain applied to leaf and soil are expressed as NL (NL2.5, NL3.5, and NL4.5) and NS (NS2.5, NS3.5 and NS4.5) respectively (Zhang et al., 2021b).

Each treatment was replicated six times. The leaves were collected from each treatment at end of the experiment.

Simulated N deposition experiment

The simulated N deposition experiment was conducted at the same time with an acid deposition experiment. Five N deposition levels (i.e., 30, 60, 100, 150, and 200 kg N ha^{-1} y^{-1}represented by N3, N6, N10, N15, and N20, respectively) and CK (only received filtered water) were included in this experiment. The N addition was conducted every 15 days, with 20 additions for the entire duration of the pot experiment. Different NH_4NO_3 aqueous solutions (prepared according to the treatment concentrations) of 300 ml were added to corresponding treatment pots and a similar volume of water was added to the CK. Each treatment was replicated six times. Daily field management routines such as irrigation and weeding were kept the same with the simulated acid deposition experiments. The leaves samples were collected from each treatment at end of the experiment.

Wild reintroduction experiment

Various light environments in forest

Acer catalpifolium with the same growth features was selected and transplanted to its natural habitat (located in Western Asia Alpine Botanical Garden, Institute of Plants, Chinese Academy of Sciences) in November 2017. Five A. *catalpifolium* were planted at a spacing of 2 m × 2 m under each light condition (including unshaded land, forest edge, gap and understory) in the forest (n=5).

Soil fertilization experiment

In this experiment, we included six soil amendments, which were N fertilizer (urea, 46% N, 1 kg per plant), P fertilizer (calcium superphosphate, 12% P_2O_5, 4 kg per plant), NP fertilizer (1 kg urea per plant plus 4 kg calcium superphosphate per plant), vermicompost (10 kg per plant), charcoal (10 kg per plant). *A. catalpifolium* planted at the spacing of 2 m × 2 m, soil amendments were applied to different treatments in two times (the first is planting time and the second is in April 2018). Daily weeding, pest control, and irrigation were carried out to ensure the normal growth of *A. catalpifolium*.

Chemical analysis of soil and plant samples

Fully expanded and disease-free leaves of *A. catalpifolium* were collected from field investigation, simulation experiments and wild reintroduction experiments and leave samples were oven-dried with 105 °C for 30 mins and then 85 °C for 72 h until a constant weight resulted. Leaf samples were ground and digested by H_2SO_4-H_2O_2 solution and determined the N and P content using an AA3 continuous flow analyzer. Soil properties such as soil pH, soil organic matter, soil total N content, soil available nitrogen (NO_3^--N and NH_4^+-N), phosphorus and potassium were measured using the determination methods described by Sha et al. (2020).

Data analysis

In order to clarify the effects of explanatory variables on nutrient concentration and L-N/P characteristics of *A. catalpifolium*, explanatory variables were divided into soil factors, geographical factors and species factors, and the strong colinearity and irrelevant variables were eliminated through multiple linear regression analysis combined with stepwise regression analysis model.

The IBM SPSS 22 (IBM Corp, 2013) was used to analyze the significant difference in leaf N and P content as well as L-N/P under different treatments ($p<0.05$). Multivariate regression analysis were performed using R Program 4.1.1 (R Core Team, 2021). Figures were developed by using Origin 9.0 and R 4.1.1.

Results

Leaf N and P stoichiometric characteristics of *Acer catalpifolium* and its drivers

The LNC and LPC of *A. catalpifolium* were 20.02 mg g^{-1} (14.49-25.44), 2.27 mg g^{-1} (1.29-3.81) (Figures 1A, B), and the mean L-N/P of *A. catalpifolium* were 8.75 (4.87-13.93) (Figure 1C).

LNC was significantly correlated with soil available N (SAV_N), potassium (SAV_K) (Figure 2), the correlation coefficients were 0.39 and 0.39. The LPC was significantly correlated with soil available P (SAV_P) and the correlation coefficient was 0.42. Tree height (TH) was negatively correlated with longtitude, latitude and elevation, and positively correlated with SAV_N, the correlation coefficients were -0.45, -0.45, -0.61 and 0.37 respectively.

The changes in LNC were mainly controlled by soil pH, total N, available N, available K, altitude and DBH, and the overall explanation rate of N concentration of *A. catalpifolium* was 31% (Table 1). The LPC was only related to soil available P, and its explanation rate for LPC change was 15%. In terms of L-N/P, consistent with Pearson correlation analysis and redundancy analysis, the L-N/P of *A. catalpifolium* was mainly affected by

10.3389/fpls.2022.1052565

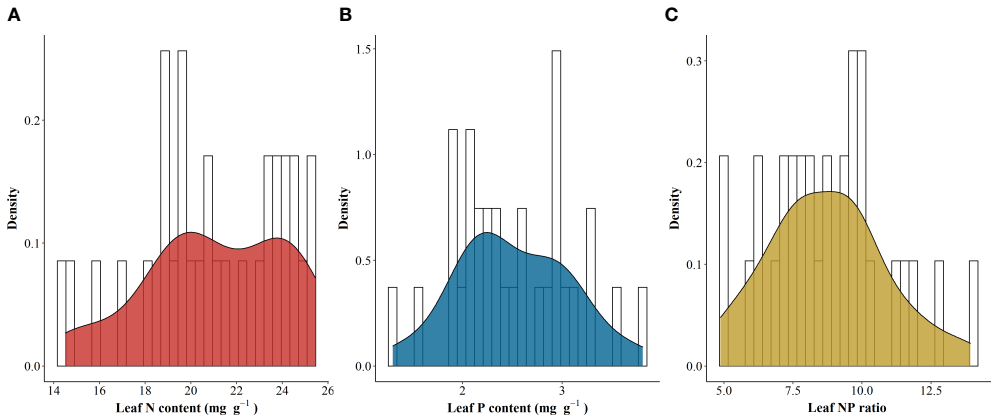

FIGURE 1
Leaf N and P stoichiometry traits of *Acer catalpifolium*. **(A)** leaf N content, **(B)** leaf P content and **(C)** leaf N/P ratio.

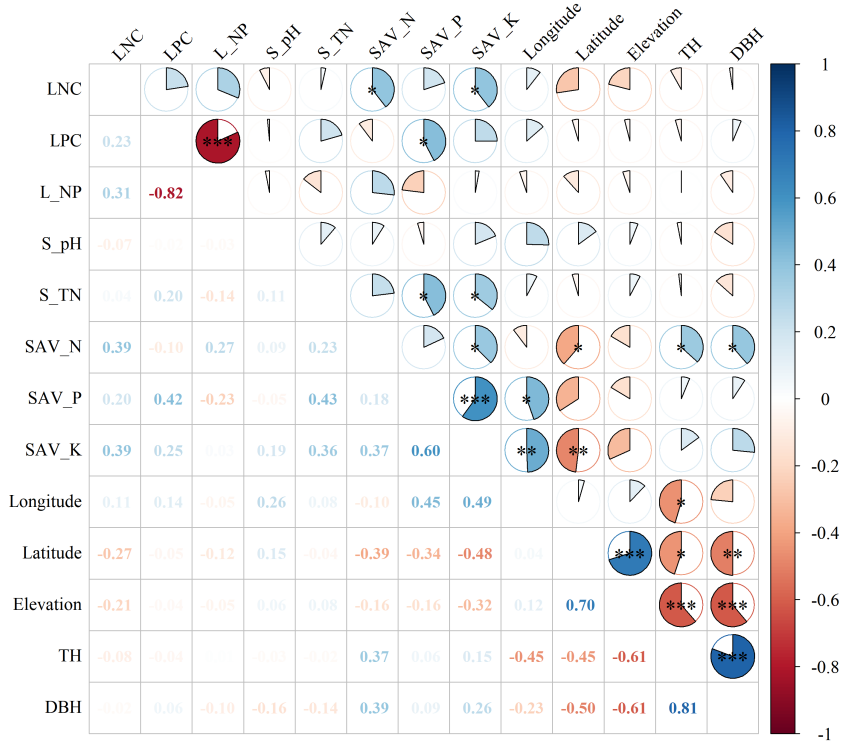

FIGURE 2
Pearson's correlation matrix of leaf nutrition and environmental explanatory variables. Note: S_pH, S_TN, SAV_N, SAV_P, SAV_K, TH, and DBH represent soil pH, soil total nitrogen, soil available nitrogen, soil available phosphorus, soil available potassium, tree height, and DBH, respectively. Asterisk (*) indicated significant correlation with *, ** and *** indicating significance levels at 0.05 0.01 and 0.001, respectively.

soil available N and P, and the explanation rate of L-N/P variation was 19%.

At the single factor level, the explanation rate of soil available N to the change of L-N/P was only 7.1% (Figure 3A), and that of available P was 5.3% (Figure 3B).

Effects of water and light on N and P stoichiometric characteristics

Different water and light supply regimes have changed foliar N and P composistion of *A. catalpifolium*. The LNC was high in L1 light

TABLE 1 Multivariate regression analysis of N/P in the foliage of *Acer catalpifolium*.

Variables		LNC		LPC		L-N/P	
		Estimate	*P*	Estimate	*P*	Estimate	*P*
	(Intercept)	75.82	0.21	16.53	0.22	-14.93	0.76
Soil	S_pH	-0.61	0.32	0.08	0.53	-0.56	0.26
	S_TN	-0.34	0.17	0.01	0.88	-0.17	0.38
	SAV_N	0.42	0.02*	-0.04	0.26	0.25	0.06
	SAV_P	0.00	0.74	0.01	0.05	-0.02	0.10
	SAV_K	0.01	0.05	0.00	0.54	0.00	0.49
Geography	Longitude	-0.64	0.28	-0.16	0.22	0.30	0.52
	Latitude	0.69	0.36	0.09	0.59	-0.15	0.80
	Elevation	-0.01	0.06	0.00	0.90	-0.00	0.69
Species	TH	-0.14	0.24	-0.03	0.21	0.09	0.30
	DBH	-0.07	0.23	0.02	0.21	-0.11	0.04*
F		2.05		0.92		1.09	
R^2		0.25		0.02		0.03	
P		0.08		0.52		0.41	
Variables		**LNC**		**LPC**		**L-N/P**	
		Estimate	***P***	**Estimate**	***P***	**Estimate**	***P***
	(Intercept)	27.96	0.00***	2.35	0.00***	7.43	0.00***
Soil	S_pH	-0.76	0.14	—	—	—	—
	S_TN	-0.30	0.16	—	—	—	—
	SAV_N	0.39	0.01**	—	—	0.17	0.04*
	SAV_P	—	—	0.01	0.02*	-0.01	0.06
	SAV_K	0.01	0.04*	—	—	—	—
Geography	Longitude	—	—	—	—	—	—
	Latitude	—	—	—	—	—	—
	Elevation	-0.00	0.11	—	—	—	—
Species	TH	—	—	—	—	—	—
	DBH	-0.12	0.01**	—	—	—	—
F value		3.25		6.35		3.50	
R^2		0.31		0.15		0.19	
P		0.02*		0.02*		0.04*	

Asterisk (*) indicated significant impact, with *, ** and *** indicating significance levels at 0.05 0.01 and 0.001, respectively.

condition, of which L1W2 and L1W3 treatments were significantly higher than those of L2W1 and L3 light treatments ($p<0.05$) (Figure 4A). The LPC was also higher under L1 light, but under the same light condition, there was no significant difference in LPC among different water treatments ($p>0.05$) (Figure 4B). The L-N/P in L3W3 treatment was significantly higher than that in W1 and W3 treatment under L1 light ($p<0.05$) (Figure 5C).

Effects of simulated acid deposition on stoichiometric characteristics of N and P in *Acer catalpifolium* leaves

Significant variations in foliar N and P content under different acid deposition patterns were observed. Leaf acid spraying did not significantly change the LNC of *A. catalpifolium* with CK. The LNC under NL4.5 treatment was significantly higher than that under NL2.5 treatment ($p<0.05$) (Table 2). The LNC under NS3.5 and NS4.5 treatments were significantly higher than that under NL2.5 treatment ($p<0.05$). The LPC of NS2.5 and SS2.5 was significantly higher than that of CK, NL2.5, and NL2.5 ($p<0.05$). The L-N/P of NS2.5 and SS2.5 was significantly lower than that of NL3.5 and NL4.5 ($p<0.05$).

Effects of simulated nitrogen deposition on stoichiometric characteristics of N and P in *Acer catalpifolium* leaves

Simulated different N deposition levels have altered foliar nutrients status, significantly increased the LNC of *A. catalpifolium* ($p<0.05$) and the LNC increased with the increase of N addition (Figure 5A). The changes of LPC in the

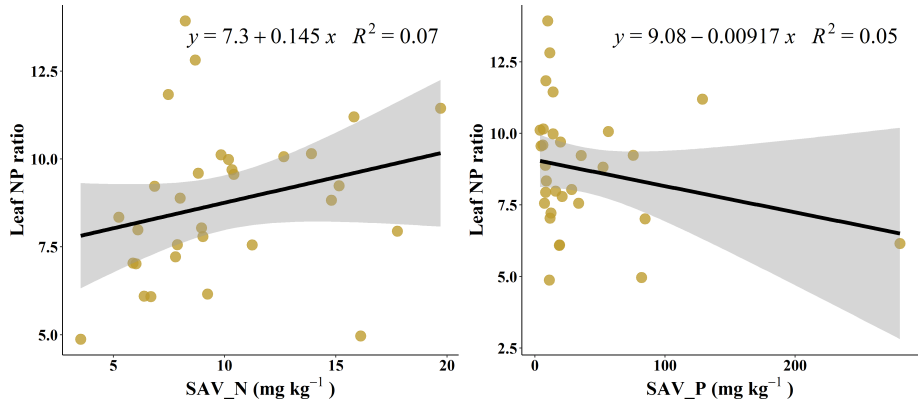

FIGURE 3
Correlation of leaf NP ratio with soil available nutrients.

leaf of *A. catalpifolium* under simulated N deposition were similar to those of LNC (Figure 5B). The LPC under N10 treatment was significantly higher than CK ($p<0.05$) (Figure 5B). The L-N/P under N20 treatment was significantly higher than CK ($p<0.05$) (Figure 5C).

Effect of different canopy density on leaf N and P stoichiometric characteristics of *Acer catalpifolium* leaves

Under different canopy density habitats, LNC of leaves of *A. catalpifolium* was higher in the light environment of the understory, but there was no significant difference among treatments ($p>0.05$) (Figure 6A). On the contrary, the LPC of *A. catalpifolium* was lower in understory light and significantly lower than that of no shading treatment ($p<0.05$) (Figure 6B). The L-N/P under gap and understory light was higher than that that of no shading ($p<0.05$) (Figure 6C).

Effects of soil amendment on leaf N and P stoichiometric characteristics of *Acer catalpifolium*

The amendments application changed soil nutrients pool. N fertilizer application increased the LNC of *A. catalpifolium* which was significantly higher than that of CK and P fertilizer ($p<0.05$) (Figure 7A). Different soil amendment applications had little effect on the LPC of *A. catalpifolium* (Figure 7B). The L-N/P ratio of leaves treated with P fertilizer was lower compared to N fertilizer and vermicompost ($p<0.05$) (Figure 7C).

Discussion

The results from field investigation, simulation experiments and wild reintroduction experiments provided a quantitative perspective of the effect of environmental changes in leaf N and P stoichiometric characteristics of *Acer catalpifolium*. The LNC and LPC of *A. catalpifolium* in this study were found higher than that of the data synthesis study which indicated the average LNC and LPC of woody plants (based on the global plant leaf N and P stoichiometry dataset) are 18.22 g kg^{-1} and 1.10 g kg^{-1}, respectively (Tian et al., 2017). Stoichiometric studies of 753 species in China also showed relatively low LNC (18.6 g kg^{-1}) and LPC (1.21 g kg^{-1}), but the L-N/P (14.4) was higher compared to this study (Han et al., 2005). L-N/P is an important indicator of plant nutrient restriction. Previous studies have pointed out that when L-N/P < 14, nutrients are N limited, l-N/P > 16 is P limited, and when 14 < L-N/P < 16, it is common N and P limited (Güsewell, 2004; Wassen et al., 2005). The range of L-N/P of *A. catalpifolium* was 4.87 ~ 13.93 in the rain zone of west China, indicating that there was a strong N limitation in the distribution area of *A. catalpifolium*. The L-N/P is affected by factors such as geography, climate and soil, the temperature-physiology hypothesis holds that plant metabolism is more sensitive to temperature, and plant physiological domestication and adaptation increase plant LNC and LPC, while L-N/P increases with the decrease of temperature (Reich and Oleksyn, 2004). Results from a global database confirm that plant LNC and LPC are higher at high latitudes (Tian et al., 2017), and change from relative P limit to N limit (i.e., L-N/P increase) with increasing latitudes (Du et al., 2020).

Acer catalpifolium had a small geographical distribution gradient (the mid-latitude variation range in this survey was

10.3389/fpls.2022.1052565

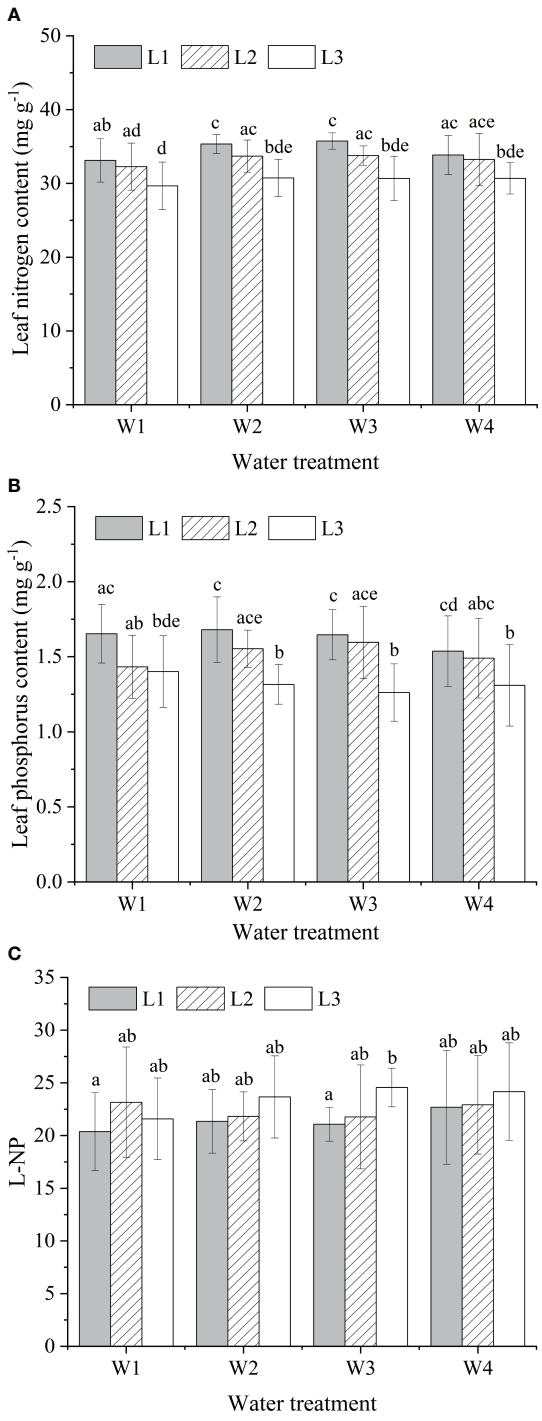

FIGURE 4
Effects of water and light on characteristics of leaf N and P of *Acer catalpifolium*. **(A)** leaf N content, **(B)** leaf P content and **(C)** leaf N/P ratio.

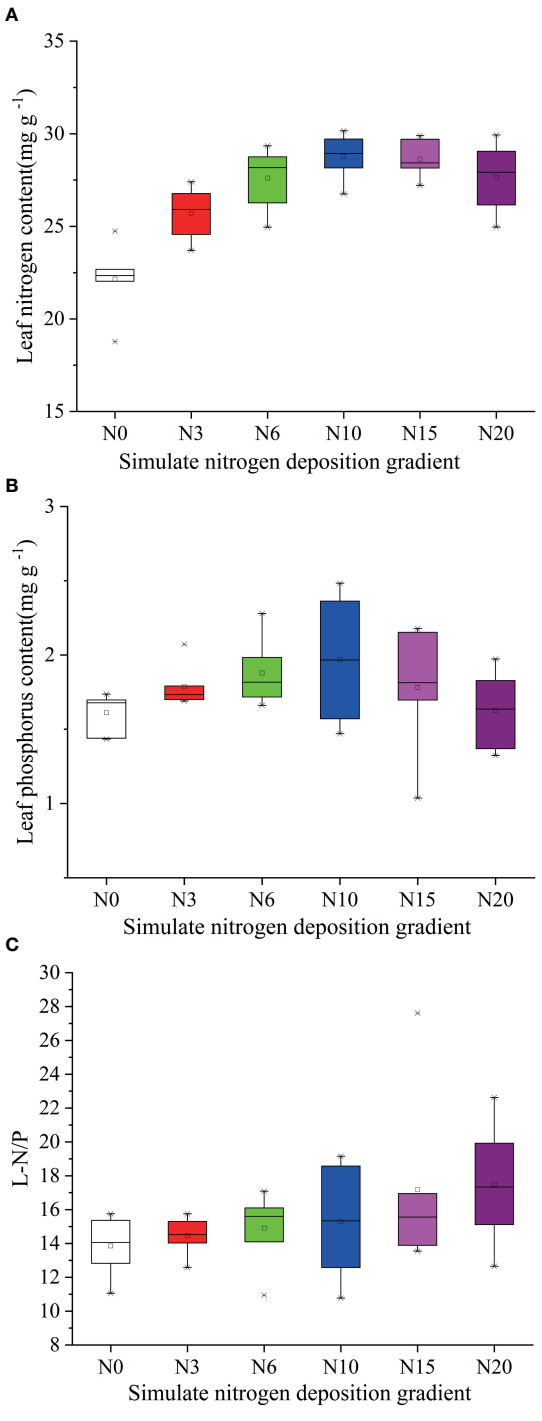

FIGURE 5
Effects of simulated N deposition on characteristics of leaf N and P of *Acer catalpifolium*. **(A)** leaf N content, **(B)** leaf P content and **(C)** leaf N/P ratio.

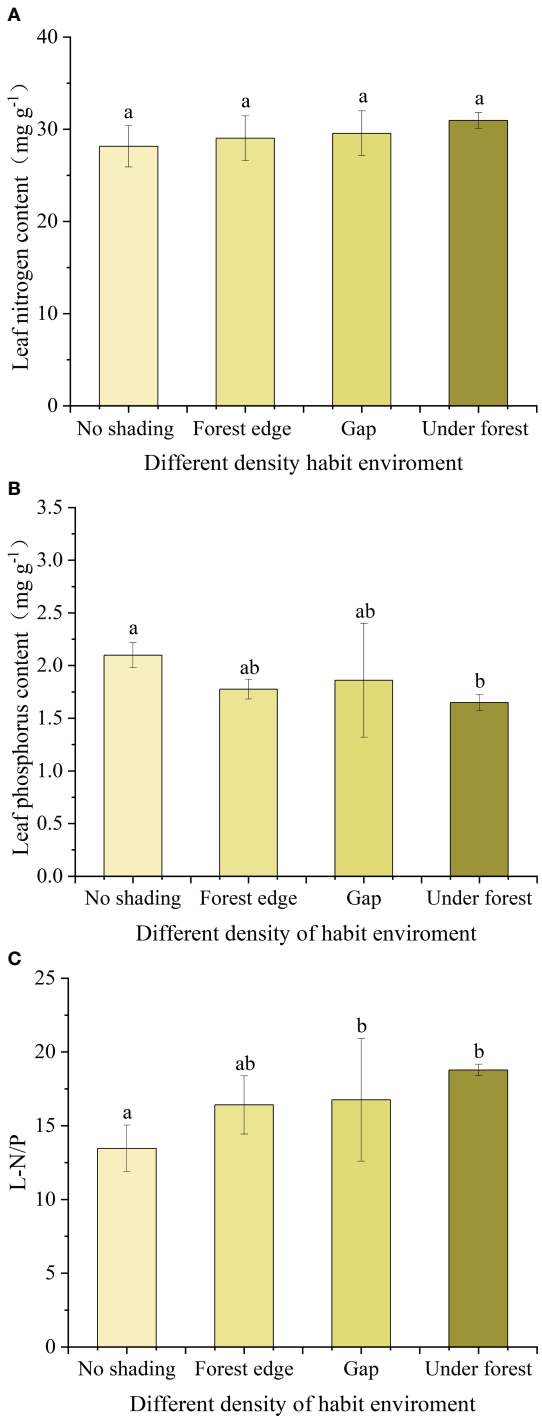

FIGURE 6
Effects of different light conditions on characteristics of leaf N and P of *Acer catalpifolium*. **(A)** leaf N content, **(B)** leaf P content and **(C)** leaf N/P ratio.

only 29.36°~32.24°). Therefore, the contribution of geographical explanation variables to N and P stoichiometry of *A. catalpifolium* was weak according to stepwise regression analysis. The soil substrate age hypothesis predicts that the restriction of P increases gradually from geologically young Arctic to tropical regions and is mainly limited by less weathered phosphate rock (Chadwick et al., 1999), and the biogeochemical hypothesis pointed out the storage capacity of plants available nutrients in the soil largely reflect the current status of leaf nutrients (McGroddy et al., 2004). In this study, soil available N (ammonium N + nitrate N) and soil available P (Olsen-P) contributed the most to the changes of N and P stoichiometry of *A. catalpifolium*, both of which reached significant levels. Among species factors, stepwise regression analysis showed that there was a negative correlation between DBH of *A. catalpifolium* and LNC, which was inconsistent with previous studies (Liu et al., 2020). In this survey, the DBH of *A. catalpifolium* had a large variation range (The DBH ranges from 8 cm to 54 cm), and the correlation between DBH and LNC used different tree ages which may be responsible for the difference from previous findings.

Light and water are key factors that limit plant growth, plant growth rate hypothesis holds that the relative growth rate of plants depends on the rate of protein synthesis (restricted by P-rich ribosomal RNA), in other words, the relative growth rate of plants is positively correlated with plant P concentration and P/N (Ågren, 2008; Peng et al., 2011). The relative growth rate of *A. catalpifolium* decreased with the decrease of light conditions (Zhang et al., 2019), and its corresponding LNC and LPC also decreased (especially under W2 and W3 moisture conditions), while L-N/P showed an increasing trend. This is consistent with previous studies (Wang et al., 2013); The plants in the water-light test had significantly higher LNC but lower LPC than those in the *A. catalpifolium* distribution area, and the higher LNC was mainly due to the high frequency of water recharge in the greenhouse test that facilitated soil N mineralization (Dijkstra et al., 2016), while the soil used in this study was typical calcareous fluvo-aquic soil in north China, and the reaction between soil P and calcium limited the effectiveness of P thus making the LPC relatively (Graf, 1980). Moreover, differences in NP stoichiometry at different growth stages (saplings were studied in the water and light trials) likewise made an important contribution to the differences in leaf nutrients between the two sites.

In the acid deposition study, the LNC of *A. catalpifolium* was similar to that of plants in the distribution area but differed significantly from the Beijing water and light test (Figure 4), consistent with previous studies on *Acer mono* at different study sites also found large differences in LNC concentrations (27.91 ± 0.58 mg g^{-1} in Beijing and 12.99 ± 1.30 mg g^{-1} in Shanxi) but small differences in LPC (Song et al., 2019). Acid rain acting on plant leaves alters cell permeability thereby leaching important elements from the leaves thus affecting leaf morphology and physiological functions (Zeng et al., 2005; Liu et al., 2018). LNC was significantly lower in the NL2.5 treatment but similar changes were not observed under sulfuric acid dominant acid rain treatment, further demonstrating that HNO_3 has a stronger

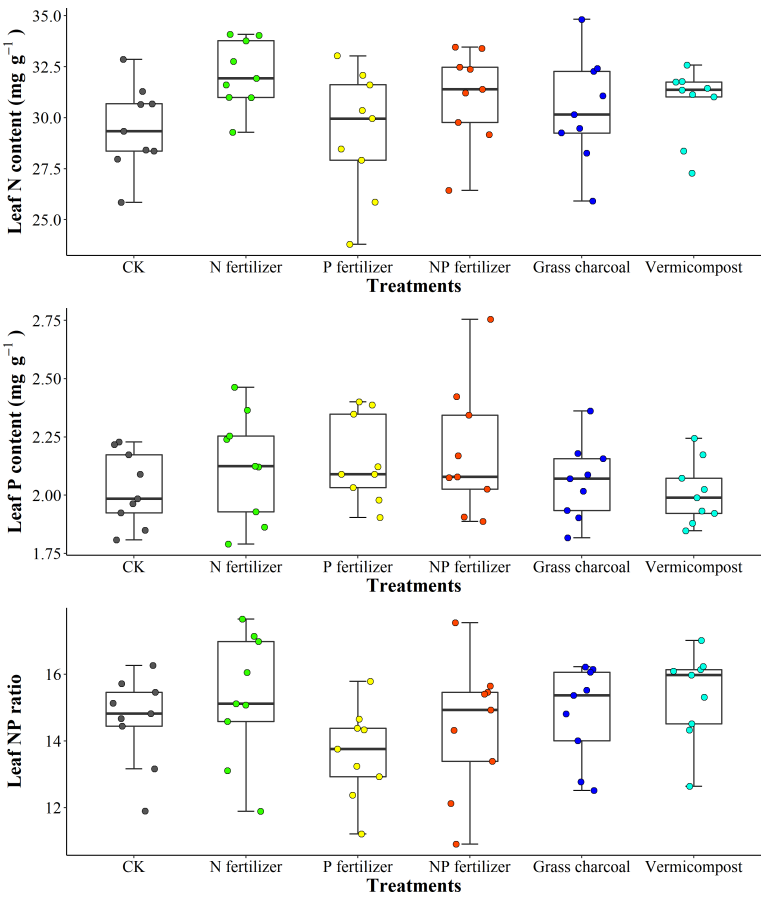

FIGURE 7
Effects of different soil fertility improvement measures on characteristics of leaf N and P of *Acer catalpifolium*.

effect on leaf related to stronger oxidative stress on physiological activity than H_2SO_4. In addition, the LNC increased significantly under the low acidity treatment and was slightly higher than CK, which is consistent with previous studies (Hu et al., 2019), The presence of abundant available N in acid rain at low acidity is beneficial for leaf uptake, counteracting the negative effects of acid rain or even further enhancing leaf physiological activities such as increasing LNC, chlorophyll and photosynthetic rate (Dong et al., 2017a; Dong et al., 2017b). Differing from leaf acid spraying, soil acid addition directly enriched the available N pool in soil and aided in nutrient uptake of *A. catalpifolium*. Additionally, the soil acidification due to the continuous input of exogenous H^+ and could improve P acquisition by plants, just like the simulated forest soil acidification experiment, soil P bioeffectiveness was found to be increased by 15-30% (Ohno and Amirbahman, 2010), and similar patterns were observed in other agricultural fields and water bodies (Kopáček et al., 2015; Wang et al., 2017). In the simulated acid rain experiment, the CK of *A. catalpifolium* showed co-limitation of N and P (Table 2). Leaf acid spray did not significantly change L-N/P in our study, but the LPC elevation was high under the soil acid addition treatment (especially high acidity treatment) and the leaves shifted from NP co-limitation to N limitation. These results were consistent with Hu et al. (2019) 's study on the influence of simulated acid rain on the stoichiometry of *Camellia sinensis*. However, it is worth noting that this experiment was only conducted for one year of continuous acid addition and the results may change in long-term acid addition. With the long-term aggravation of soil acidification, the mobility of Al, Mn and other elements can further increase and make toxic conditions in the plant that limit the plant growth and P absorption efficiency (Yang et al., 2008).

Environmental N (atmospheric N deposition) into terrestrial ecosystems effectively increases N uptake by plants. Simulated N deposition (N addition) was found to increase LNC by 22% (from 225 observations) in terrestrial ecosystem plants, and LNC by 30% approximately (from128 observations) in temperate forests (Sardans et al. (2017)). Similarly, the LNC of catalpa

10.3389/fpls.2022.1052565

TABLE 2 Effects of simulated acid deposition on characteristics of leaf N and P of *Acer catalpifolium*.

Added method	Treatments	Acidity	LNC(mg g^{-1})	LPC(mg g^{-1})	L-N/P
—	CK	—	22.15 ± 1.93bcd	1.61 ± 0.14bc	13.85 ± 1.78ab
Leaf spray	NL	2.5	20.46 ± 2.96b	1.42 ± 0.29b	14.79 ± 2.89ab
		3.5	23.03 ± 3.75ab	1.48 ± 0.37bd	16.95 ± 7.11a
		4.5	24.72 ± 3.71ac	1.59 ± 0.24bc	15.82 ± 2.76ac
	SL	2.5	22.08 ± 3.35bc	1.44 ± 0.23b	15.47 ± 2.61acd
		3.5	22.52 ± 3.21ab	1.57 ± 0.18bc	14.59 ± 3.02ab
		4.5	21.72 ± 3.85bc	1.51 ± 0.28bc	14.50 ± 1.85ab
Soil added	NS	2.5	25.68 ± 1.72ad	2.41 ± 0.85a	11.44 ± 2.81b
		3.5	25.01 ± 3.35ac	1.97 ± 0.44acd	13.04 ± 2.59bc
		4.5	25.88 ± 2.36a	2.01 ± 0.29ac	13.01 ± 1.24bc
	SS	2.5	23.53 ± 3.36ab	2.22 ± 0.60a	11.33 ± 3.56b
		3.5	24.36 ± 2.37ac	2.14 ± 0.49a	11.79 ± 2.15b
		4.5	24.82 ± 3.21ac	2.16 ± 0.62ac	12.06 ± 2.83bd

maple was found to be increased by 16-30% under the influence of simulated deposition and the response of LPC to N deposition was lower relative to LNC (Sardans et al., 2017). Some studies targeting the aboveground parts of plants have also concluded that N addition significantly reduces P concentration (Li et al., 2016a; Deng et al., 2017), it has also been suggested that plants can respond to increased N resources by increasing P uptake or by enhancing P resorption capacity (Sardans et al., 2012a). The weak response of LPC to simulated N deposition found in this study, L-N/P increased significantly by 15% and *A. catalpifolium* shifted from a co-limitation of N and P to a limitation of P (especially N15 and N20 treatments). Similarly, a previous study based on data integration has found that N addition can increase L-N/P by 10-27% (Sardans et al., 2017).

In the wild reintroduction experiment, the LNC responded to the N fertilizer, P fertilizer and N, P fertilizer treatments by the same mechanism as the simulated N deposition plant response. We found that the LPC under N and P treatments increased by 6% and 8% compared to CK, respectively, which is lower than the previous findings on LPC (Sardans et al., 2017) and the difference may be related to the frequency of fertilizer addition (only twice) and treatment cycle (Li et al., 2016b; Li et al., 2019). In this study of field habitat selection, the change of L-N/P of *A. catalpifolium* was also small, and L-N/P was reduced by P application, which was consistent with previous research results (Sardans et al., 2017). However, we observed non-significant increase in L-N/P between N and NP treatments (Figure 7C). A study pointed out that long-term N addition had a more significant change in L-N/P (Fujita et al., 2010). Among the fertilization treatments, peat soil and vermicompost mainly improved soil structure and promoted root growth, and N and P concentration and N and P ratio in leaves of *A. catalpifolium* showed little response to the addition of two substrates (Figure 7C). However, further follow-up studies are needed to clarify the long-term effects of substrate addition.

In the habitat experiment with different canopy densities, the essence is to explore the effects of different light environments on the nutrients of *A. catalpifolium*. The LNC of *A. catalpifolium* showed a weak response to different canopy density treatments, but the LPC of *A. catalpifolium* growing under the forest was relatively low, resulting in a relatively high L-N/P. This is consistent with the results of the water-light experiment and is consistent with the plant growth rate hypothesis, namely, the increase of P uptake by plants with increasing light intensity is positively correlated with the P/N (Ågren, 2008; Peng et al., 2011).

Conclusion

The stoichiometric characteristics of N and P in leaves of *A. catalpifolium* in field population and applied with different treatments were studied. The results showed that the LNC, LPC and L-N/P in the field population were 14.49~25.44 mg g^{-1}, 1.29~3.81 mg g^{-1}, and 4.87~13.93 respectively. The N/P in the wild population was affected by soil available N and P. The LNC and LPC were higher under high light treatment. Under simulated N deposition, LNC and LPC of *A. catalpifolium* were the highest applied with N10 treatment, while L-N/P was the highest for N20 treatment. Under simulated acid deposition, LNC and LPC were higher in soil application with high acidity treatment and L-N/P was high in leaf application. Applied to different canopy closure habitats, LNC of *A. catalpifolium* was higher, LPC was lower in the understory, and L-N/P was higher in gap and understory habitats. The LNC of N fertilizer treatment was significantly increased compared with the CK, while the LPC of *A. catalpifolium* increased slightly under substrate and fertilization, and the L-N/P of *A. catalpifolium* was lower under P fertilization. These results provide solid guidance for field management and nutrient supply regimes

for the future protection and population rejuvenation of this species. Moreover, this provides guidelines to develop and implement a suitable management strategy such as conservation and nutrient management, and translocation plan to manage the regeneration of populations and help prevent the loss of remaining populations.

Data availability statement

The raw data supporting the conclusions of this article will be made available by the authors, without undue reservation.

Author contributions

ZS and RL conceived and designed the study and provided suggestions and comments for the manuscript. YZ and XC collected and analyzed the data and wrote the manuscript. SL and YZ collected the samples. BD, ML, and RL revised the manuscript. All authors read and approved the manuscript.

Funding

This research was supported by the National Key Research and Development Plan "Research on protection and restoration of typical small populations of wild plants" (Grant No. 2016YFC0503106).

Conflict of interest

The authors declare that the research was conducted in the absence of any commercial or financial relationships that could be construed as a potential conflict of interest.

Publisher's note

All claims expressed in this article are solely those of the authors and do not necessarily represent those of their affiliated organizations, or those of the publisher, the editors and the reviewers. Any product that may be evaluated in this article, or claim that may be made by its manufacturer, is not guaranteed or endorsed by the publisher.

References

Ackerman, D., Millet, D. B., and Chen, X. (2018). Global estimates of inorganic nitrogen deposition across four decades. *Global Biogeochem. Cycles* 33, 100–107. doi: 10.1029/2018GB005990

Ågren, G. (2008). Stoichiometry and nutrition of plant growth in natural communities. *Annu. Rev. Ecol. Evol. Syst.* 39, 153–170. doi: 10.1016/j.chnaes.2017.10.003

Allen, A., and Gillooly, J. (2009). Towards an integration of ecological stoichiometry and the metabolic theory of ecology to better understand nutrient cycling. *Ecol. Lett.* 12, 369–384. doi: 10.1111/j.1461-0248.2009.01302.x

Braun, S., Thomas, V., Quiring, R., and Flückiger, W. (2009). Does nitrogen deposition increase forest production? the role of phosphorus. *Environ. Pollut.* 158, 2043–2052. doi: 10.1016/j.envpol.2009.11.030

Chadwick, O. A., Derry, L. A., Vitousek, P. M., Huebert, B. J., and Hedin, L. O. (1999). Changing sources of nutrients during four million years of ecosystem development. *Nature* 397, 491–497. doi: 10.1038/17276

Chapin, F. S., Autumn, K., and Pugnaire, F. (1993). Evolution of suites of traits in response to environmental stress. *Am. Nat.* 142, S78–S92. doi: 10.1086/285524

Chapin, F. S., Schulze, E., and Mooney, H. A. (1990). The ecology and economics of storage in plants. *Annu. Rev. Ecol. Syst.* 21, 423–447. doi: 10.1146/ANNUREV.ES.21.110190.002231

Demars, B., and Edwards, A. (2007). Tissue nutrient concentrations in freshwater aquatic macrophytes: High inter-taxon differences and low phenotypic response to nutrient supply. *Freshw. Biol.* 52, 2073–2086. doi: 10.1111/j.1365-2427.2007.01817.x

Deng, Q., Hui, D., Dennis, S., and Reddy, K. (2017). Responses of terrestrial ecosystem phosphorus cycling to nitrogen addition: A meta-analysis. *Global Ecol. Biogeogr.* 26. doi: 10.1111/geb.12576

Dijkstra, F., Carrillo, Y., Aspinwall, M., Maier, C., Canarini, A., Tahaei, H., et al. (2016). Water, nitrogen and phosphorus use efficiencies of four tree species in response to variable water and nutrient supply. *Plant Soil* 406, 187–199. doi: 10.1007/s11104-016-2873-6

Dong, D., Sun, Z., Zeng, X., and Vries, W. (2017a). Non-linear direct effects of acid rain on leaf photosynthetic rate of terrestrial plants. *Environ. Pollut.* 231, 1442–1445. doi: 10.1016/j.envpol.2017.09.005

Dong, D., Zeng, X., Sun, Z., Jiang, X., and Vries, W. (2017b). Direct effect of acid rain on leaf chlorophyll content of terrestrial plants in China. *Sci. Total Environ.* 605-606, 764–769. doi: 10.1016/j.scitotenv.2017.06.044

Du, E., Terrer, C., Pellegrini, A. F. A., Ahlström, A., Van Lissa, C. J., Zhao, X., et al. (2020). Global patterns of terrestrial nitrogen and phosphorus limitation. *Nat. Geosci.* 13, 221–226. doi: 10.1038/s41561-019-0530-4

Elser, J., and Hamilton, A. (2007). Stoichiometry and the new biology: The future is now. *PloS Biol.* 5, e181. doi: 10.1371/journal.pbio.0050181

Fujita, Y., Robroek, B. J. M., De Ruiter, P. C., Heil, G. W., and Wassen, M. J. (2010). Increased n affects p uptake of eight grassland species: the role of root surface phosphatase activity. *Oikos* 119, 1665–1673. doi: 10.1111/j.1600-0706.2010.18427.x

Gargallo-Garriga, A., Sardans, J., PeéRez-Trujillo, M. R., Oravec, M., Urban, O., Jentsch, A., et al. (2015). Warming differentially influences the effects of drought on stoichiometry and metabolomics in shoots and roots. *New Phytol.* 207, 591–603. doi: 10.1111/nph.13377

Gargallo-Garriga, A., Sardans, J., PeéRez-Trujillo, M. R., Rivas-Ubach, A., Oravec, M., Večeřová, K., et al. (2014). Opposite metabolic responses of shoots and roots to drought. *Sci. Rep.* 4, 6829. doi: 10.1038/srep06829

Graf, D. L. (1980). Chemical equilibria in soils. *Clays Clay Miner.* 28, 319–319. doi: 10.1346/CCMN.1980.0280411

Güsewell, S. (2004). N : P ratios in terrestrial plants: variation and functional significance. *New Phytol.* 164, 243–266. doi: 10.1111/j.1469-8137.2004.01192.x

Han, W., Fang, J., Guo, D., and Zhang, Y. (2005). Leaf nitrogen and phosphorus stoichiometry across 753 terrestrial plant species in China. *New Phytol.* 168, 377–385. doi: 10.1111/j.1469-8137.2005.01530.x

He, M., and Dijkstra, F. (2014). Drought effect on plant nitrogen and phosphorus: A meta-analysis. *New Phytol.* 204, 924-931. doi: 10.1111/nph.12952

Huang, W., Zhou, G., Liu, J., Zhang, D., Xu, Z., and Liu, S. (2012). Effects of elevated carbon dioxide and nitrogen addition on foliar stoichiometry of nitrogen and phosphorus of five tree species in subtropical model forest. *Environ. pollut.* 168, 113–120. doi: 10.1016/j.envpol.2012.04.027

Hu, X., Wu, A. Q., Wang, F., and Chen, F. S. (2019). The effects of simulated acid rain on internal nutrient cycling and the ratios of mg, Al, Ca, n, and p in tea plants of a subtropical plantation. *Environ. Monit. Assess.* 191, 99. doi: 10.1007/s10661-019-7248-z

IBM Corp (2013). *IBM SPSS Statistics for windows, version 22.0* (Armonk, NY: IBM Corp).

Kopáček, J., Hejzlar, J., Kaňa, J., Norton, S., and Stuchlik, E. (2015). Effects of acidic leposition on in-lake phosphorus availability: A lesson from lakes recovering from acidification. *Environ. Sci. Technol.* 49 (5), 2895–2903. doi: 10.1021/es5058743

Li, F., Dudley, T. L., Chen, B., Chang, X., Liang, L., and Peng, S. (2016a). Responses of tree and insect herbivores to elevated nitrogen inputs: A meta-analysis. *Acta Oecol.* 77, 160–167. doi: 10.1016/j.actao.2016.10.008

Li, Y., Niu, S., and Yu, G. (2016b). Aggravated phosphorus limitation on biomass production under increasing nitrogen loading: a meta-analysis. *Global Change Biol.* 22, 934–943. doi: 10.1111/gcb.13125

Liu, X., Fu, Z., Zhang, B., Zhai, L., Meng, M., Lin, J., et al. (2018). Effects of sulfuric, nitric, and mixed acid rain on Chinese fir sapling growth in southern China. *Ecotoxicol. Environ. Saf.* 160, 154–161. doi: 10.1016/j.ecoenv.2018.04.071

Liu, M., Song, Y., Xu, T., Xu, Z., Wang, T., Yin, L., et al. (2020). Trends of precipitation acidification and determining factors in China during 2006–2015. *J. Geophys. Res.: Atmos.* 125, e2019JD031301. doi: 10.1029/2019JD031301

Li, W., Zhang, H., Huang, G., Liu, R., Wu, H., Zhao, C., et al. (2019). Effects of nitrogen enrichment on tree carbon allocation: A global synthesis. *Global Ecol. Biogeogr.* 29, 573-589. doi: 10.1111/geb.13042

McGroddy, M., Daufresne, T., and Hedin, L. (2004). Scaling of C:N:P stoichiometry in forests worldwide: Implications of terrestrial redfield-type ratios. *Ecology* 85 (9), 2390–2401. doi: 10.1890/03-0351

Ohno, T., and Amirbahman, A. (2010). Phosphorus availability in boreal forest soils: A geochemical and nutrient uptake modeling approach. *Geoderma* 155, 46–54. doi: 10.1016/j.geoderma.2009.11.022

Peng, Y., Niklas, K., and Sun, S. (2011). The relationship between relative growth rate and whole-plant c: N: P stoichiometry in plant seedlings grown under nutrient-enriched conditions. *J. Plant Ecol.* 4, 147–156. doi: 10.1093/jpe/rtq026

R Core Team (2021). *R: A language and environment for statistical computing* (Vienna, Austria: R Foundation for Statistical Computing). doi: 10.1890/0012-9658(2002)083[3097:CFHIWS]2.0.CO;2

Reich, P., and Oleksyn, J. (2004). Global patterns of plant leaf n and p in relation to temperature and latitude. *Proc. Natl. Acad. Sci. U. S. A.* 101, 11001–11006. doi: 10.1073/PNAS.0403588101

Sardans, J., Grau, O., Chen, H. Y. H., Janssens, I. A., Ciais, P., Piao, S., et al. (2017). Changes in nutrient concentrations of leaves and roots in response to global change factors. *Global Change Biol.* 23, 3849–3856. doi: 10.1111/gcb.13721

Sardans, J., Rivas-Ubach, A., and Penuelas, J. (2012a). The C:N:P stoichiometry of organisms and ecosystems in a changing world: A review and perspectives. *Perspect. Plant Ecol. Evol. Syst.* 14, 33–47. doi: 10.1016/j.ppees.2011.08.002

Sardans, J., Rivas-Ubach, A., and Peñuelas, J. (2012b). The elemental stoichiometry of aquatic and terrestrial ecosystems and its relationships with organismic lifestyle and ecosystem structure and function: a review and perspectives. *Biogeochemistry* 111, 1–39. doi: 10.1007/s10533-011-9640-9

Sha, Z. P., Lv, T. T., Staal, M., Ma, X., Wen, Z., Li, Q. Q., et al. (2020). Effect of combining urea fertilizer with p and K fertilizers on the efficacy of urease inhibitors under different storage conditions. *J. Soils Sediments* 20, 2130–2140. doi: 10.1007/s11368-019-02534-w

Song, Z., Liu, Y., Su, H., and Hou, J. (2019). N-p utilization of acer mono leaves at different life history stages across altitudinal gradients. *Ecol. Evol.* 10, 851-862. doi: 10.1002/ece3.5945

Tian, D., Yan, Z., Niklas, K., Han, W., Kattge, J., Reich, P., et al. (2017). Global leaf nitrogen and phosphorus stoichiometry and their scaling exponent. *Natl. Sci. Rev.* 5, 728-739. doi: 10.1093/nsr/nwx142

Vitousek, P. M., Porder, S., Houlton, B. Z., and Chadwick, O. A. (2010). Terrestrial phosphorus limitation: mechanisms, implications, and nitrogen-phosphorus interactions. *Ecol. Appl.* 20, 5–15. doi: 10.1890/08-0127.1

von Liebig, J. (1855). "Principles of agricultural chemistry with special reference to the late researches made in England," in *Cycles of essential elements*, vol. vol. 1 . Ed. L. R. Pomeroy (London: Dowden, Hutchinson, and Ross), 11–28.

Wang, J., Hui, D., Ren, H., Liu, Z., and Yang, L. (2013). Effects of understory vegetation and litter on plant pitrogen (N), phosphorus (P), N : P ratio and their relationships with growth rate of indigenous seedlings in subtropical plantations. *PloS One* 8, e84130. doi: 10.1371/journal.pone.0084130

Wang, C., Zhou, J., Liu, J., Wang, L., and Xiao, H. (2017). Reproductive allocation strategy of two herbaceous invasive plants across different cover classes. *Polish J. Environ. Stud.* 26, 355–364. doi: 10.15244/pjoes/64240

Wassen, M. J., Venterink, H. O., Lapshina, E. D., and Tanneberger, F. (2005). Endangered plants persist under phosphorus limitation. *Nature* 437, 547–550. doi: 10.1038/nature03950

Yang, J., Lee, W. Y., Ok, Y. S., and Skousen, J. (2008). Soil nutrient bioavailability and nutrient content of pine trees (*Pinus thunbergii*) in areas impacted by acid deposition in Korea. *Environ. Monit. Assess.* 157, 43–50. doi: 10.1007/s10661-008-0513-1

Yu, Q., Chen, Q., Elser, J. J., He, N., Wu, H., Zhang, G., et al. (2010). Linking stoichiometric homoeostasis with ecosystem structure, functioning and stability. *Ecol. Lett.* 13, 1390–1399. doi: 10.1111/j.1461-0248.2010.01532.x

Yu, Q., Elser, J., He, N., Wu, H., Quansheng, C., Zhang, G., et al. (2011). Stoichiometry homeostasis of vascular plants in the inner Mongolia grassland. *Oecologia* 166, 1–10. doi: 10.1007/s00442-010-1902-z

Zeng, G., Zhang, G., Huang, G., Jiang, Y., and Liu, H. (2005). Exchange of Ca^{2+}, Mg^{2+} and k^{+} and uptake of h^{+}, NH4+ for the subtropical forest canopies influenced by acid rain in shaoshan forest located in central south China. *Plant Sci.* 168, 259–266. doi: 10.1016/j.plantsci.2004.08.004

Zhang, Y. Y., Ma, W. B., Yu, T., Ji, H. J., Gao, J., Li, J. Q., et al. (2018). Population structure and community characteristics of *Acer catalpifolium* rehd. *Chin. J. Appl. Environ. Biol.* 24 (4), 0697–0703. doi: 10.19675/j.cnki.1006-687x.2017.09040

Zhang, Y. Y., Tian, C., Yu, T., Buddhi, D., Fu, B., Senaratne, S., et al. (2021a). Differential effects of acid rain on photosynthetic performance and pigment composition of the critically endangered *Acer amplum* subsp. catalpifolium. *Global Ecol. Conserv.* 30, e01773. doi: 10.1016/j.gecco.2021.e01773

Zhang, Y. Y., Yu, T., Ma, W. B., Buddhi, D., Kenji., I., and Li, J. Q. (2021b). Morphological, physiological and photophysiological responses of critically endangered acer catalpifolium to acid stress. *Plants* 10, 1958. doi: 10.3390/plants10091958

Zhang, Y. Y., Yu, T., Ma, W. B., Tian, C., Sha, Z. P., and Li, J. Q. (2019). Morphological and physiological response of *Acer catalpifolium* rehd. seedlings to water and light stresses. *Global Ecol. Conserv.* 19, e00660. doi: 10.1016/j.gecco.2019.e00660

Zhang, Y. Y., Yu, T., Ma, W. B., Wang, F., Tian, C., and Li, J. Q. (2020). Physiological and morphological effects of different canopy densities on reintroduced *Acer catalpifolium*. *Biodivers. Sci.* 28 (3), 323–332. doi: 10.17520/biods.2019190

frontiers | Frontiers in Plant Science

TYPE Original Research
PUBLISHED 16 November 2023
DOI 10.3389/fpls.2023.1280794

OPEN ACCESS

EDITED BY
Claudia Cocozza,
University of Florence, Italy

REVIEWED BY
Manoj Kumar Solanki,
University of Silesia in Katowice, Poland
Gabriela Jamnicka,
Slovak Academy of Sciences (SAS), Slovakia

*CORRESPONDENCE
Lazar Pavlović
lazar.pavlovic@polj.edu.rs

RECEIVED 21 August 2023
ACCEPTED 01 November 2023
PUBLISHED 16 November 2023

CITATION
Vuksanović V, Kovačević B, Kebert M, Pavlović L, Kesić L, Čukanović J and Orlović S (2023) *In vitro* selection of drought-tolerant white poplar clones based on antioxidant activities and osmoprotectant content. *Front. Plant Sci.* 14:1280794. doi: 10.3389/fpls.2023.1280794

In vitro selection of drought-tolerant white poplar clones based on antioxidant activities and osmoprotectant content

Vanja Vuksanović[1], Branislav Kovačević[2], Marko Kebert[2], Lazar Pavlović[1]*, Lazar Kesić[2], Jelena Čukanović[1] and Saša Orlović[1,2]

[1]Department of Fruit Growing, Viticulture, Horticulture and Landscape Architecture, Faculty of Agriculture, University of Novi Sad, Novi Sad, Serbia, [2]Institute of Lowland Forestry and Environment, University of Novi Sad, Novi Sad, Serbia

Introduction: In light of upcoming climate change, there is an urgent requirement for tree improvement regarding adaptability to drought-caused stress and the development of quick and reliable screening methodologies for genotypes' drought tolerance. White poplar is, despite its high adaptability, considered to be an endangered tree species in Serbia, which gives it special importance in the preservation and improvement of biodiversity of riparian ecosystems. The main goal of this research was to evaluate the tolerance of five white poplar clones to the presence of polyethylene glycol (PEG 6000 molecular weight 6000) (different concentrations (e.g. 0 g/L, 1 g/L, 10 g/L, 20 g/L, and 50 g/L) in Aspen Culture Medium (ACM).

Methods: The tolerance of the clones was evaluated by using morphological parameters (shoot fresh and dry weight, root fresh and dry weight), photosynthetic pigments (contents of chlorophyll a, chlorophyll b, carotenoids, and chlorophyll a+b), and biochemical parameters (total phenolic content, total flavonoid content, ferric reducing antioxidant power, antioxidant activities (DPPH activity and ABTS assay), free proline content and glycine betaine content.

Results and Discussion: The values of morphological and photosynthetic pigments declined with an increase in the concentration of PEG 6000. At a concentration of 50 g/L, the content of shoot fresh mass decreased by 41%, the content of Chl a by 68%, Chl b by 65%, and Car by 76% compared to the control. Also, at the same medium, there was an increase in the content of total phenols, accumulation of proline, the content of glycine betaine as well as in antioxidant activity. Based on the obtained results, it can be assumed that more drought-tolerant clones are characterized by high values for biomass, high content of photosynthetic pigments, and high content of proline and glycine betaine in conditions similar to drought *in vitro*. Clone L-80 showed better results in most of the tested parameters, especially compared to the reference clone Villafranca.

KEYWORDS

abiotic stress, polyethylene glycol, tissue culture, proline, glycine betaine

1 Introduction

Drought is one of the leading abiotic factors that negatively affect the growth and productivity of plant species, which can have incalculable ecological and economic consequences (Chen and Murata, 2011). Climate change does and is expected to bring considerable problems through extreme changes in temperature and precipitation in the 21st century (IPCC, 2023). Over the past 5 years, more than half of Europe has been affected by extreme drought conditions, with major consequences for agriculture, inland waterway transport, forestry, society, and biodiversity (Ionita et al., 2022). Researchers estimated that if no climate adaptation strategies are developed and adopted in the near future, drought disruption may result in an economic loss of more than €100 billion (Mohammed et al., 2022). There is a need to reduce this risk by improving plant growth under drought-stress conditions (Ashry et al., 2022).

White poplar (*Populus alba* L.) is an indigenous species of the Republic of Serbia, which is widely used in the production of lumber, pulp, and paper, while its biomass has great potential as a source of energy. It occurs in a wide distribution range from the Mediterranean to central Asia. It is characterized by fast growth, a powerful root system, resistance to smoke and harmful gases in the air, and many other abiotic agents except prolonged flooding. However, despite its high adaptability, according to the European Forest Genetic Resources Programme (EUFORGEN) database on forest genetic resources (2003), the white poplar is classified as endangered throughout Europe. As a component of floodplain mixed forests, which are ecosystems with high biodiversity and are seriously endangered by human activity, white poplar plays a significant ecological role. In this sense, in recent years significant projects of research and preservation of variability, restoration, and reforestation with white poplars have been carried out in most European countries (EUFORGEN).

Breeding in poplars is characterized by intense evolution: from a selection of accessions from the natural stands and controlled breeding to the implementation of contemporary biotechnological methodologies (Stanton et al., 2010). Nowadays, poplar breeding programs pay more attention to tolerance to the various abiotic agents, especially drought, due to climate change, implementing advances in genomic and phenotypic tools (Rosso et al., 2023). Estimation of a plant's tolerance to drought is a very complex process due to various interactions between drought and various physiological and biochemical phenomena that affect plant growth and development (Razmjoo et al., 2008). (Rubio et al., 2002) state that the symptoms of drought can also occur with other abiotic factors, such as salinity, and high and low temperature. In this sense, *in vitro* culture is one of the suitable models for quick assessment of the forest trees' tolerance to abiotic agents in relatively controlled conditions opposite to all limitations in field trials caused by multiannual growth and development of tree species, such as a large area that is needed for the establishment of experiments in the field conditions, as well as the hardly controllable influence of the external multifactorial stressors present in the natural environment. The basic approach to overcoming the problem of climate change, and thus drought as a leading abiotic stressor, is precisely the selection of species and the creation of tolerant varieties. That is why it is very important to know the underlying mechanisms of tolerance of plants, especially forest woody species, to drought. As the white poplar is considered to be a model forest tree species in biotechnological research (Confalonieri et al., 2000), the development of *in vitro* drought tolerance assessment methodology is important for the improvement of testing and selection process in white poplar, but also in other forest tree species. The *in vitro* technique has been proven as an effective, cheap, and fast method in the vegetative propagation of white poplar. Also, the advantages of testing white poplar clones *in vitro* conditions compared to field trials are multiple: a greater number of repetitions, a quick response, a greater number of clones, controlled conditions, and testing can be done throughout the year. One of the main disadvantages is the fact that conditions in the field are not controlled and usually the plant is not affected only by one but a series of abiotic and biotic factors. In contrast, *in vitro*, techniques provide good opportunities for studying and understanding the effect of single stress on different physiological processes and interactions and the selection of promising clones in conditions that can be efficiently controlled. *In vitro* cultures have been used to assess drought tolerance in numerous plant species: potato (*Solanum tuberosum* L.) (Hanász et al., 2022), rice (Biswas et al., 2002), guava (*Psidium guajava* L.) (Youssef et al., 2016), blueberry (*Vaccinium corymbosum* L.) (Molnar et al., 2022), "Mexican lime" (*Citrus aurantifolia* (Christ.) Swingle) (Jafari and Shahsavar, 2022), Mexican marigold (*Tagetes minuta* L.) (Babaei et al., 2021), *Stevia rebaudiana* (Bertoni) (Hajihashemi and Sofo, 2018), *Agave salmiana* (Puente-Garza et al., 2017), Wild cherry (*Prunus avium* L.) (Vuksanović et al., 2022), olives (*Olea europaea* L.) (Silvestri et al., 2017), kiwifruit (*Actinidia chinensis* Planch.), (Wu et al., 2019), fig tree (*Ficus carica* L.) (Abdolinejad and Shekafandeh, 2022) and euramerican poplar (Popović et al., 2017). Erst and Karakulov (2023) analyzed resistance of three *Populus alba*×*P. bolleana* and *P. davidiana*×*P. bolleana* regenerants *in vitro* to osmotic stress induced by d-mannitol. Beside numerous drought tolerance studies in hydroponic (Popović et al., 2016; Ždero-Pavlović et al., 2020), greenhouse (Cocozza et al., 2016; Kebert et al., 2022a), and field (Lei et al., 2006) conditions, there is still a small amount of data on drought tolerance of forest tree species *in vitro*.

Since polyethylene glycol (PEG 6000), a neutral high-molecular weight polymer, simulates a water deficit by forming multiple hydrogen bonds with water and rendering it inaccessible to plants, it is widely used to induce osmotic stress *in vitro* (Mozafari et al., 2018; Hanász et al., 2022). Drought frequently results in oxidative stress, which modifies the redox status of plants. An imbalance between the generation of reactive oxygen species (ROS) in cells and tissues and the antioxidant defense systems that neutralize these detrimental ROS is known as oxidative stress. To overcome oxidative stress, plants evolved various defense mechanisms, including enhanced biosynthesis of compounds with strong antioxidant capacity such as polyphenols, carotenoids, proline, glycine betaine, etc. (Safaei Chaeikar et al., 2020; Babaei et al., 2021). Because of their unique structure of highly conjugated system and abundance of hydroxyl groups, particularly the 3-

hydroxy groups in flavonols, phenolic compounds have a potent antioxidant effect in higher plants (Urquiaga and Leighton, 2000). Polyphenols are able to directly scavenge ROS, prevent initiation of lipid peroxidation by chelating iron ions that catalyze Fenton like reactions (Tsao, 2010). Furthermore, drought upregulates overexpression of certain transcription factors and genes (such as PFG3) that are involved in flavonoid biosynthesis (Baozhu et al., 2022). Frequently, higher amounts of accumulated flavonoids are accompanied with more tolerant species varieties, genotypes to drought stress (Selmar, 2008; Agati et al., 2012).Because of its chaperone-like activity and a key role in protecting macromolecules from oxidative stress and reactive oxygen species (ROS), free proline, as a compatible osmolyte and multifunctional amino acid, is thought to be the most important indicator of drought (Kishor et al., 2005; Szabados and Savoure, 2010). Additionally, glycine betaine is one of the quaternary ammonium compounds that plays a significant role in reducing oxidative stress and drought. Although increased generation of ROS during drought leads to deterioration and oxidation of the photosynthetic systems, chloroplast membrane, and subsequent reduction of photosynthesis, some of the ROS and RNS (reactive nitrogen species), like H2O2 and NO, are important signaling molecules, which can induce stomata closing during drought and prevent water loss and drought (Babaei et al., 2021).

Numerous studies have emphasized the importance of increased total antioxidant activity and drought tolerance in different tree plants including *Populus deltoides* × *Populus nigra* (Guo et al., 2010); *Citrus aurantifolia* (Christ.) Swingle) (Jafari and Shahsavar, 2022); Persian Oak and Black Poplar (Karimi et al., 2022); Oaks (Kebert et al., 2022a); *Populus przewalskii* (Lei et al., 2006); *Morus nigra* (Özelçi et al., 2022); *Populus* × *canadensis* (Popović et al., 2017); *Olea europaea* L. (Silvestri et al., 2017).

The research is based on the hypothesis that tolerance of examined white poplar clones on the induced drought-like conditions *in vitro* could be determined on the base of morphological parameters, photosynthetic pigments, and biochemical parameters. The main goal of this research was to study the response of white poplar clones to drought-like conditions *in vitro* to select drought-tolerant clones, and analyze the relationship between examined traits. Such studies can serve as a preliminary test for the further assessment of tolerance and adaptability of clones in field conditions.

2 Materials and methods

2.1 Plant material and micropropagation

The study involved five clones of white poplar (*Populus alba* L.). There were four Serbian clones: L-80, L-12, and LBM, selected in the natural stands, and LCM, a clone of *Populus alba* var. Bolleana, a variety popular in horticulture, as well as the well-known Italian clone Villafranca (Table 1). Clone Villafranca is one of the most widespread clones of white poplar in the world, characterized by the female gender, excellent rooting of hardwood cuttings, straightness of the trunk, and vigorous growth (Confalonieri et al., 2000; Vuksanović et al., 2019a; Vuksanović et al., 2019b). Thus, in this study, it is considered as a reference clone, and the reaction of other clones on examined treatments is compared with its reaction. The selected clones have exposed a high level of variability in both phenotypic and molecular evaluation (Kovačević et al., 2013). This experiment was performed in the tissue culture laboratory of the Institute for Lowland Forestry and Environment, University of Novi Sad, Serbia at the beginning of 2019. The technique of tissue culture (micropropagation by shoot tips) was applied to obtain a sufficient quantity of virus-free and genetically identical plant material in the shortest possible time. During the dormant period of the vegetation from the collection of white poplar clones of the Institute for Lowland Forestry and Environment, the culture of shoot tips was initiated based on the buds formed from apical meristem (on modified Aspen Culture Medium (ACM) with the addition of 9 g/L agar and 20 g/L sucrose, 1 μM kinetin, 1 μM BAP and 100 mg myoinositol, adjusted to pH 5.5 before autoclaving). All of the procedures of micropropagation were carried out in a sterile environment.

TABLE 1 Examined white poplar clones.

Name of clone	Origin[a)]	Description
Villafranca	Italy	Model clone, straight, narrow tree shape
L-12	Serbia	Experimental clone, vigorous straight tree shape
L-80	Serbia	Experimental clone, vigorous straight tree shape
LCM	Serbia	Horticultural clone, "Bolleana" tree shape
LBM	Serbia	Horticultural clone, straight pyramidal tree shape

Legend: [a)]All examined clones were selected in the Institute of Lowland Forestry and Environment, Novi Sad, Serbia, except the clone "Villafranca", which was selected at Poplar Research Institute in Casa le Monferrato, Italy.

2.2 *In vitro* drought treatments

After multiplication, shoots of the same age and height (about 2.0 cm) were cultivated in sterile glass jars containing 25 ml rooting medium, consisting of ACM medium, with the addition of 9 g/L agar and 20 g/L sucrose, that was supplemented with/without polyethylene glycol (PEG 6000 SIGMA^{TM}) in the following concentrations; 0 g/L (control), 1 g/L (PEG1), 10 g/L (PEG10), 20 g/L (PEG20), and 50 g/L (PEG50), adjusted to pH 5.5 before autoclaving. The range of concentrations of PEG 6000 was made based on our preliminary tests (Vuksanović, 2019), in order to find the medium that provides considerable osmotic stress, but also achieves proper agar solidification (Osmolovskaya et al., 2018, Molnar et al. (2022), and Vuksanović et al. (2022). The sterilization of the medium was performed using an autoclave at a temperature of 121°C for 20 min. For 35 days, the plantlets were allowed to develop and grow to test the clones' tolerance to drought. The cultures were grown in controlled conditions at a temperature of t = 26 ± 2°C, under a white light of 3500 lx m^{-2} emitted by LED lamps in a 16h/8h day/night regime. The temperature was the same

during the day/night regime, and the LED lamps were turned on suddenly after the night regime. The experiment was designed as completely randomized. There were 5 explants cultured in each jar. The average value of five explants at the level of one jar represented one replication. There were three jars (replications) for each tested treatment of interaction Clone × PEG concentration.

2.3 Measurement of morphological parameters

In this research, the following parameters were measured and expressed in grams: shoot fresh weight (SFW), shoot dry weight (SDW), root fresh weight (RFW), and root dry weight (RDW). After 35 days of cultivation on the experimental medium, the plants were removed from the jars and the fresh mass of roots and leaves was measured separately on an analytical scale. After measuring the fresh weight, the plant material was freeze-dried (lyophilized) for 72 hours at a temperature gradient from -30°C to 30°C. After drying, the dry mass of roots and leaves was measured and expressed in grams.

2.4 Measurement of photosynthetic pigments

For measurements of the content of photosynthetic pigments, about 0.01 g of fresh plant material was macerated in 1 mL of 96% ethanol and centrifuged at 4000 rpm for 10 min. The content of photosynthetic pigments was determined spectrophotometrically, using a MultiScan spectrophotometer (Thermo Fisher Scientific, model Multiscan GO, USA), according to (Lichtenthaler and Wellburn, 1983). Measurements included chlorophyll a (Chl a), chlorophyll b (Chl b), carotenoids (Car), and the following derived parameter chlorophyll a+b (Chl a+b). The obtained values were expressed in mg g^{-1}.

2.5 Measurement of biochemical parameters

Ethanol extracts obtained by extracting 0.01 g of dry mass in 1 mL of 96% ethanol were used to measure biochemical parameters (excluding proline and glycine betaine).

Total phenolic content (TPC) was determined spectrophotometrically with Folin-Ciocalteu reagent according to the methodology proposed by (Kim et al., 2003), using gallic acid as the standard. Briefly, samples (25 mL ethanolic extract) were introduced into a microplate, and then, 125 µL of 0.1 mol/L Folin-Ciocalteu's reagent and 100 µL of Na_2CO_3 7.5% (w/v) were added. The results were expressed as mg of gallic acid equivalent (GAE) per g of dry weight (mg GAE g^{-1} DW).

Total flavonoid content (TFC) was measured by a spectrophotometric method as described by (Chang et al., 2002). The 30 µL of ethanolic extract was mixed with 90 µL MeOH, 6 µL 1M $NaCH_3COO$, 6 µL 10% w/v $AlCl_3$, and 150 µL of distilled water. The calibration curve was obtained from the absorbance of known concentrations of quercetin for the quantification of total flavonoids and the results were given as mg of quercetin equivalent per g of dry weight (mg QE g^{-1} DW).

Ferric-reducing antioxidant power (FRAP) was determined spectrophotometrically according to the method (Benzie and Strain, 1996). Briefly, 225 µl of FRAP reagent was added to 20 µl of ethanol extract, which was obtained by mixing acetate buffer, TPTZ solution, and $FeCl_3 \times H_2O$ in a ratio of 10:1:1. After incubation (5 minutes) the absorbance was read at 593 nm. A standard curve was constructed using ascorbic acid (AS). The obtained results are expressed in mg AS g^{-1} DW.

Determination of Antioxidant Activities (DPPH Activity and ABTS Assay) The ability to neutralize ABTS (2,2′-azinobis-(3-ethylbenzothiazoline-6-sulfonic acid) radicals was determined by the method according to (Miller and Rice-Evans, 2007), while the ability to neutralize DPPH (2, 2-diphenyl-2-picrylhydrazyl) radicals was determined spectrophotometrically by the method by (Arnao, 2000). The obtained results are expressed in percentages of RSC (radical scavenger capacity). RSC or radical scavenging capacity, represents the percentage of radical species that were neutralized by antioxidants that were present in the leaf extract. The higher the RSC of the extracts, the more efficient the extract is in scavenging and neutralize radicals is, thus higher is its antioxidant potential of extract. The percentages of RSC determined by the formula:

$$\% \text{ RSC} = 100 - (A_A - A_B) \times 100/A_C$$

where: A_A - absorption of tested extract solution, A_B - absorption of the sample dissolved in the solvent, A_C - of absorption blank sample which contains only DPPH reagent and solvent.

Free proline content (PRO) was determined spectrophotometrically with the use of the method of (Bates et al., 1973). The reaction mixture was obtained by dissolving 20 mg of lyophilized plant material in 1 ml of 3% sulfosalicylic acid, the mixture was homogenized, then vortexed, and finally centrifuged for 10 minutes at 13000 rpm. The obtained supernatant (700 µL) was mixed with 700 µL of glacial acetic acid and 700 µL of ninhydrin solution. After an hour of incubation in a water bath (t=95°C), a colored complex was formed as a result of the reaction of proline and ninhydrin. Extraction was performed with 2 mL of toluene, and absorbance was measured at 520 nm, and the result was expressed in µmol PRO g^{-1} DW.

Glycine betaine (GB) was quantified by the modified spectrophotometrical method according to (Grieve and Grattan, 1983). The 10 mg of lyophilized plant material was homogenized with 500 µL of 1M H_2SO_4 and centrifuged at 13000 rpm for 30 minutes at 0°C. Then, 100 µl of cold KI/I_2 was added to 250 µL of the supernatant and the mixture was left for 16 h at a temperature of 4°C. After incubation, and centrifugation at 13200 rpm, 30 minutes at 0°C, the supernatant carefully using a pipette, and triiodide crystals were dissolved in 9 ml of 1,2 - dichloroethane absorbance was read at 365 nm. The results were expressed in mg GB g^{-1}DW.

2.6 Data analysis

The obtained results were processed by the method of two-way factorial analysis of variance, and the significance of the difference between individual PEG concentrations, clones, and their interactions was tested by Fisher's least significant difference test (LSD test) for a significance level of p=0.05. The relationship between the investigated parameters was described using the Pearson correlation coefficient and principal component analysis (PCA). In the principal component analysis, a correlation matrix was used for data entry, and the relationship between the traits was analyzed based on their loadings with the first two principal components. The STATISTICA 13 software package (TIBCO Software Inc, 2020) was used for data processing. For visualization of data, R packages ggplot2 (Wickham, 2016) and corrplot (Wei and Simko, 2021) were used.

3 Results

The results of the analysis of variance indicate that the concentration of PEG had a significant effect on all examined parameters (Table 2). Regarding the applied concentration, the clearest differences in comparison to the control treatment were achieved on treatment PEG50, in which were also found the most distinctive differences between clones.

TABLE 2 Results of F-test on examined characters in White poplar clones[1].

Trait	Clone (A)	PEG concentration (B)	Interaction A×B
Shoot fresh weight	3.28*	9.70**	0.65 ^{ns}
Shoot dry weight	3.11^{ns}	4.06**	0.96 ^{ns}
Root fresh weight	1.69 ^{ns}	3.23**	0.95 ^{ns}
Root dry weight	1.85 ^{ns}	4.28**	1.49 ^{ns}
Chlorophyll a	5.42**	61.03**	2.08**
Chlorophyll b	4.14**	48.59**	1.50 ^{ns}
Carotenoids	2.56*	27.36**	1.57 ^{ns}
Chlorophyll a + b	5.28**	61.86**	1.91**
Total phenolic content	15.04**	4.37**	0.79 ^{ns}
Total flavonoids content	5.15**	46.56**	1.75 ^{ns}
Ferric reducing antioxidant power	28.18**	4.74**	0.81 ^{ns}
ABTS radical scavenging activity	26.74**	14.29**	0.65 ^{ns}
DPPH radical scavenging activity	9.98**	16.65**	1.02 ^{ns}
Free proline content	256.35**	264.10**	11.87**
Glycine betaine	24.40**	97.55**	8.42**

[1] (ns), non-significant; (*): p<0.05; (**): p<0.01.

3.1 Variability of morphological traits

In total, the values of SFW and SDW on PEG20 and PEG50 are lower than on the control treatment, while values for RFW and RDW are the highest on PEG10 (Supplementary Table 1). Clone L-80 stood out as the clone with the highest values of the fresh and dry mass of shoots and roots on the PEG50 medium. It had a significantly higher shoot dry weight (SDW) than LBM and LCM, but not compared to Villafranca (Figure 1B). In all clones, higher values of all examined morphological parameters (fresh and dry weight of shoots and roots) were observed on PEG1 compared to the control. However, this increase was not statistically significant. Compared to the control medium, only clone LCM showed a significant reduction in shoot fresh and dry weight on the PEG50 medium: SFW was reduced by 72% (Figure 1A), and SDW was reduced by 56% compared to the control (Figure 1B). There was no statistically significant difference in root fresh (Figure 1C) and dry weight (Figure 1D) between the examined clones on the PEG50.

3.2 Variability of photosynthetic pigments

An increase in PEG 6000 concentrations resulted in a decrease in photosynthetic pigments' contents However, applied PEG6000 concentrations of 1 mg/L and 10 mg/L did not significantly affect the content of photosynthetic pigments compared to the control treatment (Supplementary Table 1). In most clones, all photosynthetic pigments were lower on PEG50 compared to the control (Figure 2A).

The examined clones showed a different response to PEG50 compared to the control. Clone Villafranca showed the lowest percentage of reduction in Chl a (66%) (Figure 2A), Chl b (65%) (Figure 2B), and Car (69%) (Figure 2C), while clone LCM had the highest percentage of reduction in Chl a (77%), Chl b (77%), and Car (86%). For the parameter Chl a+b on the PEG50 medium, there was no significant difference between the examined clones (Figure 2D).

3.3 Variability of biochemical traits

The results of the analysis of variance showed that both the clones and the applied PEG concentrations had a statistically significant influence on the variation of investigated biochemical parameters. The total phenolic content (TPC) increased with increasing concentration of PEG in the media reaching 5.3 mg GAE g^{-1} DW on PEG50 (Supplementary Table 1). In all clones, the highest TPC was recorded in the PEG50 treatment. Clone L-80 had the lowest TPC on PEG50 treatment (3.3 mg GAE g^{-1} DW), however, this difference was not significant compared to the clone Villafranca. The highest TPC was measured in clone LBM (8.1 mg GAE g^{-1} DW) whose TPC content was statistically significantly

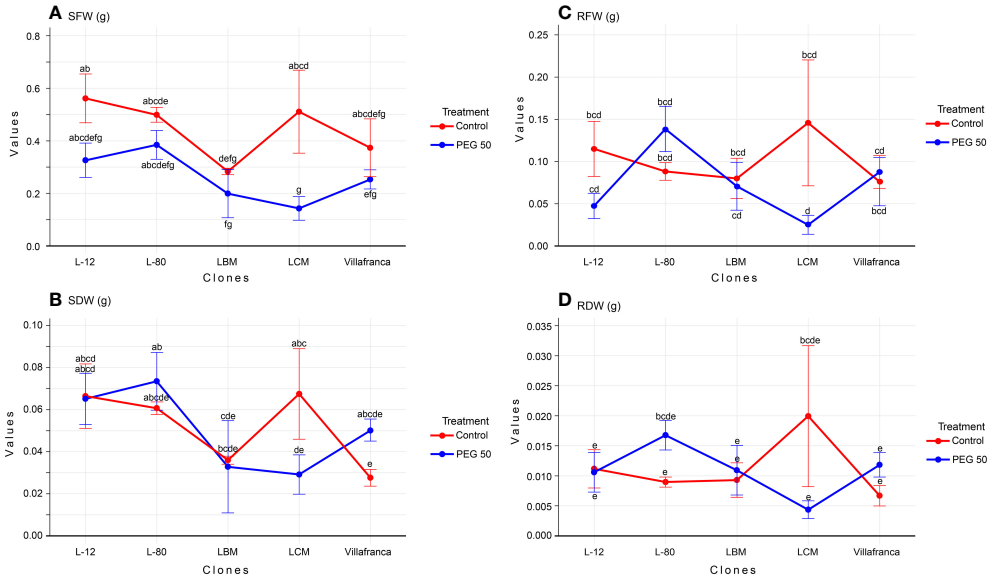

FIGURE 1
Changes in: **(A)** shoot fresh weight (SFW; g); **(B)** shoot dry weight (SDW; g); **(C)** root fresh weight (RFW; g); **(D)** root dry weight (RDW; g). Treatments: C: control (0 g/L PEG 6000); PEG50 (50 g/L PEG 6000). Differences between values of the same trait that are labeled with the same letter are not statistically significant (p>0.05). Error bars represent standard error (± SE).

higher than that of the reference clone Villafranca (Figure 3A). Unlike TPC, TFC decreased with increasing PEG concentration in the medium. The highest TFC on the PEG50 medium was measured in clone Villafranca and L-80 (4.2 and 3.9 mg QE g^{-1} DW, respectively), while the lowest TFC content was measured in clone LCM (0.8 mg QE g^{-1} DW) (Figure 3B).

FRAP values, as well as values of DPPH and ABTS, were increasing in a dose-dependent manner (Supplementary Table 1). Compared to the control treatment, in the PEG50 treatment, FRAP values increased significantly in clone L-12 by 76% reaching 20.2 mg AS g^{-1} DW, clone LBM by 59% reaching 37.2 mg AS g^{-1} DW, and clone LCM by 34% reaching 31 mg AS g^{-1} DW, while the increase in clones L-80 and Villafranca was not significant (Figure 4A). With the increase in stress levels, there was a significant increase in all clones in the ability of their samples to neutralize DPPH radicals compared to the control. The average

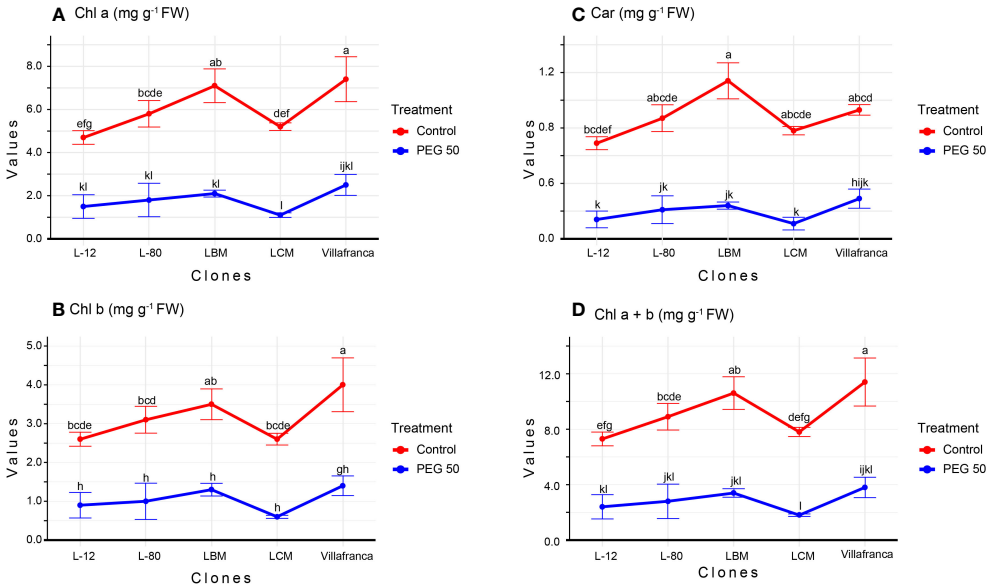

FIGURE 2
Changes in: **(A)** Chlorophyll a (Chl a; mg g^{-1} FW); **(B)** Chlorophyll b (Chl b; mg g^{-1} FW); **(C)** Carotenoide (Car; mg g^{-1} FW); **(D)** Chlorophyll a + Chlorophyll b (Chl a +b mg g^{-1} FW). Treatments: C: control (0 g/L PEG 6000); PEG50 (50 g/L PEG 6000). Differences between values of the same traits that are labeled with the same letter are not statistically significant (p>0.05). Error bars represent standard error (± SE).

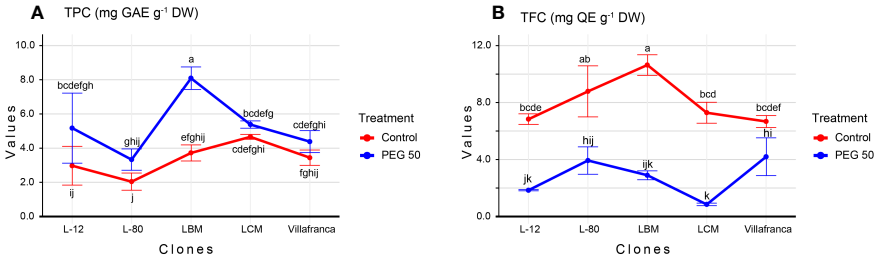

FIGURE 3
Changes in: **(A)** Total phenolic content (TPC; mg GAE g^{-1} DW); **(B)** Total flavonoid content (TFC; mg QE g^{-1} DW). Treatments: C: control (0 g/L PEG 6000); PEG50 (50 g/L PEG 6000). Differences between values of the same traits that are labeled with the same letter are not statistically significant ($p>0.05$). Error bars represent standard error (± SE).

value for the ability to neutralize DPPH radicals on the control was 54.4%, while the average value for neutralization on PEG50 was 70.9%., This was especially pronounced in the LBM clone where DPPH values increased by more than twice reaching 85.7% on PEG50 compared to the control where the ability to neutralize was 34.4% (Figure 4B).

Clone LBM (71.3%) achieved the highest ability to neutralize ABTS radicals in PEG50 treatment, while clone L-80 had the lowest ABTS radical neutralization ability (44.7%), both significantly differing from moderate performance of Villafranca (Figure 4C). The ability to neutralize ABTS radicals increased with increasing concentration of PEG 6000 (59.5% on PEG50) regarding control (18.5%). Also, all clones achieved a significant increase of this parameter on PEG50 treatment in comparison to the control.

In total, free proline content (PRO) increased as the concentration of the examined osmotic inducer increased. Thus, in the control, the average content of free proline was measured in the value of 1.7 µmol g^{-1} DW, while the average content of total proline on PEG50 was 5.6 µmol PRO g^{-1} DW (Supplementary Table 1). In the control treatment, the value of PRO varied among clones: from 0.5 µmol PRO g^{-1} DW for cloneL-80 to 4.10 µmol PRO g^{-1} DW for Villafranca. Also, in the PEG50 treatment, the highest free proline content was measured in the Villafranca clone (9.10 µmol PRO g^{-1} DW), while significantly lower proline content was measured in clones L-80, L-12, and LBM (Figure 5A). However, the greatest increase in free proline content was achieved by clone L-80, where the proline content increased by more than eight times on the PEG50 treatment (reaching 4.3 µmol PRO g^{-1} DW) compared to the control (0.5 µmol PRO g^{-1} DW). The smallest increase was recorded by clone Villafranca, where the proline content increased by only 2-fold reaching 9.1 µmol PRO g^{-1} DW compared to the control where the value was 4.1 µmol PRO g^{-1} DW.

The content of glycine betaine (GB) significantly changed depending on the concentration of PEG 6000. In total, there was a significant increase in the content of GB on PEG10 (reaching 350.5 mg GB g^{-1} DW) compared to the control (where the value was 72.8 mg GB g^{-1} DW), then it was significantly reduced on PEG20 (147.9 mg GB g^{-1} DW) compared to PEG10 treatment, while the maximum value in the content of GB plants was reached on PEG50 (reaching 557.5 mg GB g^{-1} DW) (Supplementary Table 1). The values for GB content ranged from 29.7 mg GB g^{-1} DW in clone Villafranca (control) up to 822.5 mg GB g^{-1} DW clone L-12 (PEG50). The clones with the greatest increase in GB content in the PEG50 treatment compared to the control were L-80 (reaching 647 mg GB g^{-1} DW) and Villafranca (reaching 358.9 mg GB g^{-1} DW), which increased their GB content by as much as 12-fold (Figure 5B). The smallest and non-significant increase and also the lowest GB content on PEG50 have been recorded in clone LCM (179.7 mg GB g^{-1} DW).

3.4 Relationship between examined parameters

Based on the results of the correlation analysis (Figure 6), there was a positive correlation between parameters that describe the content of photosynthetic pigments, as well as between them, and TFC. On the other side, there was a positive correlation between parameters that described oxygen radical scavenging ability (ABTS, FRAP, DPPH) and TPC, and this group was in negative or poor correlation with the photosynthetic pigments' content and TFC. The correlation of PRO and GB with the "ROS scavenging ability" group was positive, but relatively poor to moderate. However, their correlation with the contents' of photosynthetic pigments and TFC was stronger but negative. Among morphological parameters, the strongest correlation with examined photosynthetic pigments and biochemical parameters was recorded for shoot fresh weight (SFW). The fresh mass of the shoot (SFW) was negatively correlated with most of the examined biochemical parameters (TPC, FRAP, ABTS, DPPH, and PRO). With TFC and the contents' of photosynthetic pigments, it showed a positive correlation.

The first two principal components explained 71.0% of the total variation. According to their loadings with examined parameters, most of the parameters have their highest loadings with the first principal component. In accordance with the results of correlation analysis, this group could also be divided on contents of photosynthetic pigments TFC which were in negative correlation with ROS scavenging ability parameters and TPC. Only parameters describing the fresh and dry weight of roots and dry weight of

10.3389/fpls.2023.1280794

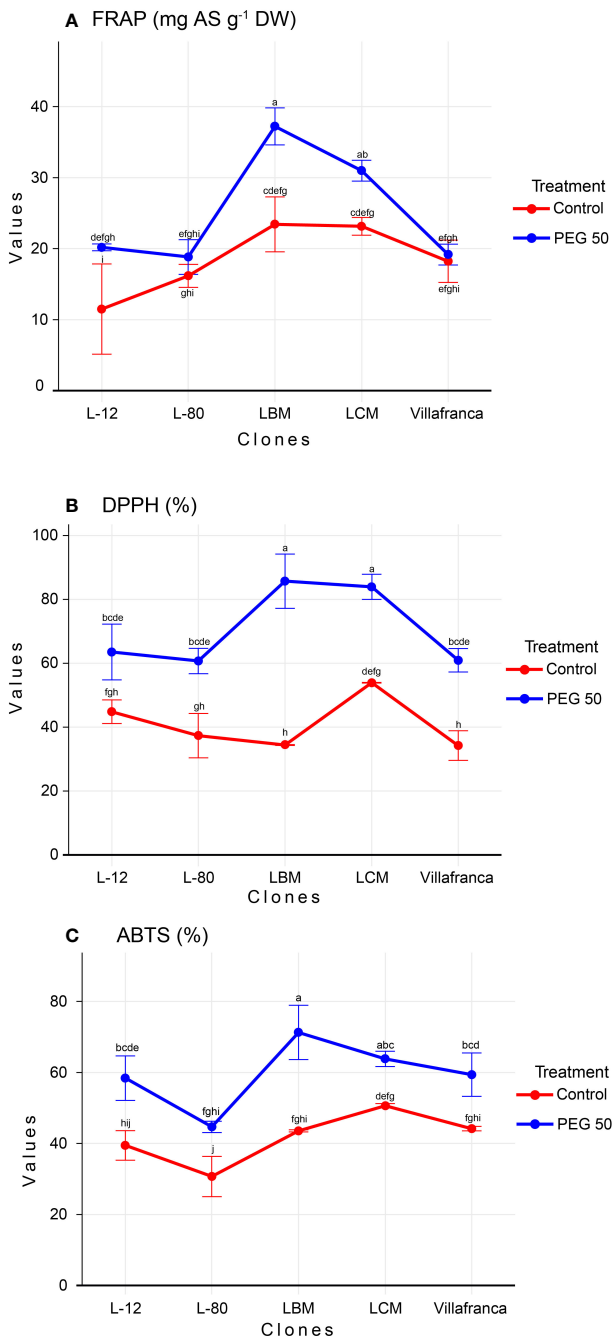

FIGURE 4
Changes in: **(A)** Ferric reducing antioxidant power (FRAP; mg AS g^{-1} DW); **(B)** 2,2′-azinobis-3-ethylbenzothiazoline-6-sulfonic acid (ABTS; %); **(C)** 2, 2-diphenyl-2-picrylhydrazyl (DPPH; %). Treatments: C: control (0 g/L PEG 6000); PEG50 (50 g/L PEG 6000). Differences between values of the same trait that are labeled with the same letter are not statistically significant ($p>0.05$). Error bars represent standard error (± SE).

shoots had their highest loadings with the second principal component. Relatively moderate relation with this (second) group of parameters showed the only content of betaine glycine and fresh shoot mass. Shoot fresh and dry weight achieved their strongest, although negative, correlation with parameters describing ROS scavenging ability, TPC, and PRO (Figure 7).

4 Discussion

Global climate change will undoubtedly affect the frequency and duration of droughts that may destroy forest ecosystems in the future (Salahvarzi et al., 2021). That is why an understanding of the underlying drought tolerance mechanisms of plants is of essential importance, especially in forest tree species. Studies on the tolerance of white poplar to various abiotic and biotic factors have been conducted, such as: tolerance to acidity stress (Vuksanović et al., 2019d); salinity (Sixto, 2005; Vuksanović et al., 2019c; Zhang et al., 2019), drought (Yang et al., 2016), heavy metals (Kebert et al., 2017; Kovačević et al., 2020; Kebert et al., 2022b; Katanić et al., 2015; Fischerová et al., 2006). Polyethylene glycol has several advantages (Osmolovskaya et al., 2018) and allows a convenient way to assess the effects of drought on plant growth and development in controlled conditions (Vuksanović et al., 2022). In the present study, five white poplar clones were examined for their drought tolerance *in vitro* and different clones were exposed to four different concentration ranges of PEG 6000 and control, used to induce drought-like stress conditions, had their potential drought tolerance examined *in vitro*. This research was focused on tracking poplar clones' responses at morphological, photosynthetic, and biochemical level. Generally, most of the examined parameters decreased in a dose-dependent manner, except for TFC, root biomass traits, and GB. The treatment PEG50 provided the most intense drought-like stress effect and achieved the most clear distinction between examined white poplar clones, which was proposed it for further *in vitro* drought tolerance studies.

4.1 Morphological traits

Based on the obtained results, it can be concluded that high PEG concentrations induced a decrease in shoot and root weight accumulation (Figure 8). The reduction of fresh and dry weight under the influence of polyethylene glycol was also recorded in other plant species. For example, (Akte et al., 2011) examining the tolerance of rice *in vitro*, found that the dry and fresh mass was significantly reduced when PEG was added to the MS medium at a concentration of 4%. Compared to the control, the significantly lower fresh weight of *Stevia rebaudiana* leaves was also measured by (Hajihashemi and Sofo, 2018) in the treatment with PEG 15% (w/v). Also, (Jaafar et al., 2021) performed a screening of 12 lines of cotton and observed that shoot and root weight decreased with an increase in PEG concentration from 0 to 15%. (Zhong et al., 2018), also found that fresh shoot weight decreased with increasing concentration of PEG 8000 in kiwifruit (*Actinidia* sp.) Therefore, it could be assumed that the drop in the fresh weight of the plant under the influence of drought is a consequence of the reduced growth of the plants as well as the limited capacity of the roots to provide water to the leaves. The results of this analysis suggest that although the difference was not statistically significant, it seems that the fresh and dry mass of the roots tend to increase in clone L-80 as the concentration of PEG in the medium increased. An increase in dry matter *in vitro* seeds was also obtained in tomato tolerance tests

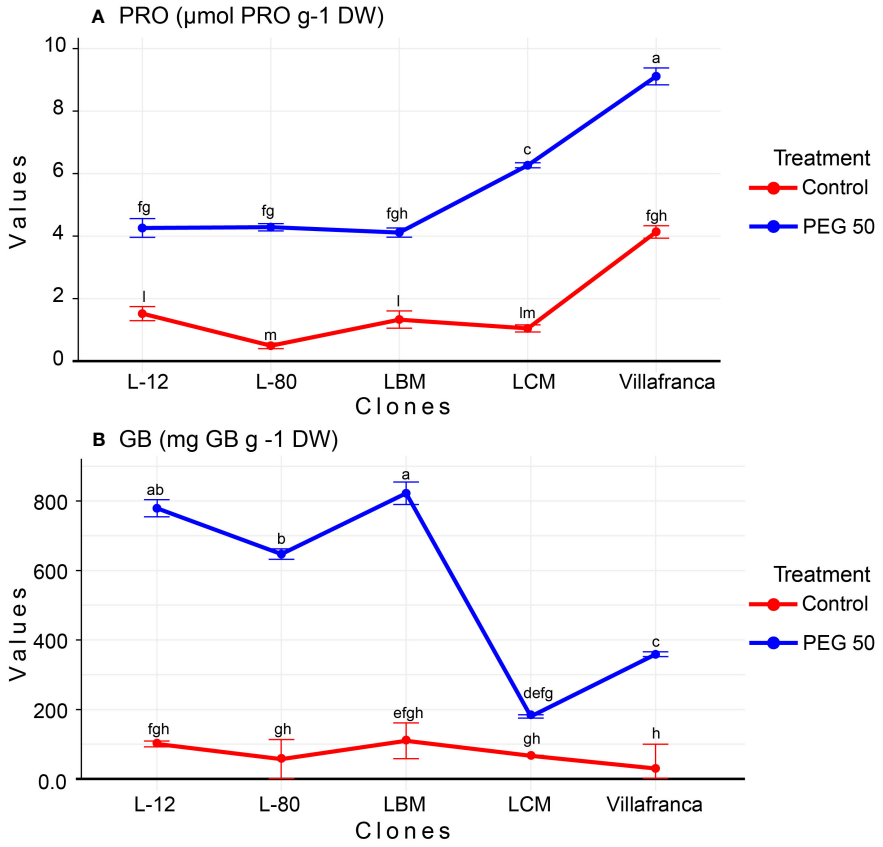

FIGURE 5
Changes in: **(A)** Free proline content (PRO; µmol PRO g^{-1} DW); **(B)** Glycine betaine (GB; mg GB g^{-1} DW). Treatments: C: control (0 g/L PEG 6000); PEG50 (50 g/L PEG 6000). Differences between values of the same trait that are labeled with the same letter are not statistically significant (p>0.05). Error bars represent standard error (± SE).

in vitro by adding PEG in the concentration range of 0-295 g/L (Aazami et al., 2010). Given that the root has an important role in the uptake of nutrients and water, it can be assumed that clones tolerant to drought showed a greater mass of roots compared to less tolerant ones. This could be explained by faster osmotic adjustment and retention of a larger amount of water in the roots.

If we consider the shoot's fresh and dry mass as an ultimate result of the ability of the plant to cope with the drought stress, it is important to relate these parameters with the examined photosynthetic pigments and biochemical parameters to evaluate their significance. Due to their close relationship with the response of the plant to disturbances of the oxidative and osmotic status of the cell, they could provide information on the importance of the regulation of these characteristics of the cell's metabolism in the mitigation of drought stress. In this study, a close negative relationship is found between shoot fresh and dry mass and some biochemical parameters, namely: FRAP, ABTS, DPPH, and TPC, but relatively moderate positive with photosynthetic pigments and TFC (Figures 6, 7). The clear negative correlation of shoot mass with and parameters of ROS scavenging ability suggest that those clones that considerably increased production of antioxidant substances to cope with disturbances of oxidative status related to drought conditions could be considered as less tolerant. These results are consistence with the results of (Vuksanović et al., 2019c) who studied the reaction of white poplar clones on rooting media differing in NaCl concentration. However, in work dealing with wild cherry clones on multiplication media differing in PEG concentration by (Vuksanović et al., 2022), TPC appeared to be in positive correlation with morphometric parameters that described shoot number and height, while FRAP and ABTS achieved with those morphological parameters poor correlation. Also, FRAP, DPPH, ABTS, as well as TPC, and TFC were not correlated with shoot fresh and dry mass in the study of (Vuksanović et al., 2019d) dealing with the reaction of white poplar clones on rooting media differing in pH from pH 3.0 to pH 5.5, suggesting that this topic needs further studies.

4.2 Photosynthetic pigments

A large embodiment of literature demonstrated that drought conditions induce a reduction of photosynthetic pigments' content and thus a decrease in the intensity of photosynthesis (Jaleel et al., 2009; Xia et al., 2022). In this study, the contents of all examined photosynthetic pigments were in strong positive correlation (Figures 6, 7), suggesting that the reaction of clones on examined treatments was similar by all of them. All examined white poplar clones significantly reduced the content of all photosynthetic

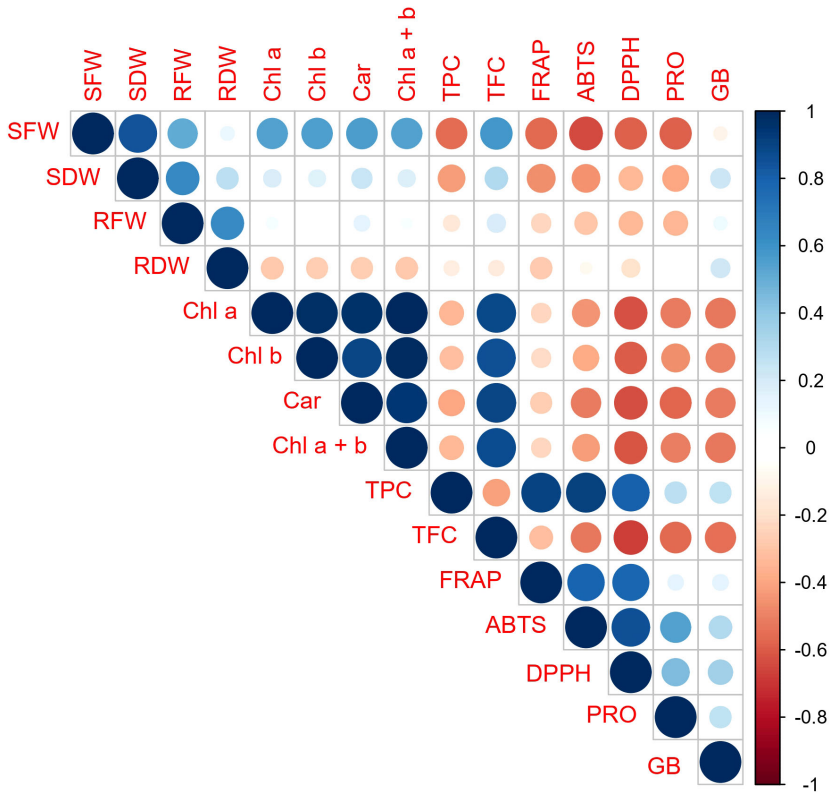

FIGURE 6
Pearson's correlation matrix of analyzed morphological, physiological, and biochemical parameters. Abbreviations present examined parameters: shoot fresh weight (SFW); shoot dry weight (SDW); root fresh weight (RFW); root dry weight (RDW); Chlorophyll a (Chl a); Chlorophyll b (Chl b); Carotenoide (Car); Chlorophyll a + Chlorophyll b (Chl a +b); total phenolic content (TPC); total flavonoid content (TFC)); ferric reducing antioxidant power (FRAP); 2,2′-azinobis-3-ethylbenzothiazoline-6-sulfonic acid (ABTS); 2, 2-diphenyl-2-picrylhydrazyl (DPPH); free proline content (PRO); glycine betaine (GB)). Error bars represent standard error (± SE).

pigments on PEG50 compared to the control. (Lei et al., 2006), in their work on poplar (*Populus przewalskii*), showed that the reduced content of photosynthetic pigments was a consequence of the increased activity of enzymes (superoxide dismutase (SOD), guaiacol peroxidase (GPX), and glutathione reductase (GR)) enrolled in degradation of chlorophyll under drought conditions. Similar results were obtained by (Guo et al., 2010), investigating the tolerance of hybrid poplar *Populus deltoides* × *Populus nigra* clones, where there was also reduced chlorophyll content due to different regimes of limited water availability. A decrease in the content of photosynthetic pigments with an increase in PEG concentration was also recorded in other plant species. Thus, (Ghassemi-Golezani et al., 2018), observed reduced total chlorophyll and carotenoids content upon treatment with 16 mM PEG *in vitro* in *Allium hirtifolium*, while (Hussein et al., 2017), reported that total chlorophyll content was significantly reduced in strawberries treated with 2% PEG *in vitro*. Additionally, a reduction in total chlorophyll content due to drought-induced by PEG has also been documented in *Stevia rebaudiana* under treatment with PEG 15% (w/v) (Hajihashemi and Sofo, 2018) and in peanuts (*Arachis hypogaea*) under treatment with PEG-6000; 20% (w/v) (Shivakrishna et al., 2018). In this study, clones L-80 and L-12 stood out as they achieved the lowest percentage reduction in pigment content under PEG50 treatment, almost twice lower than clone Villafranca. This suggests their good tolerance against examined drought-like *in vitro* conditions, particularly in comparison with clone Villafranca. A decrease in the content of Chl a, Chl b, and Car was recorded by (Razavizadeh et al., 2019), who investigated the influence of different concentrations (2, 4, 6, and 8% (v/w)) of PEG 6000 on the tolerance of *Thymus vulgaris* L. (thyme) *in vitro*. Also, (Mehmandar et al., 2023), in their investigation of the responses of three Iranian melon genotypes to PEG (0.009, 0.012, and 0.015 M) state that there was a decrease in Chl a, Chl b, and Car content when using this osmolyte. Interestingly, (Radi et al., 2023), investigated the influence of PEG concentrations (0, 50, 100, and 150 g/L) on cactus pear (*Opuntia ficus indica*) and reported that the highest chlorophyll b content was recorded in shoots grown for 3 weeks on MS medium containing 150 g/L PEG.

4.3 Biochemical traits

4.3.1 Antioxidant activities

Previous research showed that under the influence of drought, there were numerous changes in plant metabolism (Jaleel et al., 2009). This study showed a high accumulation of total phenols in poplar genotypes under the influence of PEG 6000. The total

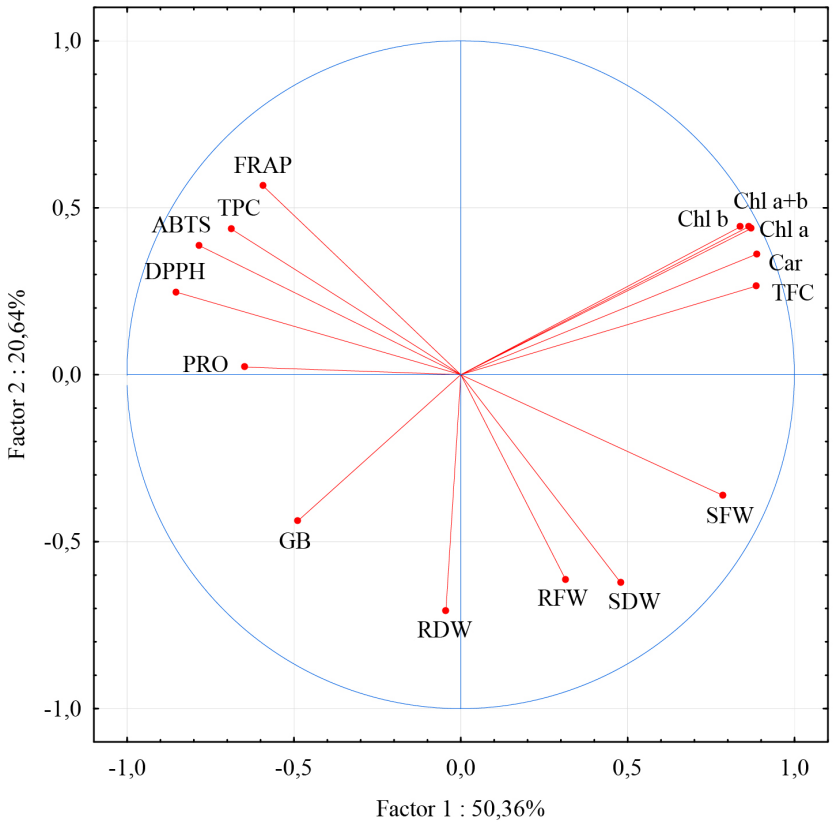

FIGURE 7
Loadings of the first two principal components for morphological physiological and biochemical parameters. Abbreviations present examined parameters: shoot fresh weight (SFW); shoot dry weight (SDW); root fresh weight (RFW); root dry weight (RDW); Chlorophyll a (Chl a); Chlorophyll b (Chl b); Carotenoide (Car); Chlorophyll a + Chlorophyll b (Chl a +b); total phenolic content (TPC); total flavonoid content (TFC); ferric reducing antioxidant power (FRAP); 2,2′-azinobis-3-ethylbenzothiazoline-6-sulfonic acid (ABTS); 2,2-diphenyl-2-picrylhydrazyl (DPPH); free proline content (PRO); glycine betaine (GB). Error bars represent standard error (± SE).

phenolic content increased by 56% on PEG50 compared to the control. Phenolics as secondary metabolites play an important role in plants' protection against diseases, pests, and adverse environmental conditions including drought (Li et al., 2011). Increased phenolic content under the influence of stress caused by polyethylene glycol was also obtained in other plant species: *Thymus vulgaris* L. (6% PEG 6000) (Razavizadeh et al., 2019) *Morus nigra* cv. 'Eksi Kara' (355 g/L PEG 8000) (Özelçi et al., 2022); *Stevia rebaudiana* (4% PEG 6000) (Ahmad et al., 2020); *Allium hirtifolium* (16 mM) (Ghassemi-Golezani et al., 2018).

In this research, the concentration of PEG 6000 of 50 g/L led, in total, to a decrease in the content of total flavonoids by 63% compared to the control (Supplementary Table 1). Clones L-80, Villafranca, and L-12 achieved the highest content of flavonoids on PEG50. Furthermore, it can be assumed that the clones that exhibited the lowest flavonoid content are the least tolerant to drought stress caused by the addition of PEG 6000. Given that clone L-80 accumulated the highest amounts of flavonoids on PEG50, it can be assumed that it is the most tolerant clone according to this parameter. The TPC and TFC differed in the correlation with other parameters: TPC was positively correlated with FRAP, ABTS, and DPPH, and negatively with all examined photosynthetic pigments, while the opposite was in the case of TFC. Also, although both deceased on PEG50, the correlation between them was weak, indicating a clone specificity in their reaction to drought-like conditions with these two parameters. The clone L-80 achieved the lowest values of TPC on PEG 50, but not significantly lower than Villafranca, suggesting its good performance according to this parameter.

The ABTS, DPPH, and FRAP inhibition activities are the most commonly used assays based on electron transfer mechanisms to assess antioxidant capacity during drought stress. The obtained research results show a strong positive correlation between them and that the examined clones significantly increased the antioxidant activity (ABTS, DPPH, FRAP) on PEG50. A strong positive correlation among biochemical assays based on electron transfer mechanisms has been thoroughly explained (Huang et al., 2005). Increased antioxidant activity under drought stress conditions was previously reported in *Agave salmiana* exposed to 30% PEG; (Sarker and Oba, 2018), as well as in *Amaranthus tricolor* where plants were exposed to drought induced by reduced watering regimen and water field capacity (FC) drought from 0 to 30% FC, but also in the wild cherry *in vitro* after medium supplementation with 50 g/L of PEG (Vuksanović et al., 2022), Furthermore, increasing patterns of antioxidant power were noted in *Quercus robur* and *Quercus cerris* exposed to drought stress (Kebert et al., 2022a) However, some authors found that drought induced by 100

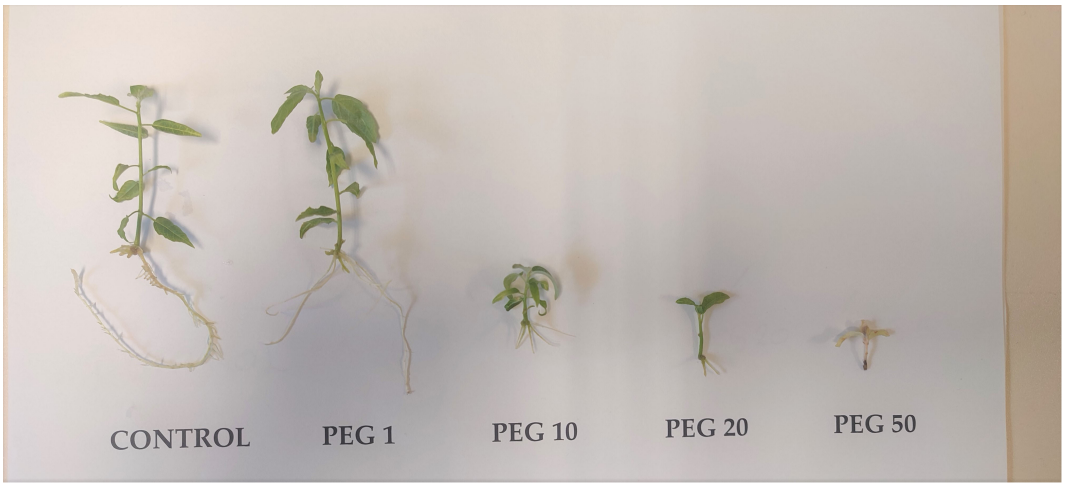

FIGURE 8
Explants of clone L-12 after cultivation on examined PEG concentrations. (control): 0; (PEG1): 1 g/L PEG 6000; (PEG10): 10 g/L PEG 6000; (PEG20): 20 g/L PEG 6000; (PEG50): 50g/L PEG 6000. Error bars represent standard error (± SE).

and 200 mOsm PEG 6000 in hydroponic culture caused significant decrease of DPPH and FRAP values in hybrid black poplar (Popović et al., 2017). Interestingly, clones L-80 and Villafranca for that the positive reaction by shoot and root dry mass, as well as clones L-12 and LCM for that negative reaction by the same parameters was recorded on PEG50 compared to control treatment, achieved relatively moderate increment of antioxidant capacity, considerably weaker than clone LBM. This clone showed no significant difference between two treatments by biomass parameters, but considerable difference in examined parameters of antioxidant capacity. Relatively moderate increment of antioxidant capacity was also recorded in white poplar clones tolerant to salty (100 mM NaCl) (Vuksanović et al., 2019c) and acidic (pH 3) (Vuksanović et al., 2019d) medium.

4.3.2 Clone-specific osmolyte (glycine betaine and proline) variability

A significant amount of literature has been devoted to elucidating how the increased content of various osmolytes, such as proline or glycine betaine, is related to the increased stress tolerance to drought in plants (Kebert et al., 2023). Proline is a multifunctional amino acid and a crucial marker of abiotic stress that acts as an antioxidant and ROS quencher involved in the control of redox balance, osmotic pressure, energy status, nutrient availability, photosynthesis, and mitochondrial respiration as well as serving as a signaling molecule that modifies gene expression (Szabados and Savoure, 2010; Alvarez et al., 2022). In our study, all examined PEG 6000-treated clones showed a clearly increased level of free proline when compared to controls, with clones LCM and Villafranca standing out the most. A similar increasing trend of free proline was also reported in vitro in other plant species such as Prunus dulcis (Mill.) when it was treated with 7.5% PEG 6000 in MS medium (Karimi et al., 2022) as well as in Tacca leontopetaloides (Martin et al., 2021). Other plant species, including rice (Akte et al., 2011), almond (Akbarpour et al., 2017), mango (Pradhan et al., 2021), potato (Kumar et al., 2020), and Fragaria ananasa (Hussein et al., 2017), have also shown a drought-induced increase in free proline levels. In addition, greenhouse pot experiment under drought conditions with woody plant species such as pedunculate oak (Kebert et al., 2023), Persian oak (Quercus brantii Lindl.) and European black poplar (Populus nigra L.) also exhibited increased proline content (Karimi et al., 2022). Increased proline levels may be linked to improved plant tolerance to various abiotic stresses, including drought, because of the strong positive correlation between proline and antioxidant potential (FRAP and ABTS) that was observed in this study. Another explanation for elevated levels of proline may be related to the fact that drought alters the metabolism of proline by upregulating the proline biosynthetic gene P5CS1 and downregulating the proline catabolic gene ProDH (Yoshiba et al., 1997; Alvarez et al., 2022). Regarding quaternary nitrogen compounds, on the other hand, it was discovered that all inspected poplar clones were affected by the drought and that there was a high level of variation among them in terms of the response to the drought-induced glycine betaine response. All clones exhibited higher amounts of GB compared to untreated controls, but the clones L-12 and LBM were the most prominent in terms of GB levels under drought. Intriguingly, the PEG-treated clones LCM and Villafranca that showed the greatest increases in proline levels also showed the lowest increases in GB levels compared to non-treated controls. This might indicate the clone-specificity, where the same PEG50 treatment in some clones induces a proline response (as it did in LCM and Villafranca) while in other clones (LBM, L-80, and L-12) it induced a more dramatic GB response. Given that both metabolites utilize the same available nitrogen sources for their biosynthesis, this reciprocity between glycine betaine and proline is already known (Carrilo et al., 2008; Carrilo, 2018). The duration of the stress also affects whether the nitrogen is directed to proline or GB biosynthesis, as proline typically responds more quickly to short-term stresses while GB biosynthesis is temporally delayed in comparison to other significant osmolytes, such as proline (Carrilo et al., 2008; Woodrow et al., 2017; Carrilo, 2018). Similarly, drought-induced increasing

patterns of GB were also recorded in pedunculate oak (Kebert et al., 2023), vanilla (Martínez-Santos et al., 2021), and sugar cane (Hernández-Pérez et al., 2021). In addition, increased content of glycine betaine under drought stress (induced by PEG; 50–150 g/L) was recently reported in the cactus in vitro (Radi et al., 2023). This increment in GB may be attributed to enhanced drought tolerance due to the high osmoprotective properties of GB since it is also known that GB can activate various antioxidant enzymes such as peroxidases, catalase, and SOD (Chen and Murata, 2008). Finally, GB can serve as a stabilizer and chaperone to photosynthetic proteins including oxygen-evolving PSII complex, and protect them from oxidative damage (Ashraf and Foolad, 2007).

5 Conclusions

The use of biochemical tests *in vitro* research is of great importance considering the rare implementation of these tests in research on the tolerance of woody species to abiotic factors. There was a negative correlation of shoot mass with and parameters of ROS scavenging ability, suggesting low drought tolerance of clones with high production of antioxidant substances. There was clear of agglomeration of examined clones to those that accumulated proline and those that accumulated glycine betaine as a response to drought-like conditions. We assume that clone L-80 is more tolerant to drought than the other examined white poplar clones, but not considerably better than the reference clone Villafranca. Namely, in conditions similar to drought *in vitro*, this clone achieved high values for biomass and content of photosynthetic pigments, but moderate values of parameters describing ROS scavenging ability. At the same time it accumulated a low content of proline and a high content of glycine betaine. On the other side, clone LCM could be regarded as the most susceptible, because of its relatively strong decrease in biomass, low content of photosynthetic pigments, and low values of TFC and GB, along with high values of TPC, FRAP, ABTS, DPPH, and PRO in examined drought-like conditions. According to the results of the study, medium with 50 g/L PEG could be proposed for further studies on variability of the responses of white poplar clones to drought stress *in vitro*. Also, examined biochemical parameters proved to be indicative in the selection of drought-tolerant clones, but should be further studied in future research on drought tolerance in white poplar.

Data availability statement

The original contributions presented in the study are included in the article/Supplementary Material. Further inquiries can be directed to the corresponding author.

Author contributions

VV: Conceptualization, Data curation, Formal Analysis, Investigation, Methodology, Project administration, Software, Validation, Visualization, Writing – original draft, Writing – review & editing. BK: Conceptualization, Data curation, Formal Analysis, Investigation, Methodology, Software, Supervision, Validation, Visualization, Writing – original draft, Writing – review & editing. MK: Conceptualization, Data curation, Investigation, Methodology, Software, Supervision, Validation, Visualization, Writing – original draft, Writing – review & editing. LP: Data curation, Software, Visualization, Writing – original draft, Writing – review & editing. LK: Validation, Writing – original draft, Writing – review & editing. JC: Writing – original draft, Writing – review & editing. SO: Conceptualization, Funding acquisition, Project administration, Resources, Supervision, Writing – original draft, Writing – review & editing.

Funding

The author(s) declare financial support was received for the research, authorship, and/or publication of this article. This research has been supported by the Ministry of Science, Technological Development and Innovation of the Republic of Serbia, Contract No. 451-03-47/2023-01/200117 and 451-03-47/2023-01/200197. In addition, this manuscript covered one of the research topics conducted by the researchers gathered in the Center of Excellence Agro-Ur-For at the Faculty of Agriculture in Novi Sad, supported by the Ministry of Science, Technological Development and Innovations, contract number 451-03-1524/2023-04/17.

Acknowledgments

We acknowledge the Ministry of Science, Technological Development, and Innovation of the Republic of Serbia.

Conflict of interest

The authors declare that the research was conducted in the absence of any commercial or financial relationships that could be construed as a potential conflict of interest.

Publisher's note

Supplementary material

The Supplementary Material for this article can be found online at: https://www.frontiersin.org/articles/10.3389/fpls.2023.1280794/full#supplementary-material

References

Aazami, M. A., Torabi, M., and Jalili, E. (2010). *In vitro* response of promising tomato genotypes for tolerance to osmotic stress. *Afr J. Biotechnol.* 9, 4014–4017.

Abdolinejad, R., and Shekafandeh, A. (2022). Tetraploidy Confers Superior in *vitro* Water-Stress Tolerance to the Fig Tree (*Ficus carica*) by Reinforcing Hormonal, Physiological, and Biochemical Defensive Systems. *Front. Plant Sci.* 12. doi: 10.3389/fpls.2021.796215

Agati, G., Azzarello, E., Pollastri, S., and Tattini, M. (2012). Flavonoids as antioxidants in plants: location and functional significance. *Plant Sci.* 196, 67–76. doi: 10.1016/j.plantsci.2012.07.014

Ahmad, M. A., Javed, R., Adeel, M., Rizwan, M., and Yang, Y. (2020). PEG 6000-stimulated drought stress improves the attributes of in *vitro* growth, steviol glycosides production, and antioxidant activities in Stevia rebaudiana Bertoni. *Plants* 9, 1–10. doi: 10.3390/plants9111552

Akbarpour, E., Imani, A., and Yeganeh, S. F. (2017). Physiological and morphological responses of almond cultivars under in *vitro* drought stress. *J. Nuts* 8, 61–72.

Akte, J., Yasmin, S., Bhuiyan, M., Khatun, F., Roy, J., and Goswami, K. (2011). *In vitro* screening of rice genotypes for drought tolerance using polyethylene glycol. *Acta Physiol. Plant* 33, 2209–2217. doi: 10.1007/s11738-011-0760-6

Alvarez, M. E., Savouré, A., and Szabados, L. (2022). Proline metabolism as regulatory hub. *Trends Plant Sci.* 27, 39–55. doi: 10.1016/j.tplants.2021.07.009

Arnao, M. B. (2000). Some methodological problems in the determination of antioxidant activity using chromogen radicals: A practical case. *Trends Food Sci. Technol.* 11, 419–421. doi: 10.1016/S0924-2244(01)00027-9

Ashraf, M., and Foolad, M. R. (2007). Roles of glycine betaine and proline in improving plant abiotic stress resistance. *Environ. Exp. Bot.* 59, 206–216. doi: 10.1016/j.envexpbot.2005.12.006

Ashry, N. M., Alaidaroos, B. A., Mohamed, S. A., Badr, O. A. M., El-Saadony, M. T., and Esmael, A. (2022). Utilization of drought-tolerant bacterial strains isolated from harsh soils as a plant growth-promoting rhizobacteria (PGPR): Utilization of drought-tolerant bacterial strains. *Saudi J. Biol. Sci.* 29, 1760–1769. doi: 10.1016/j.sjbs.2021.10.054

Babaei, K., Moghaddam, M., Farhadi, N., and Ghasemi Pirbalouti, A. (2021). Morphological, physiological and phytochemical responses of Mexican marigold (*Tagetes minuta* L.) to drought stress. *Sci. Hortic. (Amsterdam).* 284, 110116. doi: 10.1016/j.scienta.2021.110116

Baozhu, L., Ruonan, F., Yanting, F., Runan, L., Hui, Z., Tingting, C., et al. (2022). The flavonoid biosynthesis regulator PFG3 confers drought stress tolerance in plants by promoting flavonoid accumulation. *EEB* 196, 104792. doi: 10.1016/j.envexpbot.2022.104792

Bates, L. S., Waldren, R. P., and Teare, I. D. (1973). Rapid determination of free proline for water-stress studies. *Plant Soil 1973 391* 207, 205–207. doi: 10.1007/BF00018060

Benzie, I. F. F., and Strain, J. J. (1996). The ferric reducing ability of plasma (FRAP) as a measure of "Antioxidant power": the FRAP assay. *Anal. Biochem.* 239, 70–76. doi: 10.1006/ABIO.1996.0292

Biswas, J., Chowdhury, B., Bhattacharya, A., and Mandal, A. B. (2002). *In vitro* screening for increased drought tolerance in rice. *Vitr. Cell. Dev. Biol. Plant* 38, 525–530. doi: 10.1079/IVP2002342

Carillo, P. (2018). GABA shunt in durum wheat. *Front. Plant Sci.* 9. doi: 10.3389/fpls.2018.00100

Carillo, P., Mastrolonardo, G., Nacca, F., Parisi, D., Verlotta, A., and Fuggi, A. (2008). Nitrogen metabolism in durum wheat under salinity: accumulation of proline and glycine betaine. *Funct. Plant Biol.* 35, 412–426. doi: 10.1071/FP08108

Chang, C. C., Yang, M. H., Wen, H. M., and Chern, J. C. (2002). Estimation of total flavonoid content in propolis by two complementary colometric methods. *J. Food Drug Anal.* 10, 178–182. doi: 10.38212/2224-6614.2748

Chen, T. H. H., and Murata, N. (2008). Glycinebetaine: an effective protectant against abiotic stress in plants. *Trends Plant Sci.* 13, 499–505. doi: 10.1016/j.tplants.2008.06.007

Chen, T. H. H., and Murata, N. (2011). Glycinebetaine protects plants against abiotic stress: Mechanisms and biotechnological applications. *Plant Cell Environ.* 34, 1–20. doi: 10.1111/j.1365-3040.2010.02232.x

Cocozza, C., De Miguel, M., Pšidová, E., Ditmarová, L. U., Marino, S., Maiuro, L., et al. (2016). Variation in ecophysiological traits and drought tolerance of beech (*Fagus sylvatica* L.) seedlings from different populations. *Front. Plant Sci.* 7. doi: 10.3389/fpls.2016.00886

Confalonieri, M., Belenghi, B., Balestrazzi, A., Negri, S., Facciotto, G., Schenone, G., et al. (2000). Transformation of elite white poplar (*Populus alba* L.) cv. "Villafranca" and evaluation of herbicide resistance. *Plant Cell Rep.* 19, 978–982. doi: 10.1007/s002990000230

Erst, A. A., and Karakulov, A. V. (2023). Drought tolerance of ornamental Poplar forms cultured in *vitro*. *Contemp. Probl. Ecol.* 16, 339–345. doi: 10.1134/S1995425523030058

Fischerová, Z., Tlustoš, P., Száková, J., and Šichorová, K. (2006). A comparison of phytoremediation capability of selected plant species for given trace elements. *Environ. pollut.* 144 (1), 93–100. doi: 10.1016/j.envpol.2006.01.005

Ghassemi-Golezani, K., Farhadi, N., and Nikpour-Rashidabad, N. (2018). Responses of in *vitro*-cultured *Allium hirtifolium* to exogenous sodium nitroprusside under PEG-imposed drought stress. *Plant Cell. Tissue Organ Cult.* 133, 237–248. doi: 10.1007/s11240-017-1377-2

Grieve, C. M., and Grattan, S. R. (1983). Rapid assay for determination of water soluble quaternary ammonium compounds. *Plant Soil* 70, 303–307. doi: 10.1007/BF02374789

Guo, X. Y., Zhang, X. S., and Huang, Z. Y. (2010). Drought tolerance in three hybrid poplar clones submitted to different watering regimes. *J. Plant Ecol.* 3, 79–87. doi: 10.2478/s11756-013-0165-7

Hajihashemi, S., and Sofo, A. (2018). The effect of polyethylene glycol-induced drought stress on photosynthesis, carbohydrates and cell membrane in *Stevia rebaudiana* grown in greenhouse. *Acta Physiol. Plant* 40, 1–9. doi: 10.1007/s11738-018-2722-8

Hanász, A., Dobránszki, J., Mendler-Drienyovszki, N., Zsombik, L., and Magyar-Tábori, K. (2022). Responses of Potato (*Solanum tuberosum* L.) Breeding Lines to Osmotic Stress Induced in *In vitro* Shoot Culture. *Horticulturae* 8, 1–24. doi: 10.3390/horticulturae8070591

Hernández-Pérez, C. A., Gómez-Merino, F. C., Spinoso-Castillo, J. L., and Bello-Bello, J. J. (2021). *In vitro* screening of sugarcane cultivars (*Saccharum* spp. hybrids) for tolerance to polyethylene glycol-induced water stress. *Agronomy* 11, 598. doi: 10.3390/agronomy11030598

Huang, D., Ou, B., and Prior, R. L. (2005). The chemistry behind antioxidant capacity assays. *J. Agric. Food Chem.* 53 (6), 1841–1856. doi: 10.1021/jf030723c

Hussein, E. A., El-Kerdany, A. Y., and Afifi, M. K. (2017). Effect of drought and salinity stresses on two strawberry cultivars during their regeneration in *vitro*. *IJISET-International J. Innov. Sci. Eng. Technol.* 4, 83–93.

Intergovernmental Panel on Climate Change (IPCC) (2023). *Climate change 2022 – Impacts, Adaptation and Vulnerability: Working Group II Contribution to the Sixth Assessment Report of the Intergovernmental Panel on Climate Change* (Cambridge: Cambridge University Press). doi: 10.1017/9781009325844

Ionita, M., Nagavciuc, V., Scholz, P., and Dima, M. (2022). Long-term drought intensification over Europe driven by the weakening trend of the Atlantic Meridional Overturning Circulation. *J. Hydrol. Reg. Stud.* 42, 101176. doi: 10.1016/j.ejrh.2022.101176

Jaafar, K. S., Mohammed, M. A., and Mohammed, S. M. (2021). Screening for drought tolerance in cotton (*Gossypium hirsutum* L.) using in *vitro* technique. *J. Dryland Agric.* 7 (4), 52–59. doi: 10.5897/JODA2021.0067

Jafari, M., and Shahsavar, A. R. (2022). Sodium nitroprusside: its beneficial role in drought stress tolerance of "Mexican lime" (*Citrus aurantifolia* (Christ.) Swingle) under in *vitro* conditions. *Vitr. Cell. Dev. Biol. - Plant* 58, 155–168. doi: 10.1007/s11627-021-10218-9

Jaleel, C. A., Manivannan, P., Wahid, A., Farooq, M., Al-Juburi, H. J., Somasundaram, R., et al. (2009). Drought stress in plants: A review on morphological characteristics and pigments composition. *Int. J. Agric. Biol.* 11, 100–105.

Karimi, A., Tabari, M., Javanmard, Z., and Bader, M. K. F. (2022). Drought effects on morpho-physiological and biochemical traits in persian oak and black poplar seedlings. *Forests* 13, 339. doi: 10.3390/f13030399

Katanić, M., Kovačević, B., Đorđević, B., Kebert, M., Pilipović, A., Klašnja, B., et al. (2015). Nickel phytoremediation potential of white poplar clones grown in *vitro*. *Rom. Biotechnol. Lett.* 20 (1), 10085–10096.

Kebert, M., Kostić, S., Stojnić, S., Čapelja, E., Gavranović Markić, A., Zorić, M., et al. (2023). Fine-tuning of the plant hormones, polyamines and osmolytes by ectomycorrhizal fungi enhances drought tolerance in pedunculate oak. *Int. J. Mol. Sci.* 24 (8), 7510. doi: 10.3390/ijms24087510

Kebert, M., Kostić, S., Vuksanović, V., Gavranović Markić, A., Kiprovski, B., Zorić, M., et al. (2022b). Metal- and organ-specific response to heavy metal-induced stress mediated by antioxidant enzymes' Activities, polyamines, and plant hormones levels in *populus deltoides*. *Plants* 11 (23). doi: 10.3390/plants11233246

Kebert, M., Rapparini, F., Neri, L., Bertazza, G., Orlović, S., and Biondi, S. (2017). Copper-induced responses in poplar clones are associated with genotype-and organ-specific changes in peroxidase activity and proline, polyamine, ABA, and IAA levels. *J. Plant Growth Regul.* 36, 131–147. doi: 10.1007/s00344-016-9626-x

Kebert, M., Vuksanović, V., Stefels, J., Bojović, M., Horák, R., Kostić, S., et al. (2022a). Species-Level Differences in Osmoprotectants and Antioxidants Contribute to Stress Tolerance of *Quercus robur* L., and *Q. cerris* L. Seedlings under Water Deficit and High Temperatures. *Plants* 11 (13), 1744. doi: 10.3390/plants11131744

Kim, D. O., Jeong, S. W., and Lee, C. Y. (2003). Antioxidant capacity of phenolic phytochemicals from various cultivars of plums. *Food Chem.* 81 (3), 321–326. doi: 10.1016/S0308-8146(02)00423-5

Kishor, P. K., Sangam, S., Amrutha, R. N., Laxmi, P. S., Naidu, K. R., Rao, K. S., et al. (2005). Regulation of proline biosynthesis, degradation, uptake and transport in higher plants: its implications in plant growth and abiotic stress tolerance. *Curr. Sci.* 88, 424–438.

Kovačević, B., Miladinović, D., Katanić, M., Tomović, Z., and Pekeč, S. (2013). The effect of low initial medium pH on in *vitro* white poplar growth. *Bull. Fac For.* 108, 67–80. doi: 10.2298/gsf1308067k

Kovačević, B., Tišma, G., Nikolić, N., Milović, M., Vuksanović, V., and Orlović, S. (2020). *In vitro* lead tolerance testing in white poplar genotypes on acidic medium. *South-east Eur.* 11 (2), 153–160.

Kumar, S., Kumar, D., Kumar, P., Malik, P. S., and Kumar, M. (2020). Proline accumulation in the leaves of four potato cultivars in response to water stress. *Plant Arch.* 20, 3510–3514.

Lei, Y., Yin, C., and Li, C. (2006). Differences in some morphological, physiological, and biochemical responses to drought stress in two contrasting populations of *Populus przewalskii*. *Physiol. Plant* 127, 182–191. doi: 10.1111/j.1399-3054.2006.00638.x

Li, C. M., Wang, Y., and Yu, W. X. (2011). Dynamic changes of phenolic compound contents in leaf and bark of poplar during autumn temperature drop. *J. For. Res.* 22, 481–485. doi: 10.1007/s11676-011-0191-7

Lichtenthaler, H. K., and Wellburn, A. R. (1983). Determinations of total carotenoids and chlorophylls a and b of leaf extracts in different solvents. *Biochem. Soc Trans.* 11, 591–592. doi: 10.1042/bst0110591

Martin, A. F., Hapsari, B. W., and Ermayanti, T. M. (2021). Determination of growth and antioxidant activity assay of in *vitro* gamma-irradiated Tacca leontopetaloides shoots. *IOP Conf. Ser. Earth Environ. Sci.* 741, 012021. doi: 10.1088/1755-1315/741/1/012021

Martínez-Santos, E., Cruz-Cruz, C. A., Spinoso-Castillo, J. L., and Bello-Bello, J. J. (2021). *In vitro* response of vanilla (*Vanilla planifolia* Jacks. ex Andrews) to PEG-induced osmotic stress. *Sci. Rep.* 11, 1–10. doi: 10.1038/s41598-021-02207-0

Mehmandar, M. N., Rasouli, F., Giglou, M. T., Zahedi, S. M., Hassanpouraghdam, M. B., Aazami, M. A., et al. (2023). Polyethylene glycol and sorbitol-mediated *In vitro* Screening for Drought Stress as an Efficient and Rapid Tool to Reach the Tolerant *Cucumis melo* L. Genotypes. *Plants* 12, 870. doi: 10.3390/plants12040870

Miller, N. J., and Rice-Evans, C. A. (2007). Factors influencing the antioxidant activity determined. *Free Radic. Res.* 26 (3), 195–199. doi: 10.3109/10715769709097799

Mohammed, S., Alsafadi, K., Enaruvbe, G. O., Bashir, B., Elbeltagi, A., Széles, A., et al. (2022). Assessing the impacts of agricultural drought (SPI/SPEI) on maize and wheat yields across Hungary. *Sci. Rep.* 12, 1–19. doi: 10.1038/s41598-022-12799-w

Molnar, S., Clapa, D., and Mitre, V. (2022). Response of the five highbush blueberry cultivars to *in vitro* induced drought stress by polyethylene glycol. *Agronomy* 12, 1–16. doi: 10.3390/agronomy12030732

Mozafari, A., Havas, F., and Ghaderi, N. (2018). Application of iron nanoparticles and salicylic acid in *in vitro* culture of strawberries (*Fragaria* × *ananassa* Duch.) to cope with drought stress. *Plant Cell. Tissue Organ Cult.* 132, 511–523. doi: 10.1007/s11240-017-1347-8

Osmolovskaya, N., Shumilina, J., Kim, A., Didio, A., Grishina, T., Bilova, T., et al. (2018). Methodology of drought stress research: Experimental setup and physiological characterization. *Int. J. Mol. Sci.* 19, 4089. doi: 10.3390/ijms19124089

Özelçi, D., Beker Akbulut, G., and Yiğit, E. (2022). Effects of Melatonin on *Morus nigra* cv. "Eksi Kara" Exposed to Drought Stress. *Tarim Bilim. Derg.* 28, 555–569. doi: 10.15832/ankutbd.953558

Popović, B. M., Štajner, D., Ždero-Pavlović, R., Tari, I., Csiszár, J., Gallé, Á., et al. (2017). Biochemical response of hybrid black poplar tissue culture (*Populus* × *canadensis*) on water stress. *J. Plant Res.* 130, 559–570. doi: 10.1007/s10265-017-0918-4

Popović, B. M., Stajner, D., Zdero-Pavlović, R., Tumbas-Saponjac, V., Canadanović-Brunet, J., and Orlović, S. (2016). Water stress induces changes in polyphenol profile and antioxidant capacity in poplar plants (*Populus* spp). *Plant Physiol. Biochem.* 105, 242–250. doi: 10.1016/j

Pradhan, S., Singh, S. K., Srivastav, M., Prakash, J., Lal, S. K., Padaria, J. C., et al. (2021). Poly ethylene glycol mediated in *vitro* screening and physico-biochemical changes induced in mango callus due to moisture stress. *Plant Cell. Tissue Organ Cult.* 145, 155–172. doi: 10.1007/s11240-020-01999-9

Puente-Garza, C. A., Meza-Miranda, C., Ochoa-Martínez, D., and García-Lara, S. (2017). Effect of in *vitro* drought stress on phenolic acids, flavonols, saponins, and antioxidant activity in *Agave salmiana*. *Plant Physiol. Biochem.* 115, 400–407. doi: 10.1016/j.plaphy.2017.04.012

Radi, H., Bouchiha, F., El Maataoui, S., Oubassou, E. Z., Rham, I., Alfeddy, M. N., et al. (2023). Morphological and physio-biochemical responses of cactus pear (*Opuntia ficus indica* (L.) Mill.) organogenic cultures to salt and drought stresses induced in *vitro*. *Plant Cell. Tissue Organ Cult.* 154, 337–350. doi: 10.1007/s11240-023-02454-1

Razavizadeh, R., Farahzadianpoor, F., Adabavazeh, F., and Komatsu, S. (2019). Physiological and morphological analyses of *Thymus vulgaris* L. in *vitro* cultures under polyethylene glycol (PEG)-induced osmotic stress. *Vitr. Cell. Dev. Biol. Plant* 55, 342–357. doi: 10.1007/s11627-019-09979-1

Razmjoo, K., Heydarizadeh, P., and Sabzalian, M. R. (2008). Effect of salinity and drought stresses on growth parameters and essential oil content of *Matricaria chamomila*. *Int. J. Agric. Biol.* 10, 451–454.

Rosso, L., Cantamessa, S., Bergante, S., Biselli, C., Fricano, A., Chiarabaglio, P. M., et al. (2023). Responses to drought stress in poplar: what do we know and what can we learn? *Life* 13 (2), 533. doi: 10.3390/life13020533

Rubio, M. C., González, E. M., Minchin, F. R., Webb, K. J., Arrese-Igor, C., Ramos, J., et al. (2002). Effects of water stress on antioxidant enzymes of leaves and nodules of transgenic alfalfa overexpressing superoxide dismutases. *Physiol. Plant* 115, 531–540. doi: 10.1034/j.1399-3054.2002.1150407.x

Safaei Chaeikar, S., Marzvan, S., Jahangirzadeh Khiavi, S., and Rahimi, M. (2020). Changes in growth, biochemical, and chemical characteristics and alteration of the antioxidant defense system in the leaves of tea clones (*Camellia sinensis* L.) under drought stress. *Sci. Hortic. (Amsterdam).* 265, 109257. doi: 10.1016/j.scienta.2020.109257

Salahvarzi, M., Nasr Esfahani, M., Shirzadi, N., Burritt, D. J., and Tran, L. S. P. (2021). Genotype-and tissue-specific physiological and biochemical changes of two chickpea (*Cicer arietinum*) varieties following a rapid dehydration. *Physiol. Plant* 172 (3), 1822–1834. doi: 10.1111/ppl.13452

Sarker, U., and Oba, S. (2018). Drought stress enhances nutritional and bioactive compounds, phenolic acids and antioxidant capacity of *Amaranthus* leafy vegetable. *BMC Plant Biol.* 18 (1), 1–15. doi: 10.1186/s12870-018-1484-1

Selmar, D. (2008). Potential of salt and drought stress to increase pharmaceutical significant secondary compounds in plants. *Landbauforschung Volkenrode Agric. For. Res.* 58 (1/2), 139–144.

Shivakrishna, P., Reddy, K. A., and Rao, D. M. (2018). Effect of PEG-6000 imposed drought stress on RNA content, relative water content (RWC), and chlorophyll content in peanut leaves and roots. *Saudi J. Biol. Sci.* 25 (2), 285–289. doi: 10.1016/j.sjbs.2017.04.008

Silvestri, C., Celletti, S., Cristofori, V., Astolfi, S., Ruggiero, B., and Rugini, E. (2017). Olive (*Olea europaea* L.) plants transgenic for tobacco osmotin gene are less sensitive to in *vitro*-induced drought stress. *Acta Physiol. Plant* 39, 1–9. doi: 10.1007/s11738-017-2535-1

Sixto, H. (2005). Response to sodium chloride in different species and clones of genus. *Populus L. Forestry* 78, 93–104. doi: 10.1093/forestry/cpi009

Stanton, B. J., Neale, B. D., and Li, S. (2010). "*Populus* breeding: from the classical to the genomic Approach," in *Genetics and Genomics of Populus. Plant Genetics and Genomics: Crops and Models*, vol. 8 . Eds. S. Jansson, R. Bhalerao and A. Groover (New York, NY: Springer). doi: 10.1007/978-1-4419-1541-2_14

Szabados, L., and Savouré, A. (2010). Proline: A multifunctional amino acid. *Trends Plant Sci.* 15, 89–97. doi: 10.1016/j.tplants.2009.11.009

TIBCO Software Inc (2020) *Data science work-bench*. Available at: http://www.tibco.com/products/data-science.

Tsao, R. (2010). Chemistry and biochemistry of dietary polyphenols. *Nutrients* 2 (12), 1231–1246. doi: 10.3390/nu2121231

Urquiaga, I. N. E. S., and Leighton, F. (2000). Plant polyphenol antioxidants and oxidative stress. *Biol. Sci.* 33 (2), 55–64. doi: 10.4067/S0716-97602000000200004

Vuksanović, V., Kovačević, B., Orlović, S., Kebert, M., and Kovač, M. (2019a). The influence of drought on growth and development of white poplar shoots *In Vitro. Poplar*. 203, 13–18.

Vuksanović, V. (2019b). Tolerance of white poplar assortments against abiotic factors in *vitro* (Serbia: University of Novi Sad).

Vuksanović, V., Kovačević, B., Kebert, M., Milović, M., Kesić, L., Karaklić, V., et al. (2019c). *In vitro* modulation of antioxidant and physiological properties of white poplar induced by salinity. *Bull. Fac. For.* 120, 179–196. doi: 10.2298/GSF1920179V

Vuksanović, V., Kovačević, B., Kebert, M., Katanić, M., Pavlović, L., Kesić, L., et al. (2019d). Clone specificity of white poplar (Populus alba L.) acidity tolerance in *vitro*. *Fresenius Environ. Bull.* 28 (11), 8307–8313.

Vuksanović, V., Kovačević, B., Stojnić, S., Kebert, M., Kesić, L., Galović, V., et al. (2022). Variability of tolerance of Wild cherry clones to PEG-induced osmotic stress in *vitro*. *IForest* 15, 265–272. doi: 10.3832/ifor4033-015

Wei, T., and Simko, V. (2021) *R package 'corrplot': Visualization of a Correlation Matrix*. Available at: https://github.com/taiyun/corrplot.

Wickham, H. (2016). *ggplot2: Elegant Graphics for Data Analysis* (New York: Springer-Verlag). Available at: https://ggplot2.org.

Woodrow, P., Ciarmiello, L. F., Annunziata, M. G., Pacifico, S., Iannuzzi, F., Mirto, A., et al. (2017). Durum wheat seedling responses to simultaneous high light and salinity involve a fine reconfiguration of amino acids and carbohydrate metabolism. *Physiol. Plant* 159 (3), 290–312. doi: 10.1111/ppl.12513

Wu, R., Wang, T., Richardson, A. C., Allan, A. C., Macknight, R. C., and Varkonyi-Gasic, E. (2019). Histone modification and activation by SOC1-like and drought stress-related transcription factors may regulate AcSVP2 expression during kiwifruit winter dormancy. *Plant Sci.* 281, 242–250. doi: 10.1016/j.plantsci.2018.12.001

Xia, Q., Fu, L. J., Tang, H., Song, L., Tan, J. L., and Guo, Y. (2022). Sensing and classification of rice (*Oryza sativa* L.) drought stress levels based on chlorophyll fluorescence. *Photosynthetica* 60, 102–109. doi: 10.32615/ps.2022.005

Yang, C., Yao, J., Li, S., Ni, H., Liu, Y., Zhang, Y., et al. (2016). Growth and physiological responses to drought stress and comprehensive evaluation on drought tolerance in Leuce clones at nursery stage. *J. Beijing For. Univ.* 38 (5), 58–66.

Yoshiba, Y., Kiyosue, T., Nakashima, K., Yamaguchi-Shinozaki, K., and Shinozaki, K. (1997). Regulation of levels of proline as an osmolyte in plants under water stress. *Plant Cell Physiol.* 38, 1095–1102. doi: 10.1093/oxfordjournals.pcp.a029093

Youssef, M., Mohamed, E.-S. A., El-Sayed, E.-S. N., and Abouzaid, E. (2016). Establishment of an in *vitro* evaluation method for drought tolerance in guava. *Res. J. Appl. Biotechnol.* 5, 32–38.

Ždero-Pavlović, R., Blagojević, B., Latković, D., Agić, D., Mićić, N., Štajner, D., et al. (2020). Drought-induced changes in antioxidant system and osmolyte content of poplar cuttings. *Balt. For.* 26 (2). doi: 10.46490/BF420

Zhang, X., Liu, L., Chen, B., Qin, Z., Xiao, Y., Zhang, Y., et al. (2019). Progress in understanding the physiological and molecular responses of Populus to salt stress. *Int. J. Mol. Sci.* 20 (6), 1312. doi: 10.3390/ijms20061312

Zhong, Y. P., Li, Z., Bai, D. F., Qi, X. J., Chen, J. Y., Wei, C. G., et al. (2018). *In vitro* variation of drought tolerance in five actinidia species. *J. Am. Soc Hortic. Sci.* 143, 226–234. doi: 10.21273/JASHS04399-18

frontiers | Frontiers in Forests and Global Change

TYPE Original Research
PUBLISHED 29 November 2023
DOI 10.3389/ffgc.2023.1243352

OPEN ACCESS

EDITED BY
Hülya Torun,
Duzce University Duzce, Türkiye

REVIEWED BY
Yadav Ankit,
Indian Institute of Science Education and Research Mohali, India
Kevin Smith,
Forest Service (USDA), United States

*CORRESPONDENCE
Ravi S. Maurya
✉ ravishankarmaurya94@gmail.com
Krishna G. Misra
✉ kgmisrabsip@gmail.com

RECEIVED 21 June 2023
ACCEPTED 06 November 2023
PUBLISHED 29 November 2023

CITATION
Maurya RS, Misra KG, Vishwakarma S, Singh V, Misra S and Yadava AK (2023) Analyses of intra-annual density fluctuation signals in Himalayan cedar trees from Himachal Pradesh, western Himalaya, India, and its relationship with apple production.
Front. For. Glob. Change 6:1243352.
doi: 10.3389/ffgc.2023.1243352

Analyses of intra-annual density fluctuation signals in Himalayan cedar trees from Himachal Pradesh, western Himalaya, India, and its relationship with apple production

Ravi S. Maurya[1,2]*, Krishna G. Misra[1,2]*, Sadhana Vishwakarma[1,3], Vikram Singh[1,4], Sandhya Misra[1] and Akhilesh K. Yadava[1]

[1]Birbal Sahni Institute of Palaeosciences, Lucknow, India, [2]Academy of Scientific and Innovative Research, Ghaziabad, Uttar Pradesh, India, [3]Department of Botany, Institute of Science, Banaras Hindu University, Varanasi, India, [4]Department of Geology, University of Lucknow, Lucknow, India

Intra-annual density fluctuation (IADF) refers to anatomical changes in the tree ring caused by a sudden change in wood density triggered by a combination of climate variations and various biotic and abiotic influences. To reveal the occurrence of IADFs, we analyze the growth rings of Himalayan cedar (*Cedrus deodara*) growing over the Kullu region, Himachal Pradesh, western Himalaya. Using 30 increment cores, we precisely dated and developed a 214-year-long tree-ring chronology extending back to AD 1808. The tree–growth–climate relationship using ring-width chronology and observed climate data revealed that cool and moist condition provides favorable condition for Himalayan cedar tree growth. Delving deeper into wood anatomy of growth rings, we revealed the frequent occurrences of IADFs in both earlywood (IADF*e*) and latewood (IADF*l*). The formation of IADFs in earlywood (IADF*e*) is related to the reduced precipitation from April to July, causing moisture stress in the soil and surrounding climate. However, wetter conditions in the late growing season, mainly August–October, activated the formation of IADFs in latewood (IADF*l*). The study revealed several IADF years in earlywood and latewood, such as 1901, 1902, 1903, 1914, 1915, 1919, 1920, 1923, 1925, 1943, 1958, 1959 and 1937, 1955, 1956, 1988, respectively. These IADF years corresponded with unusual climatic fluctuations that severely affected apple production, the major cash crop in the region. The analyses demonstrated that the IADF chronology of Himalayan cedar would be a valuable proxy to understand abrupt and unusual climatic fluctuations from a long-term perspective for the data-scarce western Himalayan region.

KEYWORDS

intra-annual density fluctuation, earlywood, latewood, Himalayan cedar, cambium, western Himalaya

1 Introduction

In the late 1400s, Leonardo da Vinci noticed that the number of rings in the tree's branches designates their age (translation of Leonardo da Vinci's Treatise on Painting) and tree-ring width is associated with the climate conditions during the year of their formation (Stallings, 1937; Sarton, 1954; Corona, 1986). Furthermore, cross-dating was initially employed by French

naturalists Duhamel and Buffon to pinpoint the 1709 frost ring in the samples collected in 1737 (Dean, 1978; Webb, 1986). In 1827, Twining played a crucial role in bringing the process to light (Dean, 1978), while Babbage notably elaborated on it in 1838 (Babbage, 1838), consistently championing its significance. Later, Douglass made significant advancements by developing the primary skeleton plotting method, and refining the cross-dating technique in 1904, which is supported by extensive testing and documentation (Webb, 1986; Nash, 1999). However, since Douglass's (1914) dendrochronological investigations, relationships between annual tree-growth changes and climatic conditions have been recognized. Tree rings are expressed as "well-defined increments surrounding the entire tree" and are generated in response to climatic and genetic factors. Each tree ring is subsequently dated to one calendar year, the same year of tree-ring formation, and is a fundamental concept of dendrochronology. However, IADFs are characterized by the appearance of latewood-like cells in earlywood or earlywood-like cells in latewood (Fritts, 2001). These IADFs are identifiable as a layer of cells within a tree ring recognized by distinct characteristics, such as shape, size, and wall thickness (Kaennel and Schweingruber, 1995). Mostly, IADFs are also accepted as false rings (Schulman, 1938), multiple rings (Kozlowski, 1971), or intra-annual growth bands (Fritts, 1976), and they are formed in annual rings in accordance with short-term climatic variability throughout the growing season. The formation of IADFs is not limited to a specific group of trees but extends to several species, including both hardwood trees like Himalayan birch (*Betula utilis*) and oak (*Quercus* spp.) and softwood trees like Himalayan cedar (*Cedrus deodara*), strawberry tree (*Arbutus unedo*), and Aleppo pine (*Pinus halepensis*) in different climates globally (Cherubini et al., 2003; De Micco et al., 2016). Therefore, IADFs comprise an essential tool to examine and evaluate intra-annual changes in climatic factors, giving enormous seasonal level clues worldwide (Copenheaver et al., 2006; De Luis et al., 2007; Battipaglia et al., 2010; Edmondson, 2010; Olivar et al., 2012; Gao et al., 2021; Tucker et al., 2022). The formation of IADF reflects tree's ability to modify wood anatomical characters to temporary fluctuation in climatic conditions. This adaptation helps them balance hydraulic efficiency and protection instead of embolism throughout wet and dry spells, respectively (De Micco and Aronne, 2009; Wilkinson et al., 2015). IADFs have been occasionally linked to disruptions or reductions in photosynthesis due to environmental limitations, including severe aridity, frost events, and defoliation resulting from fire or pathogen attacks (De Micco et al., 2007; Schweingruber, 2007). However, precipitation and temperature are the most commonly examined factors when studying the occurrence of IADF, as they play a crucial role in interpreting the ecological significance of IADF formation (De Micco et al., 2016). Besides the climate variables, IADF can offer valuable insights into climate modeling, such as analyzing climate variations at a seasonal temporal scale and comparing modeled climate data with observed IADF patterns, which can assess the accuracy of model outputs and make necessary adjustments. Using IADFs in climate modeling contributes to our understanding of short-term climate variability, enhance our capacity to predict and adapt to changing environmental conditions.

Globally, the occurrence of IADF is known to exhibit variability based on several tree-related factors, such as tree's age, sex, size, and width of tree ring (Rigling et al., 2001; Wimmer, 2002; Campelo et al., 2007, 2013; De Luis et al., 2009; Vieira et al., 2009; Olano et al., 2015). According to Vogel et al. (2001), the formation of false rings is also more likely to occur in younger trees and trees that grow faster. The increased likelihood of IADFs in juvenile tree rings can be attributed to the early reactivation of the cambium resulting in an extended growing season, along with a rapid physiological and morphological response to environmental alterations (Villalba and Veblen, 1996; Vieira et al., 2009). However, younger trees with shallower root systems may also be more vulnerable to environmental changes, which can lead to the production of the IADF in response to changes in water availability (Ehleringer and Dawson, 1992; Battipaglia et al., 2014). Pacheco et al. (2016) discovered the link between a higher IADF frequency in tree rings and a shallower root system, indicating that the shallow-rooted Spanish juniper (*Juniperus thurifera*) in north-eastern Spain is more susceptible to summer and autumn rains than the deeper-rooted Aleppo pine (*Pinus halepensis*). According to the Carvalho et al. (2015) hypothesis, higher spring cell production rates contribute latewood to developing IADFs, successively increasing the number of cells undergoing enlargement following the summer drought and forming wider rings. A range of variations in the occurrence of IADF across species dispersion is often mentioned (Novak et al., 2013; Nabais et al., 2014). From the Mediterranean climate, a higher frequency of IADF in cluster pine (*Pinus pinaster*) was reported in younger trees than older ones (Bogino and Bravo, 2009; Vieira et al., 2009). A homogeneous age trend has been analyzed in Aleppo pine growing over the Iberian Peninsula. Specifically, the relative age and size of IADF frequency in both Aleppo pine and cluster pine species have been observed, revealing that the highest frequency of IADF is seen in trees of age ~27 years old, in the juvenile stage, and characterized by wider than narrower tree rings (Novak et al., 2013). In Spain, the occurrences of IADF in cluster pine have been conversely correlated with secondary growth rates (Bogino and Bravo, 2009). Notably, no significant relationship between IADF frequency with age and tree-ring width has been observed in young trees with age < 35 years from the wetter north-western region of Spain. In the case of Scots pine (*Pinus sylvestris*) growing in dry sites within the central Alps, a distinct relationship between IADF frequencies and tree age has been identified (Rigling et al., 2001, 2002). An extensive investigation of a database of cluster pine, aleppo pine, and stone pine (*Pinus pinea*) trees within the Mediterranean region revealed that IADFs appeared more frequently in juvenile trees with wide rings (Zalloni et al., 2016). However, a higher frequency of IADF was reported in tree rings of black spruce (*Picea mariana*) and jack pine (*Pinus banksiana*) from eastern Manitoba (Hoffer and Tardif, 2009), which showed no remarkable relationship between IADF occurrence and tree-ring width.

Moreover, the IADF-based studies carried out to understand the impact of sudden climatic changes in tree's radial growth focusing on intra-seasonal and seasonal resolution (Priya and Bhat, 1998; Braüning, 1999; Speer et al., 2004; Copenheaver et al., 2010; Gonda-King et al., 2012; Palakit et al., 2012; De Micco et al., 2014; Campelo et al., 2015; Ren et al., 2015). The western Himalayan region has not yet received much attention on IADF research, primarily focusing on the high-latitude temperate and Mediterranean regions. In India, tree-ring studies have predominantly confined to the application of ring-width chronologies in climatic reconstructions (Singh et al., 2009; Yadav et al., 2014, 2015, 2017; Misra et al., 2015, 2021; Yadava et al., 2016, 2021; Shekhar et al., 2017; Shah et al., 2019; Singh et al., 2021, 2022). However, few studies have been carried out on wood density (Hughes and Davies, 1987; Hughes, 1992, 2001; Borgaonkar et al., 2001), stable isotopes (Ramesh et al., 1985, 1986; Managave et al.,

2011, 2020; Sano et al., 2017), and IADFs from northeast India (Singh et al., 2016; Thomte et al., 2022). Considering the significance of IADFs, efforts have been made to analyze the short-term intra-annual climatic changes from the western Himalaya.

2 Materials and methods

2.1 Study area and tree-ring data

Himalayan cedar (*Cedrus deodara*) is a long-lived conifer generally growing over steep rocky slopes with well-drained soil cover and moderate-to-heavy winter snowfall at an elevation varying from 1,200 to 3,300 masl (Raizada and Sahni, 1960; Champion and Seth, 1968). To comprehend the effect of climate on Himalayan cedar, we selected the Jari (31° 59′ 43″ N, 77° 14′ 16″ E) restricted forest area located in Parvati Valley, Kullu, Himachal Pradesh (Figure 1). The lithology around Jari village comprises carbonaceous phyllites, quartz schist with recrystallized limestone bands (overlying thrust sheet) that form a semi-klippen structure over the Manikaran Quartzite with a thrust contact (Choubey et al., 1997).

For the tree-ring sampling, healthy undisturbed trees free from any visible mark of injury were chosen and cored at breast height (~1.4 m) perpendicular to the slope. For this study, 30 core samples from 25 trees were collected during May 2022. Subsequently, the transverse surface of increment core samples was mounted on wooden frames and polished using abrasives of varying grits (220 and 400 grit) until the cellular features were discernible under the stereozoom binocular microscope. The established dendrochronological procedures were adopted for cross-dating of each series (Fritts, 1976).

Using LINTAB (Rinn, 2003) measuring machine connected to a personal computer, the ring widths of accurately dated increment core samples were measured with a resolution of 0.01 mm. The dating quality control program COFECHA demonstrated robust coherence in the growth patterns of the trees. It showed a high correlation among the radii, $n = 30$ (mean $r = 0.84$), indicating common climate factors affecting tree growth over the site (Holmes, 1983). The statistical program ARSTAN (Cook, 1985) was used to develop tree-ring chronology and removed the juvenile growth trend and other noises in the samples by curve fitting. A 67% cubic smoothing spline with a 50% frequency response cutoff was applied to detrend the ring-width data series. To stabilize the variation in each series, the tree-ring-width series were power transformed before being detrended (Cook and Peters, 1997). Detrending was accomplished by biweight robust mean computed (Cook, 1985), and mean chronology was developed by merging all standardized series. The resulting 214-year-long ring-width chronology (AD 1808–2021) of Himalayan cedar was developed from Kullu, Himachal Pradesh (Figure 2). A sufficient number of increment cores were used with a threshold value of expressed population signal (EPS) > 0.85 from AD 1855, which reflects the validation of chronology for analyses (Figure 2). The chronology statistics, such as mean sensitivity, standard deviation, and first-order autocorrelation, showed strong signals of interannual climatic variations (Table 1).

2.2 Climate signal in ring-width chronology

The climate over the orography-dominated Himalayan region varies from valley to valley or within a very short distance in the valley. Meteorological data for the western Himalayan region are geographically erratic and restricted to short duration (Singh et al., 2021, 2022). For the

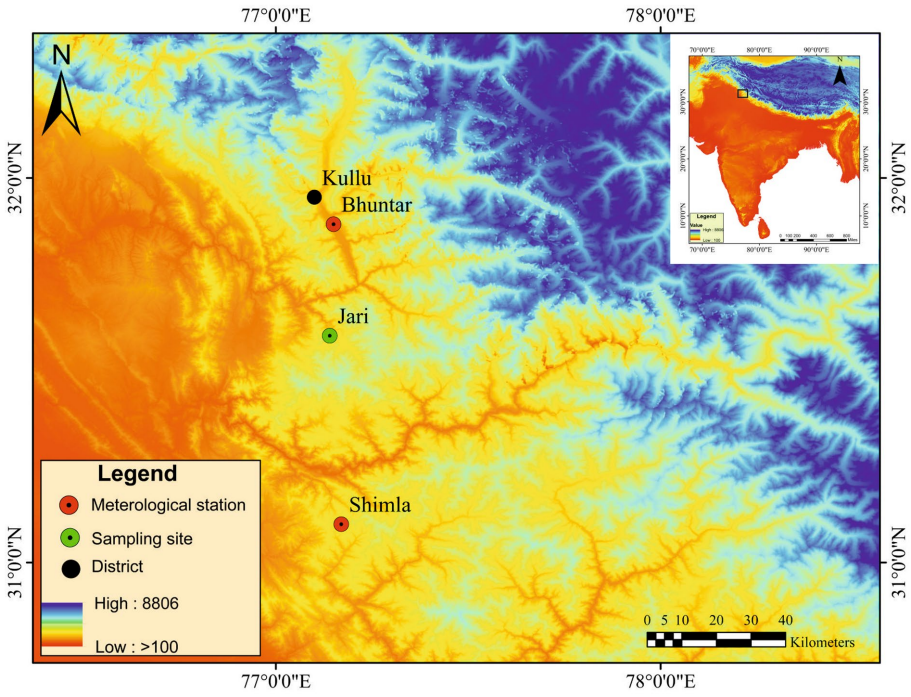

FIGURE 1
Location of the study area, tree-ring sampling site, and meteorological station used in the present study.

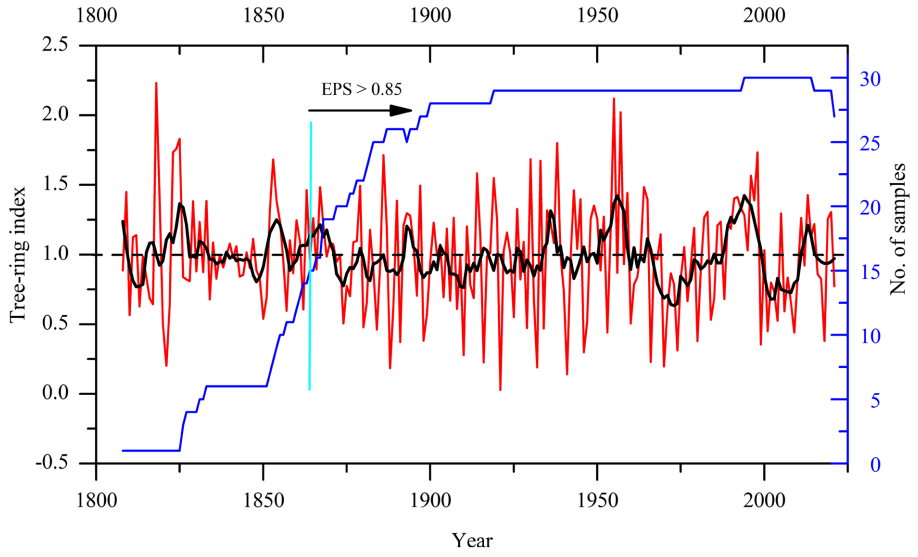

FIGURE 2
Himalayan cedar tree-ring chronology developed from Kullu, Himachal Pradesh (AD 1808–2021), with the number of samples used in the development of chronology.

TABLE 1 Himalayan cedar tree-ring chronology statistics developed from Jari, Kullu, Himachal Pradesh, India (1808–2021).

Site	Latitude (N)	Longitude (E)	Elevation (masl)	Cores/ trees	Chronology Span AD (years)	Chronology with EPS > 0.85, AD	MI	MS	SD	AR1
Jari, Kullu	31° 59′ 43″	77° 14′ 16″	1,702 m	30/25	1808–2021 (214)	1855–2021	0.97	0.46	0.39	0.24

EPS, expressed population signal; MI, mean index; MS, mean sensitivity; SD, standard deviation; AR1, first-order autocorrelation.

present study, monthly precipitation data (1901–2010) from Bhuntar and mean monthly temperature data (1876–1998) from Shimla were selected for the analyses (Figure 3). Bootstrap correlation analysis was performed using the program DENDROCLIM2002 (Biondi and Waikul, 2004) for the tree–growth–climate relationship (Figure 4). This analysis using residual chronology specified that the radial growth of the Himalayan cedar has a direct correlation with precipitation throughout the year except for June and August.

From the previous year November to the current year May month's precipitation plays a significant positive role in the Himalayan cedar growth. Analyses with temperature data showed an inverse relationship with tree growth during the whole year except for the monsoon months (July–September). Current-year February–May are the significant months for tree growth. However, an increase in the February–May temperature initiates high evapotranspiration during these months, resulting slowdown in the tree growth. Overall correlation analyses showed that cool and wet conditions favor the Himalayan cedar tree growth over the study site.

2.3 Cambium activity and growth ring in Himalayan cedar

The Himalayan cedar is a conifer tree species native to Himalaya, thrives across a range extending from Afghanistan to Garhwal Himalaya, and is also found in patches within the Kumaun Himalaya. Sub-tropical to temperate climate in a monsoon and monsoon shadow region of western Himalaya provides favorable conditions for its growth. Most trees and woody plants possess a thin tissue layer known as the cambium, located between the xylem and phloem that develops new cells and is responsible for secondary growth (increase in radial growth; Wang et al., 2021). In temperate climates, cambium exhibits a seasonal rhythm of activity responsible for the xylem formation throughout a prolonged growing period from March to November. In the winter, cambium activity goes dormant from December to February. During the growing season, cells are larger and lighter in color; on the other hand, in autumn, cells become smaller and darker in color.

2.4 Intra-annual density fluctuations

This study involved precisely dated growth ring sequences with Intra-annual density fluctuation (IADF) in cores under a stereozoom binocular microscope with magnification capabilities of up to 50×. IADFs are observed as thin bands of tracheids with thick walls (resembling latewood) within the earlywood portion, which is close to both sides by tracheids with thinner walls and larger diameters (Singh et al., 2016). On the other hand, the IADFs in the latewood portion are thin-walled tracheids (earlywood-like) neighboring on

10.3389/ffgc.2023.1243352

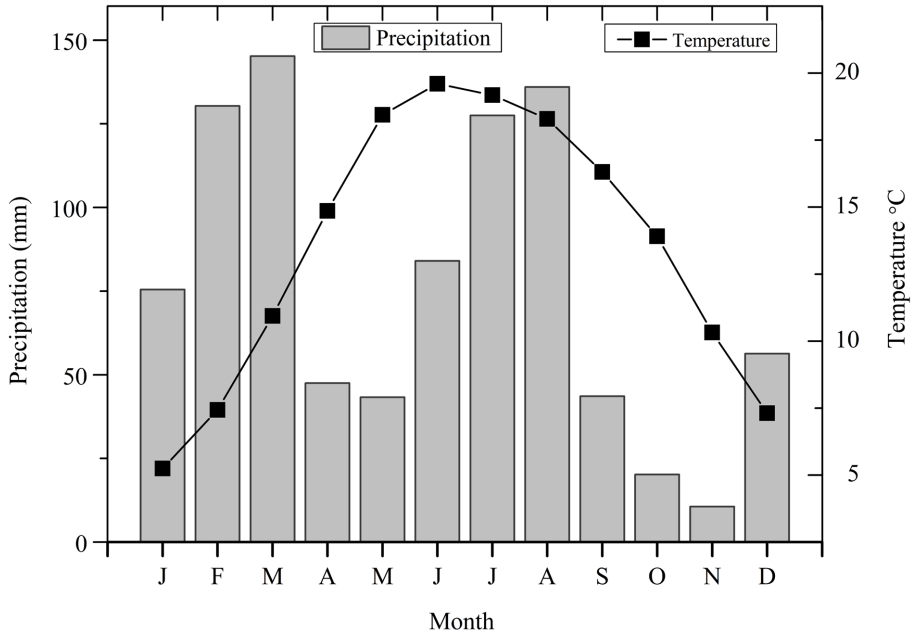

FIGURE 3
Recorded monthly variation in precipitation from Bhuntar and mean temperature from Shimla of Himachal Pradesh.

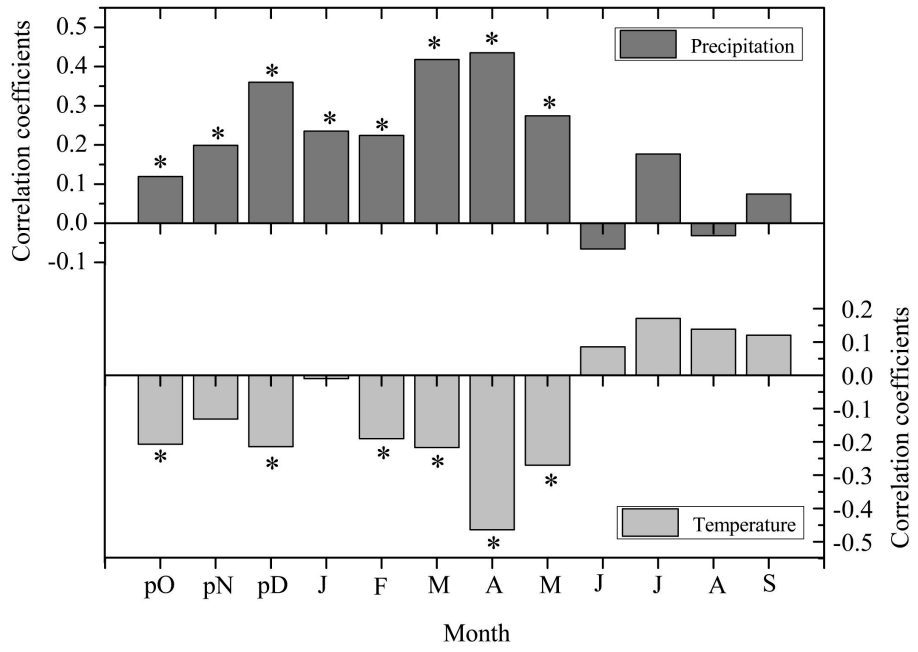

FIGURE 4
Bootstrap correlation between ring-width chronology and climate variables (Precipitation and temperature). *Represents correlation values significant at a 95% confidence level.

both sides by thicker walled, smaller diameter latewood tracheids (Singh et al., 2016). Their precise location within the ring may serve as a robust proxy of the climatic variables on the resolution of the intra-seasonal level, as the formation of IADFs takes place by climatic variation during the growing season. In the present study, IADFs were recorded in trees when both cores from a tree contained an IADF in an annual ring. However, when only one core from a tree was present, the IADFs in the associated rings were considered, with the single core representing one tree. With precisely dated increment core samples, the percentage (F) and occurrence of IADFs in growth rings of samples for respective years were calculated as ratios: $F = 100^{*}\ n/N$ where n is the number of trees that developed IADF in a particular year in early/latewood along with N is the total number of trees in that specific year.

3 Results

3.1 Correlation between seasonalized precipitation and tree-ring index

Tree growth and climate relationship using residual chronology specified that the radial growth of Himalayan cedar has a significant positive correlation with the monthly precipitation, especially March–April–May (MAM). Specifically, the correlation coefficient (r) was calculated at 0.62, spanning the years from 1901 to 2010. This correlation coefficient value indicates a relatively strong and consistent relationship between MAM precipitation and tree-ring growth (Figure 5). The observed positive correlation between the ring-width chronology and monthly precipitation can likely be attributed to the increased soil moisture content resulting from snow melting, which accumulates during winter. When the snow begins to melt, it effectively acts as a slow-release fertilizer, gradually providing essential nitrogen to the trees. This nitrogen is thought to be attached to snowflakes as they fall through the atmosphere, and when the snow accumulates on the ground and then melts, it releases this nitrogen into the soil. As a result, the trees experience improved growth conditions due to the enhanced soil moisture and the gradual nitrogen supply.

3.2 Relationship between IADF frequency and tree age

A variation in the timing and length of xylem development may account for the age-dependent IADF frequency. In our study, when we examined the relationship between the frequency of IADF and the age of Himalayan cedar trees, we observed that there was a higher incidence of IADF during the juvenile stage of the trees, which typically falls within the age range of ~50–150 years (Figure 6). Interestingly, we also noted that the highest occurrences of IADF were predominantly found within the wider growth rings of the trees, as depicted in Figure 7. This suggests that IADF is more prevalent and pronounced in the earlier years of the tree's life, particularly in the broader annual growth rings.

3.3 Climatic implications of IADFs

In investigation, we observed IADFs within the annual growth rings of Himalayan cedar. It is intriguing that these IADFs were not confined to a specific portion of the growth ring but rather appeared consistently in both the earlywood and latewood. This uniform presence suggests a similarity in moisture fluctuation patterns throughout the growing season, as visually represented in Figure 7. To shed light on the factors responsible for forming these IADFs, we conducted a thorough analysis of climate data for the years that exhibited a high incidence of IADFs. This approach aimed to uncover any climatic patterns or anomalies that might offer insight into the underlying causes of these density fluctuations within the annual growth rings. By examining the climatic conditions during these specific years, we sought to establish potential links between climate variations and the occurrence of IADFs, providing a deeper understanding of the ecological and environmental drivers of this phenomenon.

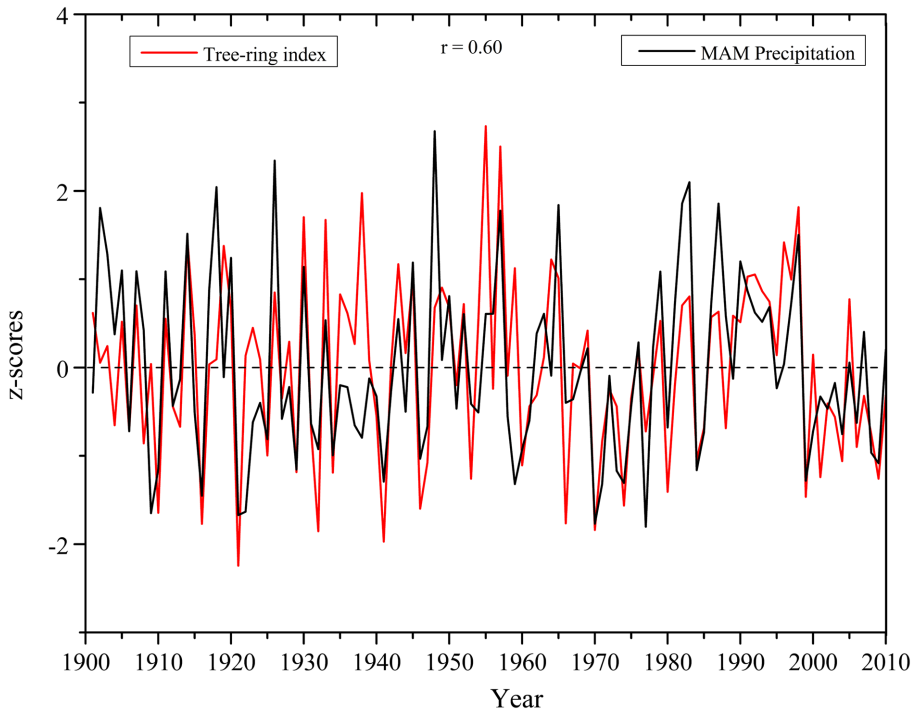

FIGURE 5
Ring-width chronology and seasonalized March–April–May (MAM) precipitation plotted together to show the relationship. The two series showed Pearson correlation of 0.62 (1901–2010, two-tailed $p = 0.01$).

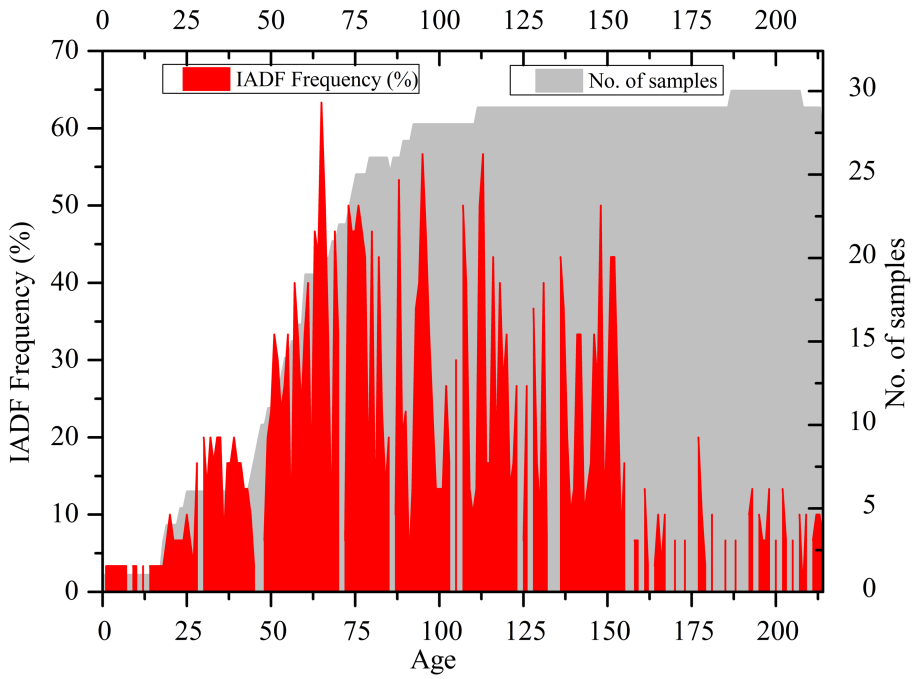

FIGURE 6
Relationship between IADF frequency and tree age.

4 Discussion

4.1 Climatic interpretation of IADFs in earlywood

IADFs in earlywood (IADF*e*) are characterized by thin-lumen, thick-walled tracheids that are bordered on both sides by large-diameter, thin-walled tracheids typical of earlywood.

These IADF*e* tracheids are due to lack of soil moisture throughout the early growing period (Kuo and McGinnes, 1973). Our analysis showed that the IADFs in earlywood were more frequent than in the latewood of Himalayan cedar tree rings growing in Kullu, Himachal Pradesh (Figure 8). Due to inequality in the length of climate data, a common period for precipitation and temperature from 1901 to 1998 was taken, and IADF investigation restricted between them. IADF chronology showed major occurrences of IADF*e* in growth rings of a threshold value of 40% has been taken. The 40% to above IADFe years are 1901, 1902, 1903, 1914, 1915, 1919, 1920, 1923, 1925, 1943, 1958, and 1959 (Figure 9).

Monthly precipitation data from Bhuntar indicated that during the year 1901, precipitation depicted in the months of April was only 39.1 mm, which was very low as compared with the 1901–1998 mean of 80 mm for April month, causing the moisture scarcity and formation of IADF*e*. Successively, in the year 1902, winter precipitation during January (15.2 mm) and February (28.7 mm) was meager as compared with the 1901–1998 mean of January 106 mm and February 114 mm, causing soil moisture deficiency in the growing period, and formation of IADFs takes place. However, high temperature in January (7.5°C) and February (8°C) compared with the 1901–1998 mean of January (5.3°C) and February (6.68°C) triggered snow melting before the vegetation period and moisture scarcity in upcoming months. Like April 1901, precipitation depicted in April at only 29.2 mm significantly deviated from the 1901–1998 mean of 80 mm for April month, causing the moisture scarcity in 1903 to form IDAF*e*. Only 26.4 mm of precipitation in January 1914 and 8.1 mm in May 1915 were the influential factors for IADF*e* in 1914 and 1915, respectively. In 1915, May temperature (20.6°C) was much higher compared with the 1901–1998 mean of 18.51°C, which increased evapotranspiration and formation of IADFs in earlywood. Notably, 1915 was marked by a moderate annual drought in Una, Keylong, and Kilba as reported by Chandel and Brar (2013). Premonsoon precipitation failure in June 1919, 1920, and 1923, only 6.9, 25.9, and 21.1 mm, respectively, that was very low compared to the 1901–1998 mean of 53 mm for June caused the formation of IADF*e* in the respective years. Increased June temperatures for 1919 (20.2°C) and 1923 (20.5) were higher than the 1901–1998 mean 19.7°C of June. Moderate annual drought years were recorded in the year 1915 from Una, Keylong, and Kilba; in the year 1919, drought conditions were reported from Kilba and in the year 1920 from Una and Dehra Gopipur of Himachal Pradesh (Chandel and Brar, 2013). For the year 1919, on average, 43.66 mm of June month precipitation was below the average of 90.26 mm (for the period 1901–2002) in the whole of Himachal Pradesh state (Randhawa et al., 2015). Yadav et al. (2015) also reported a 5-year mean SPI of May (SPI7-May) analysis, which revealed drought conditions in 1920–1924 from the Kumaun Himalaya.

Precipitation during January–April (182 mm) was 2.4 times less than the 1901–1998 mean of January–April (436 mm), causing the moisture deficiency in the growing period in the year 1925. However, the increased April temperature (17.2°C) was much higher than the 1901–1998 mean of April (14.7°C), triggering the formation of IADF*e*. According to Randhawa et al. (2015), in the year 1925, January–May precipitation in the whole state was 69.08 mm compared to the previous year's January–May month precipitation of 157.5 mm. In

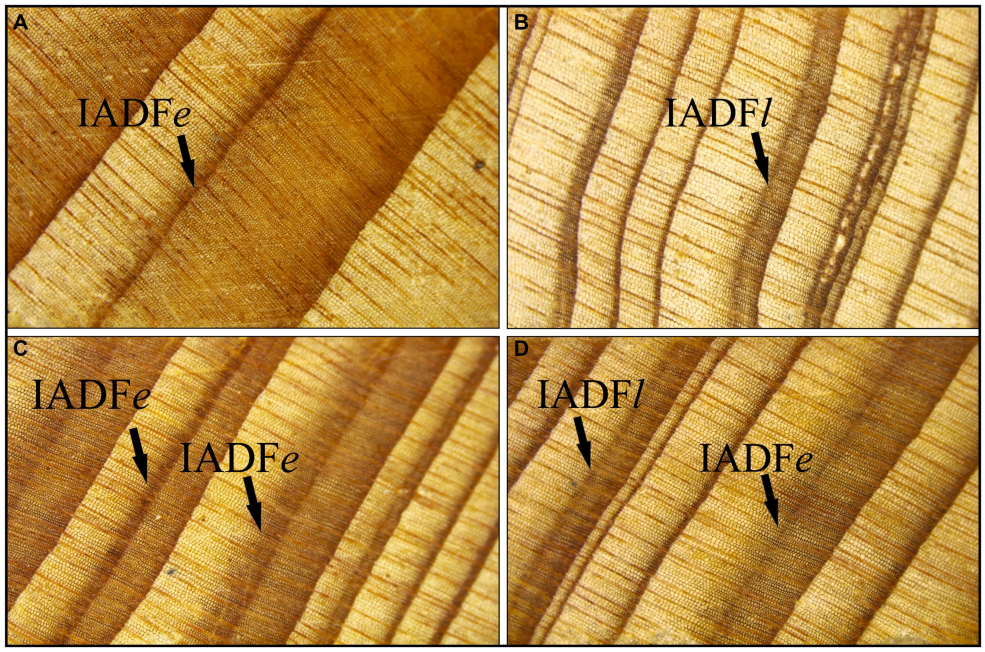

FIGURE 7
Images showing the intra-annual density fluctuations (IADFs); **(A)** IADF in earlywood, **(B)** two successive IADFs in earlywood, **(C)** IADFs in latewood, **(D)** IADFs in both early and latewood.

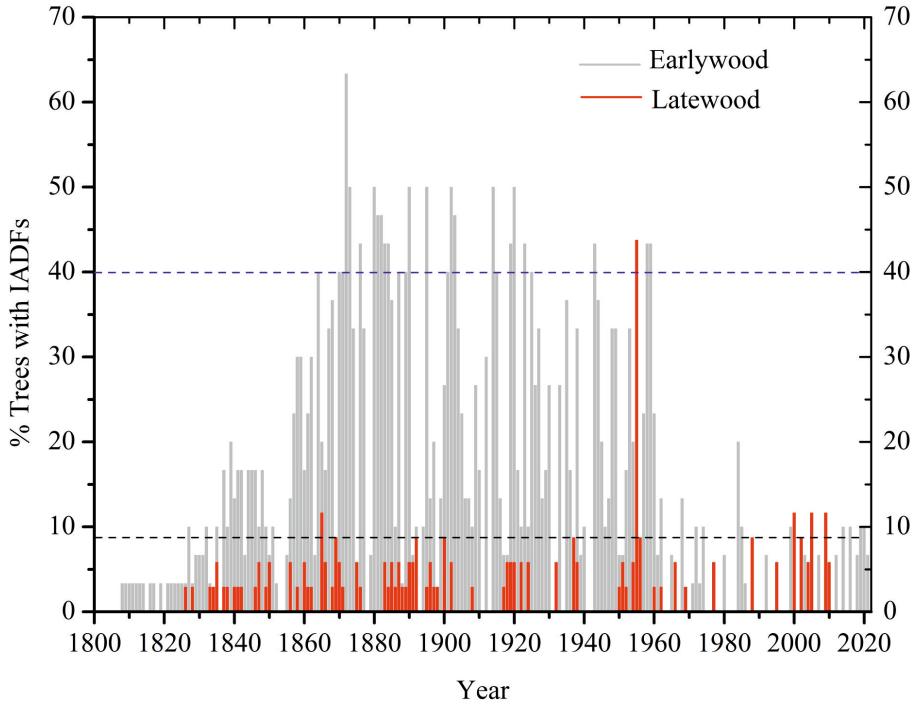

FIGURE 8
Earlywood and latewood IADF chronology of Himalayan cedar trees from Kullu, Himachal Pradesh.

1925, a La Nina phase was observed in winter and spring, which triggered the scarcity of rainfall in this region NOAA Physical Sciences Laboratory (n.d.). Precipitation during June months in the years 1943 (12 mm) and 1958 (17 mm) was meager as compared to the 1901–1998 mean of 53 mm; and in 1959, May month precipitation of 7.8 mm was also very low as compared to 1901–1998 mean for May 56.6 mm. For the years 1958 and 1959, June month temperature was too high as compared to the average of 19.7°C for 1901–1998, causing

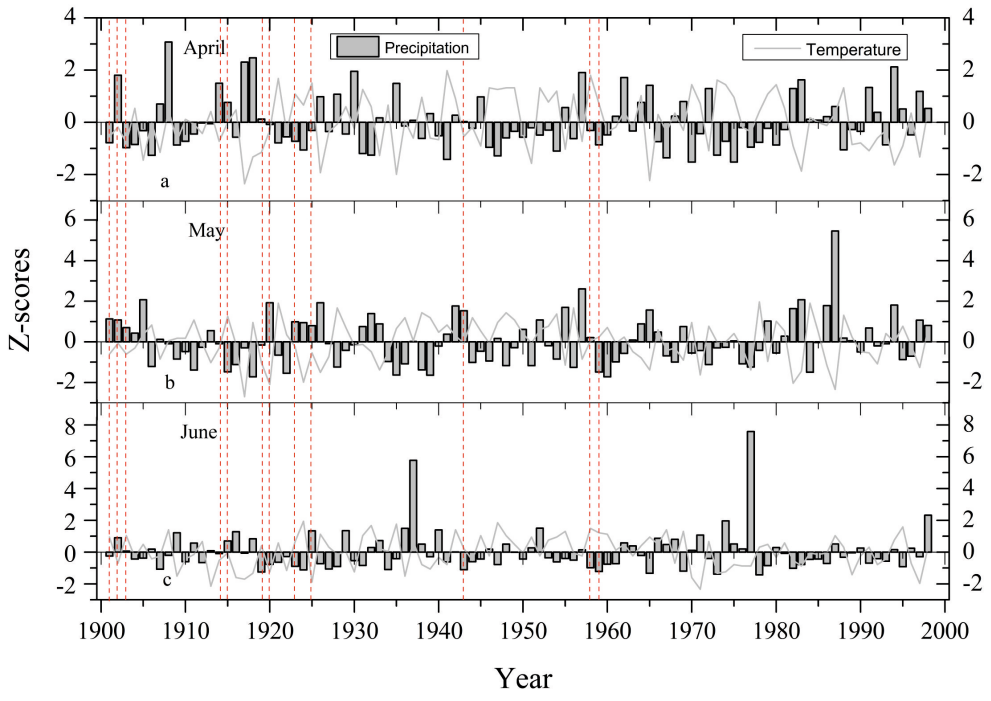

FIGURE 9
Z-scores of climatic variables (precipitation and temperature) for the period of 1901–1998. The red vertical dotted lines represent the years of intense IADF development in earlywood.

increased evapotranspiration and moisture deficiency in early monsoon month and annual high mean temperature anomaly recorded in the year 1958–1959 in comparison with the previous year 1957 (Anonymous, 2022). According to the NOAA Physical Science Laboratory (PSL), the years 1958 and 1959 were hit by a strong El Niño Southern Oscillation (ENSO) incident that caused the failure of monsoonal rainfall.

4.2 Climatic interpretation of IADFs in latewood

The IADFs in latewood (IADF*l*) are characterized as large thin-wall tracheids in latewood due to the sudden increase in soil moisture throughout the late growing season (Uggla et al., 2001). To investigate, the triggering climatic factor for IADF*l* was analyzed and a threshold value of up to 8% or more was observed in the chronology (Figure 10). The years 1937, 1955, 1956, and 1988 were the years in which IADF*l* was formed. Precipitation in September 1937 was 2.6 times higher than the 1901–1998 mean of September (73 mm), causing sudden moisture availability during the closing phase of the tree ring and formation of IADF*l*. Similarly, heavy precipitation during the month of October 1955 (346.7 mm) and 1956 (151.6 mm) was very high as compared to the 1901–1998 mean of October (30.1 mm). Increased moisture content in the month of October for two consecutive years (1955 and 1956) lowered the temperature to 13.6°C than the average range 1901–1998 for October (14.58°C). The year 1955 was reported as a year of surplus rainfall in the Chamba, Hamirpur, Mandi, and Una districts (Anonymous, 2017). On 4–6 October 1955, a massive flood destroyed the flood embankments of the Bambanwala–Ravi–Bedian–Dipalpur link canal in the Ravi basin (Groot et al., 2018). Again, in September 1988, heavy precipitation (260.4 mm) compared to August (130.2 mm) triggered the formation of IADF*l*. In September 1988, a cloud burst created flash flood conditions, causing massive landslide incidents along the eastern slope of Soldan Khad. The 20-m bridge on Soldan Khad washed away, and a 2-km-long road leading to Ponda was destroyed. The sudden flash flood destroyed agricultural land, houses, and apple trees and killed 32 people. Furthermore, the landslide-induced blockage temporarily halted the Satluj River flow, creating a temporary lake dimension roughly 6 km long (Anonymous, 2017). However, in the same year, excessive rainfall was reported in the Sirmour, Chamba, Hamirpur, Mandi, and Una districts of Himachal Pradesh (Anonymous, 2017).

4.3 Socioeconomic relevance of IADF chronology

Apple is the state's main fruit crop, which has recently overtaken other fruit harvests as the most valuable cash crop. After Jammu and Kashmir, Himachal Pradesh is India's second-largest apple-producing state (Wani and Songara, 2018). Apple tree belongs to the "Rosaceae" family and the "Malus" genus. Apple can be cultivated at 1,500 to 2,700 masl (National Horticulture Board, 2012). The climate plays a crucial role in influencing apple fruit growth, and a typical apple orchard needs between 21°C and 24°C temperature during the growing season and 100–130 cm of uniform annual rainfall. However, extremely cold temperatures could also harm the apple crop (National Horticulture Board, 2012).

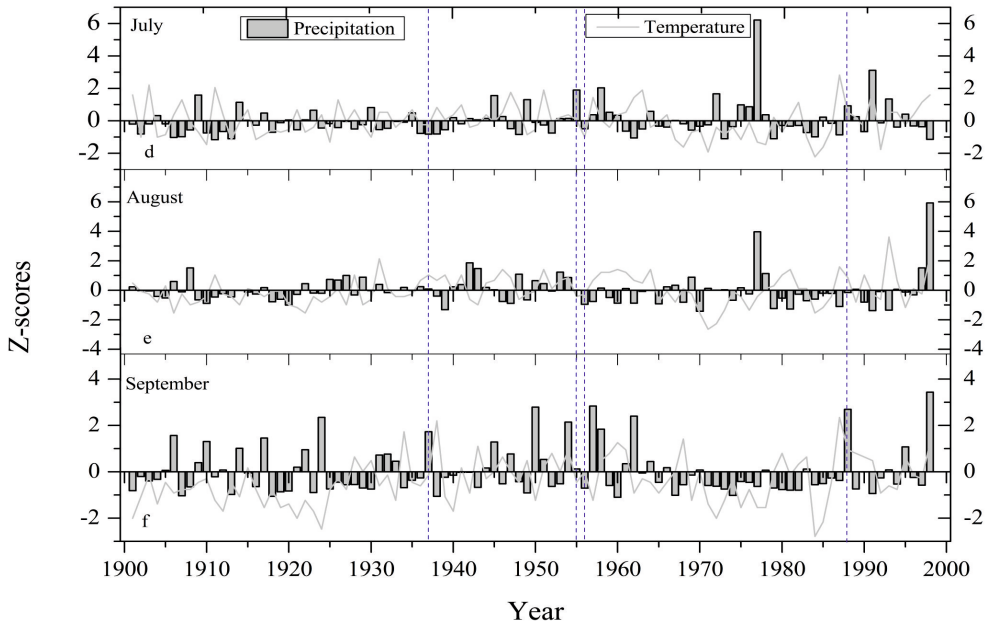

FIGURE 10
Z-scores of climatic variables (precipitation and temperature) data for the period of 1901–1998. The blue vertical dotted lines are the years of the intense formation of IADFs in latewood.

To analyze the socioeconomic relevance of IADFs chronology of Himalayan cedar growing over Kullu, Himachal Pradesh, we studied the variability in apple production data available from 1973 to 2015 (Singh et al., 2012; Randhawa et al., n.d.). In Himachal Pradesh, the apple crop set up approximately 49% of the total area, giving lucrative employment to millions of people. The apple production data of Kullu (1973–2015) showed that apple crop production was deficient at 1.43 tons/ha in the year 1974. The year 1974 featured the presence of IADF*e* in Himalayan cedar trees in the study area. This year, the precipitation is below the mean average for all the months. However, precipitation of February was extremely reduced to only 0.2 mm compared to the 1901–1998 average. In 1984, a deficient apple production of 2.41 tons/ha was recorded due to only 7.3 mm precipitation in May, that is, very low compared to the 1901–1998 average of 56.6 mm and failure of upcoming monsoon precipitation. Low precipitation induced dry conditions in the year 1984 was reported and about 1,497 forest fire cases identified, causing, burnt a large area of 50,364 ha in the state (Parikh et al., 2015). The year 1984 drought also triggers severe crop damage in Shimla and Kangra districts. In only Kangra district, approximately 3,100 villages were affected, and crops worth 24 crore rupees were damaged (Chandel and Brar, 2013). Low apple productivity of 3.10 tons/ha in the year 1988 was due to three times higher precipitation in September month average that caused heavy damage to apple crops due to unusually heavy and prolonged spell of rainfall from 22 to 27 September over the north-western part of India (Chandel and Brar, 2013; Punjab, Himachal Pradesh, and Jammu and Kashmir) with an exceptionally heavy rain of 30–50 cm/day. This surplus spell initiated a catastrophic flood in Punjab (Prasad, 1992). Surplus precipitation in July 2000 was more than two times higher than the average, causing very low apple crop productivity in the year 2000, i.e., 0.38 tons/ha. Excess precipitation in July 2000 triggered flash flood conditions and washed away a large cultivated area (1887.50 bighas) in Kinnaur, Kullu, and Shimla, resulting in a loss of 31.92 crores (Kumar, 2022). Meager precipitation, only 6.8 mm in April 2007, caused moisture scarcity during the early flowering season of the apple crop, causing heavy loss in apple production, i.e., 2.0 tons/ha, and the year 2007 coincided with the presence of IADF in earlywood. Early in 2007, the Himachal Pradesh region experienced a drought-like condition that severely affected the apple crop in the higher areas while also causing damage to the potato, wheat, and oil seed crops in the lower regions (Chandel and Brar, 2013). Prevailed dry conditions initiated 550 forest fire incidents and brunt approximately 8,393-ha area in the state (Parikh et al., 2015). These findings elevate the importance of IADF chronologies to understand short-term climate incidents from a socioeconomic perspective.

5 Conclusion

For the present study, a 214-year-long Himalayan cedar tree-ring-width chronology extending back to AD 1808 was developed from the Kullu, Himachal Pradesh. The Himalayan cedar trees growing over poorly porous crystalline rock surfaces provide favorable conditions to record moisture signals during precipitation events, encouraging us for the IADF study. The tree–growth–climate relationship revealed that cool and moist condition favors tree growth, and increased evapotranspiration during the growing season hampers tree growth. IADFs, which reflect short-term fluctuations in the precipitation during the growing and autumn season, offer fascinating, unusual, but varying climatic impressions from associated ring-width series. Analyses revealed sometimes successively multiyear IADF years in earlywood and latewood such as 1901, 1902, 1903, 1914, 1915, 1919, 1920, 1923, 1925, 1943, 1958, 1959 and 1937, 1955, 1956, 1988,

respectively. Occurrences of IADF*e* during the growing season positively correlate to apple crop failure due to moisture scarcity during the flowering and fruiting period. However, the IADF*l* formation in autumn revealed that surplus rainfall causes heavy loss of apple crop production at the ripening time. The several low apple crop production years were 1974, 1984, 1988, 2000, and 2007 associated with IADF*e*/*l*. In 1974, only 1.3848 tons/ha of apple production occurred due to precipitation being below the mean average for all the months. However, in the year 2000, surplus precipitation in the month of July badly affected apple production up to 0.38 tons/ha. The present IADF analyses of Himalayan cedar from western Himalaya, performed for the first time, have enormous potential to study short-term climate fluctuations. Furthermore, adding an extensive network of IADF chronologies will be helpful socioeconomically in understanding climatic fluctuations more precisely over the western Himalayan region.

Data availability statement

The raw data supporting the conclusions of this article will be made available by the authors, without undue reservation.

Author contributions

RSM and KGM drafted the manuscript. RSM, KGM, and SV collected, processed, and cross-dated the tree-ring samples. RSM, KGM, SV, VS, SM, and AY evaluated the results and provided comments to improve the manuscript. All authors contributed to the article and approved the submitted version.

Acknowledgments

The authors sincerely acknowledge to Director, Birbal Sahni Institute of Palaeosciences, Lucknow, for providing the necessary facilities, support, and permission (BSIP/RDCC/05/2023-24) to publish this study. We also thank the Forest Department, Himachal Pradesh, for providing all essential assistance and logistical support during the collection of tree-ring samples. RSM was thankful to the Department of Science and Technology, New Delhi, for INSPIRE Fellowship (IF 180864, IVR No. 201800028174) and KGM to SERB-DST, New Delhi (SCP/2022/000706). We sincerely thank both the reviewers for their valuable suggestions, which greatly improved the manuscript.

Conflict of interest

The authors declare that the research was conducted in the absence of any commercial or financial relationships that could be construed as a potential conflict of interest.

Publisher's note

References

Anonymous (2017). Himachal Pradesh State Disaster Management Plan. *Himachal Pradesh State Disaster Management Authority*. 1–262.

Anonymous (2022). Statement on climate for the state of Himachal Pradesh: 2022. *Indian Meteorological Department, Pune*, 1–16.

Babbage, C. (1838). "On the age of strata, as inferred from the rings of trees embedded in them" in *The ninth Bridgewater treatise, a fragment*. *2nd* ed (John Murray, London), 256–264.

Battipaglia, G., De Micco, V., Brand, W. A., Linke, P., Aronne, G., Saurer, M., et al. (2010). Variations of vessel diameter and δ13C in false rings of *Arbutus unedo* L. reflect different environmental conditions. *New Phytol.* 188, 1099–1112. doi: 10.1111/j.1469-8137.2010.03443.x

Battipaglia, G., De Micco, V., Brand, W. A., Saurer, M., Aronne, G., Linke, P., et al. (2014). Drought impact on water use efficiency and intra-annual density fluctuations in *Erica arborea* on Elba (Italy). *Plant Cell Environ.* 37, 382–391. doi: 10.1111/pce.12160

Biondi, F., and Waikul, K. (2004). DENDROCLIM2002: a C++ program for statistical calibration of climate signals in tree-ring chronologies. *Comput. Geosci.* 30, 303–311. doi: 10.1016/j.cageo.2003.11.004

Bogino, S., and Bravo, F. (2009). Climate and intraannual density fluctuations in *Pinus pinaster* subsp. mesogeensis in Spanish woodlands. *Can. J. For. Res.* 39, 1557–1565. doi: 10.1139/X09-074

Borgaonkar, H. P., Rupa Kumar, K., Pant, G. B., Okada, N., Fujiwara, T., and Yamashita, K. (2001). Climatic implications of tree-ring density variations in Himalayan conifers. *Palaeobotanist* 50, 27–34. doi: 10.54991/jop.2001.1801

Braüning, A. (1999). Dendroclimatological potential of drought-sensitive tree stands in southern Tibet for the reconstruction of monsoonal activity. *IAWA J.* 20, 325–338. doi: 10.1163/22941932-90000695

Campelo, F., Nabais, C., Freitas, H., Gutierrez, E., and Cristina, N. (2007). Climatic significance of tree-ring width and intra-annual density fluctuations in Pinus pine a from a dry Mediterranean area in Portugal. *Ann. For. Sci.* 64, 229–238. doi: 10.1051/forest:2006107

Campelo, F., Vieira, J., Battipaglia, G., de Luis, M., Nabais, C., Freitas, H., et al. (2015). Which matters most for the formation of intra-annual density fluctuations in *Pinus pinaster*: age or size? *Trees* 29, 237–245. doi: 10.1007/s00468-014-1108-9

Campelo, F., Vieira, J., and Nabais, C. (2013). Tree-ring growth and intraannual density fluctuations of *Pinus pinaster* responses to climate: does size matter? *Trees* 27, 763–772. doi: 10.1007/s00468-012-0831-3

Carvalho, A., Nabais, C., Vieira, J., Rossi, S., and Campelo, F. (2015). Plastic response of tracheids in *Pinus pinaster* in a water-limited environment: adjusting lumen size instead of wall thickness. *PloS One* 10:136305. doi: 10.1371/journal.pone.0136305

Champion, H. G., and Seth, S. K. (1968). *The revised survey of the Forest types of India*, Manager of Publications, New Delhi.

Cherubini, P., Gartner, B. L., Tognetti, R., Bräker, O. U., Schoch, W., and Innes, J. L. (2003). Identification, measurement, and interpretation of tree rings in woody species from Mediterranean climates. *Biol. Rev.* 78, 119–148. doi: 10.1017/S1464793102006000

Choubey, V. M., Sharma, K. K., and Ramola, R. C. (1997). Geology of radon occurrence around Jari in Parvati valley, Himachal Pradesh, India. *J. Environ. Radioact.* 34, 139–147. doi: 10.1016/0265-931X(96)00024-0

Cook, E. R. (1985). A time series analysis approach to tree-ring standardization. Ph.D. thesis. Tucson, Arizona, USA: University of Arizona.

Cook, E. R., and Peters, K. (1997). Calculating unbiased tree-ring indices for the study of climatic and environmental change. *Holocene* 7, 361–370. doi: 10.1177/095968369700700314

Copenheaver, C. A., Gartner, H., Schafer, I., Vaccari, F. P., and Cherubini, P. (2010). Drought-triggered false ring formation in a Mediterranean shrub. *Botany* 88, 545–555. doi: 10.1139/B10-029

Copenheaver, C. A., Pokorski, E. A., Currie, J. E., and Abrams, M. D. (2006). Causation of false ring formation in *Pinus banksiana*: a comparison of age, canopy class, climate, and growth rate. *For. Ecol. Manage.* 236, 348–355. doi: 10.1016/j.foreco.2006.09.020

Corona, E. (1986). *Dendrocronologia: principi e applicazioni. In: Dendrocronologia: Principi e Applicazioni. Atti del Seminario a Verona nei giorni 14–15 November 1984*. Istituto Italiano di Dendrocronologia, Verona, Italy, 7–32.

Chandel, V. B. S., and Brar, K. K. (2013). Drought in Himachal Pradesh, India: A Historical-Geographical Perspective, 1901–2009. *Trans. Inst. Indian Geogr.* 35, 259–273. doi: 10.17501/icfow.2018.1102

De Luis, M., Gricar, J., Cufar, K., and Raventos, J. (2007). Seasonal dynamics of wood formation in *Pinus halepensis* from dry and semi-arid ecosystems in Spain. *IAWA J.* 28, 389–404. doi: 10.1163/22941932-90001651

De Luis, M., Novak, K., Cufar, K., and Raventós, J. (2009). Size mediated climate-growth relationships in Pinus halepensis and *Pinus pinea*. *Trees* 23, 1065–1073. doi: 10.1007/s00468-009-0349-5

De Micco, V., and Aronne, G. (2009). Seasonal dimorphism in wood anatomy of the Mediterranean *Cistus incanus* L. subsp. incanus. *Trees* 23, 981–989. doi: 10.1007/s00468-009-0340-1

De Micco, V., Battipaglia, G., Cherubini, P., and Aronne, G. (2014). Comparing methods to analyse anatomical features of tree rings with and without intra-annual density fluctuations (IADFs). *Dendrochronologia* 32, 1–6. doi: 10.1016/j.dendro.2013.06.001

De Micco, V., Campelo, F., de Luis, M., Braüning, A., Grabner, M., Battipaglia, G., et al. (2016). Formation of intra-annual-density-fluctuations in tree rings:how, when, where and why? *IAWA J.* 37, 232–259. doi: 10.1163/22941932-20160132

De Micco, V., Saurer, M., Aronne, G., Tognetti, R., and Cherubini, P. (2007). Variations of wood anatomy and δ13C within tree rings of coastal *Pinus pinaster* Ait. Showing intra-annual density fluctuations. *IAWA J.* 28, 61–74. doi: 10.1163/22941932-90001619

Dean, J. (1978). Tree-ring dating in archaeology. in University of Utah Anthropological Papers: Misc. Paper, edited by J. S. Jennings University of Utah Press, Salt Lake City. pp. 24 129–163.

Douglass, A. E. (1914). A method of estimating rainfall by the growth of trees. *Geol. Soc. Am. Bull.* 46, 321–335. doi: 10.2307/201814

Edmondson, J. R. (2010). The meteorological significance of false rings in eastern red cedar (*Juniperus virginiana* L) from the southern great plains USA. *Tree-Ring Res.* 66, 19–33. doi: 10.3959/2008-13.1

Ehleringer, J. R., and Dawson, T. E. (1992). Water-uptake by plants – perspectives from stable isotope composition. *Plant Cell Environ.* 15, 1073–1082. doi: 10.1111/j.1365-3040.1992.tb01657.x

Fritts, H. C. (1976). *Tree-rings and climate, 567*. London: Academic Press.

Fritts, H. C. (2001). *Tree rings and climate*, *2nd* Edn.; The Blackburn Press: Caldwell, NJ, USA.

Gao, J., Rossi, S., and Yang, B. (2021). Origin of intra-annual density fluctuations in a semi-arid area of northwestern China. *Front. Plant Sci.* 12:777753. doi: 10.3389/fpls.2021.777753

Gonda-King, L., Radville, L., and Preisser, E. L. (2012). False ring formation in eastern hemlock branches: impacts of hemlock woolly Adelaid and elongate hemlock scale. *Environ. Entomol.* 41, 523–531. doi: 10.1603/EN11227

Groot, A., Singh, T., Pandey, A., Gioli, G., Ahmed, B., Ishaq, S., et al. (2018). *Literature review of critical climate-stress moments in the Hindu Kush Himalaya: A resource kit*. HI-AWARE Resource Kit, Kathmandu.

Hoffer, M., and Tardif, J. C. (2009). False rings in jack pine and black spruce trees from eastern Manitoba as indicators of dry summers. *Can. J. For. Res.* 39, 1722–1736. doi: 10.1139/X09-088

Holmes, R. L. (1983). Computer-assisted quality control in tree-ring dating and measurement. *Tree-Ring Res.* 43, 69–78. doi: 10.4324/9781315748689-14

Hughes, M. K. (1992). "Dendroclimatic evidence from the western Himalaya" in *Climate since 1500 AD*. eds. R. S. Bradley and P. D. Jones (London: Routledge), 415–431.

Hughes, M. K. (2001). An improved reconstruction of summer temperature at Srinagar, Kashmir since 1660 a D, based on tree ring width and maximum latewood density of Abies pindrow (Royle) Spach. *Palaeobotanist* 50, 13–19.

Hughes, M. K., and Davies, A. C. (1987). "Dendrochronology in Kashmir using ring widths and densities in sub-alpine conifers" in *Methods of dendrochronology: East/west approaches*. eds. L. Kairiukstis, Z. Bednarz and E. Feliksik (Laxenburg: IIASA/Polish Academy of Sciences), 163–176.

Kaennel, M., and Schweingruber, F. H. (1995). *Multilingual glossary of dendrochronology. Terms and definitions in English, Spanish, Italian, Portuguese, and Russian*. Swiss Federal Research Institute WSL, Birmensdorf/Haupt, Bern.

Kozlowski, T. T., (1971). *Growth and development of trees*. Vol. *II*, Academic Press, New York.

Kuo, M., and McGinnes, E. A. (1973). Variation of anatomical structure of false rings in eastern red cedar. *Wood Sci.* 5, 205–210.

Kumar, V. (2022). Floods and flash floods in Himachal Pradesh. *J. Geogr. Nat. Disasters* 12:1000252. doi: 10.35841/2167-0587.22.12.252

Managave, S. R., Sheshshayee, M. S., Ramesh, R., Borgaonkar, H. P., Shah, S. K., and Bhattacharyya, A. (2011). Response of cellulose oxygen isotope values of teak trees in differing monsoon environments to monsoon rainfall. *Dendrochronologia* 29, 89–97. doi: 10.1016/j.dendro.2010.05.002

Managave, S. R., Shimla, P., Yadav, R. R., Ramesh, R., and Balakrishnan, S. (2020). Contrasting centennial-scale climate variability in High Mountain Asia revealed by a tree-ring oxygen isotope record from Lahaul-Spiti. *Geophys. Res. Lett.* 47:e2019GL086170. doi: 10.1029/2019GL086170

Misra, K. G., Singh, V., Yadava, A. K., Misra, S., Maurya, R. S., and Vishwakarma, S. (2021). Himalayan blue pine deduced precipitation records from cold arid Lahaul-Spiti, Himachal Pradesh, India. *Front. Earth Sci.* 9:645959. doi: 10.3389/feart.2021.645959

Misra, K. G., Yadav, R. R., and Misra, S. (2015). Satluj river flow variations since AD 1660 based on tree-ring network of Himalayan cedar from western Himalaya, India. *Quat. Int.* 371, 135–143. doi: 10.1016/j.quaint.2015.01.015

Nabais, C., Campelo, F., Viera, J., and Cherubini, P. (2014). Climatic signals of tree-ring width and intra-annual density fluctuations in Pinus pinaster and *Pinus pinea* along a latitudinal gradient in Portugal. *Forestry* 87, 598–605. doi: 10.1093/forestry/cpu021

Nash, S. E. (1999). *Time, trees, and prehistory: Tree-ring dating and the development of north American archaeology, 1914–1950*. The University of Utah Press: Salt Lake City.

National Horticulture Board. (2012). Available at: https://nhb.gov.in/report_files/apple/APPLE.htm

Novak, K., Saz-Sánchez, M. A., Čufar, K., Raventós, J., and De Luis, M. (2013). Age, climate and intraannual density fluctuations in *Pinus halepensis* in Spain. *IAWA J.* 34, 459–474. doi: 10.1163/22941932-00000037

NOAA Physical Sciences Laboratory (n.d.). El Niño Southern Oscillation (ENSO). Available at: https://psl.noaa.gov/enso/climaterisks/years/top24enso.html

Olano, J. M., García-Cervigón, A. I., Arzac, A., and Rozas, V. (2015). Intraannual wood density fluctuations and tree-ring width patterns are sex and site-dependent in the dioecious conifer Juniperus thurifera L. *Trees* 29, 1341–1353. doi: 10.1007/s00468-015-1212-5

Olivar, J., Bogino, S., Spiecker, H., and Bravo, F. (2012). Climate impact of growth dynamic and intra-annual density fluctuations in Aleppo pine (*Pinus halepensis*) trees of different crown classes. *Dendrochronologia* 30, 35–47. doi: 10.1016/j.dendro.2011.06.001

Pacheco, A., Camarero, J. J., and Carrer, M. (2016). Linking wood anatomy and xylogenesis allows pinpointing of climate and drought influences on growth of coexisting conifers in continental Mediterranean climate. *Tree Physiol.* 36, 502–512. doi: 10.1093/treephys/tpv125

Palakit, K., Siripattanadilok, S., and Duangsathaporn, K. (2012). False ring occurrences and their identification in teak (*Tectona grandis*) in North-Eastern Thailand. *J. Trop For Sci.* 24, 387–398.

Parikh, J., Sharma, A., Singh, C., Gupta, M. K., Kaushik, A., and Dhingra, M. (2015). Final technical report: Socio economic vulnerability of Himachal Pradesh to climate change, 1–94.

Prasad, K. (1992). A diagnostic study of flood producing rainstorm of September, over Northwest India with the aid of a fine mesh numerical analysis system. *Mausam* 43, 71–76. doi: 10.54302/mausam.v43i1.3320

Priya, P. B., and Bhat, K. M. (1998). False ring formation in teak (*Tectona grandis* L f) and the influence of environmental factors. *For. Ecol. Manage.* 108, 215–222. doi: 10.1016/S0378-1127(98)00227-8

Raizada, M. B., and Sahni, K. C. (1960). Living Indian gymnosperms, part 1 (Cycades, Ginkgoales and Coniferales). *Indian For Rec.* 5, 1–150.

Ramesh, R., Bhattacharya, S. K., and Gopalan, K. (1985). Dendrochronological implications of isotope coherence in trees from Kashmir, India. *Nature* 317, 802–804. doi: 10.1038/317802a0

Ramesh, R., Bhattacharya, S. K., and Gopalan, K. (1986). Climatic correlations in the stable isotope records of silver fir (Abies pindrow) trees from Kashmir, India. *Earth Planet. Sci. Lett.* 79, 66–74. doi: 10.1016/0012-821X(86)90041-5

Randhawa, S. S., Randhawa, S., and Rai, I. (2015). *Himachal Pradesh state Centre on climate change. Seasonal, Monthly and Annual Rainfall Trends in Himachal Pradesh during 1901-2002*, 1–13.

Randhawa, S. S., Sharma, Y. P., Vaidya, P., Chakrabarty, N., Randhawa, S., Lata, K., et al. (n.d.). Status report: Impact of climate change assessment on horticulture sector in district Kullu Himachal Pradesh, 1–77.

Ren, P., Rossi, S., Gricar, J., Liang, E., and Cufar, K. (2015). Is precipitation a trigger for the onset of xylogenesis in Juniperus przewalskii on the north-eastern Tibetan plateau? *Ann. Bot.* 115, 629–639. doi: 10.1093/aob/mcu259

Rigling, A., Bräker, O., Schneiter, G., and Schweingruber, F. (2002). Intra-annual tree-ring parameters indicating differences in drought stress of *Pinus sylvestris* forests within the Erico-pinion in the Valais (Switzerland). *Plant Ecol.* 163, 105–121. doi: 10.1023/A:1020355407821

Rigling, A., Waldner, P. O., Forster, T., Bräker, O. U., and Pouttu, A. (2001). Ecological interpretation of tree-ring width and interannual density fluctuations in *Pinus sylvestris* on dry sites in the Central Alps and Siberia. *Can. J. For. Res.* 31, 18–31. doi: 10.1139/x00-126

Rinn, F. (2003). *TSAP-win time series analysis and presentation for dendrochronology and related applications, version 0.53 for Microsoft windows*. Rinn Tech, Heidelberg, Germany.

Sano, M., Dimri, A. P., Ramesh, R., Xu, C., Li, Z., and Nakatsuka, T. (2017). Moisture source signals preserved in a 242-year tree-ring δ18O chronology in the western Himalaya. *Global Planet. Change* 157, 73–82. doi: 10.1016/j.gloplacha.2017.08.009

Sarton, G. (1954). When was tree-ring analysis discovered? *Isis* 45, 383–384. doi: 10.1086/348359

Schulman, E. (1938). Classification of false annual rings in Monterey pine. *Tree Ring Bull.* 4, 4–7.

Schweingruber, F. H. (2007). *Wood structure and environment*. Springer-Verlag, Berlin, Heidelberg.

Shah, S. K., Pandey, U., Mehrotra, N., Wiles, G. C., and Chandra, R. (2019). A winter temperature reconstruction for the Lidder Valley, Kashmir, northwest Himalaya based on tree rings of *Pinus wallichiana*. *Climate Dynam.* 53, 4059–4075. doi: 10.1007/s00382-019-04773-6

Shekhar, M., Bhardwaj, A., Singh, S., Ranhotra, P. S., Bhattacharyya, A., Pal, A. K., et al. (2017). Himalayan glaciers experienced significant mass loss during later phases of little ice age. *Sci. Rep.* 7, 1–14. doi: 10.1038/s41598-017-09212-2

Singh, V., Misra, K. G., Singh, A. D., Yadav, R. R., and Yadava, A. K. (2021). Little ice age revealed in tree-ring-based precipitation record from the northwest Himalaya, India. *Geophys. Res. Lett.* 48:e2020GL091298. doi: 10.1029/2020GL091298

Singh, V., Misra, K. G., Yadav, R. R., Yadava, A. K., Vishwakarma, S., and Maurya, R. S. (2022). High-elevation tree-ring record of 263-year summer temperature for a cold-arid region in the Western Himalaya, India. *Dendrochronologia* 73:125956. doi: 10.1016/j.dendro.2022.125956

Singh, R., Vaidya, C. S., Saraswat, S. P., Singh, I., and Pawan Verma, M. (2012). *Impact of high-density apple plantation under horticulture in Himachal Pradesh*, 1–126.

Singh, N. D., Yadav, R. R., Venugopal, N., Singh, V., Yadava, A. K., Misra, K. G., et al. (2016). Climate control on ring width and intra-annual density fluctuations in Pinus kesiya growing in a sub-tropical forest of Manipur, Northeast India. *Trees* 30, 1711–1721. doi: 10.1007/s00468-016-1402-9

Singh, J., Yadav, R. R., and Wilmking, M. (2009). A 694-year tree-ring based rainfall reconstruction from Himachal Pradesh, India. *Climate Dynam.* 33, 1149–1158. doi: 10.1007/s00382-009-0528-5

Speer, J. H., Orvis, K. H., Grissino-Mayer, H. D., Kennedy, L. M., and Horn, S. P. (2004). Assessing the dendrochronological potential of Pinus occidentalis Swartz in the cordillera central of the Dominican Republic. *Holocene* 14, 563–569. doi: 10.1191/0959683604hl732rp

Stallings, W. S. (1937). Some early papers on tree-rings: J. Kuechler. *Tree-Ring Bull* 3, 27–28.

Tucker, C. S., Pearl, J. K., Elliott, E. A., Bregy, J. C., Friedman, J. M., and Therrell, M. D. (2022). Baldcypress false ring formation linked to summer hydroclimatic extremes in the South-Eastern United States. *Environ. Res. Lett.* 17:114030. doi: 10.1088/1748-9326/ac9745

Thomte, L., Shah, S. K., Mehrotra, N., Bhagabati, A. K., Saikia, A. (2022). Influence of climate on multiple tree-ring parameters of Pinus kesia from Manipur, Northeast India. *Dendrochronologia* 71:125906. doi: 10.1016/j.dendro.2021.125906

Uggla, C., Magel, E., Moritz, T., and Sundberg, B. (2001). Function and dynamics of auxin and carbohydrates during earlywood/latewood transition in scots pine. *Plant Physiol.* 125, 2029–2039. doi: 10.1104/pp.125.4.2029

Vieira, J., Campelo, F., and Nabais, C. (2009). Age-dependent responses of tree-ring growth and intra-annual density fluctuations of *Pinus pinaster* to Mediterranean climate. *Trees* 23, 257–265. doi: 10.1007/s00468-008-0273-0

Villalba, R., and Veblen, T. T. (1996). A tree-ring record of dry spring wet summer events in the forest-steppe ecotone northern Patagonia, Argentina. *Tree Rings Environ Human*, 107–116.

Vogel, J. C., Fuls, A., and Visser, E. (2001). Radiocarbon adjustments to the dendrochronology of a yellowwood tree. *South Afr. J. Sci.* 97, 164–166.

Wang, D., Chen, Y., Li, W., Li, Q., Lu, M., Zhou, G., et al. (2021). Vascular cambium: the source of wood formation. *Front. Plant Sci.* 12:700928. doi: 10.3389/fpls.2021.700928

Wani, F. A., and Songara, A. (2018). Status and position of apple crop in area, production, and productivity in Himachal Pradesh. *Int. J. Multidiscip. Res. Dev.* 5, 106–111.

Webb, G. E. (1986). Solar physics and the origins of dendrochronology. *Isis* 77, 291–301. doi: 10.1086/354133

Wilkinson, S., Ogee, J., Domec, J. C., Rayment, M., and Wingate, L. (2015). Biophysical modelling of intra-ring variations in tracheid features and wood density of *Pinus pinaster* trees exposed to seasonal droughts. *Tree Physiol.* 35, 305–318. doi: 10.1093/treephys/tpv010

Wimmer, R. (2002). Wood anatomical features in tree-rings as indicators of environmental change. *Dendrochronologia* 20, 21–36. doi: 10.1078/1125-7865-00005

Yadav, R. R., Gupta, A. K., Kotlia, B. S., Singh, V., Misra, K. G., Yadava, A. K., et al. (2017). Recent wetting and glacier expansion in the northwest Himalaya and Karakoram. *Sci. Rep.* 7:6139. doi: 10.1038/s41598-017-06388-5

Yadav, R. R., Misra, K. G., Kotlia, B. S., and Upreti, N. (2014). Premonsoon precipitation variability in Kumaon Himalaya, India over a perspective of ~300 years. *Quat. Int.* 325, 213–219. doi: 10.1016/j.quaint.2013.09.005

Yadav, R. R., Misra, K. G., Yadava, A. K., Kotlia, B. S., and Misra, S. (2015). Tree-ring footprints of drought variability in last ~300 years over Kumaun Himalaya, India and its relationship with crop productivity. *Quat. Sci. Rev.* 117, 113–123. doi: 10.1016/j.quascirev.2015.04.003

Yadava, A. K., Braüning, A., Singh, J., and Yadav, R. R. (2016). Boreal spring precipitation variability in the cold arid western Himalaya during the last millennium, regional linkages, and socio-economic implications. *Q. Sci. Rev.* 144, 28–43. doi: 10.1016/j.quascirev.2016.05.008

Yadava, A. K., Misra, K. G., Singh, V., Misra, S., Sharma, Y. K., and Kotlia, B. S. (2021). 244 YEAR long tree-ring based drought records from Uttarakhand, western Himalaya, India. *Quat. Int.* 599-600, 128–137. doi: 10.1016/j.quaint.2020.12.038

Zalloni, E., de Luis, M., Campelo, F., Novak, K., De Micco, V., Di Filippo, A., et al. (2016). Climatic signals from intra-annual density fluctuation frequency in Mediterranean pines at a regional scale. *Front. Plant Sci.* 7:579. doi: 10.3389/fpls.2016.00579

frontiers | Frontiers in Plant Science

TYPE Original Research
PUBLISHED 10 January 2024
DOI 10.3389/fpls.2023.1337700

OPEN ACCESS

EDITED BY
Hülya Torun,
Düzce University, Türkiye

REVIEWED BY
Andrej Pilipovic,
University of Minnesota Duluth, United States
Gürcan Güleryüz,
Bursa UludağUniversity,
Türkiye

*CORRESPONDENCE
Olga Kostić
olgak@ibiss.bg.ac.rs

RECEIVED 13 November 2023
ACCEPTED 21 December 2023
PUBLISHED 10 January 2024

CITATION
Kostić O, Jarić S, Pavlović D, Matić M, Radulović N, Mitrović M and Pavlović P (2024) Ecophysiological response of *Populus alba* L. to multiple stress factors during the revitalisation of coal fly ash lagoons at different stages of weathering. *Front. Plant Sci.* 14:1337700. doi: 10.3389/fpls.2023.1337700

Ecophysiological response of *Populus alba* L. to multiple stress factors during the revitalisation of coal fly ash lagoons at different stages of weathering

Olga Kostić*, Snežana Jarić, Dragana Pavlović, Marija Matić, Natalija Radulović, Miroslava Mitrović and Pavle Pavlović

Department of Ecology, Institute for Biological Research 'Siniša Stanković' - National Institute of the Republic of Serbia, University of Belgrade, Belgrade, Serbia

The enormous quantities of fly ash (FA) produced by thermal power plants is a global problem and safe, sustainable approaches to reduce the amount and its toxic effects are still being sought. Vegetation cover comprising long-living species can help reduce FA dump-related environmental health issues. However, the synergistic effect of multiple abiotic factors, like drought, low organic matter content, a deficit of essential nutrients, alkaline pH, and phytotoxicity due to high potentially toxic element (PTE) and soluble salt content, limits the number of species that can grow under such stressful conditions. Thus, we hypothesised that *Populus alba* L., which spontaneously colonised two FA disposal lagoons at the 'Nikola Tesla A' thermal power plant (Obrenovac, Serbia) 3 years (L3) and 11 years (L11) ago, has high restoration potential thanks to its stress tolerance. We analysed the basic physical and chemical properties of FA at different weathering stages, while the ecophysiological response of *P. alba* to multiple stresses was determined through biological indicators [the bioconcentration factor (BCF) and translocation factor (TF) for PTEs (As, B, Cr, Cu, Mn, Ni, Se, and Zn)] and by measuring the following parameters: photosynthetic efficiency and chlorophyll concentration, non-enzymatic antioxidant defence (carotenoids, anthocyanins, and phenols), oxidative stress (malondialdehyde (MDA) concentrations), and total antioxidant capacity (IC50) to neutralise DPPH free radical activity. Unlike at L3, toxic As, B, and Zn concentrations in leaves induced oxidative stress in *P. alba* at L11, shown by the higher MDA levels, lower vitality, and reduced synthesis of chlorophyll, carotenoids, and total antioxidant activity, suggesting its stress tolerance decreases with long-term exposure to adverse abiotic factors. Although *P. alba* is a fast-growing species with good metal accumulation ability and high stress tolerance, it has poor stabilisation potential for substrates with high As and B concentrations, making it highly unsuitable for revitalising such habitats.

KEYWORDS

***Populus alba*, fly ash, revitalisation, multiple abiotic stresses, potentially toxic elements, ecophysiological response**

1 Introduction

Fly ash (FA), the main by-product of coal-fired thermal power plants is a complex, heterogeneous material whose highly variable physical and chemical properties and toxicity are determined by the coal's geological origin, the combustion process, the disposal method, the time the ash has been exposed to atmospheric conditions (age of the ash), and vegetation development (Haynes, 2009; Izquierdo and Querol, 2012; Bhatt et al., 2019; Kostić et al., 2022a). The intensification of activities related to this type of electricity generation is one of the major environmental problems today because the disposal of FA in dry or wet lagoons near thermal power plants contributes to the leaching of potentially toxic elements (PTEs) into soil and groundwater, while windblown micrometre-sized and poorly aggregated particles of FA from the dry surfaces of landfills pollute agricultural land and endanger the flora, fauna, and health of residents of nearby settlements (Raja et al., 2015; Ćujić et al., 2016; Khan and Umar, 2019).The formation of a vegetation cover, i.e. the revitalisation of FA landfills, is a cost-effective and environmentally sound method and the best method when it comes to stabilising this mobile substrate physically and chemically (Haynes, 2009; Yan et al., 2020; Kostić et al., 2022b). However, the synergistic effect of multiple abiotic stress factors, such as drought, low organic matter content, lack of essential nutrients (N, P, Mn, etc.), alkaline pH, and phytotoxicity due to high PTE and soluble salt content, limits the number of species that can grow under such conditions (Kostic et al., 2018; Kalashnikova et al., 2021). Due to its dark grey colour, FA absorbs enormous amounts of heat from the sun, which increases surface temperatures at the landfill and reduces humidity. This is further decreased by the ash's sandy texture, which reduces water and nutrient retention capacity (Carlson and Adriano, 1991; Pavlović et al., 2004). Increased salinity, which can be as high as 13 dS m^{-1} in raw FA, can have a similar effect to drought on plants growing in landfills (Carlson and Adriano, 1993). When coal is burned, carbon (C) and nitrogen (N) are oxidised and transition to the gas phase, meaning FA is poor in both (Carlson and Adriano, 1993; Haynes, 2009). During and after combustion, the mineral fraction of coal undergoes various transformations that make the chemical elements bound in the original coal matrix susceptible to leaching during transport and disposal in landfills, especially when in contact with water (Izquierdo and Querol, 2012). In addition to the aluminosilicate matrix containing Si, Al, Fe, Ca, Mg, Na and K, the chemical composition of FA includes numerous microelements (As, B, Cu, Cr, Cd, Mn, Ni, Pb, Co, Mo, Zn, Se, etc.) whose concentrations in FA can be 4-10 times higher compared to the parent coal (Tian et al., 2018). Some of these elements are essential for plants in minimal amounts, while their presence in high concentrations can be potentially toxic. The most susceptible to leaching, and therefore most accessible to plants, are the partially volatile chemical elements (As, B, Cr, Se, and Zn) that condense in the surface layer of ash particles as the flue gases cool during the coal combustion process, while the less volatile elements such as Mn and Ni accumulate in the inner layer and are not directly exposed to leaching (Tian et al., 2018). The alkalinity of FA can cause the formation of insoluble forms of elements and thus a deficit of essential nutrients, most commonly phosphorus (P), manganese (Mn), and copper (Cu), but also increased solubility of arsenic (As), boron (B), and selenium (Se) and their accumulation in plants in toxic concentrations (Pandey et al., 2011; Gajić et al., 2020; Kostic et al., 2022c).

Abiotic stress factors lead to an overproduction of reactive oxygen species (ROS). These toxic products of incomplete oxygen reduction, which are common by-products of regular aerobic metabolic processes, are most commonly formed in chloroplasts, mitochondria, and cytoplasm, but also in membrane-bound exocellular enzymes involved in redox reactions, especially during photosynthetic electron transport and respiration (Sharma et al., 2020; Sachdev et al., 2021). Abiotic stresses such as high temperatures, drought, high salinity, and heavy metal pollution, as well as the combination of these stresses, disrupt the metabolic balance of cells, leading to increased production of ROS (Qadir et al., 2021; Mishra et al., 2023). In plants, this causes oxidative damage that disrupts many physiological processes, including photosynthesis as the main process of plant metabolism (Pavlović et al., 2007; Mitrović et al., 2012; Huang et al., 2019; Muhammad et al., 2021; Della Maggiora et al., 2023). Despite all the physical and chemical limitations and toxicity of FA, various plant species have been found growing on it (Kostić et al., 2012; Técher et al., 2012; Mukhopadhyay et al., 2017; Yadav et al., 2022). Thanks to the development of adaptation mechanisms based on accumulation and exclusion, tolerant species survive under conditions of PTE deficiency or toxicity in the substrate. By regulating the transfer between soil and roots and between roots and leaves, concentrations of these elements are kept within a normal range in their tissue (Pandey et al., 2012; Mukhopadhyay et al., 2017; Kostić et al., 2022b). Tolerant plant species also respond to abiotic stress by increasing their antioxidant capacity, which helps them to maintain a normal cellular balance between production and binding, degradation, and neutralisation of ROS by enzymatic or non-enzymatic antioxidants (carotenoids and anthocyanins) and secondary metabolites (phenols) (Cervilla et al., 2012; Gajić et al., 2020; Kebert et al., 2022; Vuksanović et al., 2022). Intolerant species exibit decreased antioxidant capacity and fewer mechanisms for detoxification in relation to ROS production, resulting in chain reactions in which free radicals damage important biomolecules, such as chloroplast pigments, lipids, and nucleic acids, oxidatively. Inactivation of enzymes and disruption of membrane structure follows, which leads to tissue damage and finally cell death (Moreno-Jiménez et al., 2009; Love et al., 2013; Stojnić et al., 2016; Gajić et al., 2020; Pilipović et al., 2020). In this sense, choosing the right plant species is an important factor in determining the efficiency of the FA landfill revitalisation process.

Previous studies have shown that autochthonous, long-living woody species characterised by high below- and above-ground biomass and rapid growth, as well as the ability to reproduce vegetatively and capacity to tolerate various stressors, are best suited to stabilising FA landfills and reducing health problems associated with FA while restoring ecosystem functions (Carlson and Adriano, 1991; Kostić et al., 2012; Mitrović et al., 2012;

Pietrzykowski et al., 2018; Kostić et al., 2022b). Species from the *Salicaceae* family stand out when it comes to being used for the phytoremediation and revitalisation of polluted habitats, and in particular those from the *Populus* genus, which is characterised by high tolerance to a variety of environments (Zacchini et al., 2009; Guerra et al., 2011). However, species of *Populus*, as a thoroughly mapped genus, differ widely in their uptake patterns, as well as adaptation abilities under varying abiotic conditions (Dos Santos Utmazian et al., 2007; Zacchini et al., 2009; Di Lonardo et al., 2011; Tőzsér et al., 2023). To date, research has mostly focused on accumulation, phytoremediation potential, and tolerance of poplars to metal pollution (Madejón et al., 2004; Robinson et al., 2005; Borghi et al., 2008; Todeschini et al., 2011; Kostić et al., 2022b) or their physiological response to individual stress factors such as drought, salinity or high temperatures (Chen and Polle, 2010; Yoon et al., 2014; Zhang et al., 2019; Kim et al., 2022). However, studies on the ecophysiological response of *Populus alba* L. to the combined effects of multiple stress factors are rare, particularly at FA landfills. Therefore, the aim of this study is to contribute to the expansion of knowledge on the ecophysiological response of *P. alba* to single and combined multiple abiotic stresses at FA landfills and to test its suitability for the potential revitalisation of such habitats. We hypothesised that *P. alba*, which spontaneously colonised two FA disposal lagoons at the 'Nikola Tesla A' thermal power plant (TENT A), Obrenovac, Serbia, 3 years ago (L3) and 11 years ago (L11), has high restoration potential thanks to its stress tolerance. The first research objective was to evaluate some of the abiotic stress factors in FA lagoons at different stages of weathering by analysing (1) basic physical and chemical properties and (2) PTE (As, B, Cr, Cu, Mn, Ni, Se, and Zn) concentrations. The second objective was to assess the ecophysiological response of *P. alba* to abiotic stresses based on (1) determining its ability to regulate PTE transfer from soil to root and root to leaf and (2) its photosynthetic efficiency parameters (Fv/Fm), photosynthetic pigment content, non-enzymatic antioxidant defence parameters (carotenoids, anthocyanins, and phenols), oxidative stress parameters by measuring the concentration of malondialdehyde (MDA), and the total antioxidant capacity (IC50) for neutralizing the activity of DPPH free radicals. The results of this study, which would determine the temporal dynamics of the ecophysiological response of *P. alba* to single and combined abiotic stresses, could be of importance both for its application in the planned revitalisation of the TENT A landfill and for restoring similar landfills around the world.

2 Materials and methods

2.1 Description of the study sites

The TENT A FA landfill (44°40'19"N, 20°09'18"E) occupies 382 ha of the riparian section of the Sava River in the Belgrade municipality of Obrenovac, Serbia (Figure 1). This region is mainly characterised by a moderate-continental climate with warm summers and cold winters. The mean annual temperature is 12°C and total annual precipitation is 530 mm. During the year, periods of drought most often occur in August and September and are accompanied by extremely high temperatures (e.g. maximum temperatures in the period from July to August range from 38 to 42°C) (https://www.meteoblue.com/sr/vreme/historyclimate/weatherarchive/%D0%9E%D0%B1%D1%80%D0%B5%D0%BD%D0%BE%D0%B2%D0%B0%D1%86_%D0%A1%D1%80%D0%B1%D0%B8%D1%98%D0%B0_787516). In addition to data obtained from weather stations, we took measurements 5 cm above the surface of the ash during field research, which revealed temperatures ranging from 42.5°C in May to as high as 56°C in August.

The TENT A landfill is divided into three lagoons, one of which is always active in cycles of 6-12 years and into which 520 tonnes of ash and slag mixed with water (1:10) are hydraulically discharged every hour. After the two inactive lagoons have dried out, a grass-legume mixture is sown (*Arrhenatherum elatius* (L.) P. Beauv., *Dactylis glomerata* L., *Festuca rubra* L., *Lolium multiflorum* Lam., *Lotus corniculatus* L., *Medicago sativa* L., *Secale cereale* L., and *Vicia villosa* Roth.; 270-300 kg ha^{-1}) directly onto the ash without an insulating soil layer in order to prevent the dispersal of FA. Until the vegetative cover forms, each lagoon is also irrigated and fertilised (800 kg ha-1 of 15N:15P:15K) (Kostic et al., 2018). The study was conducted on the two inactive lagoons, L3 (three years after the start of revitalisation) and L11 (eleven years after the start of revitalisation), which at the time of the study had been spontaneously colonised by 99 species (55 at L3 and 80 at L11), 91% of which were herbaceous and 9% woody (4 at L3 and 9 at L11). Of the woody species present at both lagoons, *P. alba* was only sporadically present at L3, while it covered 30% of the area of L11 (Kostic et al., 2018). Control individuals of *P. alba* were selected in its natural habitat on the bank of the Kolubara River (Control), which is 10 km away from the TENT A FA landfill (Figure 1).

During analysis of the leaves of the examined individuals, small necrotic spots were observed on leaves from L3 (Figures 2A–D), as well as chlorosis and marginal necrosis. At L11 (Figures 2E–H), the leaves were visibly smaller and thicker and leaf damage symptoms in the form of chlorosis and reddish-brown necrosis affecting a larger area of the leaf's surface were also observed, while some leaves had completely dried out.

2.2 Plant species description

P. alba is a deciduous, anemophilous, mesophilous, and heliophilous woody species that tolerates frost and a wide range of different soil types and disturbed habitats, meaning it emerges spontaneously and grows rapidly under a variety of challenging conditions such as wildfires, clearings, and clearcuts. Because of its good adaptability to wet environments, it is most common on floodplains near rivers, lakes, and canals (Palancean et al., 2018). It naturally grows on all floodplains along major rivers in eastern, central, and southwestern Europe, as well as in southwestern and central Asia, but especially on the floodplains of the Danube River and its tributaries (Caudullo et al., 2017). Thanks to its wide ecological range, it is naturalised worldwide. *P. alba* is propagated by seeds, but also vegetatively thanks to its widely branched surface veins and great sprouting capacity. Due to its distinctive root system and tolerance to salt and sandy soil, it is used to strengthen and

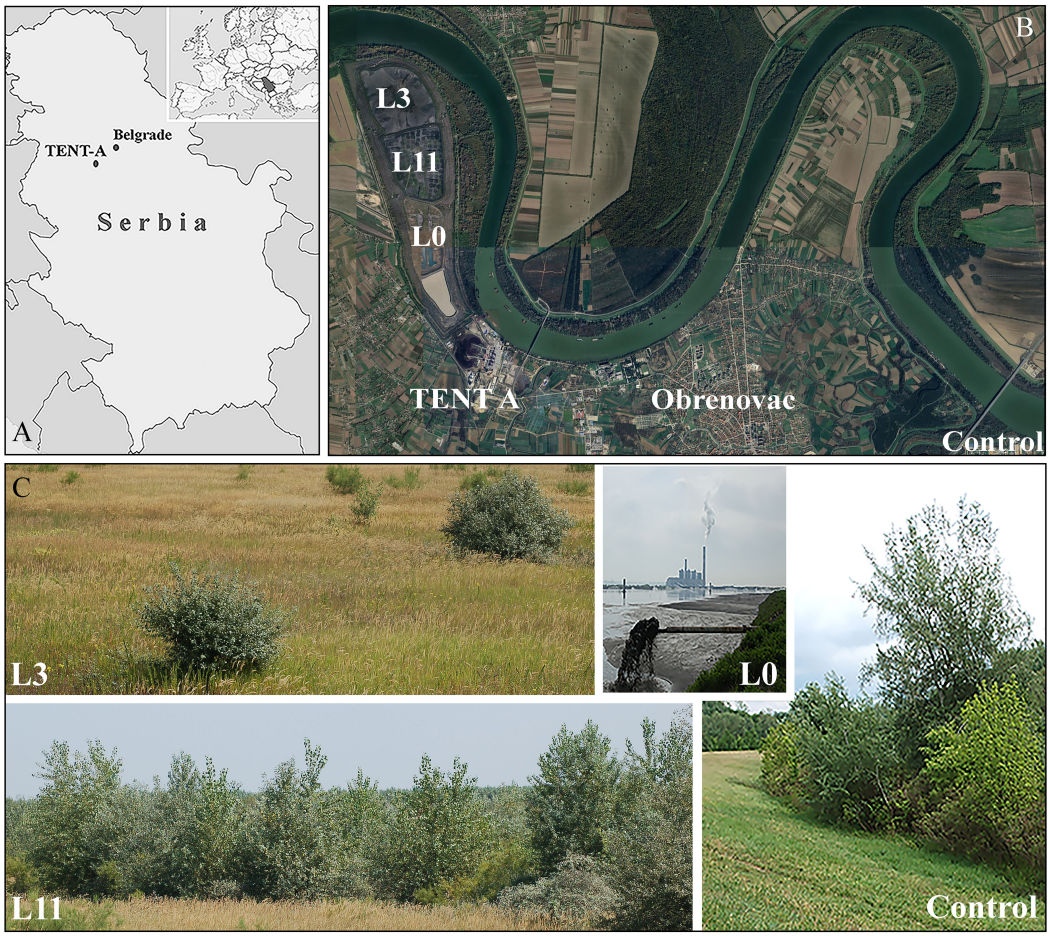

FIGURE 1
Study sites: **(A)** Geographical location of 'Nikola Tesla A' thermal power plant (TENT A) (images obtained from https://d-maps.com/carte.php?num_car=27552&lang=es; https://sh.wikipedia.org/wiki/Spisak_pozivnih_brojeva_u_Srbiji#/media/Datoteka:Serbia_in_Europe.svg, accessed on 21 July 2023), **(B)** Location of TENT A landfill (satellite image is obtained from GoogleEarth (https://earth.google.com/web/@44.69764779,20.15472413,76.16877517a,15536.9216476d,35y,0h,0t,0r/data=OgMKATA, accessed on 20 July 2023), **(C)** active lagoon (L0), and study sites at lagoons L3 and L11 and the natural habitat of *P. alba* on the bank of the Kolubara River (Control).

stabilise coastal dunes by preventing them from being washed away during floods (Caudullo and de Rigo, 2016).

2.3 Sample collection and preparation

Samples of rhizosphere FA and soil (at a depth of 0-30 cm) and plant material (roots and leaves of *P. alba*) were collected from five sampling plots (15 x 15 m) and from randomly selected specimens at each lagoon at approximately equal distance from the lagoon edge (25-30 m) and at the control site. Leaf samples were collected from the same height and from all four cardinal points. FA and soil samples (250 g per sample) were dried at room temperature and then sieved through a 2-mm aperture sieve before being quartered into representative samples (~500 g) for each site. For the analysis of PTE concentrations, the leaf and root samples for each site were combined, washed, and then dried at 65°C to constant weight and ground in a laboratory mill (Polymix, Kinematica AG, 2 mm aperture mesh, stainless steel sieve). The leaf samples for the analysis of the biochemical parameters were stored at -80°C until further analysis.

2.4 Analysis of physical and chemical characteristics of fly ash and control soil

pH (WTW - Germany, inoLab 7110 pH meter) and electrical conductivity (EC µS.cm^{-1}, Knick, Germany, Portamess 911 conductivity meter) in FA and soil samples were determined in a 1:5 suspension of FA (soil) to distilled water. Total organic carbon (C%) was determined using Simakov's modified Turin method (Simakov, 1957) and total nitrogen (N%) was determined using the semi-micro Kjeldahl method. Particle size distribution was carried out using a combined pipette and sieve technique with a 0.4 N sodium pyrophosphate solution, while fractionation was performed according to Atterberg (Atterberg, 1911). Based on the sand, silt and clay content, FA and soil texture was determined using the International Soil Texture Triangle (Soil Survey Division

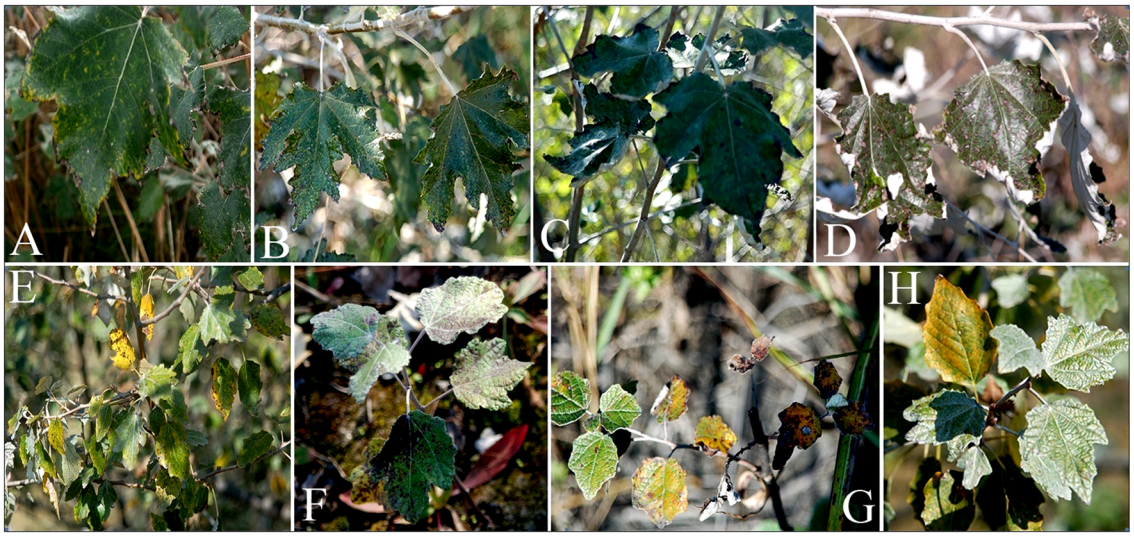

FIGURE 2
P. *alba* leaf damage symptoms at L3 **(A–D)** and L11 **(E–H)**.

Staff, 2017). The C/N ratio was calculated using Equation (1), as the ratio of the average content of total organic carbon (C) to the average content of total nitrogen (N) in FA and soil, for each of the three study sites.

$$C/N = \frac{C}{N} \quad (1)$$

2.5 Analysis of concentrations of potentially toxic elements in fly ash, soil, and plant samples

Inductively coupled plasma optical emission spectrometry (ICP-OES, Spectro Genesis, Spectro-Analytical Instruments GmbH, Kleve, Germany) was used to determine PTE concentrations (mg kg^{-1}) in FA, soil, and plant (root and leaf) samples. Prior to analysis, samples were subjected to wet digestion in a microwave oven (CEM, Mars 6 Microwave Acceleration Reaction System, Matthews, NC, USA). The US EPA acid digestion method 3051 [U.S. Environmental Protection Agency (USEPA), 1998] was used to determine the pseudo total concentrations of PTEs in FA and soil samples, i.e. their maximum content that can be available to plants, as this method does not ensure complete digestion of the elements bound to silicate mineral fraction. The total content of PTEs in root and leaf samples was obtained by means of US EPA acid digestion method 3052 [U.S. Environmental Protection Agency (USEPA), 1996]. The detection limits for the analysed PTEs were as follows: As - 0.005, B - 0.005, Cr - 0.001, Cu - 0.001, Mn - 0.001, Ni - 0.009, Se - 0.007, and Zn - 0.005. To verify the accuracy of the analytical procedures, certified reference materials were analysed: FA (coal ash BCR - 038), soil (clay ERM - CC141) and plant material (beech leaves BCR - 100) provided by IRMM (Institute for Reference Materials and Measurements, Geel, Belgium) and certified by EC-JRC (European Commission - Joint Research Centre).

2.6 Measurements of photosynthetic efficiency and pigment content

The maximum quantum yield of Photosystem II (PSII), or photosynthetic efficiency (Fv/Fm), was measured under field conditions using a portable fluorometer (Plant Stress Meter, BioMonitor SCI AB, Sweden) and calculated as Fm - Fo/Fm (Krause and Weis, 1991). Fo (minimum fluorescence level) was measured once *P. alba* leaves had been dark adapted for 30 minutes, while Fm (maximum fluorescence level) was measured after chlorophyll had been excited by a 2-second pulse of saturated actinic light with a density of 200-400 μmol photons $m^{-2}s^{-1}$. Photosynthetic pigments such as chlorophyll a (Chl a), chlorophyll b (Chl b), and total carotenoids (Tot Carot) were extracted from *P. alba* leaves with 80% acetone. The absorbance of the supernatant was measured at 663 nm, 645 nm, and 480 nm using a spectrophotometer (UV-Vis spectrophotometer, Shimadzu UV-160) and the chlorophyll and carotenoid content was calculated (Arnon, 1949; Wellburn, 1994) and expressed as mg g^{-1} dry weight. Total chlorophyll content (Chl a + b), their ratio (Chl a/b), and the chlorophyll to carotenoid ratio (Chl a + b/Tot Carot) were calculated.

2.7 Analysis of oxidative stress parameters and total antioxidant protection

The content of malondialdehyde (MDA; nmol g^{-1} of fresh weight) in leaf samples of *P. alba* (0.5 g) was determined after homogenisation in 5 mL of 80% ethanol with 0.05 mL of 2% butylated hydroxytoluene

(Heath and Packer, 1968). A solution of 1 mL of the supernatant, 0.5 mL of 0.65% thiobarbituric acid, and 0.5 mL of 10% trichloroacetic acid was heated to a temperature of 95°C for 15 minutesbefore being cooled on ice and centrifuged at 3,000 g for 10 minutes. The absorbance of the supernatant was measured using spectrophotometry at 450 nm, 532 nm, and 600 nm. Anthocyanin (Anthoc; mg g^{-1} of dry weight) in the leaves was extracted with 1 ml DMSO at 65°C for 2 hours and then heated at 65°C for a further 4 hours after the addition of 0.5 ml 2N HCl. The absorbance of the supernatant was measured spectrometrically at 650 nm, 620 nm, and 520 nm (Creasy, 1968; Proctor, 1974). Free phenols (Ph Free; mg g^{-1} of dry weight) in the leaves were extracted with 80% (v/v) boiling aqueous methanol solution followed by ethyl acetate. Bound phenols (Ph Bound; mg g^{-1} of dry weight) were extracted by boiling the insoluble residue of the Ph Free extraction in 2N HCl for 60 min and then it was transferred to ethyl acetate (Djurdjevic et al., 2007). Absorbance was measured spectrophotometrically at 660 nm (Feldman and Hanks, 1968) and a standard curve was constructed using different concentrations of ferulic acid (Serva, Heidelberg, Germany). The total antioxidant capacity of *P. alba* leaves was determined using free radical DPPH (1,1-diphenyl-2-picrylhydrazyl) (Brand-Williams et al., 1995). 0.5 g of leaves was homogenised in 10 mL of 95% ethanol and samples were prepared at three increasing extract concentrations (5 µL, 25 µL, and 50 µL) with the addition of 0.5 mL DPPH. Absorbance (A) was measured using spestrophometry at 517 nm. DPPH radical scavenging ability (%) was calculated as ((Acontrol - Asample)/Acontrol) x 100. The 'effective concentration' or IC50 (mg ml^{-1}), which indicates the amount of plant extract that results in DPPH activity decreasing by 50% (Molyneux, 2004), was used to determine the total antioxidant activity of *P. alba* at all the sites studied. A lower value points to higher antioxidant activity.

2.8 Statistical analysis

The comparison of means (M) with standard deviation (SD) of 5 replicates (n=5) between the three investigated sites for each analysed parameter is shown in Tables 1–3 and Figure 3. The obtained data was analysed using statistical analysis (ANOVA) and means were separated with a Bonferroni test at a level of significance of P<0.001, using the Statistica software package (Weiß, 2007). Data was checked to ensure it met the assumptions for ANOVA before it was analysed. The efficiency of *P. alba* to remove or stabilise chemical elements in FA (Figure 4) was assessed according to biological indicators such as the bioconcentration factor (BCF), calculated using Equation (2), and the translocation factor (TF), calculated using Equation (3), (Zacchini et al., 2009; Zhenggang et al., 2023).

$$BCF = \frac{C_{Root\ (Leaf)}}{C_{FA(Soil)}} \quad (2)$$

$$TF = \frac{C_{Leaf}}{C_{Root}} \quad (3)$$

To determine the link and intensity of the effect of PTE concentrations in leaves on the parameters of the ecophysiological response of *P. alba* non-parametric Spearman rank-order correlation was used at a level of significance of P<0.001 (Table 4). Canonical discriminant analysis (CDA) was conducted to detect which parameter had the greatest impact on the differences established between the plants from the study sites (Figure 5).

3 Results

3.1 Basic physical and chemical characteristics of fly ash and soil

The basic physical and chemical properties of FA from lagoons L3 and L11 and soil from the natural habitat of *P. alba* (Control), sampled in the rhizosphere layer (at a depth of 0-30 cm), are presented in Table 1.

Compared to the Control soil, FA from L3 and L11 was characterised by a higher pH and EC and a higher proportion of

TABLE 1 Physical and chemical properties of fly ash at lagoons L3 and L11 and soil (Control).

	pH_{H2O}	EC µS cm^{-1}	C %	N %	C/N	Sand 2.0-0.02 mm	Silt + Clay <0.02 mm
L3							
Mean	7.95 **a**	242.60 **a**	2.01 **b**	0.05 **c**	45.14	83.13 **a**	16.87 **c**
SD	0.08	8.14	0.25	0.01		1.34	0.60
L11							
Mean	7.70 **b**	201.80 **b**	1.43 **c**	0.12 **b**	12.35	71.80 **b**	28.20 **b**
SD	0.01	939	0.05	0.01		1.48	1.48
Control							
Mean	7.55 **c**	138.40 **c**	4.08 **a**	0.38 **a**	10.74	8.27 **c**	91.73 **a**
SD	0.02	5.59	0.12	0.04		0.93	0.93

(One-way ANOVA - Bonferroni); Data represents Mean values with standard deviation (SD) of five replicates (n=5); Means followed by the same letter in a column do not differ significantly between sites (P<0.001).

10.3389/fpls.2023.1337700

TABLE 2 Pseudo total concentrations of PTEs (mg kg^{-1}) in fly ash at lagoons L3 and L11 and soil (Control).

	As	B	Cr	Cu	Mn	Ni	Se	Zn
L3								
Min	23.70	47.64	76.84	41.12	198.84	41.50	0.97	32.93
Max	32.08	52.10	107.56	57.00	254.59	61.53	2.25	45.13
Mean	**27.52a**	**47.64a**	**86.00a**	48.12 **a**	218.22 **b**	49.42 **b**	1.68 **a**	39.45 **a**
SD	3.05	2.65	12.65	5.87	21.38	7.62	0.51	5.49
L11								
Min	13.72	41.16	52.65	38.55	205.36	49.36	1.27	31.97
Max	14.88	42.00	67.18	45.52	227.05	58.41	1.80	37.46
Mean	14.23 **b**	**41.16b**	58.10 **b**	42.96 **a**	213.13 **b**	53.15 **b**	1.49 **a**	35.48 **a**
SD	0.46	0.61	5.70	2.87	9.13	3.72	2.22	2.20
Control								
Min	8.00	2.21	55.43	15.69	430.29	68.59	0.14	39.30
Max	8.36	3.00	69.10	17.46	466.67	69.64	0.30	46.34
Mean	8.22 **c**	2.61 **c**	62.76 **ab**	16.46 **b**	443.90 **a**	68.70 **a**	0.23 **b**	42.11 **a**
SD	0.14	0.31	5.00	0.66	14.32	1.11	0.08	2.62
Threshold and average concentrations in soils								
Average range [a]	4.4-8.4	22-40	47-51	13-23	270-525	13-26	0.25-0.34	45-60
Critical for plants [b]	20-50	25 [c]	75-100	60-125	1500-3000	100	5-10	70-400
Background Kolubara River [d]	10.3		67.5	22.24		54.87		69
Average Central Serbia [e]	11		48	27		58		48
Average World [e]	10		50	30		20		50

(One-way ANOVA - Bonferroni); data represents minimum (min), maximum (max), and Mean values with standard deviation (SD) of five replicates (n=5); Means followed by the same letter in a column do not differ significantly between sites (P<0.001); Mean critical concentrations are in bold. Threshold and average concentrations in soil: [a] Kabata-Pendias and Pendias, 2001; [b] Alloway, 1990; [c] Kloke et al., 1984; [d] Čakmak et al., 2018; [e] Mrvić et al., 2009.

the Sand fraction (L3>L11>Control; P<0.001), but lower C (Control>L3>L11; P<0.001) and N content (Control>L11>L3; P<0.001) and a lower proportion of the Silt+Clay fraction (Control>L11 >L3; P<0.001). In addition, FA from L3 had a higher pH, EC, C, C/N, and sand fraction content (P<0.001), but lower N and Silt+Clay fraction content (P<0.001) compared to FA from L11 (Table 1). In terms of soil classification (Soil Survey Division Staff, 2017), the control soil was classified as silty clay loam soil, while the particle size distribution of FA revealed that the texture of FA at L3 was similar to that of loamy sand and FA from L11 similar to that of sandy loam.

3.2 Concentrations of potentially toxic elements in fly ash and soil

Pseudo total concentrations of PTEs (As, B, Cr, Cu, Mn, Ni, Se, and Zn) in FA from lagoons L3 and L11 and soil (Control) are shown in Table 2.

Significantly higher concentrations (P<0.001) of As (235%), B (1725%), Cu (192%), and Se (630%) were found at L3, as well as As (73%), B (1477%), Cu (161%), and Se (548%) at L11, compared to those in soil. Lower concentrations of Mn (51-52%) and Ni (29-23%) were found in both lagoons compared to the Control, where the content of Cr and Zn was similar to the content in FA. Concentrations of PTEs in the Control soil generally did not exceed the average values for world soils and those in central Serbia (Mrvić et al., 2009), as well as the background values for the Kolubara Basin (Čakmak et al., 2018). The exception was slightly elevated concentrations of Cr and Ni due to soil formation processes on basic and ultrabasic rocks, which have a high natural content of these elements (Geological Information System of Serbia - GEOLIS, 2010; Pavlović et al., 2021). At L3, concentrations of As (93%), B (16%), and Cr (48%), which were in the critical range for plants (Kloke et al., 1984; Alloway, 1990), were higher than at L11, where B was still in the critical range while As and Cr were in a range higher than the average for world soils (Kabata-Pendias and Pendias, 2001; Mrvić et al., 2009). Similar concentrations of Cu, Ni, and Se, which were in a range higher than the average for world soils, and Mn

10.3389/fpls.2023.1337700

TABLE 3 PTE concentrations (mg kg^{-1}) in the roots (Root) and leaves (Leaf) of *P. alba* at the study sites.

Root	As	B	Cr	Cu	Mn	Ni	Se	Zn
L3								
Min	4.86	21.16	2.17	4.24	6.35	2.99	0.50	20.93
Max	5.36	22.89	2.38	4.48	8.13	3.12	1.00	23.39
Mean	**5.04 a**	21.99 **a**	2.27 **a**	4.32 **a**	6.79 **b**	3.02 **a**	0.68 **a**	22.16 **a**
SD	0.21	0.73	0.11	0.11	0.76	0.06	0.21	0.89
L11								
Min	4.84	11.72	1.37	3.37	7.48	3.12	0.75	19.84
Max	5.72	13.02	1.61	3.97	8.06	3.23	1.37	23.84
Mean	**5.33a**	12.29 **b**	1.49 **b**	3.66 **b**	7.81 **b**	3.16 **a**	1.01 **a**	21.58 **a**
SD	0.33	0.54	0.09	0.22	0.22	0.06	0.22	1.59
Control								
Min	3.98	9.61	1.75	4.35	19.14	3.00	0.50	22.09
Max	4.87	12.11	2.50	4.88	22.97	3.75	1.12	27.01
Mean	4.47 **a**	11.41 **b**	2.15 **a**	4.62 **a**	20.80 **a**	3.49 **a**	0.82 **a**	25.19 **a**
SD	0.36	1.04	0.33	0.26	1.51	0.36	0.23	1.91
Leaf	**As**	**B**	**Cr**	**Cu**	**Mn**	**Ni**	**Se**	**Zn**
L3								
Min	3.50	481.76	0.75	8.10	24.40	5.62	2.00	104.17
Max	4.63	505.63	0.87	8.39	26.28	5.88	2.75	113.80
Mean	4.24 **b**	**491.97a**	0.85 **a**	8.29 **a**	25.49 **a**	5.73 **a**	2.33 **b**	**108.71b**
SD	0.47	9.51	0.05	0.13	0.96	0.11	0.27	3.66
L11								
Min	5.60	201.49	0.74	7.31	13.95	3.49	2.99	119.38
Max	6.23	208.49	0.75	8.12	15.23	3.87	4.24	123.30
Mean	**5.83 a**	**204.94b**	0.75 **a**	7.59 **a**	14.57 **c**	3.72 **b**	3.49 **a**	**122.00a**
SD	0.25	2.68	0.00	0.31	0.53	0.21	0.50	1.59
Control								
Min	3.23	41.21	0.37	6.58	19.63	2.73	0.37	79.91
Max	3.88	42.87	0.50	7.08	21.10	2.75	0.87	83.31
Mean	3.52 **b**	42.18 **c**	0.45 **b**	6.78 **b**	20.32 **b**	2.74 **c**	0.70 **c**	81.78 **c**
SD	0.23	0.68	0.07	0.21	0.56	0.01	0.21	1.27
Threshold and average concentrations in plants								
Deficit	–	3-30	–	2-5	10-30	–	–	10-20
Normal	1-1.7	10-100	0.01-0.5	5-30	30-300	0.1-5	0.01-2	27-150
Toxic	5-20	50-200	5-30	20-100	400-1000	10-100	5-30	100-400

(One-way ANOVA - Bonferroni); data represents minimum (min), maximum (max), and Mean values with standard deviation (SD) of five replicates (n=5); Means followed by the same letter in a column do not differ significantly between sites (P<0.001, 2); Mean toxic concentrations are in bold. Threshold and average concentrations in plants: [a] Kabata-Pendias and Pendias, 2001.

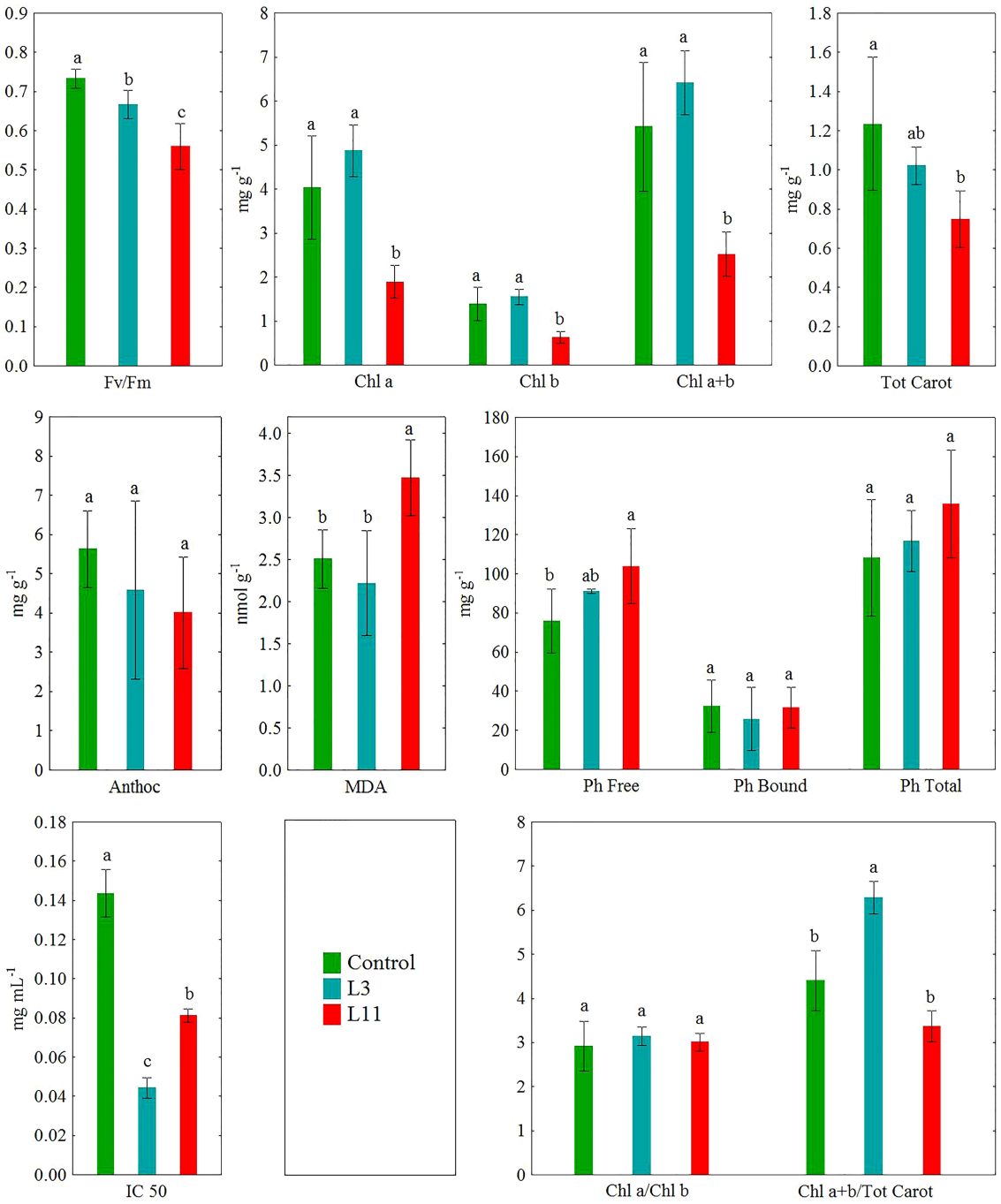

FIGURE 3
The ecophysiological response of the leaves of *P. alba* on fly ash (L3 and L11) and soil (Control). Different letters indicate significant difference between sites at P<0.001.

and Zn, which were below the average, were determined in FA from both lagoons (Table 2).

3.3 Potentially toxic elements in roots and leaves of *P. alba*

Concentrations of PTEs in *P. alba* roots and leaves at the study sites are shown in Table 3. The biological indicators BCF and TF for the examined elements in *P. alba* are shown in Figure 4.

Concentrations of As, Ni, Se, and Zn measured in the roots of *P. alba* were similar at all three sites. However, B was higher at L3 than at the control site, while Cr and Cu were lower at L11 and Mn was lower at both lagoons compared to the control. Concentrations of B, Cr, Cu, Ni, Se, and Zn in the leaves of *P. alba* at both lagoons and of As at L11 were higher than in the control individuals, for which the content of most PTEs was in the normal range. The exceptions were As, whose content in *P. alba* leaves was higher than average values, and Mn, whose content was in the deficit range for plants (Table 3;

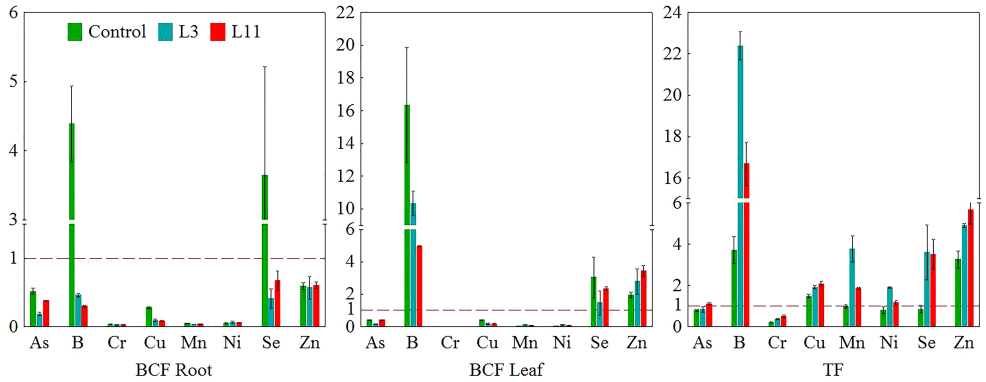

FIGURE 4
Bioconcentration factors for PTEs in roots (BCF Root) and leaves (BCF Leaf) and translocation factors (TF) for *P. alba* on fly ash (L3 and L11) and soil (Control).

Kabata-Pendias and Pendias, 2001). At L3, concentrations of B, Mn, and Ni in leaves were higher than at L11, while As, Se, and Zn levels were lower. Cr and Cu content was similar at both lagoons. Of all the elements tested, toxic concentrations of B and Zn were measured in *P. alba* leaves at L3 and of As, B, and Zn at L11, while Mn was in the deficit range at both lagoons. Cr, Se (L3 and L11), As and Ni (L3) levels in leaves were found to be in a range higher than normal but not toxic, while Cu was in the normal range at both lagoons (Table 3; Kabata-Pendias and Pendias, 2001). Analysis of BCF and TF showed that BCF in roots (BCF Root) was less than 1 for all PTEs studied at all the sites except for B and Se at the control site. BCF in leaves (BCF Leaf) was higher than 1 for B, Se, and Zn at all the sites. A TF higher than 1 was determined for B, Cu, Mn, and Zn at all three sites, for Ni and Se at L3 and L11, and for As only at L11. A general increase in the levels of the biological indicators above 1 (L3<L11) was found for As, Cu (TF), and Zn (BCF Leaf and TF) (Figure 4).

3.4 The ecophysiological response of *P. alba* to abiotic stresses at fly ash lagoons

The ecophysiological response of *P. alba*, based on Fv/Fm measurements and analysis of the content of metabolites such as Chl a, Chl b, Tot Carot, Anthoc, Ph Bound, Ph Free, MDA, and IC 50, is shown in Figure 3. The results of canonical discriminant analysis (CDA), which singles out those PTEs and ecophysiological parameters that are most responsible for the differences in the response of *P. alba* to stress factors, are shown in Figure 5. Spearman's rank correlations between all the examined ecophysiological parameters and PTE concentrations in *P. alba* leaves deviating from the range of normal values at all the sites are shown in Table 4.

In *P. alba* leaves, significantly lower values ($P<0.001$) of Fv/Fm (10%) and IC 50 (71%) were determined at L3 and of Fv/Fm (24%), Chl a (53%), Chl b (12%), Chl a+b (54%), Tot Carot (39%), and IC 50 (43%) at L11 than at the control site. Compared to the control individuals, there was a higher Chl a+b/Tot Carot ratio (39%) at L3 and a higher content of Ph Free (37%) and MDA (39%) at L11. In addition, lower values of Fv/Fm (16%), Chl a (58%), Chl b (59%), and Chl a+b (61%) were found in *P. alba* leaves at L11 compared to L3, but higher MDA (57%). Statistically significant differences in the content of Anthoc, Ph Bound, and Ph Free, as well as in the Chl a/Chl b ratio were not determined at the study sites for *P. alba* leaves (Figure 3).

In terms of the variability in concentrations of the examined PTEs in roots and leaves and the ecophysiological response of *P. alba* at the examined sites, the results of canonical discriminant analysis (CDA) showed that As, B, and Zn (Figures 5A, B), as well as IC 50, Chl a, Chl b, Tot Carot, and MDA (Figures 5C, D), had the greatest impact on the differences between the study sites. Across all the examined sites, the content of As, Se, and Zn in *P. alba* leaves correlated negatively with Fv/Fm and the Tot Carot content, but positively with Ph Free content. There was a strong negative correlation between chlorophyl content and As and a positive one with Mn content in leaves. However, the association of MDA with these elements exhibited the opposite trend. The total antioxidant activity of *P. alba* correlated negatively with B content in leaves, while the content of Ph Bound and Anthoc had a weak association with the examined PTEs in *P. alba* leaves (Table 4).

4 Discussion

At FA landfills, numerous kinds of abiotic stress simultaneously and continuously affect plants as a result of the unfavourable physical and chemical properties of the ash, the extreme microclimatic conditions, and the deficit or toxicity of essential and non-essential chemical elements. Such conditions hinder the survival and development of vegetation because they threaten the normal course of physiological processes in plants, including photosynthesis, which is extremely sensitive to heat, drought, salinity, heavy metal toxicity, and nutrient deficiency or toxicity (Muhammad et al., 2021). Research has shown that a combination of multiple stressors has a cumulative effect on almost all the physiological parameters that result in increased plant damage

TABLE 4 Spearman's correlations between ecophysiological parameters and PTE concentrations in *P. alba* leaves across all the examined sites.

Parameters	As	B	Mn	Zn
Fv/Fm	**-0.981**	-0.218	0.634	**-0.931**
Chl a	**-0.822**	0.410	**0.960**	-0.544
Chl b	**-0.872**	0.309	**0.931**	-0.629
Tot Carot	**-0.937**	-0.256	0.562	**-0.892**
Anthoc	-0.502	-0.350	0.210	-0.609
Ph Free	**0.891**	0.344	-0.457	**0.878**
Ph Bound	0.298	-0.441	-0.450	-0.019
MDA	**0.845**	-0.349	**-0.926**	0.586
IC 50	-0.405	**-0.951**	-0.343	-0.745

Bold indicates significant correlation at P<0.001.

(Pandey et al., 2015; Zandalinas et al., 2021). Many studies have shown that plants vary in terms of their ability to adapt and survive under conditions of multiple and varying stresses at ash landfills and that their survival is most often based on a strong functional response and their antioxidant capacity (Gajić et al., 2020; Kalashnikova et al., 2021; Qadir et al., 2021; Qadir et al., 2022). In addition, successful plants are able to immobilise PTEs in the root zone rather than accumulate them in leaves (Mitrović et al., 2008; Kostić et al., 2022b). Therefore, by analysing the functional properties of plants that survive in conditions of multiple stresses, it is possible to select species that are suitable for the processes of the revitalisation of polluted habitats and thus contribute to reducing pollution in the vicinity of large industrial complexes.

Analysis of chlorophyll fluorescence is a useful tool for studying the impact of abiotic stress on plants (Guidi et al., 2019). It provides information on the state of PSII, i.e. to what extent it uses the energy absorbed by chlorophyll and to what extent these stress conditions lead to damage to the photosynthetic apparatus. In this sense, calculating the photosynthetic efficiency parameter (Fv/Fm) is crucial for detecting the photoinhibition of PSII under stress

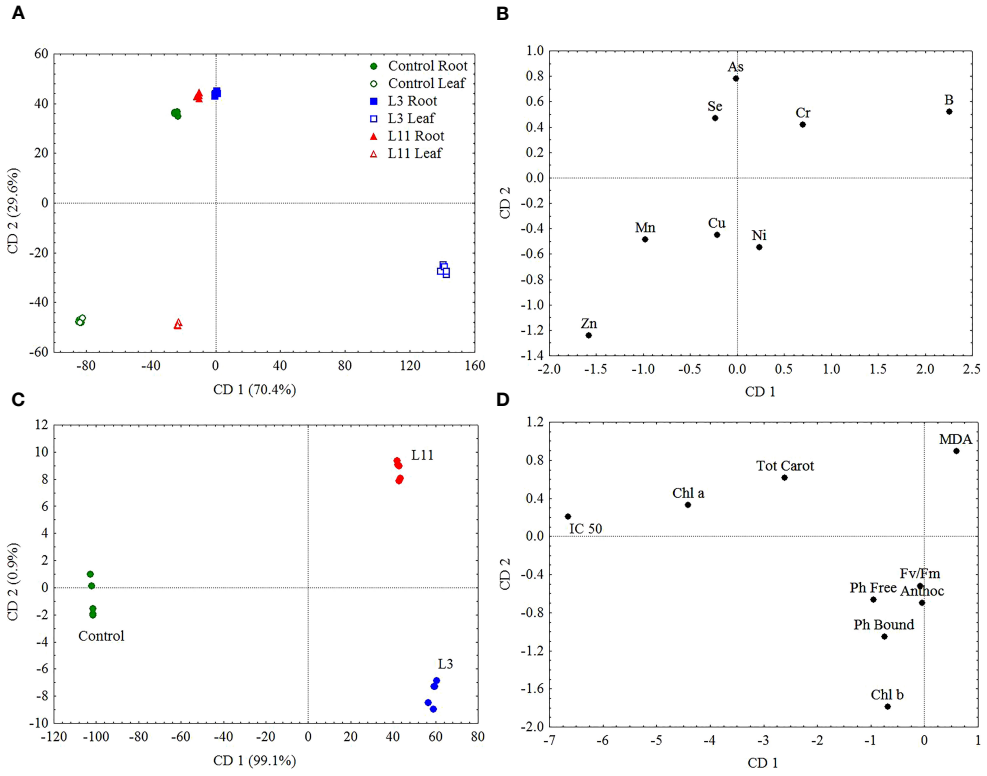

FIGURE 5
Canonical discriminant analysis (CDA) based on PTE concentrations in roots and leaves **(A)** and **(B)** and ecophysiological response parameters **(C)** and **(D)** of *P. alba* at L3, L11, and the Control site.

conditions. The results of our study showed that at the control site there was good water availability due to occasional flooding, an adequate water table, and well-structured silty clay loam. The soil was also slightly alkaline (7.4-7.8; Soil Survey Division Staff, 2017), there was an adequate mineral supply, and concentrations of the studied PTEs in the leaves of the control plants were in a range below the critical values for plants (Kabata-Pendias and Pendias, 2001). This provided optimal conditions for the growth of *P. alba* as shown by Fv/Fm values, which were in the optimal range for plants (0.750-0.850; Bjorkman and Demmig, 1987). However, Fv/Fm values for *P. alba* leaves at the FA lagoons were significantly lower at L3 (ranging between 0.650-0.687), indicating photoinhibition of PSII and a decrease in *P. alba* vitality with a tendency to further decrease at L11 (ranging between 0.510-0.585) due to prolonged stress and the accumulation of photosynthetic tissue damage, visible through pronounced morphological symptoms in the form of necrosis and leaf drying. A decrease in photosynthetic efficiency has been found in many plants at FA landfills such as *Dactylis glomerata* L., *Ricinus communis* L., *Solanum lycopersicum* L., *Tamarix tetrandra* Pall. ex M. Bieb., *Pinus sylvestris* L., *Picea abies* (L.) H. Karst., *Fagus sylvatica* L., and *Alnus glutinosa* (L.) Gaertn. (Gajić et al., 2020; Bęś et al., 2021; Kostic et al., 2022c; Qadir et al., 2022).

The general reduction in photosynthetic efficiency in the examined species at both FA lagoons is the result of the influence of multiple stressors such as drought, heat, and salt, but also inadequate mineral nutrition (PTE toxicity or deficit). In general, drought, salt, and heavy metal stress have been found to have almost similar effects on plant growth as they result in the production of ROS and oxidative stress (Zhang et al., 2019; Krzyżak et al., 2023). Specifically, the weaker binding properties of FA particles due to their texture, which corresponds to the texture of loamy sand soils, and low organic matter content resulted in the ash having a lower water-retention capacity, which exposed *P. alba* to drought stress at L3. Despite the fact that the hydraulic transport of raw FA during its disposal at L3 caused a significant reduction in the ash's salinity due to drainage of the transport water and the drying out of the FA (Kostic et al., 2018), the salt content in the ash at that lagoon was still significantly higher (242.60μS cm^{-1}) than in the control soil. This has a drought-like effect on the plants and is reflected in the reduction in photosynthetic efficiency (Técher et al., 2012). It should be noted that at L11 both abiotic (weathering) and biotic (vegetation development) factors that inevitably accompany the FA disposal process at landfills contribute to the increase in the Silt+Clay fraction and the narrowing of the C/N ratio as the best indicator of organic matter accumulation. They also result in a reduction in pH and the content of soluble salts in FA due to their leaching, which should increase the capacity of the FA to retain water and nutrients (Uzarowicz et al., 2017; Konstantinov et al., 2020; Petrović et al., 2023). However, at the time of our research, maintenance of the vegetative cover at L11 was no longer carried out (i.e. it was not watered), unlike at L3, so there was a moisture deficit despite the changes in the physical and chemical characteristics. The moisture deficit at the TENT A landfills is further intensified by the excessive heating of the surface layers of FA due to its dark grey colour, which was confirmed by the extremely high temperatures that were measured on the surface of the FA lagoons in the summer months. Moreover, due to the pozzolanic properties of FA particles, their wetting in the presence of liming material (CaSO4) cements them together, which is why compacted layers, which reduce aeration, water infiltration, and root penetration, form in places (Carlson and Adriano, 1993). Although flexible plant roots can grow horizontally or develop through zones of least resistance such as root canals, root elongation and water infiltration is reduced by the hard, compact layers of FA (Haynes, 2009). Stomatal closure as a common response to drought reduces CO2 uptake and fixation, but also reduces transpiration, limiting the cooling of the leaf's surface, resulting in thermal stress that has negative effects on metabolic processes, primarily photosynthesis. Thermal stress also causes changes in chlorophyll pigment and carotenoid content in leaves, thus affecting photoinhibition, which results in a reduced quantum yield of PSII (lower Fv/Fm), enhanced peroxidation in the leaf cell membrane (an increase in MDA), and reduced membrane thermostability (Yoon et al., 2014; Stojnić et al., 2016; Pilipović et al., 2020; Rosso et al., 2023). Increased salinity limits plant growth by inducing osmotic stress, impairing the uptake of ions leading to their imbalance or toxicity, inhibiting metabolic processes and enzyme activity, damaging thylakoid membranes, reducing photosynthetic pigments, and disrupting photosynthetic activity (Chen and Polle, 2010; Zhang et al., 2019).

Two of poplar's main strategies to cope with drought stress are avoidance mechanisms that control transpiration through the regulation of stomatal conductance, the deposition of cuticular waxes to limit non-stomatal transpiration, increased root growth, and reduced leaf area (Attia et al., 2015) and a stress tolerance strategy based on mechanisms to maintain biological functions through the synthesis of protective molecules and compounds under stress conditions (Viger et al., 2016). Salt tolerant poplar species are characterised by restricted xylem translocation and salt accumulation in the roots (Chen and Polle, 2010). However, our research found a reduction in photosynthetic efficiency of *P. alba* at both FA lagoons, which confirms earlier findings concerning *P. alba x P. glandulosa* (Yoon et al., 2014) and *P. alba* × *P. davidiana* (Kim et al., 2022) on the sensitivity of poplar to drought and salt stress, which leads to changes in their metabolic activity.

In terms of PTE pollution, among the PTEs determined in the FA at L3, As, B, and Cr were the main contaminants with concentrations exceeding critical levels for plants (As>20 mg kg^{-1}, B>25 mg kg^{-1}, Cr>75 mg kg^{-1}; Kloke et al., 1984; Kabata-Pendias and Pendias, 2001). Concentrations of Cu, Ni, and Se were higher than the average for sandy to silt-loam substrates and concentrations of Mn and Zn were lower than the range of average values (<270 mg kg^{-1} and<45 mg kg^{-1}, respectively; Kabata-Pendias and Pendias, 2001). The surface association of As, B, Cr, and Zn on FA particles contributes to their greater solubility, making these elements extremely hazardous to plants at FA landfills if they are accumulated in high concentrations (Gajić et al., 2020; Kostić et al., 2022b; Kostic et al., 2022c). However, it also contributes to their significantly lower content in FA at L11, although the content of B at L11 was still in the critical range for plants. As essential elements, B and Zn are easily transported (BCF

Leaf>1; TF>1) to leaves (Kabata-Pendias and Pendias, 2001; Robinson et al., 2005), while As and Cr as non-essential chemical elements mostly accumulate in roots (Wang et al., 2002; Singh et al., 2013). Under these conditions at the TENT A landfills, *P. alba* accumulated toxic concentrations of B and Zn (>50 mg kg^{-1}, >100mg kg^{-1}; Kabata-Pendias and Pendias, 2001) at L3 and L11 and also toxic concentrations of As (>5 mg kg^{-1}; Kabata-Pendias and Pendias, 2001) at L11, while Mn content was in the deficit range (<30 mg kg^{-1}; Kabata-Pendias and Pendias, 2001). The accumulation potential for B and Zn in *P. alba* leaves at L3 and L11 is also confirmed by earlier studies on poplars (Madejón et al., 2004; Robinson et al., 2005; Dos Santos Utmazian et al., 2007; Robinson et al., 2007; Di Lonardo et al., 2011; Rees et al., 2011; Huang et al., 2019; Pilipović et al., 2019; Kostić et al., 2022b; Tőzsér et al., 2023). The lower content of B in *P. alba* leaves at L11 compared to L3 was accompanied by changes in B content in FA because its solubility at pH>6 is conditioned only by its total concentration (Iwashita et al., 2005). The increase in Zn and As content in leaves at L11 compared to L3 is a result of their greater accumulation and translocation to leaves at this lagoon. This is due to the higher bioavailability of Zn and As, which is in line with the changed physical and chemical characteristics of FA at L11 compared to L3 – namely, a higher proportion of finer particles and organic matter, lower pH and salinity, and the absence of supplementation with phosphate fertilisers. This contributes to the greater solubility and mobility of the elements (Kostic et al., 2018; Balafrej et al., 2020; Gajić et al., 2020). Specifically, unlike at L3, where the application of phosphate fertilisers compensated for the phosphorus deficit in the FA, the cessation of phosphorus supplementation at a later stage of revitalisation and its leaching caused a deficit in the FA at L11, which can result in increased uptake of As by plants through the phosphate transport system (Wang et al., 2002). The poor solubility of Mn in FA is the cause of its characteristic deficit in plants growing at ash landfills (Adriano et al., 2002; Mitrović et al., 2008; Kostić et al., 2022b). Namely, earlier findings suggest that Mn content in *P. alba* leaves correlates to its availability in surface soil (Madejón et al., 2004) and that the accumulation potential of poplar for Mn is limited (Tőzsér et al., 2023). The higher uptake and transport of Zn through plant tissue to *P. alba* leaves at L11 may be caused by the lower Mn content in leaves resulting from its reduced bioavailability in FA at L11 due to the altered physical and chemical characteristics of FA when compared to L3 (Kabata-Pendias and Pendias, 2001; Aref, 2011). Cr content in *P. alba* leaves at L3 and L11 was higher than normal, but not toxic (>0.5 mg kg^{-1}; Kabata-Pendias and Pendias, 2001). In our study, much higher Cr concentrations were measured in *P. alba* roots than in leaves, confirming earlier findings for poplar trees (Pulford and Watson, 2003; Ancona et al., 2017; Tőzsér et al., 2023). BCF Root<1 and TF<1 make *P. alba* suitable for the phytostabilisation of this element.

The results of discriminatory analysis showed that of all the analysed PTEs in *P. alba* parts at the study sites, toxic concentrations of As, B, and Zn and a deficit of Mn contributed most to differences in the response of *P. alba* to the effects of stress. Of these differences, changes in the content of Chl a, Chl b, Tot Carot, MDA, and IC 50 were the most pronounced (Figure 5). Specifically, the toxic content of B in leaves may inhibit photosynthesis and significantly reduce Fv/Fm by damaging thylakoid membranes and reducing CO2 assimilation. This, in turn, causes disruption to photosynthetic electron transport, oxidative damage, and decreased photosynthetic enzyme activity, as well as reduced synthesis of δ-aminolevulinic acid and protochlorophyll as a precursor of chlorophyll biosynthesis as noted by a large number of researchers (Ardic et al., 2009; Han et al., 2009; Wang et al., 2011; Cervilla et al., 2012; Chen et al., 2012; Landi et al., 2012). At L3, typical visible symptoms of B toxicity were noted in the form of chlorosis and tip and marginal leaf necrosis (Rees et al., 2011). Nevertheless, the fact that there are differences in the tolerance levels of different poplar species is shown by the hybrid species *Populus nigra* × *euramericana*. Only 10% of its leaves exhibited damage at concentrations of up to 900 mg B kg^{-1}, while chlorosis occurred with concentrations of 1000-2000 mg B kg^{-1} and tissue necrosis only at concentrations greater than >2000 mg B kg^{-1} (Rees et al., 2011). Photosynthesis is the first metabolic process that will be disrupted by toxicity of Zn, which leads to a loss of plasma membrane integrity and a reduction in its permeability, damage to chloroplast functioning, and a reduction in photosynthetic electron transport (Huang et al., 2019; Balafrej et al., 2020). It has been found that high concentrations of Zn in poplar induce chlorotic and necrotic changes, alter leaf morphology and ultrastructure, leading to significant thickening of the leaf lamina and spongy tissue, and reduce above-ground biomass (Todeschini et al., 2011). It is possible that the extensive symptoms of damage in the form of chlorosis, necrosis, and leaf drying and also the visible smaller leaves with thicker lamina at L11 are the result of long-term toxic concentrations of Zn in poplar leaves. However, the toxic As levels measured in *P. alba* leaves at L11 can also adversely affect photosynthetic efficiency as it leads to disruption of the electronic transport chain, which conditions changes in the formation of NADPH and ATP and results in increased chlorophyll fluorescence (Stoeva and Bineva, 2003; Rahman et al., 2007; Gusman et al., 2013). This can be seen in our research through the decrease in Fv/Fm values, but also the visible morphological changes in the form of red-brown necrosis and the drying of older leaves (Kabata-Pendias and Pendias, 2001). Previous research has shown that *P. alba* accumulates higher amounts of As in leaves at contaminated sites than at uncontaminated ones (Madejón et al., 2004) and that the impact of As toxicity on chlorophyll synthesis is particularly pronounced (Moreno-Jiménez et al., 2009), which may be associated with the decrease in chlorophyll content at L11. Manganese is a chemical element that is directly involved in electron transport reactions and is essential for the synthesis of chlorophyll. Therefore, its deficit leads to the destruction of chloroplast thylakoid membrane structure, a reduction in the number of PSII reaction centres, and the degradation of complexes for the photolysis of water, in which four Mn atoms provide the energy necessary for the oxidation of two water molecules to oxygen (Alejandro et al., 2020).

In terms of photosynthetic pigments in leaves, measuring chlorophyll concentrations is an effective way to determine plants'

tolerance to stress. At L3, *P. alba* was found to have lower vitality, but significant differences in the content of Chl a, Chl b, Tot Carot, Anthoc, Ph Free, Ph Bound, and MDA compared to control individuals were not found. This may be the result firstly of NPK fertilisation, as N application improves the drought tolerance of poplars (Song et al., 2019), secondly of the higher Mn content in leaves compared to the other two sites as one of the mechanisms for overcoming stress (Della Maggiora et al., 2023), and thirdly the higher total antioxidant capacity of *P. alba* at this lagoon (<IC 50) as an indicator of the activation of enzymatic and non-enzymatic antioxidant systems (Zhang et al., 2019; Rosso et al., 2023). Also, the localisation of high concentrations of accumulated B in chlorotic and necrotic tissues in the tips and marginal parts of leaves is another adaptive mechanism of plants, which thus ensures a significant proportion of photosynthetic tissue remains functional (Rees et al., 2011). Unlike *P. alba* at L3 and the control site, a lower content of Chl a, Chl b, and Tot Carot and a higher content of MDA in the leaves along with a higher IC 50 was found at L11, indicating its less effective antioxidant defence system, which is consistent with the very low Fv/Fm values measured at that site. The significant correlation between As, Mn, and Zn in leaves and the analysed ecophysiological parameters (Table 4) indicates that the increase in As and Zn concentrations, as well as the decrease in Mn concentrations in leaves at L11 induces its weaker adaptive response at the older lagoon. The accumulation of both physiological and morphological damage indicates the importance of the long-term impact of stress on the process of photosynthesis in *P. alba* (Muhammad et al., 2021). Phenols as secondary metabolites contribute to physiological processes that are associated with protection against abiotic stress (Bencherif et al., 2020). As such, the higher Ph Free content in leaves at L11 when compared to the control site can be seen as the antioxidant response of *P. alba* to the environmental stresses at that particular site. However, it was not sufficient to quench lipid peroxidation and scavenge ROS under drought and salt stress conditions, as well as elevated PTE content. In particular, the toxic As and Zn concentrations contribute to this, as indicated by the positive correlation between Ph Free and the content of these two elements in leaves (Table 4). Also, the cytotoxic and prooxidative nature of phenolic compounds can be expressed in plants growing on FA due to the high content of Fe and Al oxides with the formation of phenoxy radicals, the life of which is significantly extended in the presence of Zn (Sakihama and Yamasaki, 2002). Through the synthesis of carotenoids and anthocyanins, plants also actively increase tolerance to different types of stress (Cervilla et al., 2012). However, unlike some species of plant in which a high As content in leaves induces an increased accumulation of anthocyanins (Leão et al., 2014), in woody species, such as *P. alba* in this case, and in earlier studies on *Tamarix tetrandra* at FA landfills, their antioxidant role is absent (Kostic et al., 2022c). The degradation in carotenoids for *P. alba* observed at L11 results in a reduction in the plant's resistance to ROS, which favours a rise in lipid peroxidation rates and MDA concentrations, as was also found in *T. tetrandra*, *Cassia occidentalis, and Dactylis glomerata* at FA landfills (Love et al., 2013; Gajić et al., 2020; Kostić et al., 2022b). The exposure of *P. alba* to oxidative stress at L11 is also indicated by the decrease in the Chl a + b/Tot Carot ratio compared to L3, which occurs because of the accumulation of leaf tissue damage and progressive tissue aging due to its prolonged exposure to environmental stresses (Stoeva and Bineva, 2003). This is unlike the Chl a/b ratio as an early warning indicator of the toxic effects of metal accumulation in plants (D'Addazio et al., 2023), which remains unchanged compared to L3. These results are in line with earlier research that also showed a decrease in chlorophyll and carotenoid content, as well as an increase in MDA in poplars in response to drought (Kim et al., 2022) and heavy metal stress (Chandra and Kang, 2016). A decrease in chlorophylls and carotenoids has also been found in many plants at FA landfills, such as *T. tetrandra, Robinia pseudoacacia* L., *Amorpha fruticosa* L., and *Withania somnifera* (Pavlović et al., 2004; Qadir et al., 2021; Kostic et al., 2022c).

5 Conclusion

This study was conducted with the aim of evaluating the ecophysiological response of *Populus alba* L., which spontaneously colonised two FA disposal lagoons at the 'Nikola Tesla A' thermal power plant (Obrenovac, Serbia) 3 years (L3) and 11 years (L11) before the beginning of the research, to simultaneous and continuous exposure to abiotic stressors. It was found that at both lagoons *P. alba* was exposed to multiple stress factors such as drought and salt stress, but also inadequate PTE concentrations. At L3 there were critical concentrations of As, B, and Cr in FA and at L11 critical concentrations of B, while a deficit of Mn is characteristic for all plants growing on such substrates. The *P. alba* individuals at both lagoons showed lower vitality than the individuals in their natural habitat. In addition, the effects of single and combined stressors on *P. alba* trees resulted in visible leaf damage symptoms in the form of chlorosis, necrosis, and drying of leaves. Some of these symptoms are characteristic of drought, increased salinity, toxic concentrations of B and Zn, and deficient Mn in *P. alba* leaves and were more pronounced due to the increase in toxic concentrations of As at L11. Nevertheless, care measures (e.g. watering, fertilisation) and the increased biosynthesis of enzymatic and non-enzymatic antioxidant compounds (<IC 50) at the beginning of the revitalisation process contributed to the better response of *P. alba* to stress at L3, as indicated by the absence of differences in levels of Chl a, Chl b, Tot Carot, Anthoc, Ph Free, Ph Bound, and MDA compared to the control individuals. In contrast to L3, the increased toxic concentrations of As and Zn in leaves at L11 resulted in oxidative stress in *P. alba*, as evidenced by lower vitality, reduced synthesis of chlorophyll, carotenoids and total antioxidant activity, and higher MDA content. This suggests that despite its rapid colonisation of FA lagoons, the stress tolerance of *P. alba* decreases with increasing intensity and duration of exposure to adverse abiotic factors. Furthermore, its weaker stabilisation potential for substrates with high As and B content makes *P. alba* highly unsuitable for the permanent revitalisation of such habitats. Although white poplar is a fast-growing species with a good ability to accumulate metals and a high stress tolerance, the

above characteristics could give it an advantage, but only if it were used during the temporary, short-term restoration process in the cyclical disposal of FA in the passive lagoons at the landfill and with the application of care measures such as ash moistening and NPK supplementation.

Data availability statement

The raw data supporting the conclusions of this article will be made available by the authors, without undue reservation.

Author contributions

OK: Conceptualization, Data curation, Investigation, Methodology, Writing – original draft, Writing – review & editing. SJ: Formal Analysis, Investigation, Validation, Writing – review & editing. DP: Formal Analysis, Validation, Writing – review & editing. MMa: Formal Analysis, Investigation, Writing – review & editing. NR: Formal Analysis, Investigation, Writing – original draft. MMi: Conceptualization, Methodology, Supervision, Writing – review & editing. PP: Funding acquisition, Supervision, Writing – review & editing.

Funding

The author(s) declare financial support was received for the research, authorship, and/or publication of this article. This work was supported by the Ministry of Science Technological Development and Innovation of the Republic of Serbia, grant no. 451-03-68/2023-14/200007.

Conflict of interest

The authors declare that the research was conducted in the absence of any commercial or financial relationships that could be construed as a potential conflict of interest.

Publisher's note

All claims expressed in this article are solely those of the authors and do not necessarily represent those of their affiliated organizations, or those of the publisher, the editors and the reviewers. Any product that may be evaluated in this article, or claim that may be made by its manufacturer, is not guaranteed or endorsed by the publisher.

References

Adriano, D. C., Weber, J., Bolan, N. S., Paramasivam, S., Koo, B.–J., and Sajwan, K. S. (2002). Effects of high rates of coal fly ash on soil, turfgrass, and groundwater quality. *Water Air Soil Pollut.* 139, 365–385. doi: 10.1023/A:1015895922471

Alejandro, S., Höller, S., Meier, B., and Peiter, E. (2020). Manganese in plants: from acquisition to subcellular allocation. *Front. Plant Sci.* 11. doi: 10.3389/fpls.2020.00300

Alloway, B. J. (1990). *Heavy Metals in Soil* (London: Blackie and Son Ltd.), 339.

Ancona, V., Caracciolo, A. B., Grenni, P., Di Lenola, M., Campanale, C., Calabrese, A., et al. (2017). Plant-assisted bioremediation of a historically PCB and heavy metal-contaminated area in Southern Italy. *New Biotechnol.* 38, 65–73. doi: 10.1016/j.nbt.2016.09.006

Ardic, M., Sekmen, A. H., Tokur, S., Ozdemir, F., and Turkan, I. (2009). Antioxidant response of chickpea plants subjected to boron toxicity. *Plant Biol.* 11, 328–338. doi: 10.1111/j.1438-8677.2008.00132.x

Aref, F. (2011). Influence of zinc and boron nutrition on copper, manganese and iron concentration in the maize leaf. *Aust. J. Basic Appl. Sci.* 5 (7), 52–62. ISSN 1991-8178.

Arnon, D. I. (1949). Copper enzymes in isolated chloroplasts: Polyphenoloxidase in Beta vulgaris. *Plant Physiol.* 24, 1–15. doi: 10.1104/pp.24.1.1

Atterberg, A. (1911). Über die physikalische Bodenuntersuchung und über die Plastizität der Tone. *Int. Mitt. Bodenkd.* 1, 10–43.

Attia, Z., Domec, J. C., Oren, R., Way, D. A., and Moshelion, M. (2015). Growth and physiological responses of isohydric and anisohydric poplars to drought. *J. Exp. Bot.* 66, 4373–4381. doi: 10.1093/jxb/erv195

Balafrej, H., Bogusz, D., Triqui, Z. A., Guedira, A., Bendaou, N., Smouni, A., et al. (2020). Hyperaccumulation in plants: A review. *Plants (Basel)* 9 (5), 562. doi: 10.3390/plants9050562

Bencherif, K., Trodi, F., Hamidi, M., Dalpè, Y., and Hadj-Sahraoui, A. L. (2020). "Biological overview and adaptability strategies of *Tamarix* plants, *T. articulata* and *T. gallica* to abiotic Stress," in *Plant Stress Biology*. Eds. B. Giri and M. P. Sharma (Singapore: Springer), 401–433. doi: 10.1007/978-981-15-9380-2_14

Bęś, A., Sikorski, Ł., and Szreder, K. (2021). The effect of mineral-based mixtures containing coal fly ash and sewage sludge on chlorophyll fluorescence and selected morphological parameters of deciduous and coniferous trees. *Minerals* 11 (7), 778. doi: 10.3390/min11070778

Bhatt, A., Priyadarshini, S., Mohanakrishnan, A. A., Abri, A., Sattler, M., and Techapaphawit, S. (2019). Physical, chemical, and geotechnical properties of coal fly ash: A global review. *Case Stud. Constr. Mater.* 11, e00263. doi: 10.1016/j.cscm.2019.e00263

Bjorkman, O., and Demmig, B. (1987). Photon yield of O2 evolution and chlorophyll fluorescence characteristics at 77 K among vascular plant of diverse origins. *Planta* 170, 489–504. doi: 10.1007/BF00402983

Borghi, M., Tognetti, R., Monteforti, G., and Sebastiani, L. (2008). Responses of two poplar species (*Populus alba* and *Populus x canadensis*) to high copper concentrations. *Environ. Exp. Bot.* 62 (3), 290–299. doi: 10.1016/j.envexpbot.2007.10.001

Brand-Williams, W., Cuvelier, M. E., and Berset, C. L. W. T. (1995). Use of a free radical method to evaluate antioxidant activity. *LWT Food Sci. Technol.* 28, 25–30. doi: 10.1016/S0023-6438(95)80008-5

Čakmak, D., Perović, V., Antić-Mladenović, S., Kresović, M., Saljnikov, E., Mitrović, M., et al. (2018). Contamination, risk, and source apportionment of potentially toxic microelements in river sediments and soil after extreme flooding in the Kolubara River catchment in Western Serbia. *J. Soils Sediments.* 18, 1981–1993. doi: 10.1007/s11368-017-1904-0

Carlson, C. L., and Adriano, D. C. (1991). Growth and elemental content of two tree species growing on abandoned coal fly ash basins. *J. Environ. Qual.* 20 (3), 581–587. doi: 10.2134/jeq1991.00472425002000030013x

Carlson, C. L., and Adriano, D. C. (1993). Environmental impacts of coal combustion residues. *J. Environ. Qual.* 22, 227–247. doi: 10.2134/jeq1993.00472425002200020002x

Caudullo, G., and de Rigo, D. (2016). "*Populus alba* in Europe: distribution, habitat, usage and threats," in *European atlas of forest tree species*. Eds. J. San-Miguel-Ayanz, D. de Rigo, G. Caudullo, T. Houston Durrant and A. Mauri (Luxembourg: Publications Office of the EU), 136–137.

Caudullo, G., Welk, E., and San-Miguel-Ayanz, J. (2017). Chorological maps for the main European woody species. *Data Brief* 12, 662–666. doi: 10.1016/j.dib.2017.05.007

Cervilla, L. M., Blasco, B., Rios, J. J., Rosales, M. A., Sánchez-Rodríguez, E., Rubio-Wilhelmi, M. M., et al. (2012). Parameters symptomatic for boron toxicity in leaves of tomato plants. *J. Bot.* 2012, 726206. doi: 10.1155/2012/726206

Chandra, R., and Kang, H. (2016). Mixed heavy metal stress on photosynthesis, transpiration rate, and chlorophyll content in poplar hybrids. *For. Sci. Technol.12* 2), 55–61. doi: 10.1080/21580103.2015.1044024

Chen, L. S., Han, S., Qi, Y. P., and Yang, L. T. (2012). Boron stresses and tolerance in citrus. *Afr. J. Biotechnol.* 11 (22), 5961–5969. doi: 10.5897/AJBX11.073

Chen, S., and Polle, A. (2010). Salinity tolerance of populus. *Plant Biol.* 12, 317–333. doi: 10.1111/j.1438-8677.2009.00301.x

Creasy, L. L. (1968). The role of low temperature in anthocyanin synthesis in 'McIntosh' apples. *Proc. Am. Soc Hortic. Sci.* 93, 716–724.

Ćujić, M., Dragović, S., Djordjević, M., Dragović, R., and Gajić, B. (2016). Environmental assessment of heavy metals around the largest coal fired power plant in Serbia. *Catena* 139, 44–52. doi: 10.1016/j.catena.2015.12.001

D'Addazio, V., Tognella, M. M. P., Fernandes, A. A., Falqueto, A. R., da Rosa, M. B., Gontijo, I., et al. (2023). Impact of metal accumulation on photosynthetic pigments, carbon assimilation, and oxidative metabolism in mangroves affected by the fundão dam tailings plume. *Coasts* 3 (2), 125–144. doi: 10.3390/coasts3020008

Della Maggiora, L., Francini, A., Giovannelli, A., and Sebastiani, L. (2023). Assessment of the salinity tolerance, response mechanisms and nutritional imbalance to heterogeneous salt supply in *Populus alba* L. clone 'Marte' using a split-root system. *Plant Growth Regul.* 101, 251–265. doi: 10.1007/s10725-023-01017-w

Di Lonardo, S., Capuana, M., Arnetoli, M., Gabbrielli, R., and Gonnelli, C. (2011). Exploring the metal phytoremediation potential of three *Populus alba* L. clones using an *in vitro* screening. *Environ. Sci. Pollut. Res.* 18, 82–90. doi: 10.1007/s11356-010-0354-7

Djurdjevic, L., Mitrovic, M., and Pavlovic, P. (2007). "Total phenolics and phenolic acids in plants and soils," in *Cell Diagnostics: Images, Biophysical and Biochemical Processes in Allelopathy. Section III: Methods of Analytical Biochemistry and Biophysics*. Eds. V. V. RoshChina and S. S. Narval (Enfield, CT, USA: Science Publishers), 155–168. Available at: https://radar.ibiss.bg.ac.rs/handle/123456789/3770.

Dos Santos Utmazian, M. N., Wieshammer, G., Vega, R., and Wenzel, W. W. (2007). Hydroponic screening for metal resistance and accumulation of cadmium and zinc in twenty clones of willows and poplars. *Environ. Pollut.* 148 (1), 155–165. doi: 10.1016/j.envpol.2006.10.045

Feldman, A. W., and Hanks, R. W. (1968). Phenolic content in the roots and leaves of tolerant and susceptible cultivars attacked by *Rodopholus similis*. *Phytochem.* 7, 5–12. doi: 10.1016/S0031-9422(00)88198-4

Gajić, G., Djurdjević, L., Kostić, O., Jarić, S., Stevanović, B., Mitrović, M., et al. (2020). Phytoremediation potential, photosynthetic and antioxidant response to arsenic-induced stress of *dactylis glomerata* L. Sown on fly ash deposits. *Plants* 9 (5), 657. doi: 10.3390/plants9050657

Geological Information System of Serbia - GEOLIS (2010). *Basic geological maps of Serbia* Vol. 1 (Belgrade: Institute for Geological and Geophysical Research), 100000. Available at: http://geoliss.mre.gov.rs/. 1959-1966.

Guerra, F., Gainza, F., Pérez, R., and Zamudio, F. (2011). "Phytoremediation of heavy metals using poplars (*Populus* spp.): a glimpse of the plant responses to copper, cadmium and zinc stress," in *Handbook of phytoremediation*. Ed. I. A. Golubev (New York: Nova Science Publishers Inc.), 387–413, ISBN: .

Guidi, L., Lo Piccolo, E., and Landi, M. (2019). Chlorophyll fluorescence, photoinhibition and abiotic stress: does it make any difference the fact to be a C3 or C4 species? *Front. Plant Sci.* 10. doi: 10.3389/fpls.2019.00174

Gusman, G. G., Oliveira, J. A., Farnese, F. S., and Cambraia, J. (2013). Arsenate and arsenite: the toxic effects on photosynthesis and growth of lettuce plants. *Acta Physiol. Plant* 35 (4), 1201–1209. doi: 10.1007/s11738-012-1159-8

Han, S., Tang, N., Jiang, H. X., Yang, L. T., Li, Y., and Chen, L. S. (2009). CO2 assimilation, photosystem II photochemistry, carbohydrate metabolism and antioxidant system of citrus leaves in response to boron stress. *Plant Sci.* 176, 143–153. doi: 10.1016/j.plantsci.2008.10.004

Haynes, R. J. (2009). Reclamation and revegetation of fly ash disposal sites–challenges and research needs. *J. Environ. Manage.* 90, 43–53. doi: 10.1016/j.jenvman.2008.07.003

Heath, R. L., and Packer, L. (1968). Photoperoxidation in isolated chloroplasts: I. Kinetics and stoichiometry of fatty acid peroxidation. *Arch. Biochem. Biophys.* 125, 189–198. doi: 10.1016/0003-9861(68)90654-1

Huang, X. H., Zhu, F., Yan, W. D., Chen, X. Y., Wang, G. J., and Wang, R. J. (2019). Effects of Pb and Zn toxicity on chlorophyll fluorescence and biomass production of *Koelreuteria paniculata* and *Zelkova schneideriana* young plants. *Photosynthetica* 57 (2), 688–697. doi: 10.32615/ps.2019.050

Iwashita, A., Sakaguchi, Y., Nakajima, T., Takanashi, H., Ohki, A., and Kambara, S. (2005). Leaching characteristics of boron and selenium for various coal fly ashes. *Fuel* 84, 479–485. doi: 10.1016/j.fuel.2004.11.002

Izquierdo, M., and Querol, X. (2012). Leaching behavior of elements from coal combustion fly ash: An overview. *Int. J. Coal Geol.* 94, 54–66. doi: 10.1016/j.coal.2011.10.006

Kabata-Pendias, A., and Pendias, H. (2001). *Trace Elements in Soils and Plants. 3rd Edition* (Boca Raton: CRC Press), 403.

Kalashnikova, I. V., Migalina, S. V., Ronzhina, D. A., Ivanov, L. A., and Ivanova, L. A. (2021). Functional response of Betula species to edaphic and nutrient stress during restoration of fly ash deposits in the Middle Urals (Russia). *Environ. Sci. Pollut.* 28, 12714–12724. doi: 10.1007/s11356-020-11200-5

Kebert, M., Kostić, S., Čapelja, E., Vuksanović, V., Stojnić, S., Markić, A. G., et al. (2022). Ectomycorrhizal fungi modulate pedunculate oak's heat stress responses through the alternation of polyamines, phenolics, and osmotica content. *Plants* 11, 3360. doi: 10.3390/plants11233360

Khan, I., and Umar, R. (2019). Environmental risk assessment of coal fly ash on soil and groundwater quality, Aligarh, India. *Groundw. Sustain. Dev.* 8, 346–357. doi: 10.1016/j.gsd.2018.12.002

Kim, T.-L., Lee, K., Hwang, H.-S., Oh, C., Lee, I. H., and Lim, H. (2022). Comparison of physiological and biochemical responses of two poplar species under drought stress. *Plant Breed. Biotech.* 10 (3), 145–162. doi: 10.9787/PBB.2022.10.3.145

Kloke, A., Sauerbeck, D. R., and Vetter, H. (1984). "The contamination of plants and soils with heavy metals and the transport of metals in terrestrial food chains," in *Changing Metal Cycles and Human Health. Dahlem Workshop Reports, Life Sciences Research Report*, vol. 28 . Ed. J. O. Nriagut (Berlin, Heidelberg: Springer), 113–141. doi: 10.1007/978-3-642-69314-4_7

Konstantinov, A., Novoselov, A., Konstantinova, E., Loiko, S., Kurasova, A., and Minkina, T. (2020). Composition and properties of soils developed within the ash disposal areas originated from peat combustion (Tyumen, Russia). *Soil Sci. Annu.* 71, 3–14. doi: 10.37501/soilsa/121487

Kostić, O., Gajić, G., Jarić, S., Vukov, T., Matić, M., Mitrović, M., et al. (2022b). An assessment of the phytoremediation potential of planted and spontaneously colonized woody plant species on chronosequence fly ash disposal sites in Serbia—Case study. *Plants* 11 (1), 110. doi: 10.3390/plants11010110

Kostic, O., Jaric, S., Gajic, G., Pavlovic, D., Mataruga, Z., Radulovic, N., et al. (2022c). The Phytoremediation Potential and Physiological Adaptive Response of *Tamarix tetrandra* Pall. Ex M. Bieb. during the Restoration of Chronosequence Fly Ash Deposits. *Plants* 11, 855. doi: 10.3390/plantsl1070855

Kostic, O., Jaric, S., Gajic, G., Pavlovic, D., Pavlovic, M., Mitrovic, M., et al. (2018). Pedological properties and ecological implications of substrates derived 3 and 11 years after the revegetation of lignite fly ash disposal sites in Serbia. *Catena* 163, 78–88. doi: 10.1016/j.catena.2017.12.010

Kostić, O., Mitrović, M., Knežević, M., Jarić, S., Gajić, G., Djurdjević, L., et al. (2012). The potential of four woody species for the revegetation of fly ash deposits from the 'Nikola Tesla-a' Thermoelectric plant (Obrenovac, Serbia). *Arch. Biol. Sci.* 64, 145–158. doi: 10.2298/ABS1201145K

Kostić, O., Mitrović, M., and Pavlović, P. (2022a). "Impact of weathering and revegetation on pedological characteristics and Pollutant dispersion control at coal fly ash disposal sites," in *Advances in Understanding Soil Degradation 1st edition*. Eds. E. Saljnikov, L. Müller, A. Lavrishchev and F. Eulenstein (Springer International Publishing), 473–505. doi: 10.1007/978-3-030-85682-3_22

Krause, H. M., and Weis, E. (1991). Chlorophyll fluorescence and photosynthesis: The basics. *Annu. Rev. Plant Physiol.* 42, 313–349. doi: 10.1146/annurev.pp.42.060191.001525

Krzyżak, J., Rusinowski, S., Sitko, K., Szada-Borzyszkowska, A., Stec, R., Janota, P., et al. (2023). The effect of combined drought and trace metal elements stress on the physiological response of three *Miscanthus* hybrids. *Sci. Rep.* 13, 10452. doi: 10.1038/s41598-023-37564-5

Landi, M., Degl'Innocenti, E., Pardossi, A., and Guidi, L. (2012). Antioxidant and Photosynthetic responses in plants under boron toxicity: A review. *Am. J. Agric. Biol. Sci.* 7 (3), 255–270. doi: 10.3844/ajabssp.2012.255.270

Leão, G. A., de Oliveira, J. A., Felipe, R. T. A., Farnese, F. S., and Gusman, G. S. (2014). Anthocyanins, thiols, and antioxidant scavenging enzymes are involved in *Lemna gibba* tolerance to arsenic. *J. Plant Interact.* 9 (1), 143–151. doi: 10.1080/17429145.2013.784815

Love, A., Banerjee, B. D., and Babu, C. R. (2013). Assessment of oxidative stress markers and concentrations of selected elements in the leaves of *Cassia occidentalis* growing wild on a coal fly ash basin. *Environ. Monit. Ass.* 185, 6553–6562. doi: 10.1007/s10661-012-3046-6

Madejón, P., Maranon, T., Murillo, J. M., and Robinson, B. (2004). White poplar (*Populus alba*) as a biomonitor of trace elements in contaminated riparian forests. *Environ. Pollut.* 132, 145–155. doi: 10.1016/j.envpol.2004.03.015

Mishra, N., Jiang, C., Chen, L., Paul, A., Chatterjee, A., and Shen, G. (2023). Achieving abiotic stress tolerance in plants through antioxidative defense mechanisms. *Front. Plant Sci.* 14. doi: 10.3389/fpls.2023.1110622

Mitrović, M., Jaić, S., Kostić, O., Gajić, G., Karadžić, B., Đurđević, L., et al. (2012). Photosynthetic efficiency of four woody species growing on fly ash deposits of a Serbian „Nikola tesla – A" Thermoelectric plant. *Pol. J. Environ. Stud.* 21 (5), 1339–1347.

Mitrović, M., Pavlović, P., Lakušić, D., Djurdjević, L., Stevanović, B., Kostić, O., et al. (2008). The potential of *Festuca rubra* and *Calamagrostis epigejos* for the revegetation of fly ash deposits. *Sci. Tot. Environ.* 407, 338–347. doi: 10.1016/j.scitotenv.2008.09.001

Molyneux, P. (2004). The use of the stable free radical diphenylpicrylhydrazyl (DPPH) for estimating antioxidant activity. *Songklanakarin J. Sci. Technol.* 26, 211–219.

Moreno-Jiménez, E., Esteban, E., Carpena-Ruiz, R. O., and Peñalosa, J. M. (2009). Arsenic and mercury induced phytotoxicity in the Mediterranean shrubs *Pistacia lentiscus* and *Tamarix gallica* grown in hydroponic culture. *Ecotoxicol. Environ. Saf.* 72, 1781–1789. doi: 10.1016/j.ecoenv.2009.04.022

Mrvić, V., Zdravković, M., Sikirić, B., Čakmak, D., and Kostić-Kravljanac, L. (2009). "Toxic and dangerous elements in soil," in *Fertility and content of toxic and dangerous materials in soil of Central Serbia*. Eds. V. Mrvić, G. Antonović and Lj. Martinović (Serbian: Institute of Soil Science Belgrade), 75–134.

Muhammad, I., Shalmani, A., Ali, M., Yang, Q. H., Ahmad, H., and Li, F. B. (2021). Mechanisms regulating the dynamics of photosynthesis under abiotic stresses. *Front. Plant Sci.* 11. doi: 10.3389/fpls.2020.615942

Mukhopadhyay, S., Rana, V., Kumar, A., and Kumar Maiti, S. (2017). Biodiversity variability and metal accumulation strategies in plants spontaneously inhibiting fly ash lagoon, India. *Environ. Sci. Pollut. Res.* 24, 22990–23005. doi: 10.1007/s11356-017-9930-4

Palancean, I., Alba, N., Sabatti, M., and de Vries, S. M. G. (2018). *EUFORGEN Technical Guidelines for genetic conservation and use for white poplar (Populus alba)* Vol. 6 (European Forest Genetic Resources Programme (EUFORGEN), European Forest Institute).

Pandey, P., Ramegowda, V., and Senthil-Kumar, M. (2015). Shared and unique responses of plants to multiple individual stresses and stress combinations: physiological and molecular mechanisms. *Front. Plant Sci.* 6. doi: 10.3389/fpls.2015.00723

Pandey, V. C., Singh, K., Singh, R. P., and Singh, B. (2012). Naturally growing *Saccharum munja* L. on the fly ash lagoons: A potential ecological engineer for the revegetation and stabilization. *Ecol. Eng.* 40, 95–99. doi: 10.1016/j.ecoleng.2011.12.019

Pandey, V. C., Singh, J. S., Singh, R. P., Singh, N., and Yunus, M. (2011). Arsenic hazards in coal fly ash and its fate in Indian scenario. *Resour. Conserv. Recycl.* 55 (9-10), 819–835. doi: 10.1016/j.resconrec.2011.04.005

Pavlović, P., Mitrović, M., and Djurdjević, L. (2004). An ecophysiological study of plants growing on the fly ash deposits from the "Nikola tesla – A" thermal power station in Serbia. *Environ. Manage.* 33, 654–663. doi: 10.1007/s00267-004-2928-y

Pavlović, P., Mitrović, M., Djurdjević, L., Gajić, G., Kostić, O., and Bojović, S. (2007). Ecological potential of *Spirea van-hauttei* (Briot) Zabel for urban (Belgrade city) and fly ash deposit (Obrenovac) landscaping in Serbia. *Pol. J. Environ. Stud.* 16, 427–431.

Pavlović, P., Sawidis, T., Breuste, J., Kostić, O., Čakmak, D., Djordjević, D., et al. (2021). Fractionation of potentially toxic elements (PTEs) in urban soils from salzburg, thessaloniki and belgrade: an insight into source identification and human health risk assessment. *Int. J. Environ. Res. Public Health* 18, 6014. doi: 10.3390/ijerph18116014

Petrović, M., Ivanić, M., Vidovic, N., Dolenec, M., Čermelj, B., Šket, P., et al. (2023). Physicochemical and mineral characteristics of soil materials developed naturally on two ~ 50 years old coal combustion residue disposal sites in Croatia. *Catena* 231, 107338. doi: 10.1016/j.catena.2023.107338

Pietrzykowski, M., Woś, B., Pająk, M., Wanic, T., Krzaklewski, W., and Chodak, M. (2018). The impact of alders (*Alnus* spp.) on the physico-chemical properties of technosols on a lignite combustion waste disposal site. *Ecol. Eng.* 120, 180–186. doi: 10.1016/j.ecoleng.2018.06.004

Pilipović, A., Drekić, M., Stojnić, S., Nikolić, N., Trudić, B., Milović, M., et al. (2020). Physiological responses of two pedunculate oak (*Quercus robur* L.) families to combined stress conditions – drought and herbivore attack. *Šumarski list* 144 (11-12), 573–582. doi: 10.31298/sl.144.11-12.5

Pilipović, A., Zalesny, R. S., Rončević, S., Nikolić, N., Orlović, S., Beljin, J., et al. (2019). Growth, physiology, and phytoextraction potential of poplar and willow established in soils amended with heavy-metal contaminated, dredged river sediments. *J. Environ. Manage.* 239, 352–365. doi: 10.1016/j.jenvman.2019.03.072

Proctor, J. T. A. (1974). Colour stimulation in attached apples with supplementary light. *Can. J. Plant Sci.* 54, 499–503. doi: 10.4141/CJPS74-084

Pulford, D., and Watson, C. (2003). Phytoremediation of heavy metal-contaminated land by trees – a review. *Environ. Int.* 29, 529–540. doi: 10.1016/S0160-4120(02)00152-6

Qadir, S. U., Raja, V., Siddiqui, W. A., AlYemeni, M. N., and Ahmad, P. (2021). Foliar concentrations of selected elements, assessment of oxidative stress markers and role of antioxidant defense system is associated with fly ash stress tolerance in *withania somnifera*. *J. Plant Growth Regul.* 40, 1450–1465. doi: 10.1007/s00344-020-10200-6

Qadir, S. U., Raja, V., Siddiqui, W. A., Shah, T., Alansi, S., and El-Sheikh, M. A. (2022). Ascorbate glutathione antioxidant system alleviates fly ash stress by modulating growth physiology and biochemical responses in *Solanum lycopersicum*. *Saudi J. Biol. Sci.* 29 (3), 1322–1336. doi: 10.1016/j.sjbs.2021.12.013

Rahman, M. A., Hasegawa, H., Rahman, M. M., Islam, M. N., Miah, M. A. M., and Tasmin, A. (2007). Effect of arsenic on photosynthesis, growth and yield of five widely cultivated rice (*Oryza sativa* L.) varieties in Bangladesh. *Chemosphere* 67, 1072–1079. doi: 10.1016/j.chemosphere.2006.11.061

Raja, R., Nayak, A. K., Rao, K. S., Gautam, P., Lal, B., Tripathi, R., et al. (2015). Impairment of soil health due to fly ash-fugitive dust deposition from coal-fired thermal power plants. *Environ. Monit. Assess.* 187, 679. doi: 10.1007/s10661-015-4902-y

Rees, R., Robinson, B. H., Menon, M., Lehmann, E., Günthardt-Goerg, M. S., and Schulin, R. (2011). Boron Accumulation and Toxicity in Hybrid Poplar (*Populus nigra x euroamericana*). *Environ. Sci.Technol.* 45, 10538–10543. doi: 10.1021/es201100b

Robinson, B. H., Green, S. R., Chancerel, B., Mills, T. M., and Clothier, B. E. (2007). Poplar for the phytomanagement of boron contaminated sites. *Environ. Pollut.* 150 (2), 225–233. doi: 10.1016/j.envpol.2007.01.017

Robinson, B. H., Mills, T. M., Green, S., Chancerel, B., Clothier, B., Fung, L. E., et al. (2005). Trace element accumulation by poplars and willows used for stock fodder. *New Z. J. Agric. Res.* 48 (4), 489–497. doi: 10.1080/00288233.2005.9513683

Rosso, L., Cantamessa, S., Bergante, S., Biselli, C., Fricano, A., Chiarabaglio, P. M., et al. (2023). Responses to drought stress in Poplar: What do we know and what can we learn? *Life* 13 (2), 533. doi: 10.3390/life13020533

Sachdev, S., Ansari, S. A., Ansari, M. I., Fujita, M., and Hasanuzzaman, M. (2021). Abiotic stress and reactive oxygen species: generation, signaling, and defense mechanisms. *Antioxidants* 10 (2), 277. doi: 10.3390/antiox10020277

Sakihama, Y., and Yamasaki, H. (2002). Lipid peroxidation induced by phenolics in conjunction with aluminum ions. *Biol. Plant* 45, 249–254. doi: 10.1023/A:1015152908241

Sharma, A., Kumar, V., Shahzad, B., Ramakrishnan, M., Singh Sidhu, G. P., Bali, A. S., et al. (2020). Photosynthetic response of plants under different abiotic stresses: a review. *J. Plant Growth Regul.* 39, 509–531. doi: 10.1007/s00344-019-10018-x

Simakov, V. N. (1957). The use of phenylanthranilic acid in the determination of humus by Tyurin's method. *Pochvovedenie* 8, 72–73.

Singh, H. P., Mahajan, P., Kaur, S., Batish, D. R., and Kohli, R. K. (2013). Chromium toxicity and tolerance in plants. *Environ. Chem. Lett.* 11, 229–254. doi: 10.1007/s10311-013-0407-5

Soil Survey Division Staff (2017). "Examination and description of soil profiles" in *Soil survey manual. Handbook 18.* Eds. C. Ditzler, K. Scheffe and H. C. Monge. (Washington, D.C: United States Department of Agriculture) Available at: https://www.nrcs.usda.gov/sites/default/files/2022-09/The-Soil-Survey-Manual.pdf (Accessed September 25, 2022).

Song, J., Wang, Y., Pan, Y., Pang, J., Zhang, X., Fan, J., et al. (2019). The influence of nitrogen availability on anatomical and physiological responses of *Populus alba* × *P. glandulosa* to drought stress. *BMC Plant Biol.* 19, 63. doi: 10.1186/s12870-019-1667-4

Stoeva, N., and Bineva, T. (2003). Oxidative changes and photosynthesis in oat plants grown in As-contaminated soil. *Bulg. J. Plant Physiol.* 29 (1-2), 87–95.

Stojnić, S., Pekeč, S., Kebert, M., Pilipović, A., Stojanović, D., Stojanović, M., et al. (2016). Drought Effects on Physiology and Biochemistry of Pedunculate Oak (*Quercus robur* L.) and Hornbeam (*Carpinus betulus* L.) Saplings Grown in Urban Area of Novi Sad, Serbia. *South-East Eur. For.* 7 (1), 57–63. doi: 10.15177/seefor.16-03

Tőzsér, D., Horváth, R., Simon, E., and Magura, T. (2023). Heavy metal uptake by plant parts of Populus species: a meta-analysis. *Environ. Sci. Pollut. Res.* 30, 69416–69430. doi: 10.1007/s11356-023-27244-2

Técher, D., Laval-Gilly, P., Bennasroune, A., Henry, S., Martinez-Chois, C., D'Innocenzo, M., et al. (2012). An appraisal of *Miscanthus x giganteus* cultivation for fly ash revegetation and soil restoration. *Ind. Crops Prod.* 36, 427–433. doi: 10.1016/j.indcrop.2011.10.009

Tian, Q., Guo, B., Nakama, S., and Sasaki, K. (2018). Distributions and leaching behaviors of toxic elements in fly ash. *ACS Omega* 3 10), 13055–13064. doi: 10.1021/acsomega.8b02096

Todeschini, V., Lingua, G., D`Agostino, G., Carniato, F., Roccotiello, E., and Berta, G. (2011). Effects of high zinc concentration on poplar leaves: A morphological and biochemical study. *Environ. Exp. Bot.* 71, 50–56. doi: 10.1016/j.envexpbot.2010.10.018

U.S. Environmental Protection Agency (USEPA) (1996) *Microwave Assisted Acid Digestion of Siliceous and Organically Based Matrices. In Test Methods for Evaluating Solid Waste, SW 846-Method 3052* (Washington, DC, USA: EPA). Available at: https://www.epa.gov/sites/default/files/2015-12/documents/3052.pdf (Accessed 8 February 2022).

U.S. Environmental Protection Agency (USEPA) (1998) *Microwave assisted acid digestion of sediments, sludges and oils. In Test Methods for Evaluating Solid Waste, SW 846-Method 3051* (Washington, DC, USA: EPA). Available at: https://settek.com/documents/EPA-Methods/PDF/EPA-Method-3051.pdf (Accessed 11 January 2022).

Uzarowicz, Ł., Zagórski, Z., Mendak, E., Bartmiński, P., Szara, E., Kondras, M., et al. (2017). Technogenic soils (Technosols) developed from fly ash and bottom ash from thermal power stations combusting bituminous coal and lignite. Part I. properties, classification, and indicators of early pedogenesis. *Catena* 157, 75–89. doi: 10.1016/j.catena.2017.05.010

Viger, M., Smith, H. K., Cohen, D., Dewoody, J., Trewin, H., Steenackers, M., et al. (2016). Adaptive mechanisms and genomic plasticity for drought tolerance identified in European black poplar (*Populus nigra* L.). *Tree Physiol.* 36, 909–928. doi: 10.1093/treephys/tpw017

Vuksanović, V., Kovačević, B., Stojnić, S., Kebert, M., Kesić, L., Galović, V., et al. (2022). Variability of tolerance of Wild cherry clones to PEG-induced osmotic stress *in vitro*. *iForest* 15, 265–272. doi: 10.3832/ifor4033-015

Wang, J. Z., Tao, S. T., Qi, K. J., Wu, H. Q., and Zhang, S. L. (2011). Changes in photosynthetic properties and antioxidative system of pear leaves to boron toxicity. *Afr. J. Biotechnol.* 10 (85), 19693–19700. doi: 10.5897/AJB11.2608

Wang, J. R., Zhao, F. J., Meharg, A. A., Raab, A., Feldmann, J., and McGrath, S. P. (2002). Mechanisms of arsenic hyperaccumulation in *Pteris vittata*: arsenic species uptake kinetics and interaction with phosphate. *Plant Physiol.* 130, 1552–1561. doi: 10.1104/pp.008185

Wellburn, A. R. (1994). The spectral determination of chlorophylls a and b, as well as total carotenoids using various solvents with spectrophotometers of different resolution. *J. Plant Physiol.* 144, 307–313. doi: 10.1016/S0176-1617(11)81192-2

Weiß, C. H. (2007). StatSoft, Inc., Tulsa, OK.: STATISTICA, Version 8. AStA *Adv. Stat. Anal.* 91, 339–341. doi: 10.1007/s10182-007-0038-x

Yadav, S., Pandey, V. C., Kumar, M., and Singh, L. (2022). Plant diversity and ecological potential of naturally colonizing vegetation for ecorestoration of fly ash disposal area. *Ecol. Eng.* 176, 106533. doi: 10.1016/j.ecoleng.2021.106533

Yan, A., Wang, Y., Tan, S. N., Mohd Yusof, M. L., Ghosh, S., and Chen, Z. (2020). Phytoremediation: A promising approach for revegetation of heavy metal-Polluted land. *Front. Plant Sci.* 11. doi: 10.3389/fpls.2020.00359

Yoon, S. K., Park, E. J., Choi, J. I., Bae, E. K., Kim, J. H., Park, S. Y., et al. (2014). Response to drought and salt stress in leaves of poplar (*Populus alba* × *Populus glandulosa*): Expression profiling by oligonucleotide microarray analysis. *Plant Physiol. Biochem.* 84, 158–168. doi: 10.1016/j.plaphy.2014.09.008

Zacchini, M., Pietrini, F., Scarascia Mugnozza, G., Iori, V., Pietrosanti, L., and Massacci, A. (2009). Metal tolerance, accumulation and translocation in poplar and willow clones treated with cadmium in hydroponics. *Water Air Soil Pollut.* 197, 23–34. doi: 10.1007/s11270-008-9788-7

Zandalinas, S., Sengupta, S., Fritschi, F., Azad, R., Nechushtai, R., and Mittler, R. (2021). The impact of multifactorial stress combination on plant growth and survival. *New Phytol.* 230 (3), 1034–1048. doi: 10.1111/nph.17232

Zhang, X., Liu, L., Chen, B., Qin, Z., Xiao, Y., Zhang, Y., et al. (2019). Progress in understanding the physiological and molecular responses of *populus* to salt stress. *Int. J. Mol. Sci.* 20 (6), 1312. doi: 10.3390/ijms20061312

Zhenggang, X., Li, F., Mengxi, Z., Yunlin, Z., Huimin, H., and Guiyan, Y. (2023). Physiological dynamics as indicators of plant response to manganese binary effect. *Front. Plant Sci.* 14. doi: 10.3389/fpls.2023.1145427

frontiers | Frontiers in Plant Science

TYPE Original Research
PUBLISHED 12 January 2024
DOI 10.3389/fpls.2023.1339201

OPEN ACCESS

EDITED BY
Fernanda Fidalgo,
University of Porto, Portugal

REVIEWED BY
Jorge Teixeira,
University of Porto, Portugal
Bruno Sousa,
University of Porto, Portugal

*CORRESPONDENCE
Hülya Torun
hulyatorun@duzce.edu.tr

RECEIVED 15 November 2023
ACCEPTED 22 December 2023
PUBLISHED 12 January 2024

CITATION
Torun H, Cetin B, Stojnic S and Petrík P (2024) Salicylic acid alleviates the effects of cadmium and drought stress by regulating water status, ions, and antioxidant defense in *Pterocarya fraxinifolia*. *Front. Plant Sci.* 14:1339201. doi: 10.3389/fpls.2023.1339201

Salicylic acid alleviates the effects of cadmium and drought stress by regulating water status, ions, and antioxidant defense in *Pterocarya fraxinifolia*

Hülya Torun[1]*, Bilal Cetin[2], Srdjan Stojnic[3] and Peter Petrík[4]

[1]Faculty of Agriculture, Düzce University, Düzce, Türkiye, [2]Faculty of Forestry, Düzce University, Düzce, Türkiye, [3]Institute of Lowland Forestry and Environment, University of Novi Sad, Novi Sad, Serbia, [4]Karlsruhe Institute of Technology (KIT), Institute of Meteorology and Climate Research-Atmospheric Environmental Research (IMK-IFU), Garmisch-Partenkirchen, Germany

Introduction: *Pterocarya fraxinifolia* (Poiret) Spach (Caucasian wingnut, Juglandaceae) is a relict tree species, and little is known about its tolerance to abiotic stress factors, including drought stress and heavy metal toxicity. In addition, salicylic acid (SA) has been shown to have a pivotal role in plant responses to biotic and abiotic stresses.

Methods: The current study is focused on evaluating the impact of foliar application of SA in mediating Caucasian wingnut physiological and biochemical responses, including growth, relative water content (RWC), osmotic potential (Ψs), quantum yield (Fv/Fm), electrolyte leakage, lipid peroxidation, hydrogen peroxide, and antioxidant enzymes, to cadmium (Cd; 100 μM) and drought stress, as well as their interaction. Moreover, the antioxidant activity (e.g., ascorbate peroxidase, catalase, glutathione reductase, peroxidase, and superoxide dismutase activities) of the stressed trees was investigated. The study was conducted on 6-month-old seedlings under controlled environmental conditions in a greenhouse for 3 weeks.

Results and discussion: Leaf length, RWC, Ψs, and Fv/Fm were decreased under all treatments, although the effect of drought stress was the most pronounced. An efficient antioxidant defense mechanism was detected in Caucasian wingnut. Moreover, SA-treated Caucasian wingnut plants had lower lipid peroxidation, as one of the indicators of oxidative stress, when compared to non-SA-treated groups, suggesting the tolerance of this plant to Cd stress, drought stress, and their combination. Cadmium and drought stress also changed the ion concentrations in Caucasian wingnut, causing excessive accumulation of Cd in leaves. These results highlight the beneficial function of SA in reducing the negative effects of Cd and drought stress on Caucasian wingnut plants.

KEYWORDS

antioxidant enzymes, Caucasian wingnut, photosynthesis, reactive oxygen species, water scarcity

1 Introduction

Pterocarya fraxinifolia, commonly known as the Caucasian wingnut, is a relict deciduous tree species that is a typical element of riparian and floodplain forests in lowlands of the Euxinian, Caucasian, and Irano-Turanian regions (Kutbay et al., 1999; Song et al., 2021). With its essential oil composition and high antimicrobial and antioxidant values, this plant is used as an antidiarrheal, poison, and dyeing agent by indigenous people (Akhbari et al., 2014; Tavakoli et al., 2016). Moreover, because of its high ornamental value, the genus *Pterocarya* has been utilized in urban landscape greening in recent years (Li et al., 2021). Though the Caucasian wingnut prefers moist soils, it is considered drought tolerant. However, there are a limited number of publications regarding this plant's response to stress factors.

The detrimental impact of global warming and climate change on terrestrial ecosystems is manifested through the emergence of severe environmental conditions. Plants must contend with various stresses, and their survival is significantly compromised when exposed to combinations of multiple stress factors (Zandalinas et al., 2022). The frequency and intensity of abiotic stress combinations are predicted to increase (Zandalinas et al., 2022). Among these factors, soil-associated stressors such as water scarcity and heavy metals may be more detrimental in terms of plant morphological, physiological, and biochemical processes, which could lead to decrement in growth, biomass, and yield. Known as a highly toxic heavy metal, cadmium (Cd) is released into the environment through human activities such as mining, fertilizers, pesticides, and industrial processes (Tripti et al., 2023). Plants easily accumulate Cd from the soil, and excessive Cd uptake leads to metabolic defects and growth inhibition (Zhang et al., 2023a). Drought is another well-studied abiotic stress type that also causes serious effects on plant growth and survival (Ilyas et al., 2021). Given the coexistence of multiple stressors in the natural environment, simultaneous exposure to both drought and Cd stresses results in a decline in plant growth, development, and reproductive capabilities (Zandalinas and Mittler, 2022; Zandalinas et al., 2022). Although the physiological and biochemical responses of plants to drought and Cd stresses are well documented, both as single and combined applications (Bauddh and Singh, 2012; Xia et al., 2015; Adrees et al., 2020; Zhang et al., 2023a), there is still a lack of knowledge about the effects of these stressors on riparian and floodplain vegetation.

Acclimation to multifactorial stress conditions in plants is unique when compared to their response to each of the stresses applied individually (Zandalinas et al., 2021). Moreover, when plants face simultaneous abiotic stress, they need to cope with the combined effects of multiple stressors, which can be more challenging and have synergistic or antagonistic interactions (Zandalinas and Mittler, 2022). Drought and cadmium stress can stimulate the overproduction of both oxygen radicals and their derivatives, the so-called reactive oxygen species (ROS), such as hydrogen peroxide, hydroxyl, and superoxide radicals (Hasanuzzaman et al., 2020). Even though ROS are generated in the apoplast, chloroplasts, mitochondria, peroxisomes, and plasma membranes as part of normal cellular metabolism (Singh et al., 2019), the over-accumulation of ROS causes oxidative cell injury and can lead to damage of primary metabolites. To mitigate the harmful effects of oxidative stress induced by different stress factors, including drought and Cd, plants keep them under control by enzymatic (ascorbate peroxidase, catalase, dehydroascorbate reductase, guaiacol peroxidase, glutathione reductase, monodehydroascorbate reductase, and superoxide dismutase) and non-enzymatic (α-tocopherol, alkaloids, ascorbic acid, carotenoids, flavonoids, glutathione, and phenolic acids) antioxidant defense systems that help neutralize ROS and maintain cellular redox balance (Kerchev and Van Breusegem, 2022). The equilibrium between the production of ROS and the activities of antioxidant systems is vital for plant survival and the plants' ability to withstand stress. Due to the dual role of ROS, plants have complex responses to stress conditions. However, there is no evidence that excess cellular levels of ROS induce significant damage in *P. fraxinifolia* under drought stress or Cd toxicity.

Salicylic acid (SA), a plant phenolic synthesized by the isochorismate or phenylalanine pathway in plants, is an endogenous phytohormone (Shine et al., 2016; Lefevere et al., 2020) that acts as a key signaling molecule in plant defense responses against various abiotic and biotic stress factors (Santisree et al., 2020; Song et al., 2023). As a plant growth regulator, SA interacts with other signaling molecules and phytohormones to reduce oxidative damage as well as modulate stomatal behavior (Prodhan et al., 2018; Li et al., 2023), reduce metal uptake (Sharma et al., 2020), scavenge ROS (Saleem et al., 2021), regulate nitrogen metabolism (Iqbal et al., 2022), and regulate various physiological and biochemical processes (Guo et al., 2019; González-Villagra et al., 2022; Kaya et al., 2023). However, the interaction between SA and abiotic stress in plants is a complex phenomenon and tends to vary depending on plant species, stress types, and environmental conditions (Liu et al., 2022). Therefore, understanding the role of SA in abiotic stress responses in woody plants is critical for developing strategies to enhance their resilience and productivity in the face of environmental challenges. Although several studies with SA-applied plant species have been reported, there are a limited number of studies regarding its application in simultaneously applied drought and Cd stresses. While previous studies have stated the alleviating impacts of SA on drought stress and Cd toxicity, the present study provides new insights into the mechanistic basis of this mitigation in woody plants. Furthermore, there is no conclusive evidence for the radical scavenging effect and antioxidant capacity of SA in Caucasian wingnut under drought or Cd stress.

To the best of our knowledge, there is no study investigating the effects of SA treatment on physiological and biochemical processes in *P. fraxinifolia* under drought and Cd stresses. Although agricultural plants are widely studied, studies on forest species are more limited. In addition, there are no publications on the drought and Cd stress tolerance of this species, either as a riparian species or in urban planting for its aesthetic value. Therefore, the purpose of this study was to assess the detrimental effect of single and combined treatments of drought and Cd stresses on Caucasian wingnut, as well as to investigate the potential contribution of SA to the reduction of oxidative stress. In this respect, leaf length, water

content, osmotic potential, chlorophyll fluorescence, H_2O_2 content, lipid peroxidation, antioxidant enzymes, and ion concentrations such as Ca, Cu, Fe, K, Mg, Mn, P, Zn, and Cd, were measured in Caucasian wingnut seedlings grown under singly or simultaneously applied drought and Cd stresses. We hypothesize that SA application will alleviate drought and Cd stresses *via* upregulation of the antioxidant defense system (superoxide dismutase and glutathione reductase), compared to stressed non-SA-treated groups. Moreover, it is predicted that SA-treated groups will be able to maintain higher photosynthetic capacity (quantum yield) under stress treatments, compared to non-SA-treated groups.

2 Materials and methods

2.1 Plant cultivation and treatments

Caucasian wingnut (*P. fraxinifolia*) seeds were collected from seaside areas of the village of Uğurlu located in Akçakoca, Düzce Province (41°01′27.55″E, 30°59′36.37″N, 25 m a.s.l.) in October 2019. First, to remove any dirt or debris, the seeds were cleaned by rinsing them with distilled water. After cleansing, stratification was performed on these seeds at 4°C for 30 days. Then, the seeds were planted in plastic pots (9 cm × 11 cm × 20 cm) filled with a mixture of peat and perlite (at 75:25). The seedlings were grown in a greenhouse under controlled conditions: 27°C/16 h/day and 22°C/8 h/night at a relative humidity of 70%. After the seedlings were cultured for 6 months, the treatment groups were created as control (irrigation water alone; C), cadmium (100 μM $CdCl_2$; Cd), drought (D), cadmium + drought (Cd+D), salicylic acid pretreatment (SA), salicylic acid pretreatment + cadmium (SA+Cd), salicylic acid pretreatment + drought (SA+D), and salicylic acid pretreatment + drought + cadmium (SA+Cd+D). A foliar application of SA was conducted, and 0.5 mM SA mixed with 0.1% Tween 20 was sprayed onto Caucasian wingnut leaves for 72 h before the stress treatments. The control plants were sprayed with an equal volume of water that contained only Tween 20 solution. Drought conditions were induced by maintaining soil water content below 40% of the full field capacity, and the drought treatment was considered to be leaving the plants without water. The concentrations were chosen on the basis of preliminary experiments in order to induce physiological processes without killing plants. Prior to harvesting, the plants were photographed, and the length of the leaves was measured using a standard ruler. Leaf length was defined as the distance from the base of the petiole to the apex of the terminal leaflet of the pinnate compound leaves of Caucasian wingnut. Mature leaves of this plant were harvested after 3 weeks of stress treatment, immediately frozen at −196°C, and stored at −80°C for further analysis. All chemicals used in this study were analytical-grade chemicals obtained from Sigma-Aldrich (St. Louis, MO, USA).

2.2 Relative water content

After harvesting, the fully expanded fourth leaves (n = 7) from each treatment were immediately weighed (FW). Then, the same leaves were floated in distilled water-filled tubes. Thereafter, they were reweighed to achieve the turgid weight (TW). Finally, the leaf samples were dried at 70°C until the dry weight (DW) was determined (Smart and Bingham, 1974). The relative water content (RWC) was calculated using the following formula:

$$RWC(\%) = [(FW - DW)/(TW - DW)] \times 100 =$$

2.3 Osmotic potential

After harvesting, the fully expanded fourth leaves (n = 7) from each treatment were utilized for the osmotic potential. First, a glass rod was used to crush the leaves of a Caucasian wingnut, and after centrifugation (5,000 *g* for 5 min), the supernatant was utilized for measurement using a vapor pressure osmometer (Wescor, Logan, UT, USA) (Santa-Cruz et al., 2002).

2.4 Chlorophyll fluorescence

Before harvesting, the fully expanded fourth leaves (n = 10) taken from each treatment group were used for the chlorophyll fluorescence measurements. First, the leaves were adapted to dark for 20 min with leaf clips, and then the measurements were performed using a chlorophyll fluorometer (Plant Efficiency Analyzer, Hansatech, Pentney, UK). The *Fv*/*Fm* ratio was measured for chlorophyll fluorescence to characterize the quantum efficiency of the photosystem II photochemistry.

2.5 Electrolyte leakage

Leaf disks excised using a cork borer from the fully expanded fourth leaves were utilized for the electrolyte leakage measurements (Lutts et al., 1996). Seven leaf disks from each treatment were washed with deionized water and then immersed in a test tube containing 10 mL of deionized water for 24 h at room temperature. After that, the initial electrical conductivity (EC1) of the samples was measured using a conductivity meter (Mettler-Toledo GmbH, Greifensee, Switzerland). The same test tubes were then autoclaved (120°C for 20 min) and cooled to room temperature. Then, a second electrical conductivity (EC2) measurement was taken. The EL was calculated using the following formula:

$$EL(\%) = (EC1/EC2) \times 100$$

2.6 Lipid peroxidation

Lipid peroxidation levels of the Caucasian wingnut were determined by measuring thiobarbituric acid reactive substances (TBARSs). Leaf samples (0.5 g) were homogenized with 5 mL trichloroacetic acid (TCA; 0.1%) and centrifuged at 15,000 *g* for 10 min. After centrifugation, the supernatant (1 mL) was mixed with 4 mL of 20% TCA containing 0.5% thiobarbituric acid. The

mixture solution was incubated at 95°C for 30 min. After the mixture had been cooled in ice, absorbance was recorded at 532 nm and 600 nm using a spectrophotometer (UV-VIS 1900i, Shimadzu Co., Kyoto, Japan), and the results were expressed as nmol/g FW (Heath and Packer, 1968).

2.7 Hydrogen peroxide

Hydrogen peroxide (H_2O_2) of Caucasian wingnut leaves was determined according to the method described by Liu et al. (2000). Leaf samples (0.5 g) were homogenized using TCA and centrifuged at 15,000 *g* for 10 min. After centrifugation, the supernatant (500 µL) was mixed with 1.5 mL of the reaction mixture containing 0.1% $TiCl_4$. The H_2O_2 content was determined using a standard curve prepared on a spectrophotometer (UV-VIS 1900i, Shimadzu Co., Kyoto, Japan) at 410 nm, and the results were defined as l µmol H_2O_2/g FW.

2.8 Ion content

Dried Caucasian wingnut leaf samples (0.1 g) were extracted in 40 mL of 4% HNO_3 to determine Ca, Cu, Fe, K, Mg, Mn, P, Zn, and Cd contents (Wheal and Palmer, 2010). The ion concentrations were measured using inductively coupled plasma–optical emission spectrometry (Avio 200 ICP-OES, PerkinElmer, Waltham, MA, USA).

2.9 Antioxidant enzymes

Frozen fresh leaf tissue (0.5 g) was homogenized in ice-cold 10 mL 50 mM KP buffer (pH 7.0) containing ethylenediaminetetraacetic acid (EDTA; 1 mM) and soluble polyvinylpyrrolidone (PVP; 1%) for antioxidant enzyme activity assays. Ascorbate (2 mM) was added to the same homogenization buffer for the ascorbate peroxidase (APX) activity assay. After centrifugation at 20,000 *g* for 15 min, the supernatants were obtained and further used for the enzyme activities and protein content assays. The protein content was assayed with bovine serum albumin (Bradford, 1976). Superoxide dismutase (SOD; EC.1.15.1.1) activity was measured at 560 nm according to the protocol described by Beauchamp and Fridovich (1971). The reaction solution contained 3 mL of 50 mM KP buffer (pH 7.0), 0.1 mM EDTA, 13 mM methionine, 0.075 mM nitroblue tetrazolium (NBT), and 0.002 mM riboflavin with the 50 µL enzyme extract. Then, the reaction mixture was kept under fluorescent light for 10 min. One unit of SOD was defined as the amount of enzyme that inhibited 50% of color reaction. Peroxidase (POX; EC.1.11.1.7) activity was measured at 470 nm for the activity increase with the oxidation of guaiacol (Mika and Luthje, 2003). The reaction mixture contained 3 mL of 25 mM sodium acetate buffer (pH 5.0), 10 mM H_2O_2, 10 mM guaiacol, and 50 µL enzyme extract. One unit of POX activity was defined as the amount that decomposes 1 µmol of H_2O_2 in 1 min. Catalase (CAT; EC 1.11.1.6) activity was determined at 240 nm for the absorbance activity reduction (Aebi, 1984). The reaction mixture contained 1 mL 50 mM KP buffer (pH 7.0), 10 mM H_2O_2, and 50 µL enzyme extract. One unit of CAT activity was defined as the amount that decomposes 1 µmol of H_2O_2 in 1 min. APX (EC 1.11.1.11) activity was measured at 290 nm for absorbance activity reduction (Nakano and Asada, 1981). The reaction mixture contained 1 mL 50 mM Na-P buffer (pH 7.0), 250 mM ascorbate, 5 mM H_2O_2, and 50 µL enzyme extract. One unit of APX was defined as the amount that oxidizes 1 µmol of ascorbate in 1 min. Glutathione reductase (GR; EC 1.6.4.2) activity was determined at 340 nm for the absorbance activity reduction (Foyer and Halliwell, 1976). The reaction mixture contained 1 mL of 50 mM Tris-HCl buffer (pH 7.6), 10 mM oxidized glutathione (GSSG), 5 mM NADPH, and 50 µL enzyme extract. One unit of GR was defined as the amount that reduces 1 µmol of GSSG in 1 min.

2.10 Statistical analysis

All treatments were performed with three independent biological replicates. The normal distribution of each trait was tested using the Shapiro–Wilk test, and the homogeneity of variances was analyzed by Bartlett's test. In all figures, the error bars represent the standard errors of the means. The ANOVA and principal component analyses (PCAs) were conducted in the R statistical software v4.3.2 (R Core Team, 2022). A three-way ANOVA was used with drought, Cd, and SA as factors with fixed effects. PCA was conducted on scaled and centered data using the factoextra library (Kassambara and Mundt, 2020) to explore the overall relationship between the traits and treatments.

3 Results

3.1 Leaf length

The growth of Caucasian wingnut exposed to drought or Cd stress as determined by measuring leaf length is shown in Figure 1 and morphology in Figure 2. Drought and Cd stresses resulted in significant reductions in leaf length in this study. Plants subjected to drought stress, Cd stress, and combined application of these stress factors decreased the leaf length by 26.5%, 26.9%, and 26.9%, respectively. Interestingly, under normal conditions, SA caused a 16.6% reduction in leaf length. However, exogenously applied SA caused significant increases in plant leaf length by 16.7% and 15.1%, respectively, under Cd stress (SA+Cd) and drought and Cd stresses combined (SA+Cd+D) as compared to non-SA-treated plants.

3.2 Relative water content

Drought stress alone and a combination of drought stress and Cd toxicity significantly ($p< 0.05$) reduced leaf RWC by 14% and 10.5%, respectively, compared to control plants (Figure 3A). Even though there was a reduction in RWC under stress conditions, it remained at 74% and 77% in D and Cd+D treatments, respectively. In contrast, no statistically significant effect of Cd stress was

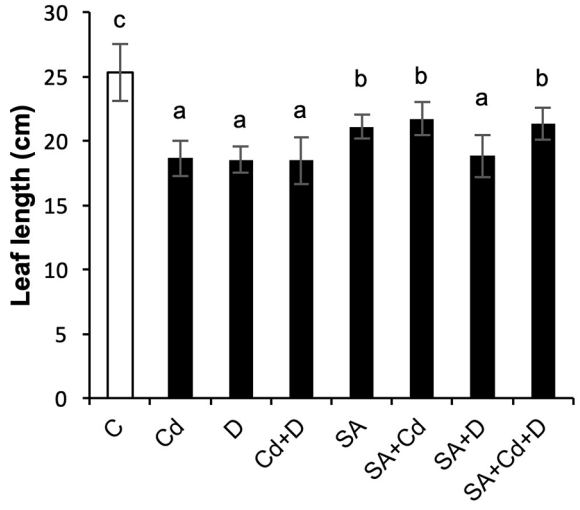

FIGURE 1
Effects of SA pretreatment on leaf length of *Pterocarya fraxinifolia* L. under drought, Cd, and the combination of these stress factors. Treatments: C, control; Cd, cadmium; D, drought; Cd+D, cadmium + drought; SA, salicylic acid pretreatment; SA+Cd, salicylic acid pretreatment + cadmium; SA+D, salicylic acid pretreatment + drought; SA+Cd+D, salicylic acid pretreatment + drought + cadmium. The bars (mean ± SD, n = 3) labeled with different letters are significantly different at $P < 0.05$ according to Duncan's multiple range test.

observed. Moreover, SA-treated control plants increased leaf RWC by 5.8% compared to non-treated control plants. In addition, RWC in SA-treated plants cultivated under drought and Cd stress treatments alone was respectively 4.7% and 12.2% higher than in non-treated plants subjected to the same stresses.

3.3 Osmotic potential

As expected, both single and combined applications of drought and Cd stresses significantly ($p< 0.05$) decreased leaf osmotic potential (Ψ_s, Figure 3B). In comparison to the control group plants, the most pronounced reduction of leaf Ψ_s (35.5%) was in plants subjected to drought stress. Cd toxicity and Cd+D reduced leaf Ψ_s by 9.03% and 26.8%, respectively. Similar to leaf length, the application of SA led to a decrease in Ψ_s of 9.7% compared to the control treatment. In contrast, SA significantly enhanced leaf Ψ_s by 2.1%, 12.8%, and 1.7% in plants exposed to Cd, D, and Cd+D stress, respectively.

3.4 Chlorophyll fluorescence

Changes in photosynthetic efficiency (Fv/Fm) of the plants depending on the effects of Cd stress, drought stress, and their combination are shown in Figure 3C. No significant ($p< 0.05$) changes in Fv/Fm were detected by the applications of Cd and Cd +D stress, whereas the application of drought stress alone reduced Fv/Fm by 9.6%, as compared to non-stress-treated plants. Similar to this trend, plants grown under Cd and Cd+D treatments did not exhibit significant changes in Fv/Fm after exogenous application of SA. However, SA increased Fv/Fm by 4.4% under drought stress alone.

3.5 Electrolyte leakage

As presented in Figure 4A, only drought alone significantly increased electrolyte leakage (by 15.6%) in comparison to controlled plants. In contrast, when comparing SA and non-SA treatments, the application of SA induced significant reductions in electrolyte leakage in D and Cd+D plants (22.8% and 20.5%, respectively).

3.6 Lipid peroxidation

Lipid peroxidation, which is evaluated from TBARS levels, increased by 26%, 48.9%, and 42.3% in Cd, D, and Cd+D treatments, respectively, compared to control plants (Figure 4B). The control plants did not exhibit any significant changes in TBARS content in response to SA pretreatment. Exogenous SA application displayed beneficial effects on lipid peroxidation and decreased TBARS levels by 11.9%, 16.3%, and 8% under Cd, D, and Cd+D treatments, respectively, as compared to non-stressed plants.

3.7 Hydrogen peroxide

As seen in Figure 4C, drought stress and the combination of drought and Cd stress treatment increased hydrogen peroxide (H_2O_2) levels by 41.5% and 37.2%, respectively, while a slight decrease in H_2O_2 (7.8%) was detected in Cd treatment compared to the control group of plants. There was no significant ($p< 0.05$) change in H_2O_2 after SA pretreatment. Contrary to TBARS, the exogenous application of SA increased H_2O_2 in all stress groups. Compared to non-SA-pretreated plants, the highest H_2O_2 accumulation (52.3%) was recorded in SA+Cd plants. Drought and combined stress also enhanced H_2O_2 levels by 15.9% and 13.9%, respectively, in comparison to the same group of plants subjected to SA.

3.8 Macro- and micronutrients

The effects of exogenous application of SA on macronutrient (P, K, Mg, and Ca) and micronutrient (Cu, Zn, Fe, and Mn) concentrations under stress conditions were investigated in the present study and are shown in Figures 5A–H. Drought stress, Cd stress, and their combination caused significant changes in the concentrations of macro- and micronutrients in Caucasian wingnut leaves. Under drought, among macronutrients, the highest accumulation was detected in K content (32.6%), and among micronutrients, in Mn content (60.9%), compared to control plants. Moreover, K, Ca, Fe, and Mn were enhanced in all stress treatments. P, Cu, and Zn displayed a slight decrease under Cd stress alone, while this reduction was recorded as 4.6% for Mg and 10.2% for Cu under Cd+D stress application when compared to non-stress-treated plants. Under non-stress conditions, exogenous SA

FIGURE 2
Effects of SA pretreatment on morphology of *Pterocarya fraxinifolia* L. under drought, Cd, and the combination of these stress factors. Treatments: C, control; Cd, cadmium; D, drought; Cd+D, cadmium + drought; SA, salicylic acid pretreatment; SA+Cd, salicylic acid pretreatment + cadmium; SA +D, salicylic acid pretreatment + drought; SA+Cd+D, salicylic acid pretreatment + drought + cadmium. Scale bar, 5 cm.

pretreatment increased P (73.2%), K (25.4%), Ca (30.5%), Mg (29.2%), Fe (14.5%), and Cu (2.3%), while it reduced Zn (1.6%) and Mn (8%). In addition, compared to non-SA-treated plants, SA application under stress tended to increase nutrient levels, although not at a high rate. Under Cd toxicity, P, K, Cu, and Zn increased by 48%, 14.4%, 4.7%, and 43.5%, respectively, with exogenous application of SA. However, Ca, Mg, Fe, and Mn decreased by 7.3%, 1.1%, 7.6%, and 15.4%, respectively, under the same conditions. Only the P level decreased by 7% with SA pretreatment under drought (SA+D) as compared to non-SA-treated plants.

3.9 Cadmium content

Cadmium stress alone and Cd + drought stress significantly increased Cd levels (64.2% and 58.6%, respectively) compared to control plants (Figure 5I). In addition, there was no Cd accumulation in non-Cd-treated plants. In contrast, foliar SA application decreased Cd level by 26.1% and 4.2% in Cd and Cd+D treatments, respectively, when compared to non-SA-treated groups.

3.10 Antioxidant defense system

As presented in Figure 6, Cd stress alone significantly decreased POX, CAT, APX, and GR activities by 16.7%, 41.7%, 50%, and 45.6%, respectively, while increasing SOD activity by 26.8%. Similarly, the combination of Cd and drought stress (Cd+D) lowered the same enzyme activities, whereas CAT activity rose by 21.2%. These reductions were detected as 19%, 33.3%, 21.2%, and 68.4%, respectively, under the combination of Cd and drought stress. Drought alone caused a significant ($p< 0.05$) increase in SOD

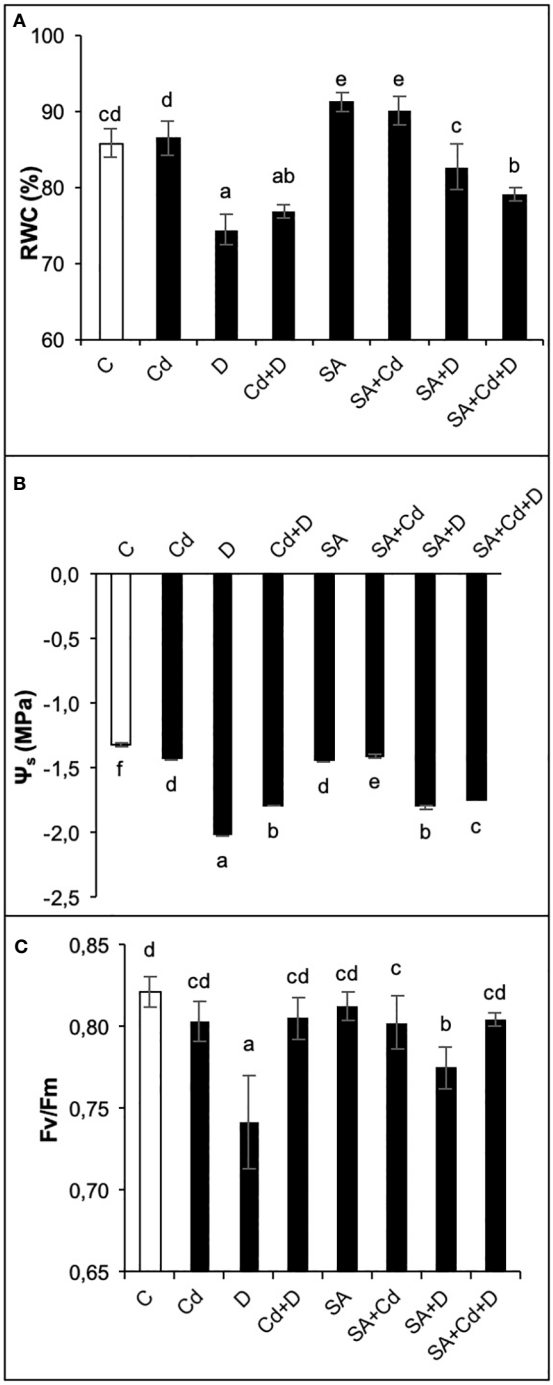

FIGURE 3
Effects of SA pretreatment on relative water content (RWC; **A**), osmotic potential (Ψ_s; **B**), and chlorophyll fluorescence (Fv/Fm; **C**) of *Pterocarya fraxinifolia* L. under drought, Cd, and the combination of these stress factors. Treatments: C, control; Cd, cadmium; D, drought; Cd+D, cadmium + drought; SA, salicylic acid pretreatment; SA+Cd, salicylic acid pretreatment + cadmium; SA+D, salicylic acid pretreatment + drought; SA+Cd+D, salicylic acid pretreatment + drought + cadmium. The bars (mean ± SD, n = 3) labeled with different letters are significantly different at $P < 0.05$ according to Duncan's multiple range test.

(41.6%), POX (9.5%), and APX (42.1%) activities and decreased both CAT (58.3%) and GR (36.8%) activities as compared to non-stress-treated plants. Moreover, the activities of these enzymes, except CAT, were enhanced further after exogenous SA pretreatment in control groups. The CAT activity of Caucasian wingnut leaves was decreased by 50% with SA application as compared to control plants. Among the measured enzymes, a significant increase in GR activity was noted with the exogenous application of SA under all stress treatments. Cd stress, drought stress, and the stress combination enhanced GR activity by 48.4%, 44.4%, and 4.3 times, respectively, in plants pretreated with SA. In addition, drought and Cd alone did not cause a significant ($p< 0.05$) change in CAT activity with exogenous SA treatment, whereas a 50% reduction was recorded in SA+Cd+D plants. Furthermore, POX activity was reduced with Cd stress, drought stress, and their combination by 14.3%, 47.8%, and 52.9%, respectively, after SA pretreatment.

3.11 Principal component analysis

PCA was employed to study the variation in physiological and biochemical parameters obtained from the control seedlings and those treated with SA and Cd stress, drought stress, and their combination (Figure 7). The PCA extracted from the data measured in the current study (Figures 1, 3–6) explained 55.7% of the total variance, where PC1 accounted for 34.2% of the variance and PC2 for only 21.5%. The analysis indicated that the macronutrients (K, Mg, and Ca) and micronutrients (Cu, Zn, Fe, and Mn), SOD activity, TBARS, H_2O_2 level, and Cd content of the Caucasian wingnut leaves were positively and significantly correlated ($p< 0.01$ or $p< 0.05$). SOD, H_2O_2, Cd, K, Ca, Cu, and Fe correlated strongly with the pretreatment of SA under drought stress alone (SA+D) and the combination of Cd and drought stress (SA+Cd+D) in the upper quadrant, but all other parameters (TBARS, Zn, and Mn) were grouped with the drought and Cd+D treatments in the right lower quadrant. Control, Cd alone, SA, and SA+Cd treatments and leaf length, RWC, osmotic potential, Fv/Fm, CAT, POX, APX, and EL were determined in the left upper and lower quadrants, with negative scores determined. These parameters were significantly ($p< 0.01$ or $p< 0.05$) negatively correlated.

4 Discussion

In the face of climate change, understanding how plants respond to more than one stress factor is critical, especially for woody plants, for developing strategies to maintain survival. Drought stress and Cd toxicity have detrimental effects on growth, membrane stability, and photosynthesis and cause osmotic and oxidative stresses (Hasanuzzaman et al., 2020; Iqbal et al., 2022; Zhang et al., 2023a). As a result of overproduction of ROS under these conditions, plants boost the antioxidant defense system with the activation of SOD, POX, CAT, APX, GR, ascorbic acid, glutathione, and secondary metabolites (Hasanuzzaman et al., 2020). Previous studies of the genus *Pterocarya* have investigated its growth performance, photosynthesis, physiological responses, and transcriptional changes in response to flooding and drought stress (Xu et al., 2015; Yang and Li, 2016; Li et al., 2021; Zhang et al., 2023b). However, to the best of our knowledge, no study to date has

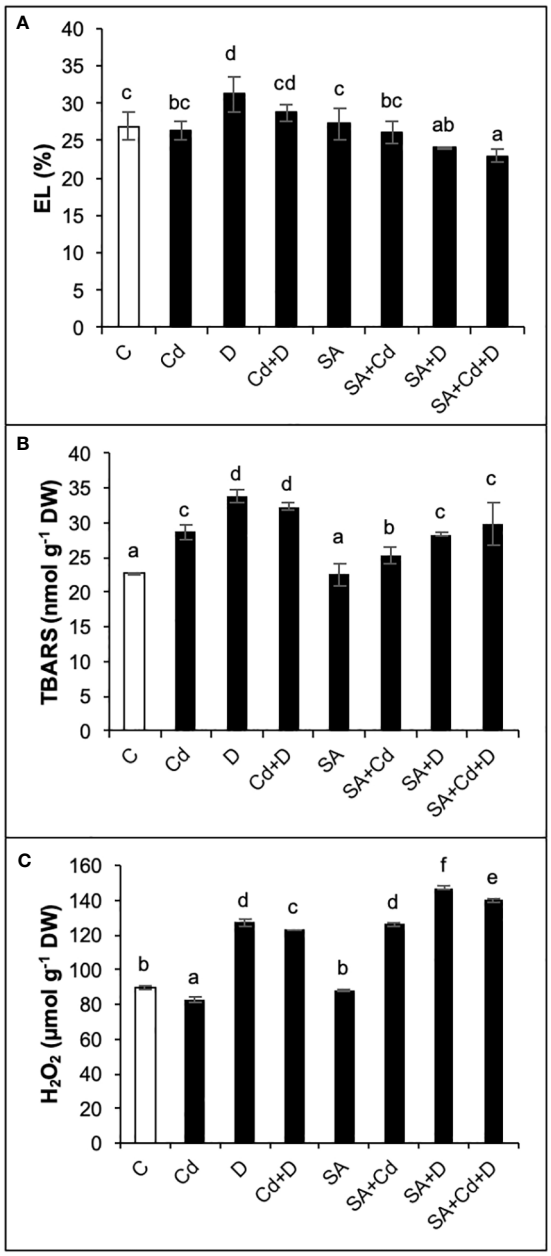

FIGURE 4
Effects of SA pretreatment on electrolyte leakage (EL; **A**), lipid peroxidation (TBARS; **B**), and hydrogen peroxide (H_2O_2; **C**) of *Pterocarya fraxinifolia* L. under drought, Cd, and the combination of these stress factors. Treatments: C, control; Cd, cadmium; D, drought; Cd+D, cadmium + drought; SA, salicylic acid pretreatment; SA+Cd, salicylic acid pretreatment + cadmium; SA+D, salicylic acid pretreatment + drought; SA+Cd+D, salicylic acid pretreatment + drought + cadmium. The bars (mean ± SD, n = 3) labeled with different letters are significantly different at $P < 0.05$ according to Duncan's multiple range test.

been conducted on the ROS regulation and antioxidant defense system of the *P. fraxinifolia* species under drought stress and Cd toxicity. Moreover, in the present study, we found that drought alone caused remarkably harmful effects on Caucasian wingnut plants compared to Cd treatment. This finding probably supports the finding of tolerance to the Cd presence of this woody species.

SA is a potential phytohormone that helps regulate plant growth and development by initiating various physiological and metabolic processes (Ding and Ding, 2020; Kaya et al., 2023). It additionally stimulates the overall antioxidant defense system at both enzymatic and non-enzymatic levels, which helps to remove excessive free radicals and alleviate the adverse impacts of abiotic stress factors (Liu et al., 2022; Kaya et al., 2023). Additionally, numerous studies have indicated that exogenous application of SA acts as a scavenger and enhances plant tolerance to drought stress and Cd toxicity by modulating the antioxidative enzymes (Guo et al., 2019; González-Villagra et al., 2022). In the present study, the function of exogenously applied SA in the regulation of growth, water content, chlorophyll fluorescence, mineral nutrients, lipid peroxidation, membrane integrity, and antioxidant enzymes under Cd stress, drought stress, and the combination of these stressors is elucidated.

In the current study, drought stress, Cd stress, and the combination of these stress factors caused a significant reduction of Caucasian wingnut leaf growth and water content. All stress treatments negatively affected leaf length, RWC, and Ψ_s, with the most pronounced reduction observed in the drought treatment. This is in accordance with previous studies, which reported a significant decrease in plant growth and water content under drought stress, Cd stress, or their combination (Bauddh and Singh, 2012; Adrees et al., 2020; González-Villagra et al., 2022). Similar to this reaction, exogenous SA-treated Caucasian wingnut plants displayed better protection in growth and water content. Exogenous SA application had a beneficial effect by improving the leaf length, RWC, and Ψ_s in terms of the single and combined treatments of Cd and drought stress, which is in agreement with prior research conducted by Iqbal et al. (2022). When plants face drought or Cd stress, osmoregulation is achieved by the production of osmolytes such as amino acids, mainly proline, soluble sugars, and organic acids (Sharma et al., 2019). In addition, Zhang et al. (2023a) reported increased proline accumulation under the combination of drought and Cd stresses in subtropical coastal tree species. SA-mediated osmolyte synthesis may be the result of osmoprotection in which the Caucasian wingnut increases resistance under Cd stress, drought stress, and their combination.

Fv/Fm is one of the chlorophyll fluorescence parameters, representing the maximum quantum yield of PSII photochemistry. To understand the adaptation of plants to various environmental stressors, Fv/Fm can be used as an indicator of plant health (Force et al., 2003). Chlorophyll fluorescence content significantly decreased in Caucasian wingnut plants subjected to drought stress alone. Moreover, the Fv/Fm level remained above 0.803 and 0.805 in Cd- and Cd+D-treated plants, respectively, indicating that the PSII photosynthetic efficiency was well-protected under both stresses. Similar findings regarding drought-induced decreases in Fv/Fm have also been observed in *Acer* genotypes (Banks, 2018) and *Coffea arabica* (de Souza et al., 2020). The decrease in Fv/Fm under drought stress can be associated with damage to the thylakoid membranes and chlorophyll degradation. ROS accumulation and increments in SOD, POX, and APX activities recorded in the current study may be the result of decreased Fv/Fm when plants were exposed to drought stress. Similar to non-SA-treated drought-stressed plants,

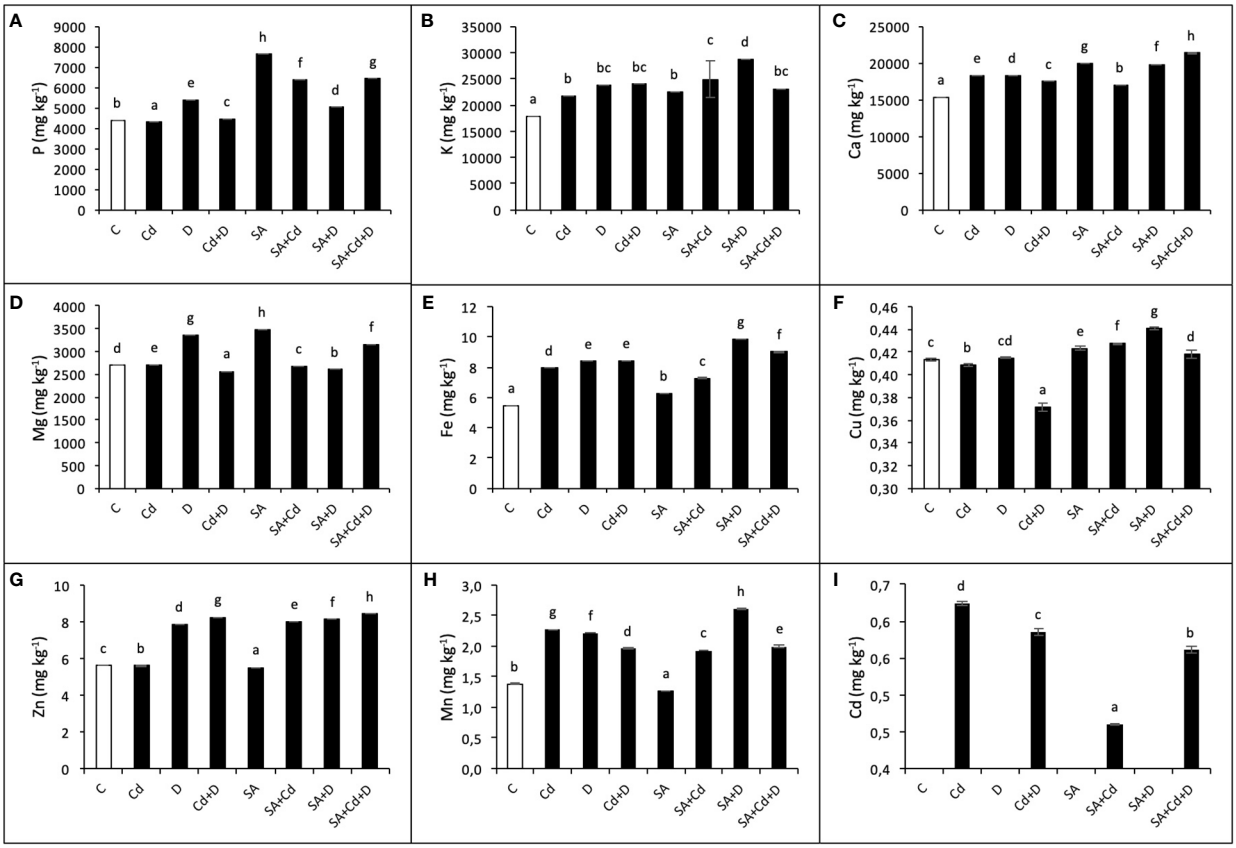

FIGURE 5
Effects of SA pretreatment on P **(A)**, K **(B)**, Ca **(C)**, Mg **(D)**, Fe **(E)**, Cu **(F)**, Zn **(G)**, Mn **(H)**, and Cd **(I)** of *Pterocarya fraxinifolia* L. under drought, Cd, and the combination of these stress factors. Treatments: C, control; Cd, cadmium; D, drought; Cd+D, cadmium + drought; SA, salicylic acid pretreatment; SA+Cd, salicylic acid pretreatment + cadmium; SA+D, salicylic acid pretreatment + drought; SA+Cd+D, salicylic acid pretreatment + drought + cadmium. The bars (mean ± SD, n = 3) labeled with different letters are significantly different at $P < 0.05$ according to Duncan's multiple range test.

exogenous SA application altered Fv/Fm in our study. It has been observed that SA treatment in *Raphanus sativus* (Henschel et al., 2022) and *Zea mays* (Xin et al., 2023) can increase Fv/Fm under drought stress. Moreover, it has also been reported that exogenously applied SA also increases photosynthetic efficiency with a photoprotective effect (Moustakas et al., 2022).

A high accumulation of TBARS and H_2O_2 accompanied by an increase in EL under stress conditions triggers oxidative damage in cells due to their high capacity to move between biological membranes and thus disrupt the stability of the plasma membrane (Bienert et al., 2006). In the current study, Caucasian wingnut leaf H_2O_2 levels, peroxidation of membrane lipids, and electrolyte leakage increased under Cd stress, drought stress, and their combination (Abbas et al., 2018; Kabała et al., 2019; Adrees et al., 2020; Kaya and Shabala, 2024), indicating an increase in oxidative stress in drought- and Cd-treated plants. Interestingly, in this study, Cd toxicity alone did not significantly change the EL level, whereas TBARS content increased. In addition, H_2O_2 levels also decreased in Cd-treated Caucasian wingnut leaves. This result correlating with unchanged RWC and Fv/Fm may be associated with reduced ROS production under these conditions. This may have been a result of tolerance to Cd by this woody species. In addition, in this study, lipid peroxidation under Cd stress was not greater than that under drought stress alone or in combination. These results suggest that the detrimental effect of stress combination on membrane lipids was greater than that of Cd stress alone, but not that of drought alone. In our study, TBARS content and EL were alleviated by foliar application of SA at a level even less than the control level. Similar conclusions have been reported in research on *Solanum tuberosum* (Li et al., 2019), *Brassica juncea* (Iqbal et al., 2022), and *A. chilensis* (González-Villagra et al., 2022). The results displayed that TBARS and EL were suppressed by exogenous SA pretreatment under Cd and drought stresses. Meanwhile, a higher accumulation of H_2O_2 was detected with SA application under these stress conditions. H_2O_2, as a potent signaling molecule, has a dual role in plants in the regulation of plant growth, metabolism, and stress tolerance (Anjum et al., 2022). Also, it has been reported that abscisic acid-induced H_2O_2 accumulation enhances antioxidant capacity against $Ca(NO_3)_2$ stress (Shu et al., 2016). The increment in H_2O_2 content accompanied by unchanged EL under SA-pretreated Cd stress suggests that SA/H_2O_2 induces ROS-scavenging machinery and activates antioxidant defense in Caucasian wingnut.

As a result of drought stress and Cd toxicity, nutrient imbalance occurred, causing an increased concentration of P, K, Mg, and Ca in

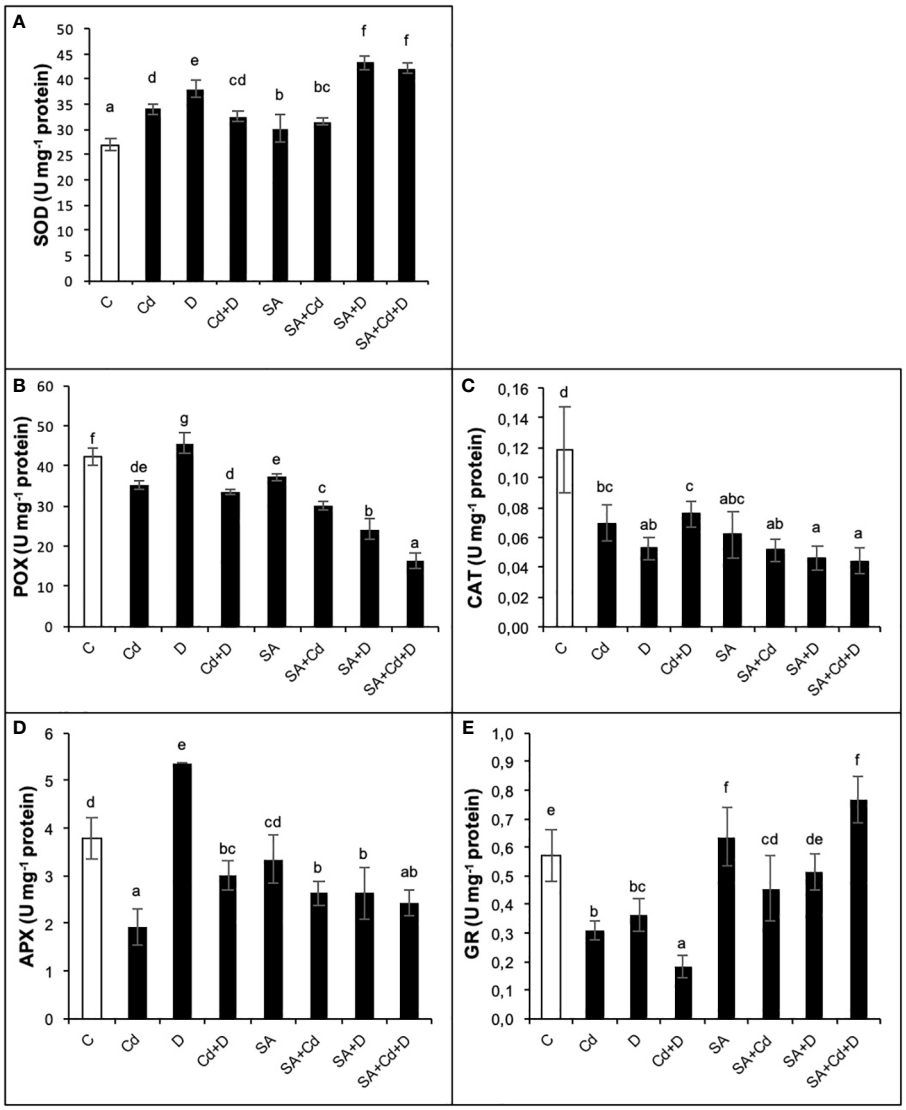

FIGURE 6
Effects of SA pretreatment on SOD **(A)**, POX **(B)**, CAT **(C)**, APX **(D)**, and GR **(E)** activities of *Pterocarya fraxinifolia* L. under drought, Cd, and the combination of these stress factors. Treatments: C, control; Cd, cadmium; D, drought; Cd+D, cadmium + drought; SA, salicylic acid pretreatment; SA+Cd, salicylic acid pretreatment + cadmium; SA+D, salicylic acid pretreatment + drought; SA+Cd+D, salicylic acid pretreatment + drought + cadmium. The bars (mean ± SD, n = 3) labeled with different letters are significantly different at $P < 0.05$ according to Duncan's multiple range test.

all the treatments (except P in Cd-stressed plants). Among micronutrients, Cu content was negatively affected by drought and Cd stress application. In contrast, Fe, Zn, and Mn tended to increase with stress conditions in Caucasian wingnut leaves. There are several studies in the literature that have similar or opposite findings to ours, for instance, studies on *Pfaffia glomerata* (Gomes et al., 2013), *Morus alba* (Guo et al., 2021), and *Brassica napus* (Dikšaitytė et al., 2023) under Cd stress and *Fagus sylvatica* (Peuke and Rennenberg, 2011) and *Ricinus communis* (Tadayyon et al., 2018) under drought stress. The results for mineral nutrient content in plants under stress conditions are contradictory due to the fact that the effects are highly dependent on plant species and experimental conditions (Mourato et al., 2019). In contrast, foliar application of SA showed a positive effect on the distribution of macro- and micronutrients in Caucasian wingnut, particularly at the Cd level under Cd stress alone and Cd+D treatments. Similar to our findings, SA pretreatment lowered Cd content in *Z. mays* (Gondor et al., 2016) and *Oryza sativa* (Wang et al., 2021).

Upregulation of the oxidative defense system is a key strategy in combating Cd or drought stress in plants (Hasanuzzaman et al., 2020). In this defense mechanism, APX, CAT, GR, POX, and SOD all fulfill specific roles, and the resulting reactions influence the homeostasis of ROS within the plant's cells. This, in turn, affects the tolerance of plants to stressful conditions. SOD is known to catalyze the dismutation of toxic superoxide by converting it into H_2O_2 and oxygen. In addition, POX and CAT, located in the cytoplasm, and APX and GR, located in the chloroplasts, act to detoxify the H_2O_2 in plant cells (Liu et al., 2006). In this study, SOD activity increased in Caucasian wingnut in response to the combination of drought and Cd stresses. Similar conclusions have been reported in research on

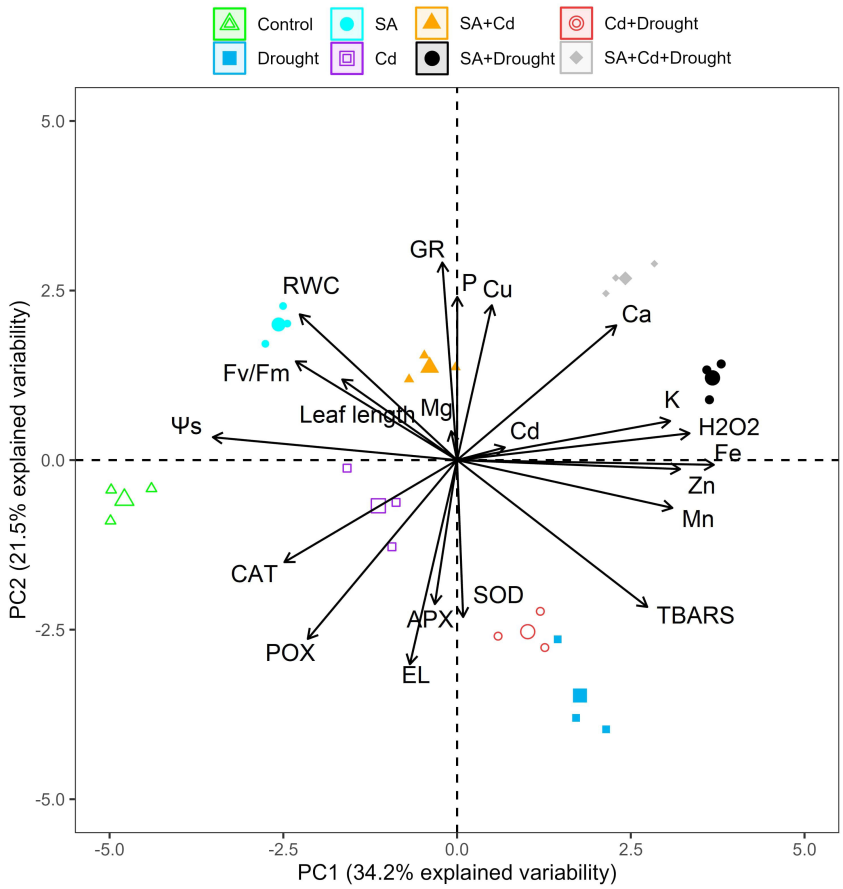

FIGURE 7
PCA bi-plots in the leaves of *Pterocarya fraxinifolia* L. under drought, Cd, and the combination of these stress factors. PCA, principal component analysis.

Pisum sativum under Cd stress (El-Amier et al., 2019), *Syzygium cumini* under water deficit (Zafar et al., 2021), *R. sativus* under cadmium and drought stress (Tuver et al., 2022), and *A. chilensis* under drought stress (González-Villagra et al., 2022). In the current study, we compared the effects of Cd and drought stress, both alone and in a combination of these two stress factors. In terms of antioxidant defense, Cd and Cd+D stress applications act similarly on the behavior of enzyme activities. POX, CAT, APX, and GR activities decreased with Cd treatments in Caucasian wingnut in this study. However, in spite of the decrease in those enzyme activities, leaf RWC, chlorophyll fluorescence content, and electrolyte leakage were maintained, and less reduction of osmotic potential and H_2O_2 was determined in this species under Cd toxicity compared to drought stress. To regulate this defense process, the activity of other enzymatic or non-enzymatic antioxidants may have been increased. Furthermore, variations in antioxidant enzyme activity may vary according to the extent of abiotic stress factors, the duration of exposure, and the developmental stage of the plants (Hasanuzzaman et al., 2020). In contrast, SA acted as a signaling molecule in this study, and foliar SA application improved the leaf antioxidant defense system and significantly increased GR activity compared to non-SA treatment in Caucasian wingnut subjected to cadmium stress, drought stress, and their combination. Similar to our findings, it was found that exogenous application of SA can help improve stress tolerance in *S. cumini* (Zafar et al., 2021) and *A. chilensis* (González-Villagra et al., 2022) under drought stress and *Cucumis melo* (Zhang et al., 2015) and *S. tuberosum* (Li et al., 2019) under Cd stress. These findings suggest that the foliar application of SA may help plants adapt to drought stress and Cd toxicity and may improve their ability to withstand the combined application of stress. Moreover, in previous studies, CAT activity was reported as inhibited with SA application (Klessig et al., 2000; Larkindale and Huang, 2004). These reports confirm the current results that the effect that SA application did not change CAT activity when Cd and drought stresses were applied alone, while it decreased CAT activity when Cd and drought stresses were applied in combination. From the findings of the study, we can conclude that drought stress alone negatively affected Caucasian wingnut when compared to drought stress applied in combination with Cd stress. Contrary to the results in most literature, cadmium stress application was not as detrimental as drought stress application. Additionally, here, we have presented a summary of the adaptive mechanisms demonstrated by the Caucasian wingnut in response to Cd toxicity, drought stress, and their combination with the exogenous application of SA. Regarding Caucasian wingnut, further studies are warranted in the future to

better understand the effects of Cd toxicity on physiological and biochemical relations in the improvement of survival and phytoremediation potential of this woody species.

5 Conclusion

The research was conducted with the aim of evaluating the role of exogenous salicylic acid in increasing the tolerance of *P. fraxinifolia* L. toward cadmium toxicity, drought stress, and their combination through the observation of physiological traits and biochemical pathways, particularly the antioxidant defense system. Our study demonstrates that SA treatment can stimulate the antioxidant defense system; reduce lipid peroxidation, electrolyte leakage, and cadmium content; enhance leaf length, osmotic potential, relative water content, and hydrogen peroxide; and upregulate macro- and micronutrients in Caucasian wingnut plants grown under cadmium stress, drought stress, and the combination of these two stressors. The tolerance of Caucasian wingnut to cadmium seems to be high, suggesting that this plant may be a possible Cd accumulator. However, the amount of Cd concentration in other vegetative organs requires measurement, and further investigation is needed.

Data availability statement

The raw data supporting the conclusions of this article will be made available by the authors, without undue reservation.

Author contributions

HT: Conceptualization, Data curation, Investigation, Writing – original draft, Writing – review & editing, Formal analysis, Methodology. BC: Formal analysis, Methodology, Writing – review & editing. SS: Data curation, Methodology, Writing – review & editing. PP: Data curation, Methodology, Writing – review & editing.

Funding

The author(s) declare financial support was received for the research, authorship, and/or publication of this article. The Research Fund of Düzce University (Project No: DÜBAP-2022.11.01.1320) provided financial support for this research.

Acknowledgments

The authors thank the reviewers for their invaluable contributions that improved the manuscript.

Conflict of interest

The authors declare that the research was conducted in the absence of any commercial or financial relationships that could be construed as a potential conflict of interest.

Publisher's note

All claims expressed in this article are solely those of the authors and do not necessarily represent those of their affiliated organizations, or those of the publisher, the editors and the reviewers. Any product that may be evaluated in this article, or claim that may be made by its manufacturer, is not guaranteed or endorsed by the publisher.

Supplementary material

The Supplementary Material for this article can be found online at: https://www.frontiersin.org/articles/10.3389/fpls.2023.1339201/full#supplementary-material

References

Abbas, T., Rizwan, M., Ali, S., Adrees, M., Mahmood, A., Zia-ur-Rehman, M., et al. (2018). Biochar application increased the growth and yield and reduced cadmium in drought stressed wheat grown in an aged contaminated soil. *Ecotoxicol. Environ. Saf.* 148, 825–833. doi: 10.1016/j.ecoenv.2017.11.063

Adrees, M., Khan, Z. S., Ali, S., Hafeez, M., Khalid, S., Ur Rehman, M. Z., et al. (2020). Simultaneous mitigation of cadmium and drought stress in wheat by soil application of iron nanoparticles. *Chemosphere* 238, 124681. doi: 10.1016/j.chemosphere.2019.124681

Aebi, H. (1984). "Catalase in vitro," in *Methods in Enzymology*, vol. 105. (Orlando: Academic Press), 121–126. doi: 10.1016/S0076-6879(84)05016-3

Akhbari, M., Tavakoli, S., and Delnavazi, M. R. (2014). Volatile fraction composition and biological activities of the leaves, bark and fruits of Caucasian wingnut from Iran. *J. Essent. Oil Res.* 26 (1), 58–64. doi: 10.1080/10412905.2013.828324

Anjum, N. A., Gill, S. S., Corpas, F. J., Ortega-Villasante, C., Hernandez, L. E., Tuteja, N., et al. (2022). Editorial: Recent insights into the double role of hydrogen peroxide in plants. *Front. Plant Sci.* 13. doi: 10.3389/fpls.2022.843274

Banks, J. M. (2018). Chlorophyll fluorescence as a tool to identify drought stress in Acer genotypes. *Environ. Exp. Bot.* 155, 118–127. doi: 10.1016/j.envexpbot.2018.06.022

Bauddh, K., and Singh, R. P. (2012). Growth, tolerance efficiency and phytoremediation potential of *Ricinus communis* (L.) and *Brassica juncea* (L.) in salinity and drought affected cadmium contaminated soil. *Ecotoxicol. Environ. Saf.* 85, 13–22. doi: 10.1016/j.ecoenv.2012.08.019

Beauchamp, C., and Fridovich, I. (1971). Superoxide dismutase: improved assays and an assay applicable to acrylamide gels. *Anal. Biochem.* 44, 276–287. doi: 10.1016/0003-2697(71)90370-8

Bienert, G. P., Møller, A. L. B., Krsitiansen, K. A., Schulz, A., Møller, I. M., Schjoerring, J. K., et al. (2006). Specific aquaporins facilitate the diffusion of hydrogen peroxide across membranes. *J. Biol. Chem.* 282, 1183–1192. doi: 10.1074/jbc.M603761200

Bradford, M. M. (1976). A rapid and sensitive method for the quantization of microgram quantities of protein utilizing the principle of the protein-dye binding. *Anal. Biochem.* 72, 248–254. doi: 10.1006/abio.1976.9999

de Souza, B. P., Martinez, H. E. P., de Carvalho, F. P., Loureiro, M. E., and Sturião, W. P. (2020). Gas exchanges and chlorophyll fluorescence of young coffee plants submitted to water and nitrogen stresses. *J. Plant Nutr.* 43 (16), 2455–2465. doi: 10.1080/01904167.2020.1771589

Dikšaitytė, A., Kniuipytė, I., and Žaltauskaitė, J. (2023). Drought-free future climate conditions enhance cadmium phytoremediation capacity by Brassica napus through improved physiological status. *J. Hazard. Mater.* 452, 131181. doi: 10.1016/j.jhazmat.2023.131181

Ding, P., and Ding, Y. (2020). Stories of salicylic acid: A plant defense hormone. *Trends Plant Sci.* 25 (6), 549–565. doi: 10.1016/j.tplants.2020.01.004

El-Amier, Y., Elhindi, K., El-Hendawy, S., Al-Rashed, S., and Abd-ElGawad, A. (2019). Antioxidant system and biomolecules alteration in *Pisum sativum* under heavy metal stress and possible alleviation by 5-aminolevulinic acid. *Molecules* 24, 4194. doi: 10.3390/molecules24224194

Force, L., Critchley, C., and van Rensen, J. J. (2003). New fluorescence parameters for monitoring photosynthesis in plants. *Photosynth. Res.* 78, 17–33. doi: 10.1023/A:1026012116709

Foyer, C. H., and Halliwell, B. (1976). The presence of glutathione and glutathione reductase in chloroplasts: a proposed role in ascorbic acid metabolism. *Planta* 133, 21–25. doi: 10.1007/BF00386001

Gomes, M., Teresa, M., and Angela, S. (2013). Cadmium effects on mineral nutrition of the Cd-hyperaccumulator *Pfaffia glomerata*. *Biologia* 68, 223–230. doi: 10.2478/s11756-013-0005-9

Gondor, O. K., Pál, M., Darkó, É., Janda, T., and Szalai, G. (2016). Salicylic acid and sodium salicylate alleviate cadmium toxicity to different extents in maize (*Zea mays* L.). *PloS One* 11, e0160157. doi: 10.1371/journal.pone.0160157

González-Villagra, J., Reyes-Díaz, M. M., Tighe-Neira, R., Inostroza-Blancheteau, C., Escobar, A. L., and Bravo, L. A. (2022). Salicylic acid improves antioxidant defense system and photosynthetic performance in *Aristotelia Chilensis* plants subjected to moderate drought stress. *Plants* 11, 639. doi: 10.3390/plants11050639

Guo, B., Liu, C., Liang, Y., Li, N., and Fu, Q. (2019). Salicylic acid signals plant defence against cadmium toxicity. *Int. J. Mol. Sci.* 20 (12), 2960. doi: 10.3390/ijms20122960

Guo, Z., Zeng, P., Xiao, X., and Peng, C. (2021). Physiological, anatomical, and transcriptional responses of mulberry (*Morus alba* L.) to Cd stress in contaminated soil. *Environ. pollut.* 284, 117387. doi: 10.1016/j.envpol.2021.117387

Hasanuzzaman, M., Bhuyan, M. H. M. B., Zulfiqar, F., Raza, A., Mohsin, S. M., Mahmud, J. A., et al. (2020). Reactive oxygen species and antioxidant defense in plants under abiotic stress: revisiting the crucial role of a universal defense regulator. *Antioxidants* 9, 681. doi: 10.3390/antiox9080681

Heath, R. L., and Packer, L. (1968). Photoperoxidation in isolated chloroplasts, I. kinetics and stoichiometry of fatty acid peroxidation. *Arch. Biochem. Biophys.* 125, 189–198. doi: 10.1016/0003-9861(68)90654-1

Henschel, J. M., Dantas, E. F. O., Soares, V. A., Santos, S. K. D., Santos, L. W. O. D., Dias, T. J., et al. (2022). Salicylic acid mitigates the effects of mild drought stress on radish (*Raphanus sativus*) growth. *Funct. Plant Biol.* 49 (9), 822–831. doi: 10.1071/FP22040

Ilyas, M., Nisar, M., Khan, N., Hazat, A., Khan, A. H., Hayat, K., et al. (2021). Drought tolerance strategies in plants: a mechanistic approach. *J. Plant Growth Regul.* 40, 926–944. doi: 10.1007/s00344-020-10174-5

Iqbal, N., Fatma, M., Gautam, H., Sehar, Z., Rasheed, F., Khan, M. I. R., et al. (2022). Salicylic acid increases photosynthesis of drought grown mustard plants effectively with sufficient-N via regulation of ethylene, abscisic acid, and nitrogen-use efficiency. *J. Plant Growth Regul.* 41, 1966–1977. doi: 10.1007/s00344-021-10565-2

Kabała, K., Zboińska, M., Głowiak, D., Reda, M., Jakubowska, D., and Janicka, M. (2019). Interaction between the signaling molecules hydrogen sulfide and hydrogen peroxide and their role in vacuolar H^+-ATPase regulation in cadmium-stressed cucumber roots. *Physiol. Plant* 166, 688–704. doi: 10.1111/ppl.12819

Kassambara, A., and Mundt, F. (2020) *Factoextra: Extract and Visualize the Results of Multivariate Data Analyses*. Available at: https://CRAN.R-project.org/package=factoextra (Accessed 2023-12-14).

Kaya, C., and Shabala, S. (2024). Melatonin improves drought stress tolerance of pepper (*Capsicum annuum*) plants via upregulating nitrogen metabolism. *Funct. Plant Biol.* 51, FP23060. doi: 10.1071/FP23060

Kaya, C., Ugurlar, F., Ashraf, M., and Ahmad, P. (2023). Salicylic acid interacts with other plant growth regulators and signal molecules in response to stressful environments in plants. *Plant Physiol. Biochem.* 196, 431–443. doi: 10.1016/j.plaphy.2023.02.006

Kerchev, P. I., and Van Breusegem, F. (2022). Improving oxidative stress resilience in plants. *Plant J.* 109 (2), 359–372. doi: 10.1111/tpj.15493

Klessig, D. F., Durner, J., Noad, R., Navarre, D. A., Wendehenne, D., Kumar, D., et al. (2000). Nitric oxide and salicylic acid signaling in plant defense. *Proc. Natl. Acad. Sci. U.S.A.* 97, 8849–8855. doi: 10.1073/pnas.97.16.8849

Kutbay, H. G., Merev, N., and Ok, T. (1999). Anatomical, phytosociological and ecological properties of *Pterocarya fraxinifolia* (Poiret). *Turk. J. Agric. For.* 23, 1189–1196.

Larkindale, J., and Huang, B. (2004). Thermotolerance and antioxidant system in *Agrostis stolonifera*: involvement of SA, abscisic acid, Ca, H_2O_2 and ethylene. *J. Plant Physiol.* 161, 405–413. doi: 10.1078/0176-1617-01239

Lefevere, H., Bauters, L., and Gheysen, G. (2020). Salicylic acid biosynthesis in plants. *Front. Plant Sci.* 11. doi: 10.3389/fpls.2020.00338

Li, X., Chang, C., and Pei, Z.-M. (2023). Reactive oxygen species in drought-induced stomatal closure: the potential roles of NPR1. *Plants* 12, 3194. doi: 10.3390/plants12183194

Li, Y., Shi, L. C., Yang, J., Qian, Z. H., He, Y. X., and Li, M. W. (2021). Physiological and transcriptional changes provide insights into the effect of root waterlogging on the aboveground part of *Pterocarya stenoptera*. *Genomics* 113 (4), 2583–2590. doi: 10.1016/j.ygeno.2021.06.005

Li, Q., Wang, G., Wang, Y., Yang, D., Guan, C., and Ji, J. (2019). Foliar application of salicylic acid alleviate the cadmium toxicity by modulation the reactive oxygen species in potato. *Ecotox. Environ. Saf.* 172, 317–325. doi: 10.1016/j.ecoenv.2019.01.078

Liu, H. T., Liu, Y. Y., Pan, Q. H., Yang, H. R., Zhan, J. C., and Huang, W. D. (2006). Novel interrelationship between salicylic acid, abscisic acid and PIP2-specific-phospholipase C in heat acclimation-induced thermotolerance in pea leaves. *J. Exp. Bot.* 57, 3337–3347. doi: 10.1093/jxb/erl098

Liu, J., Lu, B., and Xun, A. L. (2000). An improved method for the determination of hydrogen peroxide in leaves. *Prog. Biochem. Biophys.* 27, 548–551.

Liu, J., Qiu, G., Liu, C., Li, H., Chen, X., Fu, Q., et al. (2022). Salicylic acid, a multifaceted hormone, combats abiotic stresses in plants. *Life (Basel)* 12 (6), 886. doi: 10.3390/life12060886

Lutts, S., Kinet, J. M., and Bouharmont, J. (1996). NaCl-induced senescence in leaves of rice (*Oryza sativa* L.) cultivars differing in salinity resistance. *Ann. Bot.* 78, 389–398. doi: 10.1006/anbo.1996.0134

Mika, A., and Luthje, S. (2003). Properties of guaiacol peroxidase activities isolated from corn € root plasma membranes. *Plant Physiol.* 132, 1489–1498. doi: 10.1104/pp.103.020396

Mourato, M., Pinto, F., Moreira, I., Sales, J., Leitão, I., and Martins, L. L. (2019). "The effect of Cd stress in mineral nutrient uptake in plants," in *Cadmium Toxicity and Tolerance in Plants*. Eds. M. Hasanuzzaman, M. N. V. Prasad and M. Fujita (Cambridge, MA, USA: Academic Press), 327–348. doi: 10.1016/B978-0-12-814864-8.00013-9

Moustakas, M., Sperdouli, I., Adamakis, I. S., Moustaka, J., Isgoren, S., and Sas, B. (2022). Harnessing the role of foliar applied salicylic acid in decreasing chlorophyll content to reassess photosystem II photoprotection in crop plants. *Int. J. Mol. Sci.* 23 (13), 7038. doi: 10.3390/ijms23137038

Nakano, Y., and Asada, K. (1981). Hydrogen peroxide is scavenged by ascorbate specific peroxidase in spinach chloroplasts. *Plant Cell Physiol.* 22, 867–880. doi: 10.1093/oxfordjournals.pcp.a076232

Peuke, A. D., and Rennenberg, H. (2011). Impacts of drought on mineral macro- and microelements in provenances of beech (*Fagus sylvatica* L.) seedlings. *Tree Physiol.* 31, 196–207. doi: 10.1093/treephys/tpr007

Prodhan, M. Y., Munemasa, S., Nahar, M. N., Nakamura, Y., and Murata, Y. (2018). Guard cell salicylic acid signaling is integrated into abscisic acid signaling via the Ca^{2+}/CPK-dependent pathway. *Plant Physiol.* 178 (1), 441–450. doi: 10.1104/pp.18.00321

Saleem, M., Fariduddin, Q., and Castroverde, C. D. M. (2021). Salicylic acid: A key regulator of redox signalling and plant immunity. *Plant Physiol. Biochem.* 168, 381–397. doi: 10.1016/j.plaphy.2021.10.011

Santa-Cruz, A., Martinez-Rodriguez, M. M., Perez-Alfocea, F., Romero-Aranda, R., and Bolarin, M. C. (2002). The rootstock effect on the tomato salinity response depends on the shoot genotype. *Plant Sci.* 162, 825–831. doi: 10.1016/S0168-9452(02)00030-4

Santisree, P., Jalli, L. C. L., Bhatnagar-Mathur, P., and Sharma, K. K. (2020). "Emerging roles of salicylic acid and jasmonates in plant abiotic stress responses," in *Protective Chemical Agents in the Amelioration of Plant Abiotic Stress: Biochemical and Molecular Perspectives*. Eds. A. Roychoudhury and D. K. Tripathi (Wiley Online Library), 342–373. doi: 10.1002/9781119552154.ch17

Sharma, A., Shahzad, B., Kumar, V., Kohli, S. K., Sidhu, G. P. S., Bali, A. S., et al. (2019). Phytohormones regulate accumulation of osmolytes under abiotic stress. *Biomolecules* 9 (7), 285. doi: 10.3390/biom9070285

Sharma, A., Sidhu, G. P. S., Araniti, F., Bali, A. S., Shahzad, B., Tripathi, D. K., et al. (2020). The role of salicylic acid in plants exposed to heavy metals. *Molecules* 25 (3), 540. doi: 10.3390/molecules25030540

Shine, M. B., Yang, J., El-Habbak, M., Nagyabhyru, P., Fu, D., Navarre, D., et al. (2016). Cooperative functioning between phenylalanine ammonia lyase and isochorismate synthase activities contributes to salicylic acid biosynthesis in soybean. *New Phytol.* 212, 627–636. doi: 10.1111/nph.14078

Shu, S., Gao, P., Li, L., Yuan, Y., Sun, J., and Guo, S. (2016). Abscisic acid-induced H_2O_2 accumulation enhances antioxidant capacity in pumpkin-grafted cucumber leaves under $Ca(NO_3)_2$ stress. *Front. Plant Sci.* 7. doi: 10.3389/fpls.2016.01489

Singh, A., Kumar, A., Yadav, S., and Singh, I. K. (2019). Reactive oxygen species-mediated signaling during abiotic stress. *Plant Gene* 18, 100173. doi: 10.1016/j.plgene.2019.100173

Smart, R. E., and Bingham, G. E. (1974). Rapid estimates of relative water content. *Plant Physiol.* 53, 258–260. doi: 10.1104/pp.53.2.258

Song, W., Shao, H., Zheng, A., Zhao, L., and Xu, Y. (2023). Advances in roles of salicylic acid in plant tolerance responses to biotic and abiotic stresses. *Plants* 12, 3475. doi: 10.3390/plants12193475

Song, Y. G., Walas, Ł., Pietras, M., Sâm, H. V., Yousefzadeh, H., Ok, T., et al. (2021). Past, present and future suitable areas for the relict tree *Pterocarya fraxinifolia* (Juglandaceae): Integrating fossil records, niche modeling, and phylogeography for conservation. *Eur. J. Forest. Res.* 140, 1323–1339. doi: 10.1007/s10342-021-01397-6

Tadayyon, A., Nikneshan, P., and Pessarakli, M. (2018). Effects of drought stress on concentration of macro- and micro-nutrients in castor (*Ricinus communis* L.) plant. *J. Plant Nutr.* 41 (3), 304–310. doi: 10.1080/01904167.2017.1381126

Tavakoli, S., Delnavazi, M. R., and Yassa, N. (2016). Phytochemical and antimicrobial investigation of *Pterocarya fraxinifolia* leaves. *Chem. Nat. Compd.* 52, 101–103. doi: 10.1007/s10600-016-1558-y

Tripti,, Kumar, A., Maleva, M., Borisova, G., and Rajkumar, M. (2023). Amaranthus biochar-based microbial cell composites for alleviation of drought and cadmium stress: a novel bioremediation approach. *Plants* 12, 1973. doi: 10.3390/plants12101973

Tuver, G. Y., Ekinci, M., and Yildirim, E. (2022). Morphological, physiological and biochemical responses to combined cadmium and drought stress in radish (*Raphanus sativus* L.). *Rend. Fis. Acc. Lincei* 33, 419–429. doi: 10.1007/s12210-022-01062-z

Wang, F., Tan, H., Zhang, Y., Huang, L., Bao, H., Ding, Y., et al. (2021). Salicylic acid application alleviates cadmium accumulation in brown rice by modulating its shoot to grain translocation in rice. *Chemosphere* 63, 128034. doi: 10.1016/j.chemosphere.2020.128034

Wheal, M. S., and Palmer, L. T. (2010). Chloride analysis of botanical samples by ICP-OES. *J. Anal. At. Spectrom.* 25, 1946–1952. doi: 10.1039/C0JA00059K

Xia, S., Wang, X., Su, G., and Shi, G. (2015). Effects of drought on cadmium accumulation in peanuts grown in a contaminated calcareous soil. *Environ. Sci. pollut. Res. Int.* 22 (23), 18707–18717. doi: 10.1007/s11356-015-5063-9

Xin, L., Wang, J., and Yang, Q. (2023). Exogenous salicylic acid alleviates water deficit stress by protecting photosynthetic system in maize seedlings. *Agronomy* 13 (9), 2443. doi: 10.3390/agronomy13092443

Xu, L., Pan, Y., and Yu, F. (2015). Effects of water-stress on growth and physiological changes in *Pterocarya stenoptera* seedlings. *Sci. Hortic.* 190, 11–23. doi: 10.1016/j.scienta.2015.03.041

Yang, Y., and Li, C. (2016). Photosynthesis and growth adaptation of *Pterocarya stenoptera* and *Pinus elliottii* seedlings to submergence and drought. *Photosynthetica* 54, 120–129. doi: 10.1007/s11099-015-0171-9

Zafar, Z., Rasheed, F., Atif, R. M., Maqsood, M., and Gailing, O. (2021). Salicylic acid-induced morpho-physiological and biochemical changes triggered water deficit tolerance in *Syzygium cumini* L. saplings. *Forests* 12, 491. doi: 10.3390/f12040491

Zandalinas, S. I., Balfagón, D., Gómez-Cadenas, A., and Mittler, R. (2022). Plant responses to climate change: metabolic changes under combined abiotic stresses. *J. Exp. Bot.* 73 (11), 3339–3354. doi: 10.1093/jxb/erac073

Zandalinas, S. I., and Mittler, R. (2022). Plant responses to multifactorial stress combination. *New Phytol.* 234 (4), 1161–1167. doi: 10.1111/nph.18087

Zandalinas, S. I., Sengupta, S., Fritschi, F. B., Azad, R. K., Nechushtai, R., and Mittler, R. (2021). The impact of multifactorial stress combination on plant growth and survival. *New Phytol.* 230 (3), 1034–1048. doi: 10.1111/nph.17232

Zhang, S., Tan, X., Zhou, Y., and Liu, N. (2023a). Effects of a heavy metal (cadmium) on the responses of subtropical coastal tree species to drought stress. *Environ. Sci. pollut. Res. Int.* 30 (5), 12682–12694. doi: 10.1007/s11356-022-22696-4

Zhang, W., Wang, S. C., and Li, Y. (2023b). Molecular mechanism of thiamine in mitigating drought stress in Chinese wingnut (*Pterocarya stenoptera*): Insights from transcriptomics. Ecotoxicol. *Environ. Saf.* 263, 115307. doi: 10.1016/j.ecoenv.2023.115307

Zhang, Y., Xu, S., Yang, S., and Chen, Y. (2015). Salicylic acid alleviates cadmium-induced inhibition of growth and photosynthesis through upregulating antioxidant defense system in two melon cultivars (*Cucumis melo*, L.). *Protoplasma* 252, 911–924. doi: 10.1007/s00709-014-0732-y

frontiers | Frontiers in Plant Science

TYPE Original Research
PUBLISHED 08 May 2024
DOI 10.3389/fpls.2024.1380275

OPEN ACCESS

EDITED BY
Srdjan Stojnic,
University of Novi Sad, Serbia

REVIEWED BY
Milan Zupunski,
University of Novi Sad, Serbia
Radek Pokorny,
Mendel University in Brno, Czechia

*CORRESPONDENCE
Matjaž Čater
matjaz.cater@gozdis.si

RECEIVED 01 February 2024
ACCEPTED 22 April 2024
PUBLISHED 08 May 2024

CITATION
Čater M, Adamič PC and Daňenova E (2024) Response of beech and fir to different light intensities along the Carpathian and Dinaric Mountains.
Front. Plant Sci. 15:1380275.
doi: 10.3389/fpls.2024.1380275

Response of beech and fir to different light intensities along the Carpathian and Dinaric Mountains

Matjaž Čater [1,2*], Pia Caroline Adamič [1,3] and Eva Daňenova [4]

[1]Department of Yield and Silviculture, Slovenian Forestry Institute, Ljubljana, Slovenia, [2]Department of Silviculture, Faculty of Forestry and Wood technology, Mendel University, Brno, Czechia, [3]Department of Forestry and Renewable Forest Resources, Biotechnical Faculty, University of Ljubljana, Ljubljana, Slovenia, [4]Department of Department Of Matters And Energy Fluxes, Global Change Research Institute of the Czech Academy of Sciences, Brno, Czechia

Predicting global change mitigations based on environmental variables, like temperature and water availability, although yielding insightful hypothesis still lacks the integration of environmental responses. Physiological limits should be assessed to obtain a complete representation of a species' fundamental niche. Detailed ecophysiological studies on the response of trees along the latitudinal gradient are rare. They could shed light on the behaviour under different light intensities and other studied traits. The forests of the Dinaric Mountains and the Carpathians represent the largest contiguous forest complexes in south-eastern Europe. In uneven-aged Carpathian (8 plots) and Dinaric Mountain (11 plots) forests, net assimilation (A_{max}) and maximum quantum yield (Φ) were measured for beech and fir in three predefined light intensity categories according to the indirect site factor (ISF%) obtained by the analysis of hemispherical photographs in managed and old growth forests, all located above 800 m a.s.l. The measurements were carried out under fixed environmental conditions in each light category per plot for three consecutive years. Data from the last 50-year average period from the CRU TS 4.01 dataset were used for the comparison between Amax, Φ, and climate. The highest Φ for beech were observed in the central part of the Dinaric Mountains and in the south westernmost and northwesternmost part of the Carpathians for both beech and fir, while they were highest for fir in the Dinaric Mountains in the northwesternmost part of the study area. The Φ-value of beech decreased in both complexes with increasing mean annual temperature and was highest in the open landscape. For fir in the Carpathians, Φ decreased with increasing mean annual temperature, while in the Dinaric Mountains it increased with higher temperature and showed a more scattered response compared to the Carpathians. Short-term ecophysiological responses of beech and fir were consistent to long-term radial growth observations observed on same locations. The results may provide a basis and an indication of the future response of two tree species in their biogeographical range to climate change in terms of competitiveness, existence and consequently forest management decisions.

KEYWORDS

silver fir, beech, light response, Carpathian Mountains, Dinaric Mountains, temperature, precipitation

Introduction

Mixed fir-beech forests are an essential component of Central and South-Eastern European forest ecosystems and landscapes (Dobrowolska et al., 2017). Beech (*Fagus sylvatica* L.), the most common forest species in Europe (Ellenberg, 1988), grows in pure deciduous forests or in mixed forests with conifers, especially with silver fir (*Abies alba* Mill.) (hereafter fir), whose geographical distribution is comparable to that of beech, but is largely restricted to the Alpine and Carpathian arc (Bošela et al., 2018). Fir is the tallest tree in Europe and forms mixed forest stands in many regions (Aussenac, 2002; Dobrowolska et al., 2017). At its southern limit of distribution in the mountainous regions of the Iberian Peninsula and Italy, it forms mixed stands with Mediterranean tree species (Carrer et al., 2010). Species distribution modelling suggests that the current range of silver fir was determined by historical land use and which can mask the potential effects of climate change (Svenning and Skov, 2004; Tinner et al., 2013; Di Pasquale et al., 2014). However, there are several disagreements as to whether the recent increase in temperature alone or in combination with a reduction in precipitation will lead to a reduction in the species' range (Alba-Sánchez et al., 2010; Maiorano et al., 2013). Dendroecological studies have shown a decline in the growth of silver fir in the Iberian Peninsula (Linares and Camarero, 2012) and in the south-eastern European mountains (Diaci et al., 2011), which is probably due to the increase in summer water deficit in these areas (Giorgi and Lionello, 2008). The resilience of plant species or populations depends on their ability to acclimatise to the new environmental conditions. Beech, on the other hand, shows an increase in abundance and a successful ability to regenerate after large-scale disturbances such as windthrow or sleat (Čater and Diaci, 2017; Čater, 2021).

Recent research has shown that the vegetation in the Carpathian forests is changing in different intensities and directions, which can be attributed to various processes (Šamonil and Vrška, 2007), such as air pollution, soil acidification (Hédl et al., 2011), and the competitive influence of tree seedlings (Łysik, 2009). Of particular interest is the question of how ecologically and economically valuable species such as silver fir will cope with recent climate trends (Maiorano et al., 2013; Tinner et al., 2013). Adamič et al. (2023) already confirmed different stem radial growth in beech and fir since 1950s and their response to climate conditions along the Carpathians, while Darenova et al. (2024) related soil respiration spatial variability with soil water content, soil carbon and nitrogen content and no significant affect connected with canopy gaps.

Forest gaps are an integral part of forest ecosystems and play a crucial role in the regeneration of mixed beech-conifer forests and influence the future species admixture (Grassi and Bagnaresi, 2001; Čater et al., 2014). Harvests alter micrometeorological stand's conditions and ecological processes in the understorey. They result in higher soil temperature and precipitation throughfall, which temporarily increase soil respiration (Londo et al., 1999; Čater, 2021) and consequently increase the decomposition of soil organic matter. With reduced aboveground litter input, this leads to a loss of soil organic carbon (Hukić et al., 2021).

When predicting the effects of climate change on the future performance of tree species, a geographical, particularly a latitudinal gradient, can serve as a useful space-time proxy and might provide valuable reference to predict future limitations of these tree species (De Frenne et al., 2013; Čater and Levanič, 2019; Weithmann et al., 2022; Smith et al., 2023), also comparing responses in managed and old-growth forests. Many projections and predictions of global change impacts are based on theoretical specifications of temperature requirements and moisture/water availability for the life cycle of specific species (Dillaway and Kruger, 2010). Unfortunately, they do not take into account the actual response to conditions in the natural environment, which could provide a sufficient mechanistic basis for the exact nature of the constraints Physiological limits should be assessed to obtain a complete representation of a species' fundamental niche and then constrain it with biotic interactions and effects of dispersal limitation (Meier et al., 2011).

In a study on the Balkan Peninsula along the Dinaric High Karst, where diverse and well-expressed ecological factors intertwine in a relatively short geographical distance (ca. 1000 km) (Bohn et al., 2000), the response of beech and fir from the southern, warmer and drier sites already successfully served as a highly probable future prediction for the same species response on currently less extreme sites in the north (Čater and Levanič, 2019). On the contrary are the Carpathian Mountains more complex and exhibit a sufficient latitudinal and longitudinal gradient associated with significant differences in temperature/precipitation as well as differences in seasonal patterns (Micu et al., 2016). Quantum yield (Φ) in various light microsites proved that beech is more efficient in exploiting direct radiation in sun exposed parts of the gap, compared to silver fir (Čater et al., 2014). Microsite position significantly influenced Φ (Lambers et al., 1998) of young beech and firs, which changed with gap size, explaining their difference in competitive ability (Čater et al., 2014). The abundance of microsite light categories along the elevation gradient in two silvicultural systems well indicated the forest structure and its fragmentation, and after large scale disturbances (Čater and Diaci, 2017; Čater, 2021), with quantum yield (Φ) as the resulting trait. Such division may also be associated with spatial distribution of other ecological factors: direct radiation may be related with an increased evapotranspiration and higher drought probability, while diffuse radiation with rainfall patterns within gaps (Krecmer, 1967).

Our aim was to compare the physiological responses of beech and fir along the geographical gradient of the Carpathian and Dinaric Mountains (1), to assess differences in the same light categories of both species between managed and old forests (2) and to verify the relationship between climatic parameters and ecophysiological traits of both species along both geographical gradients (3).

Material and methods

Research area

The Carpathians extend over a 1500 km long arc, the width of which varies from 170 km in the eastern and western parts to less

than 80 km in the southern part of the mountain range (Warszyńska, 1995). The wide variety of favourable ecological conditions is reflected in the great diversity of plants and animals and the rich biodiversity (Mirek and Piekos-Mirkowa, 1992).

Situated on the edge of the Atlantic and continental climate regions, the western climate type with its anticyclonic weather pattern dominates over most of the Carpathians. A continental climate prevails on the eastern slopes of the Eastern Carpathians. In the foothills of the Western Carpathians the average air temperature in July is 19 ^{0}C and in the Southern Carpathians 22 ^{0}C. In the south-western part, the air temperature drops by 0.81 ^{0}C per 100 metres difference in altitude and by 0.5 ^{0}C in the south-eastern part of the Carpathians. Annual precipitation ranges from around 500 mm at the foothills of the Southern Carpathians to over 2000 mm on the peaks of the Tatra Mountains (Vološčuk, 1999) in the north. Flysch predominates in the eastern and outer Western Carpathians, crystalline and volcanic rocks in the inner band, while metamorphic rocks predominate in the Southern Carpathians (Rădulescu and Săndulescu, 1973; Golonka et al., 2018).

The Dinaric Mountain range stretches from the southern edge of the Eastern Alps in Slovenia to the mountain massif in North Macedonia; it is bordered by the Adriatic Sea to the west and the Pannonian Basin to the east (Gams, 1969). Most of the mountain range consists of Mesozoic rocks, mainly limestone and dolomite. The depth of the limestone and dolomite rocks is unique and is typically 1 to 3 kilometres, with considerable local variations (Gams, 1969). Westerly winds bring large amounts of moisture to the higher elevations along the western side of the mountain range. Precipitation at higher altitudes is relatively evenly distributed during the year, with snow cover often remaining for up to six months (Mihevc, 2010). The forest structure and composition in the region is strongly influenced by the interaction between the mountain relief, the karst area, the soils and the climatic gradient. The mountain forests above 800 metres include mainly beech-dominated forests and uneven-aged mixed forests, in which beech, fir and occasionally spruce occur to varying degrees. Large, forested areas inland have remained intact to this day and have been managed with low-intensity silvicultural systems for more than a century (Boncina et al., 2013), with several protected old-growth forest remnants scattered across the area.

Selected permanent research plots were located above an altitude of 800 m a.s.l., where mature beech and fir trees predominate and where there is abundant natural regeneration of both tree species. Eight plots were established in the Carpathian Mountains, which extend from the Czech Republic from the far north-west through Slovakia and Romania to the southern part of the mountain range, and eleven permanent observation plots in the Dinaric Mountains, which extend from Slovenia from the far north-west through Croatia, Bosnia and Herzegovina and Montenegro along the mountainous region of the Balkan Peninsula to North Macedonia in the southern part of the mountain range. Two old stands were selected in the Carpathian Mountains (plots 3 and 8) and three in the Dinaric Mountains (plots 3, 7 and 8) (Figure 1; Table 1).

Potential light categories

In each plot, three categories of different light intensities were defined based on the analysis of hemispherical photographs, taken with the Canon EOS Rebel T3 DSLR and a calibrated fisheye lens with the Regent WinScanopy pro-d accessory. Young beech and fir are strongly influenced by indirect light, which has been confirmed by our former research (Čater et al. 2014); therefore, the Indirect Site Factor (ISF %) was used, describing relative share between potential indirect (diffuse) light at the point of measurement and in the open. At least eight hemispherical photographs per every plot were made before any response measurements (Čater and Levanič, 2013) in each of three potential categories: under a closed canopy with Indirect Site Factor (ISF)<15%, at the forest edge (15%<ISF<25%) and in the open ISF>25%. Colour digital hemispherical photographs were taken

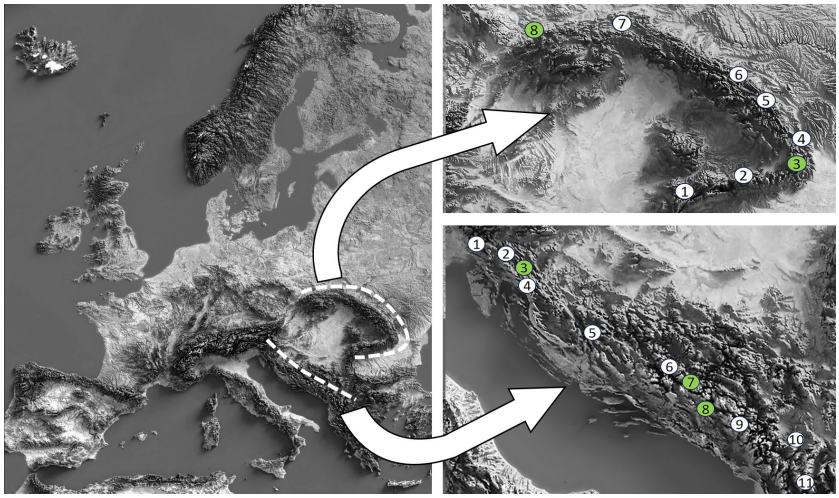

FIGURE 1
Research area and location of the permanent research plots along the Carpathian and Dinaric Mountains. The green dots represent old-growth reserves.

10.3389/fpls.2024.1380275

TABLE 1 Characteristics of the research plot; the meteorological data were obtained from the website "Climate Explorer" (http://climexp.knmi.nl) for the period 1985-2020, including the annual totals and the values for the April-September growing season.

Plot No/ Region		Altitude ASL (m)	Long. Deg (^{0})	Latit. Deg (^{0})	Annual precipitation (mm)	Average annual air T (^{0}C)	Apr.-Sept. precipit. (mm)	Average April-Sept. air T (^{0}C)
Carpathian Mts.	**1**	985	22.917°	45.169°	1073	4.7	695	10.7
	2	995	24.651°	45.460°	812	7.4	534	13.9
	3	1038	26.229°	45.614°	744	6.8	491	13.6
	4	830	26.604°	46.001°	603	8.3	412	15.6
	5	950	26.168°	46.854°	704	5.8	474	12.9
	6	850	25.683°	47.468°	738	5.4	501	12.0
	7	880	21.017°	49.255°	758	7.2	493	13.8
	8	820	18.417°	49.403°	744	7.1	491	13.4
Dinaric Mts.	**1**	814	13.757°	45.991°	1619	11.3	863	15.2
	2	807	14.464°	45.676°	1573	8.4	802	14.1
	3	871	15.004°	45.662°	1465	9.0	780	14.9
	4	1190	14.806°	45.271°	1108	9.3	616	14.9
	5	928	16.318°	44.307°	1349	8.6	645	14.5
	6	1204	18.269°	43.737°	1192	7.6	593	13.4
	7	1313	18.710°	43.320°	1229	7.7	607	13.4
	8	1408	18.646°	42.986°	1278	8.2	590	13.7
	9	1402	19.922°	42.553°	1163	6.6	548	13.1
	10	1410	20.885°	42.252°	850	8.6	418	14.6
	11	1315	20.741°	41.696°	836	8.4	357	14.0

during windless weather and standard overcast sky conditions 150 cm above the forest floor when the solar disk was completely obscured. Exposure fitting was done to above canopy conditions prior to shooting on every plot (Macfarlane et al., 2000; Zhang et al., 2005) without noteworthy blooming effects (Leblanc et al., 2005). In the process of hemispherical photograph analysis, a "standard overcast sky" (SOC) model was applied for diffuse light distribution. For the calculation within the vegetation period (30. April - 31. September), the sun's position was specified every 10 min. The solar constant was defined as 1,370 W/m^2; 0.6 was set for atmospheric transmissivity and 0.15 for the proportion of diffuse radiation compared to calculated direct potential radiation. An automatic thresholding method based on the same colour scheme was applied for the discrimination between sky and canopy elements in all digital photographs, as the thresholding is crucial and may significantly affect the calculated parameters (Ishida, 2004; Nobis and Hunziker, 2005; Schwalbe et al., 2009).

Weather and climate

Monthly mean temperatures (°C) and monthly total precipitation data were interpolated for the 0.5° grids that include each selected plot and correspond to the CRU TS 4.01 dataset (Harris et al., 2014), obtained from the Royal Netherlands Meteorological Institute 'Climate Explorer' website (http://cliexp.knmi.nl). For the comparison between maximal net assimilation (A_{max}), quantum yield (Φ) and climate data (temperature and precipitation), data from the last 50-year average period (1981-2020) were used. For the long-term comparison between climate and tree response, we extracted gridded climate data for mean monthly temperature and sum of monthly precipitation using the CRU TS 4.01 dataset with a resolution of 0.5x 0.5-degrees from the KNMI website (Figure 2).

Nitrogen content and leaf mass per area

Leaves and needles were taken from the upper canopy position of at least 12 trees per light category and location and then stored in a cool, airtight place. Age of trees was similar in all three light categories. The same trees were also used to measure the maximum assimilation rate. Total leaf nitrogen concentration (N_{tot}) [mg/g] was determined (Laboratory of Soil Science, Faculty of Forestry and Wood technology, Mendel University, Brno) to compare macronutrient status (Leco CNS-2000 analyser) (Lambers et al., 1998; Larcher, 2003) for the open, forest edge and closed canopy categories under mature trees (Čater et al., 2014). Fresh leaves were weighed and scanned for leaf area. Leaves were dried to constant weight at 105°C for 24 hours and weighed in the laboratory to determine leaf mass per area open-, forest

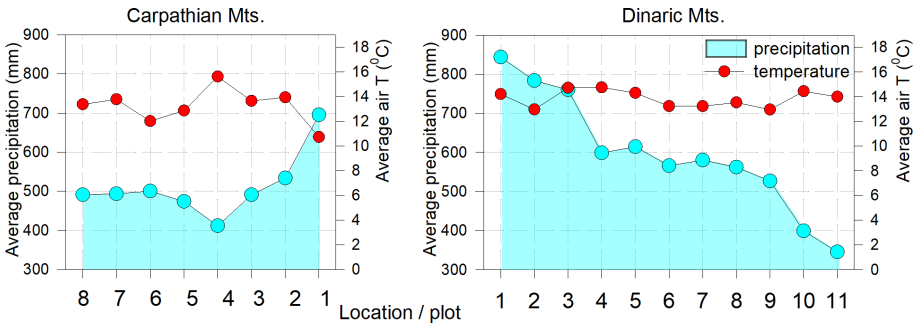

FIGURE 2
Average seasonal air temperature and precipitation (April-Sept., period 1951-2020) on the studied plots.

edge- and closed canopy-category below mature trees (Čater et al., 2014). Leaves were dried to constant weight at 105°C for 24 hours and weighed in the laboratory to determine leaf mass per area (LMA) [g/m^2].

Assimilation light response

For the light saturation measurements, which were carried out in June and July in three consecutive growing seasons, at least 8 young trees of the same height that were not obstructed by their neighbours were randomly selected (*sensu* Čater and Levanič (2019). The age of the trees varied between 5-12 years. The light response was measured with a portable LI-6400 (Li-Cor, USA) system on at least four leaves/shoots per tree located in the upper third of the tree crowns. All assimilation values were recorded after they had held constant for 2 min or until the coefficient of variability (CV%) dropped below 5%.

- Light saturation curves were generated to compare net assimilation (A_{max}) in young beech and fir trees under the same light conditions. All assimilation measurements were performed in the field at a constant temperature of the measurement block (20^{0}C), a CO_2 concentration of 420 µmol/l, an air flow of 500 µmols-1 and different light intensities: 0, 50, 250, 600 and 1500 µmol/m^2/s. The maximum assimilation rates (A_{max}) for the light saturation curves were used to compare the responses between different light categories and plots.
- The characteristic points of maximum quantum yield (Φ), defined as the maximum amount of fixed CO_2 per amount of absorbed light quanta (Lambers et al., 1998) measured as the initial slope of the light response curve of CO_2 fixation, were determined for each light category, species and plot, as described in Čater et al. (2014), using LiCOR software.

Statistical analysis

Differences between the same years for the LMA, N_{tot}, A_{max} and Φ were tested using two-way ANOVA with tree species (beech and fir) and light (open, edge, canopy) as dependent variables. Analyses of variance (ANOVA) and the HSD Tuckey *post-hoc* test were performed after testing data to meet conditions of normality. Probability values of p<0.05 (*), p<0.01 (**) and p<0.001 (***) were considered significant. Data analysis, correlation between the measured variables and multiple regression were performed using Statistica Data Analysis Software System (2011).

Results

Weather and climate

In both complexes, the long-term average temperatures show more homogeneous conditions over the longer Dinaric area and

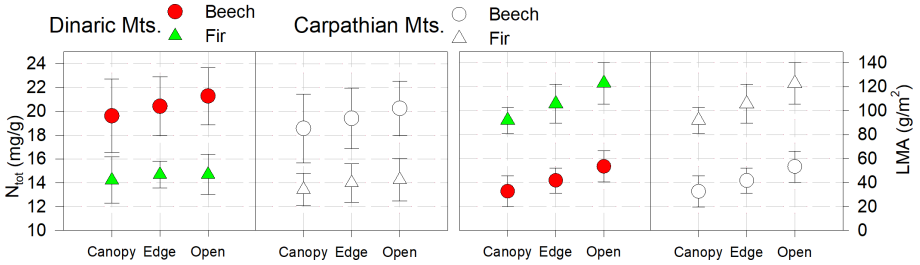

FIGURE 3
Foliar nitrogen (N_{tot}) and leaf mass per area (LMA); bars are standard errors.

10.3389/fpls.2024.1380275

more variable conditions in Carpathians. The average annual precipitation in the Carpathian region is lower and corresponds to the conditions in the southern Dinaric mountains. (plot 9) (Figure 2).

Foliar nitrogen

In all plots, N_{tot} was highest for both beech and fir in the open and lowest in the closed canopy, without significant differences between light categories and years. On all studied plots N_{tot} was within the optimal thresholds 13-15mg/g for fir and 18-22mg/g for beech, as reported by Grassi and Bagnaresi (2001); Mellert and Göttlein (2012) or even above range reported by Yang et al. (2022) and Bachofen et al. (2020). The same trend was observed for LMA.

The values of N_{tot} and LMA were slightly and not significantly lower in all categories in the Carpathian Mountains than in the Dinaric Mountains (Figure 3, Table 2).

Maximum assimilation rate and quantum yield (Φ)

In the Carpathian and Dinaric Mountains, Φ followed the pattern of precipitation and temperature; in both complexes it was highest for beech in the open light and for fir under closed canopies. In old growth reserves of the Dinaric Mountains, Φ was shifted towards the response of open light category for both species, much more so than in the Carpathian Mountains. In all cases, the absolute values were higher in all light categories than in the neighbouring managed forest stands (Figure 4, Table 3).

The highest values (Φ) for beech were observed in the central part of the Dinaric Mountains region and in the south westernmost and northwesternmost part of the Carpathian Arc for both beech and fir, while Φ for fir was highest in the Dinaric Mountains in the northwesternmost part of the studied area (Figure 4).

Post-hoc analyses revealed significant differences between all light categories for Φ in Dinaric Mountains, except in the old-growth reserves, where no significant differences between forest edge and open light were confirmed for either species. In Carpathian Mountains differences between light categories were not so pronounced (Table 4).

We confirmed positive correlation between Φ and annual precipitation, which increased with the light intensity for beech in all light categories and in both the Carpathian and Dinaric Mountains. The correlation was positive for fir, decreased with increasing light and was highest when the canopy was closed. Slope of the curve for fir was steepest for the closed canopies (Figure 5).

The quantum yield of beech in both complexes decreased with increasing mean annual temperature and was highest in the open. For fir in the Carpathian Mountains, Φ decreased with increasing mean annual temperature, while in the Dinaric Mountains it increased with higher temperature and showed a more scattered response compared to the Carpathian Mountains (Figure 5).

The relationship between Φ and five independent parameters (latitude, longitude, average annual air temperature, annual precipitation, and altitude) was tested in a linear multiple regression model for both species, both complexes and three potential light categories. As the number of variables increased, the regression coefficients for beech in the Carpathians and Dinaric Mountains became increasingly different; beech in Dinaric Mountains indicated strongest relation with annual temperatures and additional parameters did not increase correlations as much as for the beech in Carpathian Mountains. The regression coefficients for fir between Dinaric and Carpathian Mountains were at first different and highest in Carpathian Mountains and became with additional parameters increasingly similar (Figure 6).

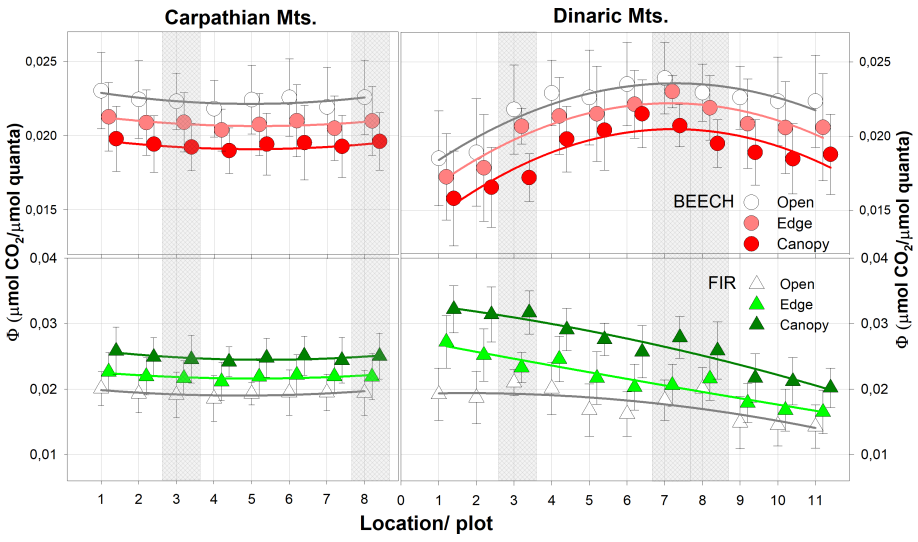

FIGURE 4
Average quantum yield (Φ) in all light categories. The shaded areas represent old growth reserves. N for each light category = 24.

10.3389/fpls.2024.1380275

TABLE 2 ANOVA for leaf nitrogen (N_{tot}) and leaf mass per area (LMA) in both regions.

Region	Trait	Df 1;2	Species		Df 1;2	Light category		Df 1;2	Species X Light category	
			F	p		F	p		F	p
Carpathian Mts.	N_{tot}	1; 47	176.2	2e-17***	2; 43	4.2	0,0278*	2; 43	1.8	0.5731^{NS}
	LMA	1; 47	3215.4	2e-17***	2; 43	345.4	2e-17***	2; 43	28.2	2e-17***
Dinaric Mts.	N_{tot}	1; 65	193.2	2e-16***	2; 60	3.6	0,0336*	2; 60	0.7	0.5197^{NS}
	LMA	1; 65	5859.9	2e-16***	2; 60	415.1	2e-16***	2; 60	46.0	7.6e-13***

p<0.05 (*), p<0.001 (***), ns – non significant.

Discussion

Shifts in climate zones and changes in forest cover directly affect regional surface temperatures through the exchange of water and energy; as warming continues, the frequency, intensity, and duration of heat-related events, including heat waves, are expected to increase (Lee et al., 2023). Climate zones are projected to shift further poleward in the mid- and high-latitudes and forest disturbances such as drought, wildfires and pest infestations are projected to increase (Lee et al., 2023). Some spatial distribution models predict a reduction in the ranges of fir and beech forests by 2100 due to climate change in favour of more drought-tolerant species (Piedallu et al., 2013); however, several studies question the predominant effects of ecological rather than macroecological and phytogeographical gradients on vegetation (Willner, 2002; Marinšek et al., 2013).

The selected sites in both studied mountain complexes were above 800m a.s.l. to ensure comparable and similar climatic conditions. Altitude is the key factor controlling the microclimate in temperate mountain forest stands (Körner et al., 2016). The average annual temperatures at the selected Carpathian sites ranged between 12 and 14 ^{0}C with the exception of sites 4 and 1, while the average annual temperatures at the Dinaric sites showed more homogeneous conditions (13 to 14 ^{0}C). The average amount of precipitation in the Dinaric Mountains decreased evenly from the north-west to south-east, while the amount of precipitation in the Carpathians decreased from west to east.

Assimilation response

In the Dinaric Mountains, Φ was highest for beech in the central area (Bosnia and Herzegovina) and for fir in the north-western part of the transect (Slovenia, Croatia), while in the Carpathians it was highest at the beginning and end of the studied transect, at the westernmost sites.

The responses (Φ) of the two species studied between the Carpathians and the Dinaric Mountains in the same light categories showed certain similarities: in both cases, Φ values were higher for beech in the open, and lowest under shaded canopies, and vice versa for fir - highest under shaded conditions and lowest in the open, confirming our previous studies (Čater and Levanič, 2013, 2019).

The differences between old-growth forest reserves and neighbouring managed forests in both mountain complexes showed the same, higher values in all light categories and species, although the response was less pronounced in the Carpathians than in the Dinaric Mountains (Figure 4). It is not clear what caused the shift of Φ in the edge light category in the old growth reserves towards the open category for both beech and fir, as leaf nitrogen values were comparable between sites and were in the optimal range on all plots. In old growth reserves Amax and Φ were significantly higher than in managed forests due to microclimate, relative air humidity (RH), higher water use-efficiency (WUE) and photosynthetic nitrogen use efficiency (PNUE) in old growth reserves (Čater and Levanič, 2013).

Despite the non-significantly lower amount of foliar nitrogen (N_{tot}) in the Carpathian categories, the variability of Φ and the differences between light categories were much higher for both beech and fir in the Dinaric Mountains (Table 3), possibly reflecting the more diverse growing conditions and more abundant water availability in the Dinaric Mountains than in the Carpathians (Micu et al., 2016). We assume that water is the most important limiting parameter, as the response of both species at all study sites in the Carpathians, except the first two, corresponded to the conditions in

TABLE 3 ANOVA for maximum assimilation rate (A_{max}) and quantum yield (Φ) for beech and fir in different light conditions and complexes.

Complex	Trait	Df 1;2	Species		Df 1;2	Light category		Df 1;2	Species X Light category	
			F	p		F	p		F	p
Carpathian Mts.	A_{max}	1; 1096	1783.5	2e-17***	2; 1096	1476.4	2e-17***	2; 1096	987.5	2e-17***
	Φ	1; 1096	622.2	2e-17***	2; 1096	214.9	2e-17***	2; 1096	2869.5	2e-17***
Dinaric Mts.	A_{max}	1; 1578	1454.3	2e-16***	2; 1578	1352.3	2e-16***	2; 1578	89.53	2e-15***
	Φ	1; 1578	73.0	2e-16***	2; 1578	231.0	2e-16***	2; 1578	775.4	2e-15***

p<0.001 (***).

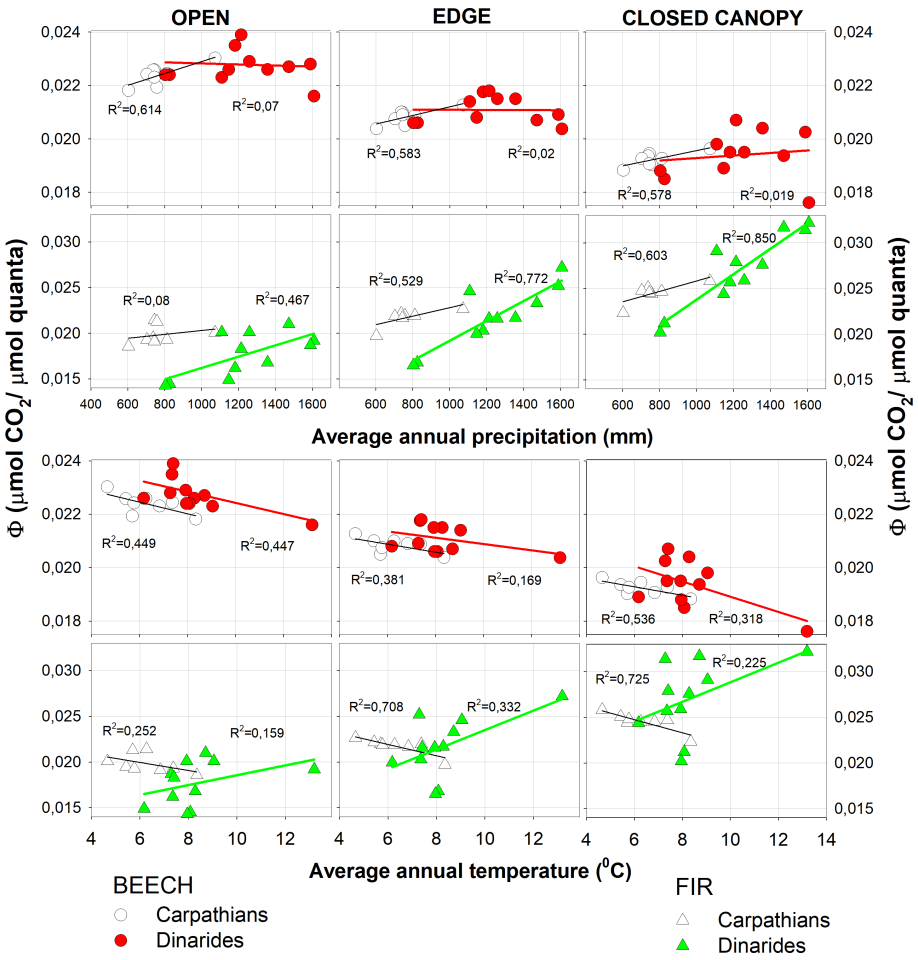

FIGURE 5
Quantum yield (Φ) as a function of precipitation and temperature.

the lower south-eastern part of the Dinaric Mountains, where the average annual precipitation was below 500 mm (Figures 2, 4).

With increasing precipitation, Φ increased in both fir and beech in the Carpathian and Dinaric Mountains, especially in fir, where the slope and dependence on shading increased. The correlation between Φ and mean annual temperature was negative at all sites for beech and fir in the Carpathians, while in the Dinaric Mountains the correlation was reversed for fir (Figure 5). The main reason for the negative correlation between Φ and increasing mean temperature in all light categories for fir could be the lower precipitation in the Carpathians.

Precipitation may not be the only reason, as the Eastern Carpathians and the southern Dinaric Mountains represent the edge of the silver fir's natural range (Mauri et al., 2016; Caudullo et al., 2017). In south-eastern Europe, a higher resistance (compared to other tree species) to climate extremes was found (Bošela et al., 2018). At the same time, two populations of fir trees were distinguished in the Carpathians (Bošela et al., 2016): the eastern population reacts to drought similarly to the populations in the Balkan region, while the western population seems to be less affected by summer droughts. The fir of the western population might therefore be better adapted to the conditions of the Western Carpathians (Bošela et al., 2018) than the beech; although we observe a long-term expansion of beech and a decline of fir there for other reasons - see Vrška et al. (2009) and might also be better adapted to climate change than the eastern fir population.

The value of the correlation coefficient of the multiple regression increased with increasing number of independent variables and Φ for the beech in the Carpathians, while it remained the same for the Dinaric Mountains, which could indicate that the independent variables influence the beech differently in both mountain complexes (Figure 6, left). Fir, on the other hand, showed a similar dependence on an increasing number of the same independent variables in both the Carpathians and the Dinaric Mountains.

Beech can tolerate a wide range of light conditions in the understorey and manages to grow under different light conditions at young growth stages (Collet et al., 2001; Stancioiu and O'Hara, 2006; Nicolini and Caraglio, 2011). Fir, on the other hand, is a late successional species that is more shade-tolerant and more sensitive to water deficits than beech (Rolland et al., 1999). Compared to beech, the competitive ability of fir is much greater under low and diffuse light conditions, but consequently lower under medium and extensive light conditions; in gaps, beech adapts better and faster to rapid changes in light intensity (Lichtenthaler et al., 2007; Wyka et al., 2007; Čater et al., 2014), while the acclimation of fir growth rate to light conditions occurs gradually over several years (Robakowski et al., 2004). Our study confirmed a better light utilisation of fir in the

10.3389/fpls.2024.1380275

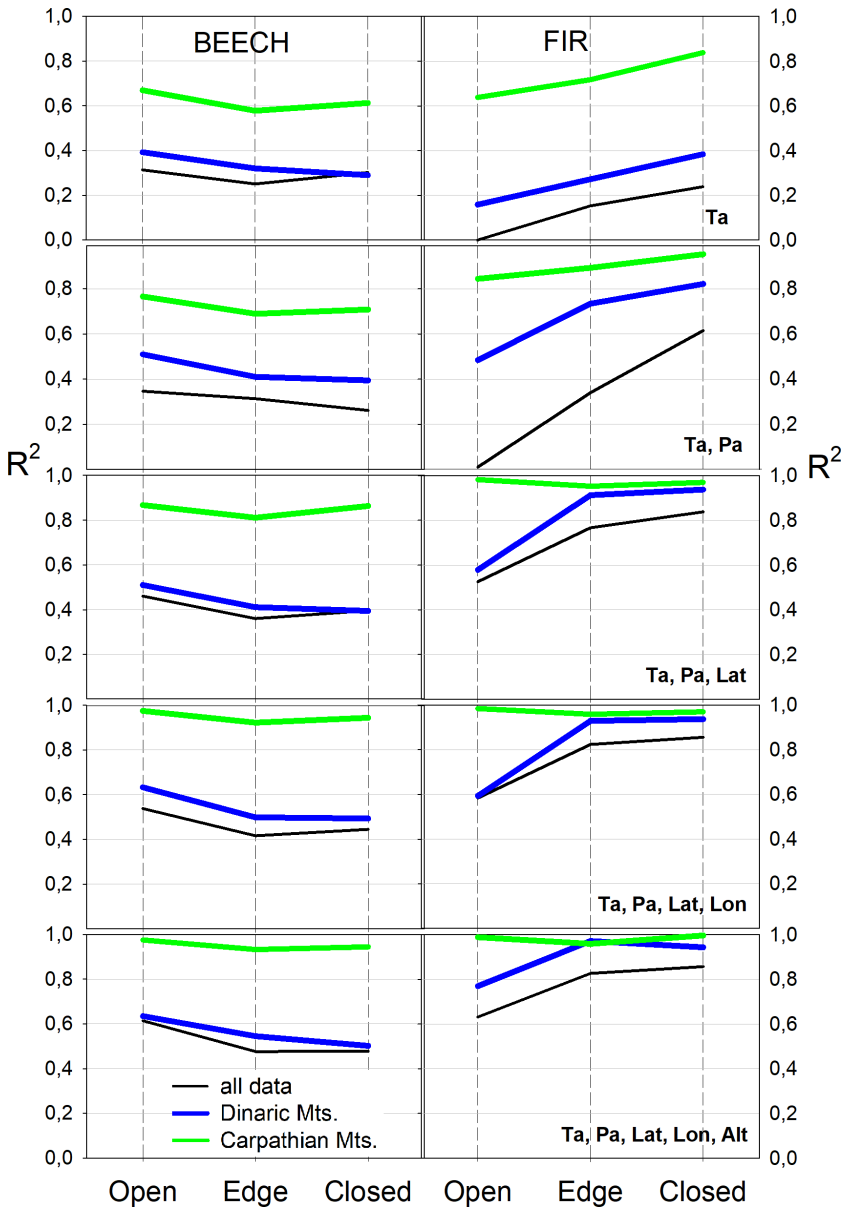

FIGURE 6
Multiple regression coefficients between independent (average annual air temperature - Ta, average annual precipitation - Pa, latitude - Lat, longitude - Lon, altitude - Alt) and dependent quantum yield (Φ) variables for both species, three light categories and two complexes.

shade and a different relationship with increased average temperatures in combination with lower precipitation. The lower Φ of fir utilisation of high-intensity solar radiation compared to beech could be a competitive disadvantage in large gaps in the canopy, which could limit the recruitment of species in the understorey or in small gaps, especially when mixed with beech.

Paralleling short term assimilation with the growth response

The dependence of tree growth on precipitation has increased over the last century, and there has been an upward trend in drought since the 1950s. The latitudinal progression of radial growth decline and the proportion of positive trends indicate a rapid northward movement of the Mediterranean climate due to global changes and their impact on tree ecology (Gazol et al., 2015). The comparison of the assimilation response in young beech and fir trees was in good agreement with the growth response in adult trees (Čater and Levanič, 2019).

The study of Adamič et al. (2023) confirmed clear differences in the growth response to climate (temperature and precipitation) between southern, eastern and northern locations on the same study plots: a significant correlation between tree growth of both species and seasonal variables (temperature, precipitation) was observed on the eastern Carpathian sites (plots 4, 5 and 6), and a less or non-significant correlation in the southern sites (plots 1, 2 and 3). The fir in the north (plot 7) showed even less significant

10.3389/fpls.2024.1380275

TABLE 4 *Post hoc* (HSD) analysis for quantum yield (Φ) for beech and fir between C (canopy), E (edge) and O (open) light conditions.

Plot No/		Beech			Fir		
Region		C-E	C-O	E-O	C-E	C-O	E-O
Carpathian Mts.	1	*	***	*	*	***	*
	2	*	***	*	*	***	*
	3	*	***	ns	*	***	ns
	4	*	***	*	*	***	*
	5	*	***	*	*	***	*
	6	*	***	*	*	***	*
	7	*	***	*	*	***	*
	8	*	***	ns	*	***	ns
Dinaric Mts.	1	***	***	**	***	***	***
	2	***	***	*	***	***	***
	3	***	***	ns	***	***	ns
	4	***	***	**	***	***	***
	5	***	***	**	***	***	***
	6	ns	***	***	***	***	**
	7	***	***	ns	***	***	ns
	8	***	***	ns	***	***	ns
	9	***	***	***	***	***	*
	10	***	***	***	***	***	*
	11	***	***	***	***	***	*

Probability values: p<0.05 (*), p<0.01 (**), p<0.001 (***), ns – non significant.

correlations than those at the southern sites, while the beech in the north showed more significant correlations than at the southern sites, but less than at the eastern sites. Beech and fir showed the same significant correlations at the eastern sites, while fir showed slightly more significant correlations in the south (Adamič et al., 2023). Accordingly, the quantum yield of beech and fir showed the lowest values in the eastern part and the highest values in the west.

Our research in the Dinaric Mountains confirmed that the growth of fir responded more strongly to climate than that of beech in the same study plots, as shown in this study (Čater and Levanič, 2019). Both temperature and precipitation had a stronger influence on the growth of fir than on that of beech. The climate signal of fir became weaker from NW to SE, with only the drought indices remaining significant, while the response of beech to climate was weaker in all plots and decreased from NW to SE, similar to fir (Čater and Levanič, 2019). In the Dinaric Mountains, four different groups were formed according to similar growth responses: two northern regions - A (including plots 1-4) and B (plot 5), and two southern regions - C (plots 6-8) and D (plots 9-11). The average Φ corresponded well to the growth response of the same group (A, B, C, D) and was more pronounced for the longer latitudinal distance than for the Carpathian Arc, which is similar in distance but shorter in latitudinal scale.

In the future, above-average summer temperatures and the absence of summer precipitation (July) are expected to become more frequent (Adamič et al., 2023), which could influence the future demography of fir towards the north and higher altitudes (Tinner et al., 2013). Especially in the Carpathian Mountains, which already show a negative correlation between young fir trees and increasing temperatures (Figure 5), the increasing number of extreme weather events is likely to affect young fir regeneration. The reaction of beech at the expense of fir and its spread in Central Europe has already been reported (Šamonil et al., 2009; Vrška et al., 2009; Janík et al., 2014, 2016).

Recent studies describe different responses of fir along its range (Diaci et al., 2011), its disappearance from warmer and drier areas and at the limit of its range (Ficko et al., 2011) and in south-western Europe (Gazol et al., 2015), especially in the Mediterranean region, where the decline of fir is often related to increasing drought (Čavlović et al., 2015). A higher resistance (compared to other tree species) to climate extremes was also found in south-east Europe (Bošela et al., 2018).

Studies also indicate a different response of the species along its distribution range. The radial growth of silver fir has increased significantly in Central Europe over the last 30 years, while it has

decreased in drought-prone Mediterranean regions (Büntgen et al., 2014). Furthermore, different growth patterns have been observed between northern and southern populations of silver fir in Italy (Carrer et al., 2010).

Understanding the light utilisation processes in the regeneration phase of uneven-aged forests, which represent the largest contiguous forest complexes in south-eastern Europe, and focusing on sites that already have lower resilience to increasing temperatures and lower precipitation could help to maintain and emphasise the necessary measures that would contribute to greater stability and ensure continuous forest cover in the long term (Schütz, 2002; Schütz et al., 2016). The future response of silver fir forests to climate warming is currently being debated by the ecological community, as millennia of human impact have greatly reduced the species' geographic distribution (Tinner et al., 2013; Di Pasquale et al., 2014). As the severity of disturbances is increasing and several Central European countries are facing unprecedented events (Nagel et al., 2017), the disadvantages of uneven-aged forest management include the dependence on shade-tolerant species that may be affected by the climatic conditions of the open areas created by disturbances. The most important silvicultural tool for the indirect promotion of silver fir is the creation of appropriately large gaps in the canopy and their temporal and spatial expansion. Most studies pointed to the predominance of fir under relatively closed canopies (Hohenadl, 1981; Stancioiu and O'Hara, 2006) and focused on different growth patterns without considering the ecophysiological processes involved.

In the present study, relatively short-term ecophysiological responses of beech and fir provided information on the behaviour at three different light intensity categories compared to long-term radial growth observations, which were consistent. The efficiency of beech increased with light intensity in all light categories and in both mountain complexes, while the response of fir was the opposite, decreasing with increasing light. The main difference between the two larger areas was the response of young fir to increasing temperatures, which correlated positively with increasing temperatures in the Dinarides and negatively in the Carpathians. In our opinion, this difference is related to the high precipitation in the Dinaric Mountains and the low precipitation in the Carpathians.

Our results may give an indication of how two important tree species in their biogeographical range will react to climate change in the future, which will affect their competitiveness, their existence and, consequently, forest management decisions.

Data availability statement

The raw data supporting the conclusions of this article will be made available by the authors, without undue reservation.

Ethics statement

No plants or animals (including human) were harmed during this study.

Author contributions

MC: Conceptualization, Data curation, Formal Analysis, Funding acquisition, Investigation, Methodology, Project administration, Resources, Supervision, Validation, Visualization, Writing – original draft, Writing – review & editing. PA: Investigation, Writing – review & editing. ED: Investigation, Visualization, Writing – review & editing.

Funding

The author(s) declare that financial support was received for the research, authorship, and/or publication of this article. The authors acknowledge the financial support from the Slovenian Research Agency (research core funding P4-0107 Program research at the Slovenian Forestry Institute, project grant No. J4-3086 and by the Young Researcher program of the Slovenian Research Agency and by the Czech Science Foundation GAČR No. 21-47163L.

Acknowledgments

Sincere thanks to Dr. J. Kermavnar, R. Krajnc, Dr. S. Poljanšek, Dr N. Potočić, BSc Ing D. Mioć, Prof Dr D. Ballian, Prof Dr O. Huseinović, BSc Ing Z. Čančar, Mr G. Damjanović, Mr R. Orbović, Mr E. Pupović, BSc Ing N. Kryeziu, Prof Dr M. Karadelev, BSc In S. Hanko and Dr. M. Hanzu.

Conflict of interest

The authors declare that the research was conducted in the absence of any commercial or financial relationships that could be construed as a potential conflict of interest.

Publisher's note

References

Adamič, P. C., Levanič, T., Hanzu, M., and Čater, M. (2023). Growth response of European beech (Fagus sylvatica L.) and Silver Fir (Abies alba Mill.) to climate factors along the Carpathian massive. *Forests* 14, 1318. doi: 10.3390/f14071318

Alba-Sánchez, F., López-Sáez, J. A., Pando, B. B., Linares, J. C., Nieto-Lugilde, D., and López-Merino, L. (2010). Past and present potential distribution of the Iberian Abies species: a phytogeographic approach using fossil pollen data and species distribution models. *Diversity Distributions* 16, 214–228. doi: 10.1111/j.1472-4642.2010.00636.x

Aussenac, G. (2002). Ecology and ecophysiology of circum-Mediterranean firs in the context of climate change. *Ann. For. Sci.* 59, 823–832. doi: 10.1051/forest:2002080

Bachofen, C., D'Odorico, P., and Buchmann, N. (2020). Light and VPD gradients drive foliar nitrogen partitioning and photosynthesis in the canopy of European beech and silver fir. *Oecologia* 192, 323–339. doi: 10.1007/s00442-019-04583-x

Bohn, U., Gollub, G., Hettwer, C., Weber, H., Neuhäuslová, Z., Raus, T., et al. (2000). *Karte der natürlichen Vegetation Europas/Map of the Natural Vegetation of Europe. Maßstab/Scale 1: 2,500,000.*

Boncina, A., Cavlovic, J., Curovic, M., Govedar, Z., Klopcic, M., and Medarevic, M. (2013). A comparative analysis of recent changes in Dinaric uneven-aged forests of the NW Balkans. *Forestry* 87, 71–84. doi: 10.1093/forestry/cpt038

Bošela, M., Lukac, M., Castagneri, D., Sedmák, R., Biber, P., Carrer, M., et al. (2018). Contrasting effects of environmental change on the radial growth of co-occurring beech and fir trees across Europe. *Sci. Total Environ.* 615, 1460–1469. doi: 10.1016/j.scitotenv.2017.09.092

Bošela, M., Popa, I., Gömöry, D., Longauer, R., Tobin, B., Kyncl, J., et al. (2016). Effects of post-glacial phylogeny and genetic diversity on the growth variability and climate sensitivity of European silver fir. *J. Ecol.* 104, 716–724. doi: 10.1111/1365-2745.12561

Büntgen, U., Tegel, W., Kaplan, J. O., Schaub, M., Hagedorn, F., Bürgi, M., et al. (2014). Placing unprecedented recent fir growth in a European-wide and Holocene-long context. *Front. Ecol. Environ.* 12, 100–106. doi: 10.1890/130089

Carrer, M., Nola, P., Motta, R., and Urbinati, C. (2010). Contrasting tree-ring growth to climate responses of Abies alba toward the southern limit of its distribution area. *Oikos* 119, 1515–1525. doi: 10.1111/j.1600-0706.2010.18293.x

Čater, M. (2021). Response and mortality of beech, fir, spruce and sycamore to rapid light exposure after large-scale disturbance. *For. Ecol. Manage.* 498, 119554. doi: 10.1016/j.foreco.2021.119554

Čater, M., and Diaci, J. (2017). Divergent response of European beech, silver fir and Norway spruce advance regeneration to increased light levels following natural disturbance. *For. Ecol. Manage.* 399, 206–212. doi: 10.1016/j.foreco.2017.05.042

Čater, M., Diaci, J., and Roženbergar, D. (2014). Gap size and position influence variable response of Fagus sylvatica L. and Abies alba Mill. *For. Ecol. Manage.* 325, 128–135. doi: 10.1016/j.foreco.2014.04.001

Čater, M., and Levanič, T. (2013). Response of Fagus sylvatica L. and Abies alba Mill. in different silvicultural systems of the high Dinaric karst. *For. Ecol. Manage.* 289, 278–288. doi: 10.1016/j.foreco.2012.10.021

Čater, M., and Levanič, T. (2019). Beech and silver fir's response along the Balkan's latitudinal gradient. *Sci. Rep.* 9, 16269. doi: 10.1038/s41598-019-52670-z

Caudullo, G., Welk, E., and ASan Miguel Ayanz, J. (2017). Chorological maps for the main European woody species. *Data In Brief* 12, 662–666. doi: 10.1016/j.dib.2017.05.007

Čavlović, J., Bončina, A., Božić, M., Goršić, E., Simončič, T., and Teslak, K. (2015). Depression and growth recovery of silver fir in uneven-aged Dinaric forests in Croatia from 1901 to 2001. *Forestry: Int. J. For. Res.* 88, 586–598. doi: 10.1093/forestry/cpv026

Collet, C., Lanter, O., and Pardos, M. (2001). Effects of canopy opening on height and diameter growth in naturally regenerated beech seedlings. *Ann. For. Sci.* 58, 127–134. doi: 10.1051/forest:2001112

Darenova, E., Adamič, P. C., and Čater, M. (2024). Effect of temperature, water availability, and soil properties on soil CO2 efflux in beech-fir forests along the Carpathian Mts. *Catena.* doi: 10.1016/j.catena.2024.107974

De Frenne, P., Graae, B. J., Rodríguez-Sánchez, F., Kolb, A., Chabrerie, O., Decocq, G., et al. (2013). Latitudinal gradients as natural laboratories to infer species' responses to temperature. *J. Ecol.* 101, 784–795. doi: 10.1111/1365-2745.12074

Diaci, J., Roženbergar, D., Anić, I., Mikac, S., Saniga, M., Kucibel, S., et al. (2011). Structural dynamics and synchronous silver fir decline in mixed old-growth mountain forests in Eastern and Southeastern Europe. *Forestry* 84, 479–491. doi: 10.1093/forestry/cpr030

Dillaway, D. N., and Kruger, E. L. (2010). Thermal acclimation of photosynthesis: a comparison of boreal and temperate tree species along a latitudinal transect. *Plant Cell Environ.* 33, 888–899. doi: 10.1111/j.1365-3040.2010.02114.x

Di Pasquale, G., Buonincontri, M. P., Allevato, E., and Saracino, A. (2014). Human-derived landscape changes on the northern Etruria coast (western Italy) between Roman times and the late Middle Ages. *Holocene* 24, 1491–1502. doi: 10.1177/0959683614544063

Dobrowolska, D., Bončina, A., and Klumpp, R. (2017). Ecology and silviculture of silver fir (Abies alba Mill.): A review. *J. For. Res.* 22, 326–335. doi: 10.1080/13416979.2017.1386021

Ellenberg, H. H. (1988). *Vegetation ecology of central Europe* (Cambridge: Cambridge University Press).

Ficko, A., Poljanec, A., and Boncina, A. (2011). Do changes in spatial distribution, structure and abundance of silver fir (Abies alba Mill.) indicate its decline? *For. Ecol. Manage.* 261, 844–854. doi: 10.1016/j.foreco.2010.12.014

Gams, I. (1969). Some morphological characteristics of the dinaric karst. *Geographical J.* 135 (4), 563–572.

Gazol, A., Camarero, J. J., Gutiérrez, E., Popa, I., Andreu-Hayles, L., Motta, R., et al. (2015). Distinct effects of climate warming on populations of silver fir (Abies alba) across Europe. *J. Biogeography* 42, 1150–1162. doi: 10.1111/jbi.12512

Giorgi, F., and Lionello, P. (2008). Climate change projections for the Mediterranean region. *Global planetary Change* 63, 90–104. doi: 10.1016/j.gloplacha.2007.09.005

Golonka, J., Pietsch, K., and Marzec, P. (2018). The north european platform suture zone in poland. *Geology Geophysics Environ.* 44, 5–16.

Grassi, G., and Bagnaresi, U. (2001). Foliar morphological and physiological plasticity in Picea abies and Abies alba saplings along a natural light gradient. *Tree Physiol.* 21, 959–967. doi: 10.1093/treephys/21.12-13.959

Harris, I., Jones, P. D., Osborn, T. J., and Lister, D. H. (2014). Updated high-resolution grids of monthly climatic observations–the CRU TS3. *10 Dataset. Int. J. climatology* 34, 623–642. doi: 10.1002/joc.3711

Hédl, R., Petřík, P., and Boublík, K. (2011). Long-term patterns in soil acidification due to pollution in forests of the Eastern Sudetes Mountains. *Environ. pollut.* 159, 2586–2593. doi: 10.1016/j.envpol.2011.06.014

Hohenadl, W. (1981). *Untersuchungen zur natürlichen Verjüngung des Bergmischwaldes: erste Ergebnisse eines Forschungsprojekts in den ostbayerischen Kalkalpen. na.*

Hukić, E., Čater, M., Marinšek, A., Ferlan, M., Kobal, M., Žlindra, D., et al. (2021). Short-term impacts of harvesting intensity on the upper soil layers in high karst Dinaric fir-beech forests. *Forests* 12, 581. doi: 10.3390/f12050581

Ishida, M. (2004). Automatic thresholding for digital hemispherical photography. *Can. J. For. Res.* 34, 2208–2216. doi: 10.1139/x04-103

Janík, D., Adam, D., Hort, L., Král, K., Šamonil, P., Unar, P., et al. (2014). Tree spatial patterns of Abies alba and Fagus sylvatica in the Western Carpathians over 30 years. *Eur. J. For. Res.* 133, 1015–1028. doi: 10.1007/s10342-014-0819-1

Janík, D., Král, K., Adam, D., Hort, L., Samonil, P., Unar, P., et al. (2016). Tree spatial patterns of Fagus sylvatica expansion over 37 years. *For. Ecol. Manage.* 375, 134–145. doi: 10.1016/j.foreco.2016.05.017

Körner, C., Basler, D., Hoch, G., Kollas, C., Lenz, A., Randin, C. F., et al. (2016). Where, why and how? Explaining the low-temperature range limits of temperate tree species. *J. Ecol.* 104, 1076–1088. doi: 10.1111/1365-2745.12574

Krecmer, V. (1967). Das mikroklima der kieferlochkahlschläge: III. *und IV. Teil. Wetter und Leben* 19, 107–115. 203–214.

Lambers, H., Chapin, F. S., and Pons, T. L. (1998). *Plant physiological ecology* (NewYork: Springer). doi: 10.1007/978-1-4757-2855-2

Larcher, W. (2003). *Physiological plant ecology: ecophysiology and stress physiology of functional groups* (New York: Springer Science & Business Media).

Leblanc, S. G., Chen, J. M., Fernandes, R., Deering, D. W., and Conley, A. (2005). Methodology comparison for canopy structure parameters extraction from digital hemispherical photography in boreal forests. *Agric. For. meteorology.* 129, 187–207. doi: 10.1016/j.agrformet.2004.09.006

Lee, H., Calvin, K., Dasgupta, D., Krinmer, G., Mukherji, A., Thorne, P., et al. (2023). *Synthesis report of the IPCC Sixth Assessment Report (AR6), Longer report* (Geneva, Switzerland: IPCC).

Lichtenthaler, H. K., Ač, A., Marek, M. V., Kalina, J., and Urban, O. (2007). Differences in pigment composition, photosynthetic rates and chlorophyll fluorescence images of sun and shade leaves of four tree species. *Plant Physiol. Biochem.* 45, 577–588. doi: 10.1016/j.plaphy.2007.04.006

Linares, J. C., and Camarero, J. J. (2012). Growth patterns and sensitivity to climate predict silver fir decline in the Spanish Pyrenees. *Eur. J. For. Res.* 131, 1001–1012. doi: 10.1007/s10342-011-0572-7

Londo, A. J., Messina, M. G., and Schoenholtz, S. H. (1999). Forest harvesting effects on soil temperature, moisture, and respiration in a bottomland hardwood forest. *Soil Sci. Soc Am. J.* 63, 637–644. doi: 10.2136/sssaj1999.03615995006300030029x

Łysik, M. (2009). A 13-year change in ground-layer vegetation of Carpathian beech forests. *Polish J. Ecol.* 57, 47–61.

Macfarlane, C., Coote, M., White, D. A., and Adams, M. A. (2000). Photographic exposure affects indirect estimation of leaf area in plantations of Eucalyptus globulus Labill. *Agric. For. meteorology.* 100, 155–168. doi: 10.1016/S0168-1923(99)00139-2

Maiorano, L., Cheddadi, R., Zimmermann, N., Pellissier, L., Petitpierre, B., Pottier, J., et al. (2013). Building the niche through time: using 13,000 years of data to predict the effects of climate change on three tree species in Europe. *Global Ecol. Biogeography* 22, 302–317. doi: 10.1111/j.1466-8238.2012.00767.x

Marinšek, A., Šilc, U., and Čarni, A. (2013). Geographical and ecological differentiation of F agus forest vegetation in SE Europe. *Appl. Vegetation Sci.* 16, 131–147. doi: 10.1111/j.1654-109X.2012.01203.x

Mauri, A., De Rigo, D., and Caudullo, G. (2016). *Abies alba in Europe: distribution, habitat, usage and threats* (Luxembourg: European Atlas of Forest Tree Species Publ. Off. EU). Available at: https://w3id.org/mtv/FISE-Comm/v01/e01493b.

Meier, E. S., Edwards, T. C. Jr., Kienast, F., Dobbertin, M., and Zimmermann, N. E. (2011). Co-occurrence patterns of trees along macro-climatic gradients and their potential influence on the present and future distribution of Fagus sylvatica L. *J. Biogeography* 38, 371–382. doi: 10.1111/jbi.2011.38.issue-2

Mellert, K. H., and Göttlein, A. (2012). Comparison of new foliar nutrient thresholds derived from van den Burg's literature compilation with established central European references. *Eur. J. For. Res.* 131, 1461–1472. doi: 10.1007/s10342-012-0615-8

Micu, D. M., Dumitrescu, A., Cheval, S., and Birsan, M.-V. (2016). *Climate of the Romanian carpathians* (Cham, Heildelberg, New York, Dordrecht, London: Springer).

Mihevc, A. (2010). "Geomorphology," in *Introduction to dinaric karst*. Eds. A. Mihevc, M. Prelovšek and N. Zupan Hajna (Postojna: IZRK, Slovenska akademija znanosti in umetnosti, Ljubljana), 30–43.

Mirek, Z., and Piekos-Mirkowa, H. (1992). Flora and vegetation of the polish tatra mountains. *Mountain Res. Dev.* 12 (2), 147–173. doi: 10.2307/3673788

Nagel, T. A., Mikac, S., Dolinar, M., Klopčič, M., Keren, S., Svoboda, M., et al. (2017). The natural disturbance regime in forests of the Dinaric Mountains: A synthesis of evidence. *For. Ecol. Manage.* 388, 29–42. doi: 10.1016/j.foreco.2016.07.047

Nicolini, É., and Caraglio, Y. (2011). L'influence de divers caract??res architecturaux sur l'apparition de la fourche chez le Fagus sylvatica, en fonction de l'absence ou de la pr??sence d'un couvert. *Can. J. Bot.* 72, 1723–1734. doi: 10.1139/b94-213

Nobis, M., and Hunziker, U. (2005). Automatic thresholding for hemispherical canopy-photographs based on edge detection. *Agric. For. meteorology.* 128, 243–250. doi: 10.1016/j.agrformet.2004.10.002

Piedallu, C., Gégout, J. C., Perez, V., and Lebourgeois, F. (2013). Soil water balance performs better than climatic water variables in tree species distribution modelling. *Global Ecol. Biogeography* 22, 470–482. doi: 10.1111/geb.12012

Rădulescu, D. P., and Săndulescu, M. (1973). The plate-tectonics concept and the geological structure of the carpathians. *Tectonophysics* 16, 155–161. doi: 10.1016/0040-1951(73)90010-3

Robakowski, P., Wyka, T., Samardakiewicz, S., and Kierzkowski, D. (2004). Growth, photosynthesis, and needle structure of silver fir (Abies alba Mill.) seedlings under different canopies. *For. Ecol. Manage.* 201, 211–227. doi: 10.1016/j.foreco.2004.06.029

Rolland, C., Michalet, R., Desplanque, C., Petetin, A., and Aimé, S. (1999). Ecological requirements of Abies alba in the French Alps derived from dendro-ecological analysis. *J. Vegetation Sci.* 10, 297–306. doi: 10.2307/3237059

Šamonil, P., Antolík, L., Svoboda, M., and Adam, D. (2009). Dynamics of windthrow events in a natural fir-beech forest in the Carpathian mountains. *For. Ecol. Manage.* 257, 1148–1156. doi: 10.1016/j.foreco.2008.11.024

Šamonil, P., and Vrška, T. (2007). Trends and cyclical changes in natural fir-beech forests at the north-western edge of the Carpathians. *Folia Geobotanica* 42, 337–361. doi: 10.1007/BF02861699

Schütz, J. P. (2002). Silvicultural tools to develop irregular and diverse forest structures. *Forestry* 75, 329–337. doi: 10.1093/forestry/75.4.329

Schütz, J.-P., Saniga, M., Diaci, J., and Vrška, T. (2016). Comparing close-to-naturesilviculture with processes in pristine forests: lessons from Central Europe. *Ann. For. Sci.* 73, 911–921. doi: 10.1007/s13595-016-0579-9

Schwalbe, E., Maas, H.-G., Kenter, M., and Wagner, S. (2009). Hemispheric image modeling and analysis techniques for solar radiation determination in forest ecosystems. *Photogrammetric Eng. Remote Sens.* 75, 375–384. doi: 10.14358/PERS.75.4.375

Smith, D. D., Adams, M. A., Salvi, A. M., Krieg, C. P., Ane, C., McCulloh, K. A., et al. (2023). Ecophysiological adaptations shape distributions of closely related trees along a climatic moisture gradient. *Nat. Commun.* 14, 7173. doi: 10.1038/s41467-023-42352-w

Stancioiu, P. T., and O'Hara, K. L. (2006). Regeneration growth in different light environments of mixed species, multiaged, mountainous forests of Romania. *Eur. J. For. Res.* 125, 151–162. doi: 10.1007/s10342-005-0069-3

Svenning, J. C., and Skov, F. (2004). Limited filling of the potential range in European tree species. *Ecol. Lett.* 7, 565–573. doi: 10.1111/j.1461-0248.2004.00614.x

Tinner, W., Colombaroli, D., Heiri, O., Henne, P. D., Steinacher, M., Untenecker, J., et al. (2013). The past ecology of Abies alba provides new perspectives on future responses of silver fir forests to global warming. *Ecol. Monogr.* 83, 419–439. doi: 10.1890/12-2231.1

Vološčuk, I. (1999). *The national parks and biosphere reserves in carpathians: The last nature paradises* (Tatranska Lomnica, Slovak Republic: Association of the Carpathian National Parks and Biosphere Reserves), 244 p.

Vrška, T., Adam, D., Hort, L., Kolář, T., and Janík, D. (2009). European beech (Fagus sylvatica L.) and silver fir (Abies alba Mill.) rotation in the Carpathians—A developmental cycle or a linear trend induced by man? *For. Ecol. Manage.* 258, 347–356. doi: 10.1016/j.foreco.2009.03.007

Warszyńska, J. (1995). *The Polish Carpathians–nature, man and his activities* (Kraków, Poland: Jagiellonian University Publication), 1–367.

Weithmann, G., Paligi, S. S., Schuldt, B., and Leuschner, C. (2022). Branch xylem vascular adjustments in European beech in response to decreasing water availability across a precipitation gradient. *Tree Physiol.* 42, 2224–2238. doi: 10.1093/treephys/tpac080

Willner, W. (2002). Syntaxonomische Revision der südmitteleuropäischen Buchenwälder Syntaxonomical revision of the beech forests of southern Central Europe. *Phytocoenologia* 32, 337–453. doi: 10.1127/0340-269X/2002/0032-0337

Wyka, T., Robakowski, P., and Zytkowiak, R. (2007). Acclimation of leaves to contrasting irradiance in juvenile trees differing in shade tolerance. *Tree Physiol.* 27, 1293–1306. doi: 10.1093/treephys/27.9.1293

Yang, F., Burzlaff, T., and Rennenberg, H. (2022). Drought hardening of European beech (Fagus sylvatica L.) and silver fir (Abies alba Mill.) seedlings in mixed cultivation. *Forests* 13, 1386. doi: 10.3390/f13091386

Zhang, Y., Chen, J. M., and Miller, J. R. (2005). Determining digital hemispherical photograph exposure for leaf area index estimation. *Agric. For. meteorology* 133, 166–181. doi: 10.1016/j.agrformet.2005.09.009

frontiers | Frontiers in Plant Science

TYPE Original Research
PUBLISHED 24 May 2024
DOI 10.3389/fpls.2024.1351392

OPEN ACCESS

EDITED BY
Srdjan Stojnic,
University of Novi Sad, Serbia

REVIEWED BY
Vasileios Tzanakakis,
Hellenic Mediterranean University, Greece
Mirjana Bojović,
Faculty of Ecological Agriculture, University Educons, Sremska Kamenica, Serbia.

*CORRESPONDENCE
Hengjia Zhang
596088683@qq.com

RECEIVED 06 December 2023
ACCEPTED 03 May 2024
PUBLISHED 24 May 2024

CITATION
Bai Y, Zhang H, Jia S, Sun D, Zhang J, Zhao X, Fang X, Wang X, Xu C and Cao R (2024) Optimized sand tube irrigation combined with nitrogen application improves jujube yield as well as water and nitrogen use efficiencies in an arid desert region of Northwest China. *Front. Plant Sci.* 15:1351392. doi: 10.3389/fpls.2024.1351392

Optimized sand tube irrigation combined with nitrogen application improves jujube yield as well as water and nitrogen use efficiencies in an arid desert region of Northwest China

Youshuai Bai[1,2], Hengjia Zhang[1]*, Shenghai Jia[2], Dongyuan Sun[2], Jinxia Zhang[2], Xia Zhao[2], Xiangyi Fang[3], Xiaofeng Wang[2], Chunjuan Xu[2] and Rui Cao[2]

[1]College of Agronomy and Agricultural Engineering, Liaocheng University, Liaocheng, China, [2]College of Water Conservancy and Hydropower Engineering, Gansu Agricultural University, Lanzhou, China, [3]Qinfeng Forestry Experimental Station of Minqin County, Wuwei, China

Efficient water-saving irrigation techniques and appropriate nitrogen (N) application are keys to solving the problems of water scarcity and irrational fertilization in jujube cultivation. In this study, first, the effects of sand tube irrigation (STI) on surface and subsurface wetted characteristics were investigated using *in-situ* infiltration tests in a jujube garden. Compared with surface drip irrigation (SD), STI reduced surface wetted area by 57.4% and wetted perimeter of the surface wetted circle by 37.1% and increased subsurface maximum infiltration distance of wetting front by 64.9%. At the optimal sand tube depth of 20 cm, surface wetted area of the surface wetted circle decreased by 65.4% and maximum infiltration distance of the wetting front increased by 70.9%, compared with SD. Two-year field experiments then investigated the effects of STI and SD on soil water storage, jujube leaf chlorophyll, net photosynthetic rate, actual water consumption, fruit yield, and water (WUE) and N (NUE) use efficiencies at four levels of N (pure nitrogen: N1, 0; N2, 286 kg ha^{-1}; N3, 381 kg ha^{-1}; N4, 476 kg ha^{-1}) at the same irrigation amount (45 mm $irrigation^{-1}$, total of 8). Compared with SD, STI increased soil water storage 18.0% (2021) and 15.6% (2022) during the entire growth period and also chlorophyll content, nitrogen balance index, and net photosynthetic rate, with both increasing and then decreasing with increasing N. Compared with SD, STI increased yields by 39.1% and 36.5% and WUE by 44.3% and 39.7% in 2021 and 2022, respectively. Nitrogen use efficiency was 2.5 (2021) and 1.6 (2022) times higher with STI than with SD. STI combined with N3 had the highest yield, WUE,

NUE, and net income and is thus recommended as the optimal water–N combination. In conclusion, STI combined with appropriate N application can be an effective water-saving irrigation technology alternative to SD in jujube cultivation in arid areas.

KEYWORDS

in-suit infiltration test, jujube yield, nitrogen, sand tube irrigation, soil water storage, surface wetted area, WUE

1 Introduction

Water scarcity is a major challenge that generally leads to the current unbalanced development in social and economic systems and ecosystem degradation in arid regions (Zhu et al., 2023). Based on World Meteorological Organization statistics on the state of the global climate in 2022, global mean temperatures have been the highest on record for the past eight years (WMO, 2023). This warming trend will increase evaporation and crop water requirements and therefore threaten the stability of crop production in arid areas (Yu et al., 2018; Habib-Ur-Rahman et al., 2022; Wang et al., 2022c). According to Food and Agriculture Organization statistics, between 691 and 783 million people faced hunger in 2022 (FAO, 2023). In addition, approximately 29.6% of the global population have unsustainable access to food, and about 900 million people suffered from serious food security problems. Thus, mankind is currently facing the multiple crises and challenges of water scarcity, climate change, and food security.

Micro-irrigation technology has provided strong impetus for sustainable development of agriculture in dry areas and has been widely applied in various crops (Madramootoo and Morrison, 2013; Mattar et al., 2021; Nazari et al., 2021; Zhang et al., 2022). Micro-irrigation delivers water and nutrients uniformly and accurately directly to the soil near crop roots at a relatively low flow rate through a pipeline system with emitters (Goyal, 2014; Liu et al., 2021). Drip irrigation is considered one of the most water-efficient micro-irrigation techniques. Integration of water and fertilizer technologies has significantly improved crop yields and water and nitrogen (N) use efficiencies and has been used extensively in arid agricultural production (Surendran et al., 2016; Fan et al., 2020; Ma et al., 2021; Cao et al., 2022). However, surface drip irrigation (SD) has a large, wetted surface area and also tends to form puddles in the saturated zone below the emitter, and therefore, surface evaporation cannot be ignored in arid environments. As a result, subsurface drip irrigation (SDI) is widely used to reduce surface evaporation and improve yields and water productivity (Payero et al., 2008; Kandelous and Šimůnek, 2010; Martínez and Reca, 2014; Sandhu and Irmak, 2022; Wang et al., 2022a). SDI reduces crop seasonal evapotranspiration by 39% because of water diffusion under the soil surface, compared with sprinkler irrigation (Valentín et al., 2020). Wang et al. (2022b) found that SDI increased yields by 19.8% compared with those with SD. SDI has gained momentum due to its advantages such as reduced evaporation and increased yields. However, drip emitter clogging is a major challenge in the application and development of drip irrigation technology (Niu et al., 2013). Similarly, drip emitter clogging is a primary obstacle to the widespread and effective application of subsurface drip irrigation technology (Niu et al., 2013; Muhammad et al., 2022). Muhammad et al. (2022) identified root invasion as the main cause of emitter clogging in subsurface drip irrigation systems. Therefore, it is urgent to explore new SDI technologies that can reduce surface evaporation, have higher flow rates and resist clogging.

Sand tube irrigation (STI) is a type of SDI in which a cylindrical soil pit is dug below the drip emitter and filled with fine sand (Meshkat et al., 1999, Meshkat et al, 2000). The fine sand can quickly infiltrate drip water down to a certain depth in the crop root system. In a laboratory experiment, Meshkat et al. (1999) reported that STI can reduce soil evaporation by about 26% over a 4-day period, compared with SD. In addition, a setup similar to that with STI for jujube trees improved jujube yield, fruit quality, and WUE and also significantly slowed secondary soil salinization (Sun et al., 2016). Bai et al. (2022) demonstrated that STI increased jujube yield and water use efficiency by increasing soil water storage and reducing soil water deficit. Therefore, STI may be one of the important alternative technologies to SD and conventional SDI.

To meet the quadrupling of global demand for food and feed, N fertilizer inputs in cropping systems increased fivefold from 1961 to 2015 (Zhang et al., 2021). Nitrogen is an essential ingredient in amino acids, proteins, nucleic acids, and chlorophyll and is therefore one of the most significant nutrient elements for plant growth and development and yield formation (Marschner, 2011; Larimi et al., 2014; Wen et al., 2020). Therefore, N utilization is one of the key factors in achieving high crop yields (Min et al., 2021). However, excessive N fertilization can lead to a series of negative effects, such as sharp declines in N use efficiency (NUE), increases in ammonia volatilization and greenhouse gas emissions, and increases in agricultural surface pollution (Zhong et al., 2016; Guo et al., 2021). Moreover, excessive N application always promotes crop vegetative growth, which inhibits the transformation of dry matter from vegetative to reproductive growth and thus reduces final crop yield (Wang et al., 2021c). Application of N fertilizers requires a compromise between increasing crop yields and avoiding serious environmental effects

(Lassaletta et al., 2023). Additionally, effective improvement in NUE and reduction in ammonia volatilization are essential for sustainable agricultural development and environmental protection (He et al., 2022). Therefore, improvements in agricultural water productivity and NUE are important measures to ensure food security (Zhang et al., 2015; Kang et al., 2017).

Jujube (*Ziziphus jujuba Mill.*) has been cultivated for more than 4000 years in China. According to the 2021 China Rural Statistics Yearbook, the national production of jujube in 2020 and 2021 is 7.7 and 7.4 million tons, respectively (Department of Rural Socio-Economic Survey, 2021). It is cultivated over 3 million hectares and accounts for more than 98% of global production (Shen et al., 2021). This jujube fruit is popular among consumers for its flavor and high nutritional value (including vitamin C, amino acids, proteins and polysaccharides) (Rashwan et al., 2020; Dou et al., 2023). Jujube trees are ecologically and economically important tree species that are drought-resistant, can survive in barren lands, and play very important roles in higher incomes for farmers, environmental protection, and ecological construction in arid areas around the world. Currently, jujube sustainable production is constrained primarily by water shortages and increased production costs.

According to the above analyses, STI is more effective than SD in increasing soil water storage and reducing soil evaporation, while N is an extremely important nutritional element for crop physiology and growth. Therefore, it is necessary to investigate the effects of different N application rates on leaf chlorophyll, nitrogen balance index (NBI), photosynthetic rate,and water consumption of jujube trees under these two irrigation methods. Simultaneously, it is essential to investigate whether there is any room for further increasing yield and WUE through reasonable N application combined with sand tube irrigation. Although studies on subsurface drip irrigation have been conducted (Meshkat et al., 1998, Meshkat et al, 2000; Sun et al., 2016), few have conducted *in-situ* infiltration tests with STI or examined effects of jujube nitrogen regulation on soil water storage and jujube growth, yield, WUE, and NUE in arid desert areas.

Thus, the study aimed to: (1) determine the optimal STI technology parameters by exploring soil wetted characteristics of surface and subsurface vertical profiles; (2) investigate the effects of different N amounts under STI and SD on soil water storage, jujube leaf chlorophyll, NBI, net photosynthetic rate, actual water consumption, jujube fruit yield, WUE, NUE, and net income.

2 Materials and methods

2.1 Field *in-situ* soil water infiltration test

The field *in-situ* soil water infiltration test was conducted in the jujube orchard (38°43'N, 103°01'E) of Qinfeng Forestry Experimental Station, Minqin County, Gansu Province, China. Following surface leveling, STI and drip irrigation infiltration systems were installed in dry soil of the jujube orchard on a sunny day. The soil moisture infiltration system consisted of a Mariotte's bottle, a water supply pipe, drip emitters (flow rate = 4 L/h), a fixed bracket, and sand tube (filled with 2–3 mm in diameter of fine sand) laid below the drip emitter (Figure 1). The test was set up with four treatments: SD (D0) and STI with sand tube depths of 10 cm (S1), 20 cm (S2), and 30 cm (S3). There were three replications of each treatment. Sand tube diameter was 10 cm in STI treatments. All surface wetting was approximately circular because the irrigation was point-source drip irrigation. Thus, surface wetting was characterized by average diameter of a wetted circle, wetted area, and wetted perimeter. A ruler (mm) was used to measure the diameter of a wetted circle during the infiltration process. The wetted surface area and perimeter were determined based on the mulching film method (Guan et al., 2016). Specifically, at the end of the test, clean, clear film was placed on the wetted surface (including horizontal surface and vertical profile), and the location of the wetted front was drawn. Subsequently, a photograph was taken directly above the drawing, imported into Auto CAD 2014 software, and the wetting front on the picture was plotted with a spline curve.

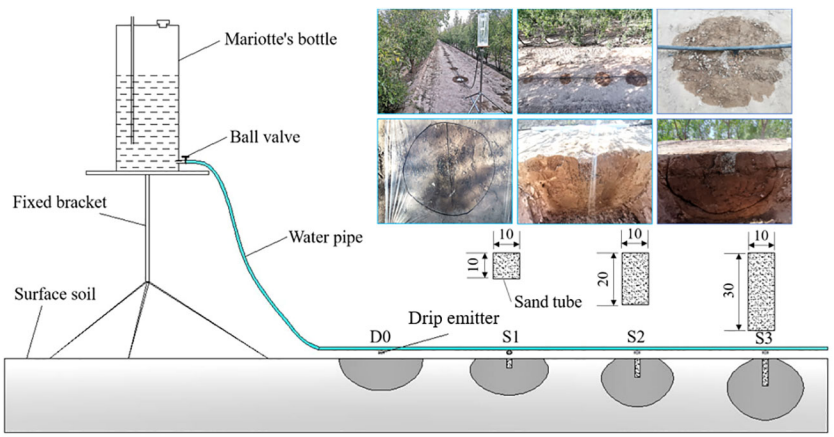

FIGURE 1
Schematic of the infiltration equipment.

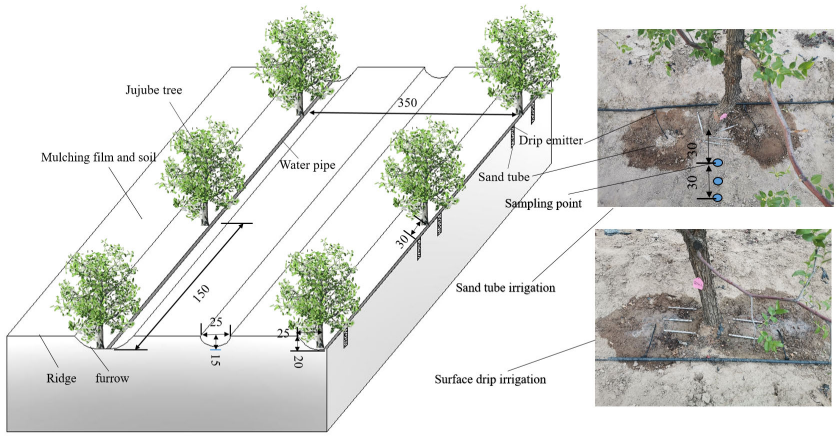

FIGURE 2
Design of field experiment.

Then, the area and perimeter were determined with the AREA command. In addition, the vertical profile was located in the center plane of the sand tube (Figure 1).

2.2 Field experiment

2.2.1 Experimental site and field conditions

The field experiments were conducted at the same locations as the *in-situ* soil infiltration tests (Figure 2). The climate of the area is continental desert climate. Annual average rainfall is 110 mm, and annual average air temperature is 7.8 °C. Groundwater depth is below 40 m. Average annual evaporation is 2,644 mm. Soil physical parameters are shown in Table 1. Field capacity and bulk density were determined by the cutting ring method (Duan et al., 2010), and soil particle size distribution was determined by the Laser Diffraction Particle Size Analyzer-Mastersizer 2000 (Malvern Instruments Co., Ltd, Malver, UK). According to the method of Bao (2000), soil nutrients contents were the following: organic matter: 5.3 g kg^{-1}; total N: 0.4 g kg^{-1}; total phosphorus: 0.5 g kg^{-1}; total potassium: 17.1 g kg^{-1}; alkaline dissolved N: 52.9 mg kg^{-1}; effective phosphorus: 18.8 mg kg^{-1}; quick-acting potassium: 85.1 mg kg^{-1}.

2.2.2 Field experimental design

Field irrigation experiments were carried out from May to October in 2021 and 2022 using 8-year-old jujube trees (*Ziziphus jujuba Mill, jun-jujube*) (Figure 2). The jujube trees monitored were of the same size (height of 250 to 300 cm), uniform and well-grown. Jujube tree row and plant spacing were 3.5 m and 1.5 m, respectively, and the field irrigation pipeline arrangement is shown in Figure 2. Irrigation water amount was controlled and monitored by a water meter (0.0001 m^3). Irrigation water met the water quality (pH, Salinity, and Electrical conductivity of 7.2, 2.9 ppt, and 6.2 μS cm^{-1}, respectively.) requirements for drip irrigation by filtration. Jujube trees were planted in furrows, and the rows were ridged with mulched film and a layer of soil.

To reduce surface evaporation and increase water content of deeper soils and preferential flow characteristics of plant root systems (Cui et al., 2021), a comprehensive assessment determined the optimal sand tube depth was 20 cm, with a tube diameter of 10 cm and with tubes filled with fine sand (2–3 mm in diameter). Each sand tube was arranged with a emitter with the 4 L h^{-1} flow rate. STI and SD were designed to provide the same irrigation amount (45 mm $irrigation^{-1}$, total of 8) under four levels of N (pure nitrogen: N1, 0; N2, 286 kg ha^{-1}; N3, 381 kg ha^{-1}; N4, 476 kg ha^{-1}) based on local, traditional fertilization experience. Nitrogen fertilizer type is urea ($CO(NH_2)_2$, 46.6% nitrogen). The method of fertilizer application is hole fertilization. Fertilizer application location is 30 cm away from the jujube tree, 20 cm in depth, and located on both sides of the jujube tree. The STI treatments were SN1, SN2, SN3, and SN4, and the SD treatments were DN1, DN2, DN3, and DN4. Each treatment was set up with 45 jujube trees as a plot and the area of each plot was 236 m^2. Each

TABLE 1 Soil physical parameters at different depths from 0 to 100 cm.

Soil depth (cm)	Soil particle size composition(mm)			Bulk density (g cm^{-3})	Field capacity (mass water content, %)
	<0.002	0.002–0.05	0.05–2		
0–20	14.87	48.77	36.36	1.43 ± 0.13	20.0
20–40	16.39	51.44	32.17	1.56 ± 0.07	
40–60	16.98	43.27	39.74	1.65 ± 0.06	
60–100	17.22	69.75	13.03	1.51 ± 0.15	16.17

TABLE 2 Field irrigation and nitrogen application management strategies for different periods of jujube growth in 2021 and 2022.

Growth period		Leaf emergence	Flowering		Fruit swelling			Fruit maturation	
2021	Irrigation date	5.11	6.1	6.21	7.6	7.21	8.6	8.21	9.6
	Irrigation amount (mm)	45	45	45	45	45	45	45	45
	Nitrogen amount (total N%)	/	30%	30%	40%			/	
2022	Irrigation date	5.7	5.28	6.18	7.4	7.2	8.6	8.19	9.1
	Irrigation amount (mm)	45	45	45	45	45	45	45	45
	Nitrogen amount (total N%)	/	30%	30%	40%			/	

treatment was three replications and three jujube trees were selected for each replication. Field irrigation and N application management strategies during different periods of jujube growth in 2021 and 2022 are shown in Table 2.

2.2.3 Measurements and calculations

2.2.3.1 Weather conditions

Meteorological data of precipitation, relative air humidity, maximum temperature, minimum temperature, air pressure, solar radiation, and wind speed were recorded at 30-min intervals based on an automated meteorological monitoring station (TRM-ZS2, Sunshine Meteorology Co., LTD., Liaoning, China) installing at the experimental site. Precipitation was 82.5 mm in 2021 and 99.7 mm in 2022, of which the effective precipitation (≥5 mm) was 50.2 mm in 2021 and 67.1 mm in 2022 during the whole growth stages. In 2021, average monthly maximum temperature was 34.4°C in July, and average monthly minimum was 6.1°C in May. In 2022, average monthly maximum temperature was 33.2°C in July, and average monthly minimum temperature was 9.1°C in May (Figure 3).

2.2.3.2 Soil water storage

Soil samples were collected at 30~60 cm (3 points uniformly) from the trunk of jujube trees with an iron soil auger (inner diameter of 40 cm) at 10-cm intervals from 0 to100 cm soil layer. Soil water content (gravimetric) was measured before and after each irrigation and determined by oven-drying. The original soil samples

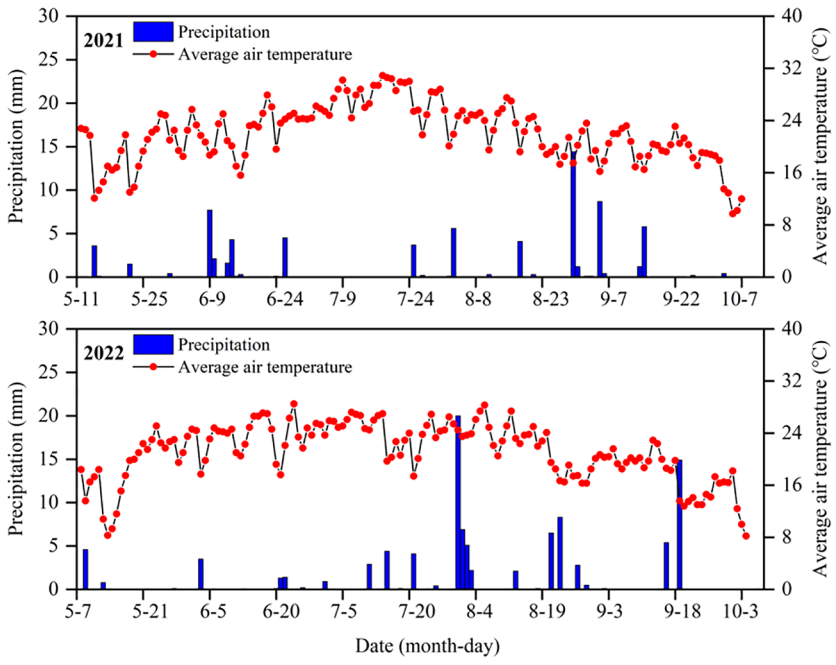

FIGURE 3
Daily precipitation and average air temperature during the growth period of jujube trees in 2021 and 2022.

were re-backfilled after soil sampling. Each treatment was three replications. Soil water storage was calculated by the following formula (Liu et al., 2018):

$$SWS = \sum_{i=10}^{n} H_i \times B_i \times \theta_i \times 10^{-1} \quad i = 10, 20, \ldots, 100 \tag{1}$$

where SWS, H_i, B_i, and θ_i are the soil water storage (mm), the soil depth (cm), the soil bulk density (g cm^{-3}), and the soil water content (gravimetric, %), respectively, of the ith soil layer.

2.2.3.3 Leaf chlorophyll content and net photosynthetic rate

Leaf chlorophyll content and NBI was measured by a Dualex 4 Scientific+ (FORCE-A, Orsay, France). Net photosynthetic rate (Pn) was measured with an Li-6400 photosynthesis system (Li-cor, Lincoln, USA). Net photosynthetic rate (μmol m^{-2} s^{-1}) was measured at 10:00 AM on a clear morning. When measurements were taken, monitoring was repeated for three consecutive days and at one-week intervals. To minimize errors due to time points, the next monitoring was done in the reverse order of the previous one. Four leaves of each jujube tree with different orientations were measured, and the average value (replicated three times) was used as the final monitoring result.

2.2.3.4 Yield, crop actual evapotranspiration, WUE, and NUE

Jujube fruits were harvested on October 7–8, 2021, and October 4–5, 2022. Jujube yield (Y, kg $plant^{-1}$) was the all fruits weight of per tree.

Crop actual evapotranspiration (ET_a, mm) was calculated by the following equation (Lu et al., 2021):

$$ET_a = I + P + \Delta W - D - R \tag{2}$$

where I, P, ΔW, D, and R are the irrigation amount (mm), the effective precipitation, the soil water storage in the 0–100 cm soil layer from leaf emergence to fruit maturation periods, the deep seepage, and the rainfall runoff, respectively. Deep seepage and rainfall runoff were ignored because of the application of drip irrigation with low flow rates and no rainfall runoff during the entire jujube growth period.

Water use efficiency (WUE, kg m^{-3}), and Irrigation water use efficiency (IWUE, kg m^{-3}) were calculated by the following two formulas:

$$\mathrm{WUE} = \frac{Y}{ET_a} \tag{3}$$

$$IWUE = \frac{Y}{I} \tag{4}$$

Nitrogen use efficiency (NUE, kg kg^{-1}) was calculated by the following formula:

$$NUE = \frac{Y_N - Y_0}{M_N} \tag{5}$$

where Y_N, Y_0, M_N are the Y (kg ha^{-1}) of an N fertilizer treatment, the Y (kg ha^{-1}) of a no N fertilizer treatment, and the total N fertilizer amount (kg ha^{-1}) for a treatment, respectively.

2.2.3.5 Comprehensive analysis of economic benefits

The comprehensive analysis of economic benefits is calculated according to the following formula:

$$E_{net} = E_{output} - E_{input} \tag{6}$$

Where E_{net} is the net income (\$ ha^{-1}), E_{output} is the total output (\$ ha^{-1}), and E_{input} is the total input (\$ ha^{-1}). The total input includes irrigation water charge, fertilizer input, labor costs, and consumables such as irrigation pipes, emitters and their accessories. The irrigation water charge is based on the cost price of water published by the local government for that year. In addition, sand tube irrigation requires additional consumables (fine sand) and labor costs compared with surface drip irrigation.

2.3 Statistical analyses

Excel 2016 (Microsoft Corporation, WA, USA) was conducted to data analysis. OriginPro 2018 (Origin Lab, MA, USA) was used to create figures. With SPSS 22 software (SPSS Inc., Chicago, IL, USA), one-way ANOVA was used to assess treatment effects, Pearson's correlation analysis was used to analyze the correlation between indicators under different treatments, and the LSD method was used to compare differences among means (p = 0.05). Auto CAD 2014 software (Autodesk, CA, USA) was used to create partial sketches and perform calculations of wetted soil area and perimeter.

3 Results

3.1 Soil water transportation under STI and SD

3.1.1 Diameter of surface wetted circle

The relation between diameter of surface wetted circle (D_c) and irrigation time is shown in Figure 4. The D_c increased with increasing irrigation time in each treatment. During the entire infiltration process, SD (D0) diameter was significantly (p< 0.01) larger than that with STI, although surface wetting occurred in S3.

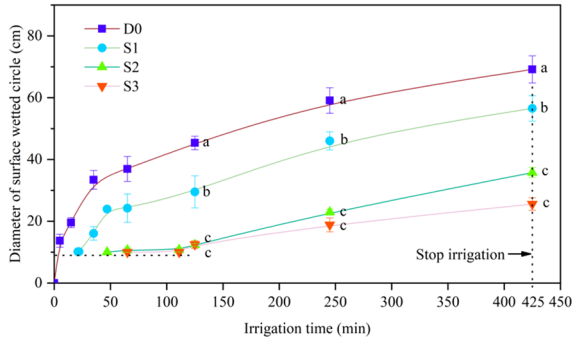

FIGURE 4
Variations in diameter of surface wetted circle with irrigation time. Different lowercase letters indicate significant differences at p< 0.05. Bars indicate the standard error.

At the end of irrigation, the D_c of D0 was 1.2, 1.9, and 2.70 times larger than that in S1, S2, and S3, respectively. In addition, the D_c in S1 was significantly larger than that in S2 and S3 by 58.1% and 121.0%, respectively, whereas there was no significant difference between S2 and S3. During the experiment, a surface water puddle was discovered at 15 min of irrigation in D0 and at 115 to 121 min in S1. Surface water puddles did not form in either S2 or S3 when irrigation ceased. At the beginning of infiltration, surface wetting in S1, S2, and S3 first appeared at 21 min, 47 min, and 111 min, respectively (Table 3). Exponential (R^2> 0.9, p< 0.001) and linear (R^2> 0.9, p< 0.01) functions best fit the variation in D_c of D0 and of STI, respectively, with irrigation time (Table 3).

3.1.2 Surface wetted characteristics after 720 min of irrigation

Variations in D_c, wetted area (A_c), and wetted perimeter (P_c) of the surface wetted circle in each treatment after 720 min of irrigation are shown in Figure 5. With an increase in sand tube depth, D_c, A_c, and P_c all decreased, and there were significant negative correlations with sand tube depth (p< 0.001). In addition, the D_c in D0 was not significantly different compared with that in S1 but was significantly different compared with that in S2 and S3, whereas there was no significant difference between S2 and S3. Both A_c and P_c were significantly greater with SD than with STI. The A_c in D0 was 1.4, 2.9, and 4.7 times greater than that in S1, S2, and S3,

TABLE 3 Functions describing relations between surface wetted circle diameter and irrigation time.

Treatment	Fitting equations	Time allocation (min)	R^2	F	P
D0	$f(t)$ =65.699−57.694$e^{-0.011t}$	t∈(0, 425)	0.951	119.659	<0.001
S1	$f(t)$ =(0,10) $f(t)$ =13.348+0.112t	t∈(0, 21) t∈(21, 425)	0.919	68.283	<0.01
S2	$f(t)$ =(0,10) $f(t)$ =4.943+0.072t	t∈(0, 47) t∈(47, 425)	0.979=	186.882	<0.001
S3	$f(t)$ =(0,10) $f(t)$ =5.989+0.047t	t∈(0, 111) t∈(111, 425)	0.975	76.840	<0.05

D0 is surface drip irrigation (SD), and S1, S2, S3 are STI with sand tube depths of 10 cm, 20 cm, and 30 cm in the in-situ infiltration test.

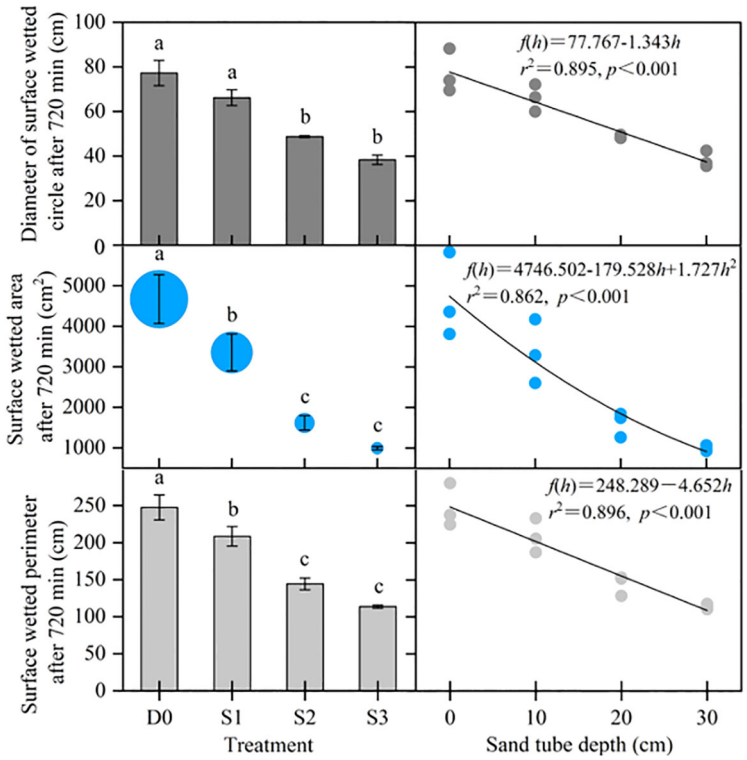

FIGURE 5
Surface wetted characteristics after 720 min of irrigation. Different lowercase letters indicate significant differences at p< 0.05. Bars indicate the standard error.

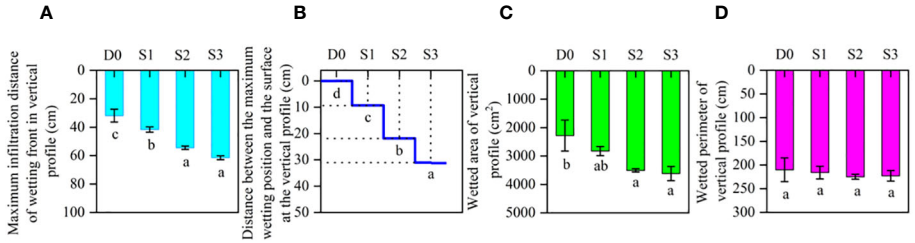

FIGURE 6
Characteristics of water infiltration in vertical soil profiles. **(A)** Maximum infiltration distance of the wetting front in vertical profile (cm). **(B)** Distance between the maximum wetting position and the surface in vertical profile (cm). **(C)** Wetted area of soil vertical profiles (cm2). **(D)** Wetted perimeter of soil vertical profiles (cm). Different lowercase letters indicate significant differences at p< 0.05. Bars indicate the standard error.

respectively. Differences in A_c between S1 and S2 and S3 were significant but not that between S2 and S3. Differences in P_c between S1 and S2 and S3 were significant but not that between S2 and S3.

3.1.3 Characteristics of water infiltration in vertical soil profile at the end of irrigation after 720 min

Variations in maximum infiltration distance of the wetting front (D_f), distance between the maximum wetting location and the surface (D_l), wetted area (A_p), and wetted perimeter (P_p) for soil vertical profiles in each treatment are shown in Figures 6A–D The D_f increased with increasing of sand tube depth, and compared with SD, STI treatments (S1, S2, and S3) significantly ($p< 0.05$) increased D_f by 30.68%, 70.9%, and 93.2%, respectively. The D_f was not significantly different between S2 and S3. The D_l of treatments changed significantly with the increase in infiltration depth. The maximum infiltration depth of D_l was in S3 (31.1 cm), and the minimum was with SD (0 cm). Compared with SD, the A_p in S2 and S3 increased significantly by 53.8% and 58.7%, respectively. Compared with D_0, although differences among treatments were not significant, the P_p in S2 and S3 increased by 7.1% and 6.1%, respectively.

3.2 Field nitrogen regulation experiments in a jujube tree orchard

3.2.1 SWS

Compared with SD, STI significantly increased ($p< 0.05$) average SWS (Equation 1) over the entire growth period 18.0% in 2021 and 15.6% in 2022 (Table 4). The maximum value of SWS in both years was in SN1, and the minimum value was in DN2. Compared with SD, in the leaf emergence period, SWS increased by 22.1% in 2021 and by 12.4% in 2022 in STI treatments. The minimum values of SWS were in SN3 and DN2. In the flowering period, compared with SDI, SWS increased by 19.5% in 2021 and by 16.0% in 2022 in STI treatments. Under the same irrigation pattern, differences in SWS among treatments were not significant, except for SN1 in 2021, which was significantly different compared with that in SN2 and SN3. The lowest SWS of STI treatments was in SN3, which was related to the increased water requirement of jujube trees due to the application of fertilizers during the period. The fruit-swelling period is the longest period with and the highest water demand and thus is the critical period of yield formation for jujube trees. Compared with SD, SWS increased by 14.2% in 2021 and by 20.8% in 2022 ($p< 0.05$) in STI treatments. In the fruit maturation period, compared with SD, SWS in STI treatments increased by

TABLE 4 Effects of different nitrogen treatments on soil water storage (mm) during growth periods of jujube trees under sand tube irrigation and surface drip irrigation in 2021 and 2022.

Treatment	Growth period									
	Leaf emergence		Flowering		Fruit swelling		Fruit maturation		Average of entire growth period	
	2021	2022	2021	2022	2021	2022	2021	2022	2021	2022
SN1	224.0 ab	239.0 a	234.3 a	230.8 a	216.3 a	231.1 a	207.6 a	231.5 a	220.6 a	233.1 a
SN2	212.2 ab	233.7 a	207.7 bc	224.7 ab	197.0 bc	229.0 a	205.4 a	218.1 ab	205.6 b	226.4 ab
SN3	208.4 bc	222.2 ab	214.4 b	214.9 abc	199.4 bc	208.6 b	204.8 a	218.6 ab	206.7 b	216.1 b
SN4	231.3 a	234.8 a	217.1 ab	238.0 a	203.9 ab	226.4 ab	210.9 a	229.3 a	215.8 ab	232.1 a
DN1	182.9 d	220.8 ab	190.5 cd	182.5 d	168.1 e	187.3 c	171.9 b	205.8 bcd	178.4 c	199.1 c
DN2	162.4 e	187.9 c	174.1 d	203.5 bcd	175.4 de	182.6 c	179.4 b	187.3 d	172.8 c	190.3 c
DN3	180.8 de	207.8 b	192.0 cd	195.4 cd	186.7 cd	187.3 c	182.2 b	191.0 cd	185.4 c	195.4 c
DN4	191.3 cd	210.5 b	174.3 d	201.5 bcd	185.1 cd	183.8 c	180.0 b	208.1 bc	182.7 c	200.9 c

Different lowercase letters indicate significant differences at p< 0.05 in the same column.

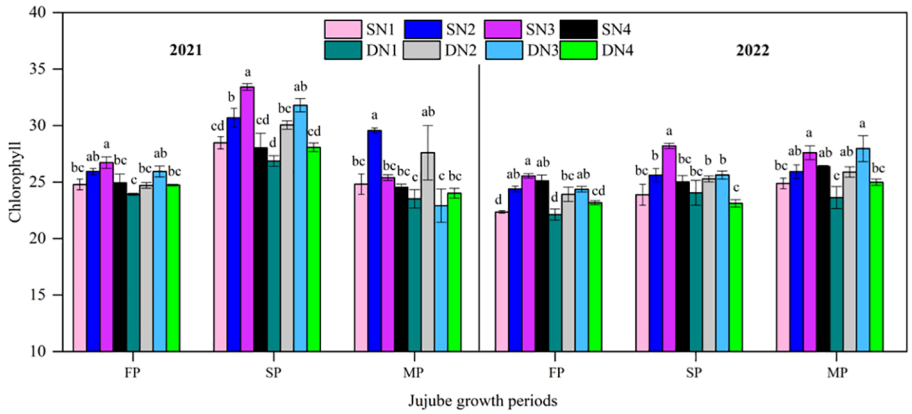

FIGURE 7
Leaf chlorophyll content in different nitrogen treatments with two irrigation methods during jujube growth periods in 2021 and 2022. FP, flowering period; SP, fruit-swelling period; MP, fruit maturation period. Different lowercase letters indicate significant differences at $p< 0.05$. Bars indicate the standard error. The same as below.

16.1% in 2021 and by 13.3% in 2022. Compared with DN3, SWS in SN3 increased significantly by 11.4% in 2021 and by 14.5% in 2022.

3.2.2 Leaf chlorophyll content and NBI

As jujube tree growth progressed, leaf chlorophyll content of treatments were showed an increase and then decline in 2021 and increased and then stabilized in 2022 (Figure 7). Compared with SD, STI increased leaf chlorophyll content over the entire growth period by 4.2% in 2021 and by 3.7% in 2022. In 2021, compared with SD, STI increased chlorophyll content by 3.1% at flowering, 3.3% at fruit swelling, and 6.4% at maturation. Similarly, in 2022, STI increased leaf chlorophyll content by 4.7% at flowering, 2.3% at fruit swelling, and 3.7% at maturation. Leaf chlorophyll content increased and then decreased with increasing N application with both STI and SD in 2021 and 2022. The maximum leaf chlorophyll content in 2021 and 2022 at flowering and fruit-swelling periods was in SN3. At fruit maturation, maximum values of chlorophyll content were in SN2 and DN3 in both years. In addition, leaf chlorophyll content in SN3 was significantly different compared with that in SN1 at both flowering and fruit swelling. At fruit maturation, leaf chlorophyll content in SN3 was significantly different from that in SN1 only in 2022. Minimum leaf chlorophyll content was in N1 treatments in both years in all growth periods under both irrigation patterns, except for the minimum value in DN3 at fruit maturation in 2021.

Figure 8 showed the changes of NBI at different growth periods for each treatment over the two years. For NBI, STI increased 6.9% (2021) and 4.9% (2022) on average compared with SD over the entire growth periods. In addition, NBI showed an increasing and then decreasing trend with increasing nitrogen application in this two irrigation methods. In both years, the SN3 was significantly higher than the SN1 at flowering and fruit swelling. Although SN4 applied more N than SN3, the former was significantly higher than the latter at fruit swelling. For SD, DN2 was the largest in 2021 and DN3 was the largest in 2022 during flowering and fruit swelling, and both were significantly higher than DN1 and DN4.

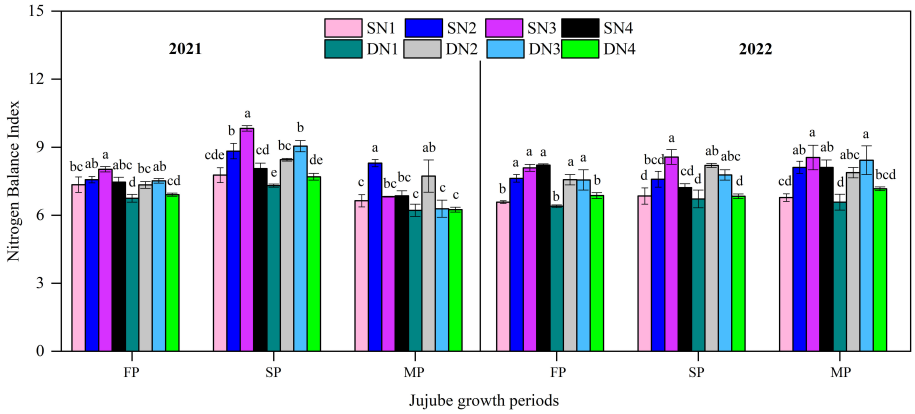

FIGURE 8
Nitrogen balance index in different nitrogen treatments with two irrigation methods during jujube growth periods in 2021 and 2022. Different lowercase letters indicate significant differences at p< 0.05. Bars indicate the standard error.

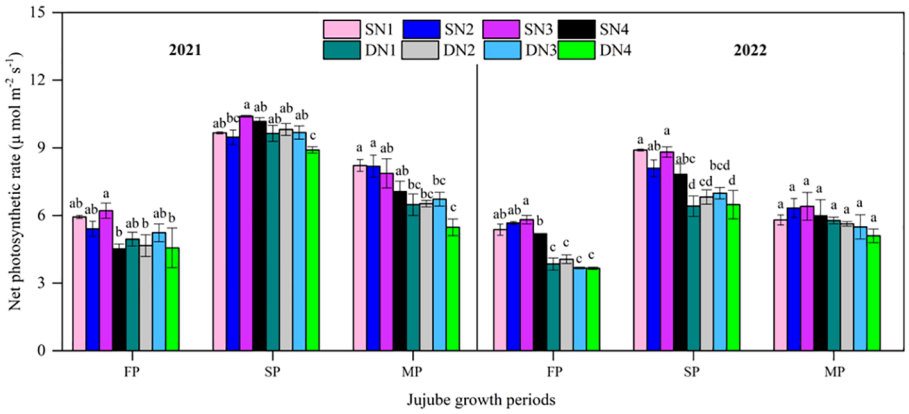

FIGURE 9
Net photosynthetic rate of different nitrogen treatments with two irrigation methods during jujube growth periods in 2021 and 2022. Different lowercase letters indicate significant differences at $p< 0.05$. Bars indicate the standard error.

3.2.3 Net photosynthesis rate

The net photosynthesis rate (Pn) in each treatment increased and then decreased during jujube growth in 2021 and 2022 (Figure 9). The maximum Pn was in the fruit swelling period, with 8.9–10.4 (2021) and 6.4–8.9 μmol m^{-2} s^{-1} (2022), and the minimum Pn was in the flowering period, with 4.5–6.2 (2021) and 3.7–5.8 μmol m^{-2} s^{-1} (2022). In 2021, compared with SD, Pn increased by 13.8% at flowering,4.4% at fruit swelling, and 24.3% at fruit maturation with STI. In 2022, compared with SD, Pn increased by 44.7% at flowering, 26.0% at fruit swelling, and 11.5% at fruit maturation. In 2021, the Pn between SN3 and SN4 at flowering and between SN2 and SN3 at fruit swelling was significantly different, whereas differences between other treatments were not significant. In 2022, the Pn in SN3 and SN4 at flowering was significantly different, whereas differences between other treatments were not significant. There were no significant differences in Pn among SD treatments for the entire growth period in either year.

3.2.4 Jujube yield, crop actual evapotranspiration, WUE, and NUE

Jujube yield (Y), crop actual evapotranspiration (ET_a, Equation 2), WUE (Equation 3), IWUE (Equation 4) and NUE (Equation 5) of each treatment are shown in Table 5. Yield increased and then decreased with increasing N amount for the same irrigation method. The yield in STI increased by 39.1% in 2021 and by 36.5% in 2022 compared with that in SD. In 2021, yield in SN3 was significantly higher than that in other treatments. In 2022, yield in SN3 was not significantly different compared with that in SN2 but was significantly different compared with that in the other treatments. Among SD treatments, the highest yields were in DN3 in both years, although differences among treatments were not significant. Compared with SD, ET_a in STI

TABLE 5 Effects of different nitrogen treatments on yield, crop actual evapotranspiration (ET_a), water use efficiency (WUE), and nitrogen use efficiency (NUE) of jujube trees under two irrigation methods in 2021 and 2022.

Treatment	2021					2022				
	Y (kg ha^{-1})	ET_a (mm)	WUE (kg m^{-3})	IWUE (kg m^{-3})	NUE (kg kg^{-1})	Y (kg ha^{-1})	ET_a (mm)	WUE (kg m^{-3})	IWUE (kg m^{-3})	NUE (kg kg^{-1})
SN1	8,782 cd	438.9 abc	2.0 cd	2.4 cd	–	9,387 bcd	424.4 bcd	2.2 bcd	2.6 bcd	–
SN2	10,325 b	388.3 c	2.7 ab	2.9 b	5.4 ab	11,560 ab	440.5 abc	2.6 ab	3.2 ab	7.6 ab
SN3	12,497 a	404.6 abc	3.1 a	3.5 a	9.8 ab	13,149 a	447.0 ab	2.9 a	3.7 a	9.9 a
SN4	9,677 bc	426.6 abc	2.3 bc	2.7 bc	1.9 b	10,177 bc	408.0 cd	2.5 abc	2.8 bc	1.7 b
DN1	6,801 e	444.1 ab	1.5 d	1.9 e	–	7,008 e	404.3 d	1.7 d	1.9 e	–
DN2	7,677 de	412.4 abc	1.9 cd	2.1 de	3.1 b	8,360 cde	455.9 ab	1.8 d	2.3 cde	4.7 ab
DN3	7,906 de	402.0 bc	2.0 cd	2.2 de	2.9 b	9,260 cde	469.3 a	2.0 d	2.6 cde	5.9 b
DN4	7,163 e	457.5 a	1.6 d	2.0 e	0.8 b	7,649 de	427.8 bcd	1.8 d	2.1 de	1.3 b

Different lowercase letters indicate significant differences at $p< 0.05$.

decreased by 3.4% in 2021 and by 2.1% in 2022. In 2021, ET_a in SN3 increased by 0.6% compared with that in DN3, but in 2022, ET_a in SN3 decreased by 4.8% compared with that in DN3, although the difference was not significant. Compared with SD, WUE in STI treatments increased by 44.3% in 2021 and by 39.7% in 2022. In addition, with both STI and SD, WUE increased and then decreased with increasing N application in 2021 and 2022. In both years, maximum WUE values were in SN3, and minimum WUE values were in DN1. In both years, WUE in STI treatments (except for SN1 and SN4 in 2021 and SN1 in 2022) was significantly higher than that in SD treatments. The IWUE is determined by the ratio of yield to irrigation amount. With both irrigation methods, IWUE increased and then decreased, with the largest value in SN3 and the smallest in DN1. In addition, IWUE with STI was 1.4 times higher than that with SD in both years. The NUE with STI was 2.5 times (2021) and 1.6 times (2022) higher than that with SD. The maximum NUE value was in SN3, and the minimum NUE value was in DN4 in both years. The NUE values in STI treatments increased and then decreased, whereas NUE values with SD showed instability (maximum values were in DN2 in 2021 and in DN3 in 2022).

Additionally, compared with N0, yield and WUE increased and then decreased with increasing N amount with the two irrigation methods. Increases in both yield and WUE were higher with STI than with SD. Specifically, the increases in yield were 23.4% in 2021 and 23.9% in 2022 with STI and 11.6% in 2021 and 20.2% in 2022 with SD. The increases in WUE were 33.6% in 2021 and 22.1% in 2022 with STI and 19.0% in 2021 and 7.7% in 2022 with SD. With STI, the maximum was in SN3, and the minimum was in SN4, and with SD, the maximum was in DN3, and the minimum was in DN4. When N treatments were compared with the previous level of treatment, yield and WUE increased in N2 and N3 treatments (SN2, SN3, DN2, and DN3) but decreased in N4 treatments (SN4 and DN4). With STI and SD at the same N level, the increases in yield were 29.2% to 57.9% in 2021 and 33.1% to 42.0% in 2022. The increases in WUE were 30.8% to 52.3% in 2021 and 27.1% to 49.0% in 2022. In addition, the maximum increases in yield and WUE were in SN3.

3.2.5 Pearson's correlation analyses

Pearson correlations between indicators under different treatments are shown in Figure 10. Yield was highly significantly ($p< 0.001$) positively correlated with WUE, IWUE, Chl, NBI, and Pn in both years. In 2021, ET_a was highly significantly negatively correlated with WUE and Chl and significantly negatively correlated with IWUE and Pn, but not in 2022. In addition, WUE was highly significantly positively correlated with IWUE, Chl, and Pn in both years. Simultaneously, IWUE was highly significantly positively correlated with both Chl, and Pn. However, ET_a and yield were not correlated.

3.2.6 Comprehensive analysis of economic benefits under two irrigation methods

There are larger differences in irrigation methods between STI and SD. The main difference between the two irrigation methods is mainly the different distribution of irrigation water in the soil. This ultimately leads to an increase in soil water storage for STI compared with SD. Additionally, there will be differences in total inputs between the two irrigation methods. The pursuit of net profit is the primary interest of the farmers. As shown in Table 6, the labor and consumables (fine sand) for arranging the sand tube increase their investment by $208 in 2021 compared with SD. In fact, fine sand is more abundant in the study area, which can reduce the cost of consumables. In 2022, the total investment was the same for both irrigation methods under the same fertilizer conditions. STI increased the net income by 23.5% (2021) and 20.3% (2022) compared with SD, respectively. The main reason for this is that the yield in STI increased by 39.1% in 2021 and by 36.5% in 2022 compared with that in SD (Table 5). The input-output ratio was also an important indicator of economic benefits. In both years, the input-output ratio of STI was lower than that of SD. When analyzed comprehensively, the SN3 treatment had the highest net income and the lowest input-output ratio in both years.

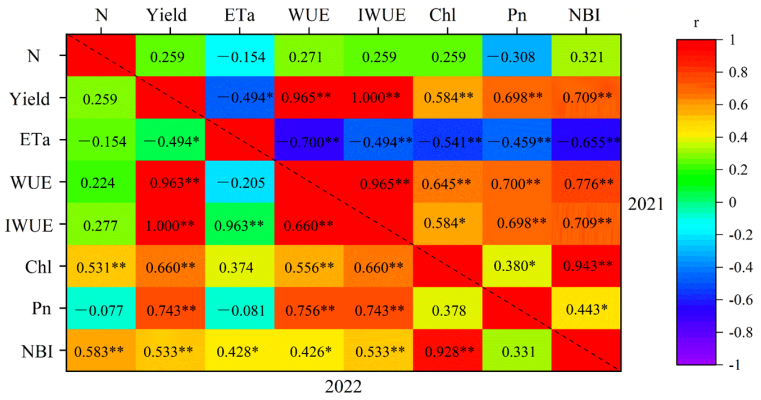

FIGURE 10
Pearson correlations (correlation coefficient *r*) between indicators under different treatments. *$p< 0.05$; **$p< 0.01$. N, nitrogen amount; Yield, jujube yield; ET_a, crop actual evapotranspiration; WUE, water use efficiency; IWUE, irrigation water use efficiency; Chl, Leaf chlorophyll content; Pn, net photosynthetic rate.

TABLE 6 Analysis of economic benefits (Equation 6) of sand tube irrigation and surface drip irrigation for jujube in 2021 and 2022.

Year	Treatment	Input ($ ha^{-1})				Output ($ ha^{-1})		Net income	Input-output ratio
		Water cost	Nitrogen cost	Labor and consumables	Total investment	Price ($ kg^{-1})	Total income	($ ha^{-1})	
2021	SN1	171	0	2,292	2,463	1	8,132	5,669	1:3.30
	SN2	171	181	2,292	2,644	1	9,561	6,917	1:3.62
	SN3	171	302	2,292	2,765	1	11,572	8,807	1:4.19
	SN4	171	363	2,292	2,825	1	8,961	6,136	1:3.17
	DN1	171	0	2,084	2,254	1	6,298	4,043	1:2.79
	DN2	171	181	2,084	2,436	1	7,109	4,673	1:2.92
	DN3	171	302	2,084	2,557	1	7,321	4,764	1:2.86
	DN4	171	363	2,084	2,617	1	6,633	4,016	1:2.53
2022	SN1	171	0	1,875	2,046	1	8,692	6,646	1:4.25
	SN2	171	181	1,875	2,227	1	10,704	8,477	1:4.81
	SN3	171	302	1,875	2,348	1	12,176	9,828	1:5.19
	SN4	171	363	1,875	2,409	1	9,424	7,016	1:3.91
	DN1	171	0	1,875	2,046	1	6,489	4,443	1:3.17
	DN2	171	181	1,875	2,227	1	7,741	5,514	1:3.48
	DN3	171	302	1,875	2,348	1	8,574	6,226	1:3.65
	DN4	171	363	1,875	2,409	1	7,083	4,674	1:2.94

4 Discussion

4.1 STI reduces surface wetted area and increases infiltration capacity

In this study, an *in-situ* test was conducted to optimize STI parameters, and then, infiltration in surface soil and subsurface soil vertical profiles was investigated in different treatments. Soil infiltration with STI has been investigated in the laboratory (Meshkat et al., 1998; Meshkat et al., 1999; Meshkat et al., 2000). However, in this study, the *in-situ* infiltration experiment was conducted in the field, with results reflecting actual soil structure and infiltration processes. The field investigation has important practical significance for selecting optimal sand tube parameters for field cultivation of jujube trees. In this study, STI significantly reduced A_c and increased maximum infiltration distance of the wetting front (Figures 5, 6). The results are in line with those of Bai et al. (2022), who reported that STI reduces A_c by 50.6% compared with SD. According to Meshkat et al. (2000), STI reduces evaporation by 39.8%, similar to the findings of the present study. Wang et al. (2020) found that introduction of infiltration holes significantly increased soil moisture (0 to 100 cm) in a semiarid, sloped shrubland. Those results are consistent with STI significantly increasing SWS compared with that with SD in this study.

The STI depth of 20 cm was selected for the cultivation of jujube trees in the field for the following reasons: (1) the main root layer of jujube trees is at 0–60 cm (Wang et al., 2015), (2) the root distribution of jujube trees and the formation of underground pore space may result in preferential flow that leads to deep seepage (Benegas et al., 2014; Cui et al., 2021; Li et al., 2023; Luo et al., 2023), (3) there was no significant difference in surface wetted area, maximum infiltration distance of the wetting front, and wetted area for vertical profiles between S2 and S3 in the *in-situ* test (Figures 5, 6), and (4) to reduce the investment in manpower and materials. In a similar study, Sun et al. (2016) developed an indirect subsurface drip irrigation system with vertical tubes (sand filled at the bottom) set at a depth of 25 cm. In addition, Wang et al. (2021) developed vertical-tube irrigation in jujube trees with a vertical-tube depth of 40 cm. The variation in technical parameters may be related to soil type, drip emitter flow rate, meteorological conditions, and tree age, among other factors, and which also needs to be determined on a case-by-case basis in conjunction with soil infiltration tests.

4.2 Nitrogen regulation with STI increases jujube chlorophyll content, NBI, and net photosynthetic rate

Because N is an essential component of chlorophyll molecular structure, N deficiency usually results in stunted plant growth and chlorotic leaves due to poor assimilate formation, which ultimately leads to premature flowering and a shortened growth cycle (Larimi

et al., 2014). In this study, chlorophyll content was highly significantly ($p< 0.001$) correlated with yield in 2021 and 2022 (Figure 10), which is in line with the findings on the application of nitrogen to jujube tree (Dai et al., 2019; Zhang et al., 2023).

In this study, chlorophyll content increased with increasing N application, but the highest N amount did not result in further increase in chlorophyll content. However, Pramanik and Bera (2013) found the highest N application had the highest chlorophyll content, although not the highest yield. The light energy converted into chemical energy by photosynthesis is absorbed by the plant green pigment chlorophyll (Simkin et al., 2022). In this study, appropriate N application was beneficial and increased chlorophyll content (Figure 7). NBI is an important indicator for assessing crop nitrogen deficiency and nitrogen management (Fan et al., 2022). Sun et al. (2018) showed that nitrogen sufficiency and deficiency were closely related to leaf color and chlorophyll content. In the present study, chlorophyll content was highly significantly positively correlated with NBI (Figure 10), and increasing nitrogen significantly increased chlorophyll content and NBI. In addition, the present study was also found that excessive nitrogen application decreased leaf chlorophyll content and NBI, which was similar to the findings of Bo et al. (2021). Leaf net photosynthetic rate varied inconsistently under both irrigation methods (Figure 9). During the flowering stage, Pn increased and then decreased with increasing N application. However, Pn decreased with increasing N application at maturity. The main reason for this result was because the low-N application had low fruit set percentage and less dry matter accumulation, which in turn reduced the excessive consumption of soil nutrients, and which was an important reason for the higher chlorophyll content under low N conditions (Figure 7).

4.3 Nitrogen regulation with STI increases jujube yield, WUE, and NUE

STI reduced the average ET_a (Table 5), which was associated with reduced evaporation of surface soil moisture. Evaporation from shallow soils increases due to the exposure of surface soils to solar radiation and soil capillary action (Andersen, 1968; Islam and Morimoto, 2015). These processes further increase soil moisture dissipation, leading to soil moisture deficit, and are one of the important factors associated with yield reduction under SD. In this study, there was no significant difference in ET_a between SN3 and DN3 (Table 6), but according to the *in-situ* infiltration test, the A_c of STI was significantly smaller than that of SD (Figure 5). This result also indicated that surface evaporation was greater in DN3 than in SN3, which was an important reason why the yield and WUE in SN3 were significantly higher than those with SD (Table 5). In this study, the average WUE with STI was 1.4 times greater than that with SD. This result is consistent with that of Wang et al. (2021c) who found that WUE of vertical-tube irrigation is 1.4–4.3 times that of SD. For average SWS, the maximum value in both years was in SN1, which was significantly higher than that in SN3. This result was related to the increase in N application, which promoted jujube growth and increased water consumption under the same irrigation condition (Table 5).

In related studies, crop yields do not increase linearly with increasing N applications (Széles et al., 2012; Guo et al., 2021). In the present study, jujube fruit yield increased and then decreased slightly with increasing N application. Similarly, Lu et al. (2021) showed that grain yields tended to increase and then remain stable with increasing N amount. In this study, WUE in SN3 increased significantly compared with that in SN1, whereas WUE in SN4 was not significantly different compared with that in SN1. Therefore, suitable N application significantly increased WUE but excessive N decreased WUE. The IWUE with STI was 1.4 times higher than that with SD in both years (Table 5), which indicated that STI is an advanced irrigation technology that increases water productivity compared with that with SD. The NUE with STI was 2.2 times higher than that with SD, which indicated that STI effectively improves NUE. The increases in SWS and yield with STI were important reasons for the increase in NUE (Table 4, Table 5). In this study, NUE increased and then decreased with increasing N application under both irrigation patterns, which are results similar to those reported by Ma et al. (2022).

In conclusion, STI combined with appropriate N increased jujube yield, WUE and NUE compared with SD. Therefore, STI can be used as an alternative technology to SD in jujube cultivation. However, limitations of this study are that the technical parameters of the sand tube are affected by soil type, physical properties, and crop species and that the nitrogen amounts applied are affected by soil fertility, crop species, and local fertilization experience.

5 Conclusion

In this study, field *in-situ* soil water infiltration tests were first conducted to optimize sand tube technical parameters. Then, nitrogen regulation experiments with sand tube irrigation (STI) and surface drip irrigation (SD) were conducted in the field using the preferred sand tube parameters. In the field *in-situ* infiltration tests, STI significantly reduced soil surface wetted area and increased water infiltration depth, compared with SD. The optimal sand tube depth for cultivating jujube trees was 20 cm. In field-cultivated jujube, STI was more effective than SD in increasing SWS, chlorophyll content, and net photosynthetic rate. STI also increased jujube fruit yield, water and nitrogen use efficiencies, and net income. Increasing nitrogen application increased chlorophyll content, nitrogen balance index, net photosynthetic rate, jujube fruit yield, and water and nitrogen use efficiencies, but excessive N application caused an unstable decline in each index under both irrigation patterns. On the basis of a comprehensive analysis, STI combined with N3 had the highest yield, WUE, NUE, and net income. This study provides a new alternate irrigation method for jujube trees that can replace SD. And, through nitrogen regulation experiments, STI combined with N3 is the optimal irrigation and nitrogen management strategy for jujube trees in this region. However, the shortcoming of this study is that there is a deviation between hole application of fertilizer and conventional

water and fertilizer integration (fertilizer dissolved in water for irrigation). This may affect the nitrogen use efficiency. In the future, it is recommended to use sand tube irrigation technology in combination with water and fertilizer integration technology in large scale application.

Data availability statement

The raw data supporting the conclusions of this article will be made available by the authors, without undue reservation.

Author contributions

YB: Conceptualization, Data curation, Formal analysis, Funding acquisition, Methodology, Writing – original draft, Writing – review & editing. HZ: Conceptualization, Methodology, Supervision, Writing – original draft, Writing – review & editing. SJ: Conceptualization, Funding acquisition, Methodology, Supervision, Writing – original draft. DS: Formal analysis, Writing – review & editing. JZ: Formal analysis, Writing – review & editing. XZ: Data curation, Writing – review & editing. XF: Data curation, Funding acquisition, Writing – original draft. XW: Data curation, Writing – review & editing. CX: Data curation, Writing – review & editing. RC: Data curation, Writing – review & editing.

Funding

The author(s) declare financial support was received for the research, authorship, and/or publication of this article. This work was supported by the Projects of the National Natural Science Foundation of China (No. 51969002), the Gansu Province Higher Education Youth Doctoral Fund Project (2022QB-070), the Tongsheng Sheng Science and Technology Innovation Fund of Gansu Agricultural University (GSAU-STS-2018–30), the School Project of Gansu Agricultural University (0722003), and the 2021 Gansu Province Higher Education Innovation Fund Project (2021B-138).

Acknowledgments

We thank everyone who helped during the manuscript writing. We also thank the reviewers for their useful comments and suggestions.

Conflict of interest

The authors declare that the research was conducted in the absence of any commercial or financial relationships that could be construed as a potential conflict of interest.

Publisher's note

References

Andersen, A. (1968). Transpiration and watering problems. *Symposium Plant production containers*. 15, 27–33. doi: 10.17660/ActaHortic.1969.15.6

Bai, Y., Zhang, H., Jia, S., Huang, C., Zhao, X., Wei, H., et al. (2022). Plastic film mulching combined with sand tube irrigation improved yield, water use efficiency, and fruit quality of jujube in an arid desert area of Northwest China. *Agric. Water Manage.* 271, 107809. doi: 10.1016/j.agwat.2022.107809

Bao, S. (2000). *Soil and agricultural chemistry analysis* (Beijing: China Agriculture Press).

Benegas, L., Ilstedt, U., Roupsard, O., Jones, J., and Malmer, A. (2014). Effects of trees on infiltrability and preferential flow in two contrasting agroecosystems in Central America. *Agr. Ecosyst. Environ.* 183, 185–196. doi: 10.1016/j.agee.2013.10.027

Bo, Y., He, H. B., Xu, H. C., Zhu, T. Z., Tao, L., Jian, K., et al. (2021). Determining nitrogen status and quantifying nitrogen fertilizer requirement using a critical nitrogen dilution curve for hybrid indica rice under mechanical pot-seedling transplanting pattern. *J. Integr. Agr.* 20, 1474–1486. doi: 10.1016/S2095-3119(21)63622-5

Cao, Y. X., Cai, H. J., Sun, S. K., Gu, X. B., Mu, Q., Duan, W. N., et al. (2022). Effects of drip irrigation methods on yield and water productivity of maize in Northwest China. *Agric. Water Manage.* 259, 107227. doi: 10.1016/j.agwat.2021.107227

Cui, Z., Huang, Z., Liu, Y., Lopez-Vicente, M., and Wu, G. L. (2021). Natural compensation mechanism of soil water infiltration through decayed roots in semi-arid vegetation species. *Sci. Total Environ.* 819, 151985. doi: 10.1016/j.scitotenv.2021.151985

Dai, Z. G., Fei, L. J., Huang, D. L., Zeng, J., Chen, L., and Cai, Y. H. (2019). Coupling effects of irrigation and nitrogen levels on yield, water and nitrogen use efficiency of surge-root irrigated jujube in a semiarid region. *Agric. Water Manage.* 213, 146–154. doi: 10.1016/j.agwat.2018.09.035

Department of Rural Socio-Economic Survey, N.B.O.S (2021). *China rural statistics yearbook* (Beijing, China: China Statistics Press). Available at: http://www.stats.gov.cn/zs/tjwh/tjkw/tjzl/202302/t20230215_1907997.html.

Dou, J.-F., Kou, X.-H., Wu, C.-E., Fan, G.-J., Li, T.-T., Li, X.-J., et al. (2023). Recent advances and development of postharvest management research for fresh jujube fruit: A review. *Sci. Hortic.* 310, 111769. doi: 10.1016/j.scienta.2022.111769

Duan, X., Xie, Y., Liu, G., Gao, X., and Lu, H. (2010). Field capacity in black soil region, northeast China. *Chin. Geographical Sci.* 20, 406–413. doi: 10.1007/s11769-010-0414-4

Fan, J. C., Lu, X. J., Gu, S. H., and Guo, X. Y. (2020). Improving nutrient and water use efficiencies using water-drip irrigation and fertilization technology in Northeast China. *Agric. Water Manage.* 241, 106352. doi: 10.1016/j.agwat.2020.106352

Fan, K., Li, F., Chen, X., Li, Z., and Mulla, D. J. (2022). Nitrogen balance index prediction of winter wheat by canopy hyperspectral transformation and machine learning. *Remote Sens.* 14 (14), 3504. doi: 10.3390/rs14143504

FAO (2023) *The state of food security and nutrition in the world 2023*. Available online at: https://www.fao.org/interactive/state-of-food-security-nutrition/en/.

Goyal, M. R. (2014). *Sustainable micro irrigation: principles and practices* (Oakville, Canada: Apple Academic Press). doi: 10.1201/b17155

Guan, Y., Lei, T., Liu, F., and Dong, Y. (2016). Measurement of wetting process of soil under dripper with automatic system for point source infiltration. *Trans. CSAE* 32, 1–7. doi: 10.11975/j.issn.1002-6819.2016.14.001

Guo, J., Fan, J., Zhang, F., Yan, S., Zheng, J., Wu, Y., et al. (2021). Blending urea and slow-release nitrogen fertilizer increases dryland maize yield and nitrogen use efficiency while mitigating ammonia volatilization. *Sci. Total Environ.* 790, 148058. doi: 10.1016/j.scitotenv.2021.148058

Habib-Ur-Rahman, M., Ahmad, A., Raza, A., Hasnain, M. U., Alharby, H. F., Alzahrani, Y. M., et al. (2022). Impact of climate change on agricultural production; Issues, challenges, and opportunities in Asia. *Front. Plant Sci.* 13, 925548. doi: 10.3389/fpls.2022.925548

He, Z., Cao, H., Liang, J., Hu, Q., Zhang, Y., Nan, X., et al. (2022). Effects of biochar particle size on sorption and desorption behavior of NH4+-N. *Ind. Crop Prod.* 189, 115837. doi: 10.1016/j.indcrop.2022.115837

Islam, M., and Morimoto, T. (2015). Evaluation of a new heat transfer and evaporative design for a zero energy storage structure. *Sol. Energy* 118, 469–484. doi: 10.1016/j.solener.2015.06.006

Kandelous, M. M., and Šimůnek, J. (2010). Comparison of numerical, analytical, and empirical models to estimate wetting patterns for surface and subsurface drip irrigation. *Irrigation Sci.* 28, 435–444. doi: 10.1007/s00271-009-0205-9

Kang, S., Hao, X., Du, T., Tong, L., Su, X., Lu, H., et al. (2017). Improving agricultural water productivity to ensure food security in China under changing environment: From research to practice. *Agric. Water Manage.* 179, 5–17. doi: 10.1016/j.agwat.2016.05.007

Larimi, S. B., Shakiba, M., Mohammadinasab, A. D., and Vahed, M. (2014). Changes in nitrogen and chlorophyll density and leaf area of sweet basil (Ocimum basilicum L.) affected by biofertilizer and nitrogen application. *Int. J. Biosci.* 5, 256–265. doi: 10.12692/ijb/5.9.256-265

Lassaletta, L., Einarsson, R., and Quemada, M. (2023). Nitrogen use efficiency of tomorrow. *Nat. Food* 4, 281–282. doi: 10.1038/s43016-023-00740-x

Li, J., Cui, P., and Yin, Y. (2023). Field observation and micro-mechanism of roots-induced preferential flow by infiltration experiment and phase-field method. *J. Hydrol.* 623, 129756. doi: 10.1016/j.jhydrol.2023.129756

Liu, Y., Hu, C., Li, B., Ding, D., Zhao, Z., Fan, T., et al. (2021). Subsurface drip irrigation reduces cadmium accumulation of pepper (Capsicum annuum L.) plants in upland soil. *Sci. Total Environ.* 755, 142650. doi: 10.1016/j.scitotenv.2020.142650

Liu, Y., Miao, H. T., Huang, Z., Cui, Z., He, H. H., Zheng, J. Y., et al. (2018). Soil water depletion patterns of artificial forest species and ages on the Loess Plateau (China). *For. Ecol. Manage.* 417, 137–143. doi: 10.1016/j.foreco.2018.03.005

Lu, J. S., Hu, T. T., Geng, C. M., Cui, X. L., Fan, J. L., and Zhang, F. C. (2021). Response of yield, yield components and water-nitrogen use efficiency of winter wheat to different drip fertigation regimes in Northwest China. *Agric. Water Manage.* 255, 107034. doi: 10.1016/j.agwat.2021.107034

Luo, Z., Niu, J., He, S., Zhang, L., Chen, X., Tan, B., et al. (2023). Linking roots, preferential flow, and soil moisture redistribution in deciduous and coniferous forest soils. *J. Soil Sediment.* 23, 1524–1538. doi: 10.1007/s11368-022-03375-w

Ma, K., Wang, Z., Li, H., Wang, T., and Chen, R. (2022). Effects of nitrogen application and brackish water irrigation on yield and quality of cotton. *Agric. Water Manage.* 264, 107512. doi: 10.1016/j.agwat.2022.107512

Ma, L., Zhang, X., Lei, Q. Y., and Liu, F. (2021). Effects of drip irrigation nitrogen coupling on dry matter accumulation and yield of Summer Maize in arid areas of China. *Field Crop Res.* 274, 108321. doi: 10.1016/j.fcr.2021.108321

Madramootoo, C. A., and Morrison, J. (2013). Advances and challenges with micro-irrigation. *Irrig. Drain.* 62, 255–261. doi: 10.1002/ird.1704

Marschner, H. (2011). *Marschner's mineral nutrition of higher plants*. *3rd edition*. Great Britain: Academic Press. 142–148. doi: 10.1016/C2009-0-63043-9

Martínez, J., and Reca, J. (2014). Water use efficiency of surface drip irrigation versus an alternative subsurface drip irrigation method. *J. Irrig. Drain. Eng.* 140, 04014030. doi: 10.1061/(ASCE)IR.1943-4774.0000745

Mattar, M. A., El-Abedin, T. Z. K., Al-Ghobari, H. M., Alazba, A. A., and Elansary, H. O. (2021). Effects of different surface and subsurface drip irrigation levels on growth traits, tuber yield, and irrigation water use efficiency of potato crop. *Irrigation Sci.* 39, 517–533. doi: 10.1007/s00271-020-00715-x

Meshkat, M., Warner, R. C., and Workman, S. R. (1998). Comparison of water and temperature distribution profiles under sand tube irrigation. *Trans. ASAE* 41, 1657–1663. doi: 10.13031/2013.17341

Meshkat, M., Warner, R. C., and Workman, S. R. (1999). Modeling of evaporation reduction in drip irrigation system. *J. Irrig. Drain. Eng.* 125, 315–323. doi: 10.1061/(ASCE)0733-9437(1999)125:6(315)

Meshkat, M., Warner, R. C., and Workman, S. R. (2000). Evaporation reduction potential in an undisturbed soil irrigated with surface drip and sand tube irrigation. *Trans. ASAE* 43, 79–86. doi: 10.13031/2013.2690

Min, J., Sun, H., Wang, Y., Pan, Y., Kronzucker, H. J., Zhao, D., et al. (2021). Mechanical side-deep fertilization mitigates ammonia volatilization and nitrogen runoff and increases profitability in rice production independent of fertilizer type and split ratio. *J. Clean Prod.* 316, 128370. doi: 10.1016/j.jclepro.2021.128370

Muhammad, T., Zhou, B., Puig-Bargu, J., Ding, C., Li, S., Manan, I., et al. (2022). Assessment of emitter clogging with multiple fouling and root intrusion in sub-surface drip irrigation during 5-year sugarcane growth. *Agric. Water Manage.* 274, 107981. doi: 10.1016/j.agwat.2022.107981

Nazari, E., Besharat, S., Zeinalzadeh, K., and Mohammadi, A. (2021). Measurement and simulation of the water flow and root uptake in soil under subsurface drip irrigation of apple tree. *Agric. Water Manage.* 255, 106972. doi: 10.1016/j.agwat.2021.106972

Niu, W., Liu, L., and Chen, X. (2013). Influence of fine particle size and concentration on the clogging of labyrinth emitters. *Irrigation Sci.* 31, 545–555. doi: 10.1007/s00271-012-0328-2

Payero, J. O., Tarkalson, D. D., Irmak, S., Davison, D., and Petersen, J. L. (2008). Effect of irrigation amounts applied with subsurface drip irrigation on corn evapotranspiration, yield, water use efficiency, and dry matter production in a semiarid climate. *Agric. Water Manage.* 95, 895–908. doi: 10.1016/j.agwat.2008.02.015

Pramanik, K., and Bera, A. (2013). Effect of seedling age and nitrogen fertilizer on growth, chlorophyll content, yield and economics of hybrid rice (Oryza sativa L.). *Int. J. Plant Prod.* 4, 3489–3499.

Rashwan, A. K., Karim, N., Shishir, M. R. I., Bao, T., Lu, Y., and Chen, W. (2020). Jujube fruit: A potential nutritious fruit for the development of functional food products. *J. Funct. Foods* 75, 104205. doi: 10.1016/j.jff.2020.104205

Sandhu, R., and Irmak, S. (2022). Effects of subsurface drip-irrigated soybean seeding rates on grain yield, evapotranspiration and water productivity under limited and full irrigation and rainfed conditions. *Agric. Water Manage.* 267, 107614. doi: 10.1016/j.agwat.2022.107614

Shen, D., Kou, X., Wu, C., Fan, G., Li, T., Dou, J., et al. (2021). Cocktail enzyme-assisted alkaline extraction and identification of jujube peel pigments. *Food Chem.* 357, 129747. doi: 10.1016/j.foodchem.2021.129747

Simkin, A. J., Kapoor, L., Doss, C. G. P., Hofmann, T. A., Lawson, T., and Ramamoorthy, S. (2022). The role of photosynthesis related pigments in light harvesting, photoprotection and enhancement of photosynthetic yield in planta. *Photosynth. Res.* 152, 23–42. doi: 10.1007/s11120-021-00892-6

Sun, Y., Tong, C., He, S., Wang, K., and Chen, L. (2018). Identification of nitrogen, phosphorus, and potassium deficiencies based on temporal dynamics of leaf morphology and color. *Sustainability* 10, 762. doi: 10.3390/su10030762

Sun, S. M., Yang, P. L., An, Q. X., Xu, R., Yao, B. L., Li, F. Y., et al. (2016). Investigation into surface and subsurface drip irrigation for jujube trees grown in saline soil under extremely arid climate. *Eur. J. Hortic. Sci.* 81, 165–174. doi: 10.17660/eJHS.2016/81.3.5

Surendran, U., Jayakumar, M., and Marimuthu, S. (2016). Low cost drip irrigation: Impact on sugarcane yield, water and energy saving in semiarid tropical agro ecosystem in India. *Sci. Total Environ.* 573, 1430–1440. doi: 10.1016/j.scitotenv.2016.07.144

Széles, A. V., Megyes, A., and Nagy, J. (2012). Irrigation and nitrogen effects on the leaf chlorophyll content and grain yield of maize in different crop years. *Agric. Water Manage.* 107, 133–144. doi: 10.1016/j.agwat.2012.02.001

Valentín, F., Nortes, P., Domínguez, A., Sánchez, J., Intrigliolo, D., Alarcón, J., et al. (2020). Comparing evapotranspiration and yield performance of maize under sprinkler, superficial and subsurface drip irrigation in a semi-arid environment. *Irrigation Sci.* 38, 105–115. doi: 10.1007/s00271-019-00657-z

Wang, C., Bai, D., Li, Y. B., Yao, B. L., and Feng, Y. Q. (2021). The comparison of different irrigation methods on yield and water use efficiency of the jujube. *Agric. Water Manage.* 252, 106875. doi: 10.1016/j.agwat.2021.106875

Wang, J., Du, Y., Niu, W., Han, J., Li, Y., and Yang, P. (2022b). Drip irrigation mode affects tomato yield by regulating root–soil–microbe interactions. *Agric. Water Manage.* 260, 107188. doi: 10.1016/j.agwat.2021.107188

Wang, N., Fu, F., Wang, H., Wang, P., He, S., Shao, H., et al. (2021c). Effects of irrigation and nitrogen on chlorophyll content, dry matter and nitrogen accumulation in sugar beet (Beta vulgaris L.). *Sci. Rep.* 11, 16651. doi: 10.1038/s41598-021-95792-z

Wang, T., Li, N., Li, Y., Lin, H., Yao, N., Chen, X., et al. (2022c). Impact of climate variability on grain yields of spring and summer maize. *Comput. Electron. Ag.* 199, 107101. doi: 10.1016/j.compag.2022.107101

Wang, H., Wang, N., Quan, H., Zhang, F., Fan, J., Feng, H., et al. (2022a). Yield and water productivity of crops, vegetables and fruits under subsurface drip irrigation: A global meta-analysis. *Agric. Water Manage.* 269, 107645. doi: 10.1016/j.agwat.2022.107645

Wang, K., Zhang, X., Ma, J., Ma, Z., Li, G., and Zheng, J. (2020). Combining infiltration holes and level ditches to enhance the soil water and nutrient pools for semi-arid slope shrubland revegetation. *Sci. Total Environ.* 729, 138796. doi: 10.1016/j.scitotenv.2020.138796

Wang, X., Zhu, D. L., Wang, Y. K., Wei, X. D., and Ma, L. H. (2015). Soil water and root distribution under jujube plantations in the semiarid Loess Plateau region, China. *Plant Growth Regul.* 77, 21–31. doi: 10.1007/s10725-015-0031-4

Wen, B., Xiao, W., Mu, Q., Li, D., Chen, X., Wu, H., et al. (2020). How does nitrate regulate plant senescence? Plant Physiol. *Biochem.* 157, 60–69. doi: 10.1016/j.plaphy.2020.08.041

WMO (2023) *State of the global climate in 2022*. Available online at: https://public.wmo.int/en/our-mandate/climate/wmo-statement-state-of-global-climate.

Yu, Y., Pi, Y., Yu, X., Ta, Z., Sun, L., Disse, M., et al. (2018). Climate change, water resources and sustainable development in the arid and semi-arid lands of Central Asia in the past 30 years. *J. Arid Land* 11, 1–14. doi: 10.1007/s40333-018-0073-3

Zhang, X., Davidson, E. A., Mauzerall, D. L., Searchinger, T. D., Dumas, P., and Shen, Y. (2015). Managing nitrogen for sustainable development. *Nature* 528, 51–59. doi: 10.1038/nature15743

Zhang, Y., Yu, H., Yao, H., Deng, T., Yin, K., Liu, J., et al. (2023). Yield and quality of winter jujube under different fertilizer applications: A field investigation in the yellow river delta. *Horticulturae* 9, 152. doi: 10.3390/horticulturae9020152

Zhang, C., Zhang, W., Yan, H., Ni, Y., Akhlaq, M., Zhou, J., et al. (2022). Effect of micro–spray on plant growth and chlorophyll fluorescence parameter of tomato under high temperature condition in a greenhouse. *Sci. Hortic-Amsterdam* 306, 111441. doi: 10.1016/j.scienta.2022.111441

Zhang, X., Zou, T., Lassaletta, L., Mueller, N. D., Tubiello, F. N., Lisk, M. D., et al. (2021). Quantification of global and national nitrogen budgets for crop production. *Nat. Food* 2, 529–540. doi: 10.1038/s43016-021-00318-5

Zhong, Y., Wang, X., Yang, J., Zhao, X., and Ye, X. (2016). Exploring a suitable nitrogen fertilizer rate to reduce greenhouse gas emissions and ensure rice yields in paddy fields. *Sci. Total Environ.* 565, 420–426. doi: 10.1016/j.scitotenv.2016.04.167

Zhu, J., Yang, Y., Liu, Y., Cui, X., Li, T., Jia, Y., et al. (2023). Progress and water stress of sustainable development in Chinese northern drylands. *J. Clean Prod.* 399, 136611. doi: 10.1016/j.jclepro.2023.136611

Frontiers in Plant Science

Cultivates the science of plant biology and its applications

The most cited plant science journal, which advances our understanding of plant biology for sustainable food security, functional ecosystems and human health.

Discover the latest Research Topics

See more →

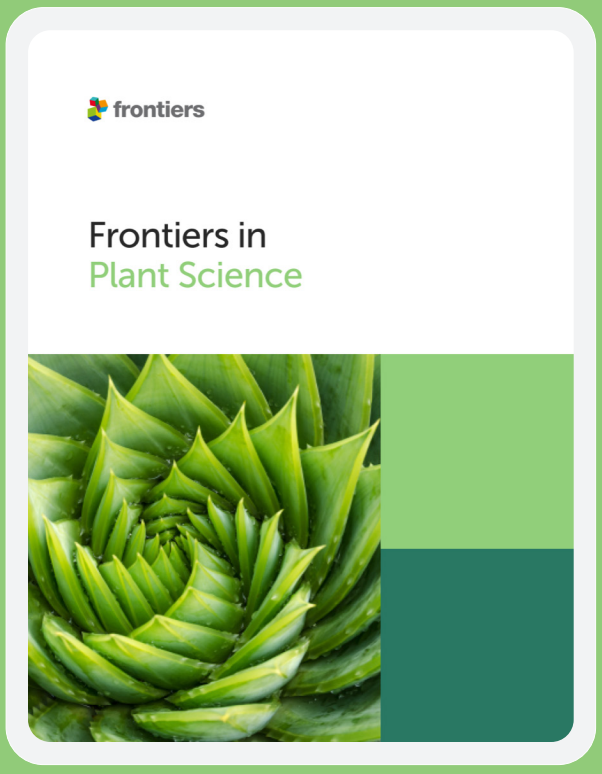

Frontiers

Avenue du Tribunal-Fédéral 34
1005 Lausanne, Switzerland
frontiersin.org

Contact us

+41 (0)21 510 17 00
frontiersin.org/about/contact